Oxidative Medicine and Cellular Longevity

# Mechanisms and Disease Pathogenesis Underlying Metal-Induced Oxidative Stress

Lead Guest Editor: Pan Chen
Guest Editors: Julia Bornhorst, M. Diana Neely, and Daiana S. Avila

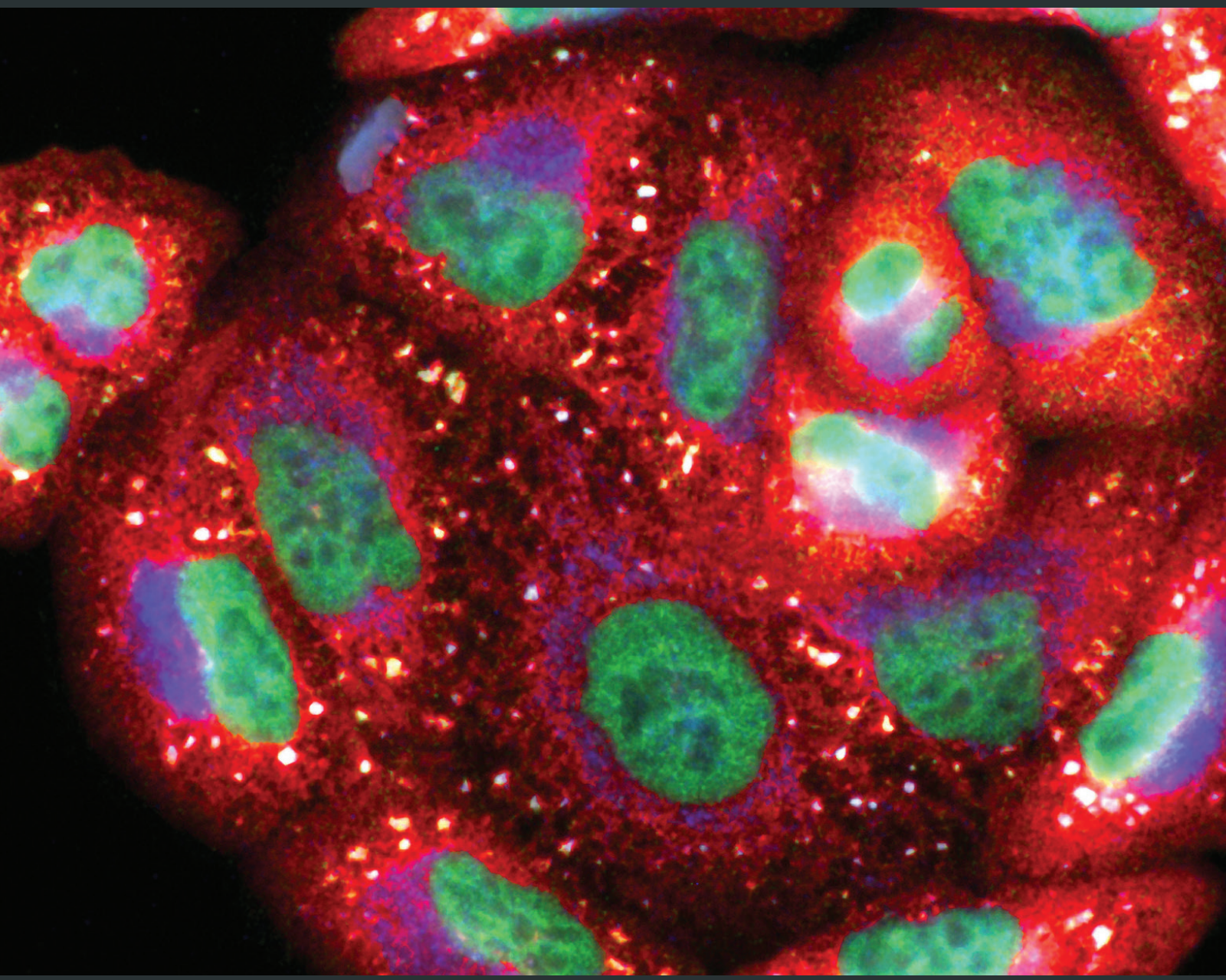

# Mechanisms and Disease Pathogenesis Underlying Metal-Induced Oxidative Stress

Oxidative Medicine and Cellular Longevity

# Mechanisms and Disease Pathogenesis Underlying Metal-Induced Oxidative Stress

Lead Guest Editor: Pan Chen
Guest Editors: Julia Bornhorst, M. Diana Neely, and Daiana S. Avila

Copyright © 2018 Hindawi. All rights reserved.

This is a special issue published in "Oxidative Medicine and Cellular Longevity." All articles are open access articles distributed under the Creative Commons Attribution License, which permits unrestricted use, distribution, and reproduction in any medium, provided the original work is properly cited.

# Editorial Board


Dario Acuña-Castroviejo, Spain
Fabio Altieri, Italy
Fernanda Amicarelli, Italy
José P. Andrade, Portugal
Cristina Angeloni, Italy
Antonio Ayala, Spain
Elena Azzini, Italy
Peter Backx, Canada
Damian Bailey, UK
Grzegorz Bartosz, Poland
Sander Bekeschus, Germany
Ji C. Bihl, USA
Consuelo Borrás, Spain
Nady Braidy, Australia
Darrell W. Brann, USA
Ralf Braun, Germany
Laura Bravo, Spain
Vittorio Calabrese, Italy
Amadou Camara, USA
Gianluca Carnevale, Italy
Roberto Carnevale, Italy
Angel Catalá, Argentina
Giulio Ceolotto, Italy
Shao-Yu Chen, USA
Ferdinando Chiaradonna, Italy
Zhao Zhong Chong, USA
Alin Ciobica, Romania
Ana Cipak Gasparovic, Croatia
Giuseppe Cirillo, Italy
Maria R. Ciriolo, Italy
Massimo Collino, Italy
Manuela Corte-Real, Portugal
Mark Crabtree, UK
Manuela Curcio, Italy
Andreas Daiber, Germany
Felipe Dal Pizzol, Brazil
Francesca Danesi, Italy
Domenico D'Arca, Italy
Claudio De Lucia, Italy
Yolanda de Pablo, Sweden
Sonia de Pascual-Teresa, Spain
Cinzia Domenicotti, Italy
Joël R. Drevet, France
Grégory Durand, France
Javier Egea, Spain
Ersin Fadillioglu, Turkey
Ioannis G. Fatouros, Greece
Qingping Feng, Canada
Gianna Ferretti, Italy
Giuseppe Filomeni, Italy
Swaran J. S. Flora, India
Teresa I. Fortoul, Mexico
Jeferson L. Franco, Brazil
Rodrigo Franco, USA
Joaquin Gadea, Spain
José Luís García-Giménez, Spain
Gerardo García-Rivas, Mexico
Janusz Gebicki, Australia
Alexandros Georgakilas, Greece
Husam Ghanim, USA
Rajeshwary Ghosh, USA
Eloisa Gitto, Italy
Daniela Giustarini, Italy
Saeid Golbidi, Canada
Aldrin V. Gomes, USA
Tilman Grune, Germany
Nicoletta Guaragnella, Italy
Solomon Habtemariam, UK
Eva-Maria Hanschmann, Germany
Tim Hofer, Norway
John D. Horowitz, Australia
Silvana Hrelia, Italy
Stephan Immenschuh, Germany
Maria Isaguliants, Latvia
Luigi Iuliano, Italy
Vladimir Jakovljevic, Serbia
Marianna Jung, USA
Peeter Karihtala, Finland
Eric E. Kelley, USA
Kum Kum Khanna, Australia
Neelam Khaper, Canada
Thomas Kietzmann, Finland
Demetrios Kouretas, Greece
Andrey V. Kozlov, Austria
Jean-Claude Lavoie, Canada
Simon Lees, Canada
Christopher Horst Lillig, Germany
Paloma B. Liton, USA
Ana Lloret, Spain
Lorenzo Loffredo, Italy
Daniel Lopez-Malo, Spain
Antonello Lorenzini, Italy
Nageswara Madamanchi, USA
Kenneth Maiese, USA
Marco Malaguti, Italy
Tullia Maraldi, Italy
Reiko Matsui, USA
Juan C. Mayo, Spain
Steven McAnulty, USA
Antonio Desmond McCarthy, Argentina
Bruno Meloni, Australia
Pedro Mena, Italy
Víctor Manuel Mendoza-Núñez, Mexico
Maria U Moreno, Spain
Trevor A. Mori, Australia
Ryuichi Morishita, Japan
Fabiana Morroni, Italy
Luciana Mosca, Italy
Ange Mouithys-Mickalad, Belgium
Iordanis Mourouzis, Greece
Danina Muntean, Romania
Colin Murdoch, UK
Pablo Muriel, Mexico
Ryoji Nagai, Japan
David Nieman, USA
Hassan Obied, Australia
Julio J. Ochoa, Spain
Pál Pacher, USA
Pasquale Pagliaro, Italy
Valentina Pallottini, Italy
Rosalba Parenti, Italy
Vassilis Paschalis, Greece
Daniela Pellegrino, Italy
Ilaria Peluso, Italy
Claudia Penna, Italy
Serafina Perrone, Italy
Tiziana Persichini, Italy
Shazib Pervaiz, Singapore
Vincent Pialoux, France
Ada Popolo, Italy
José L. Quiles, Spain
Walid Rachidi, France

Zsolt Radak, Hungary
Namakkal S. Rajasekaran, USA
Kota V. Ramana, USA
Sid D. Ray, USA
Hamid Reza Rezvani, France
Alessandra Ricelli, Italy
Paola Rizzo, Italy
Francisco J. Romero, Spain
Joan Roselló-Catafau, Spain
H. P. Vasantha Rupasinghe, Canada
Gabriele Saretzki, UK
Nadja Schroder, Brazil
Sebastiano Sciarretta, Italy
Honglian Shi, USA
Cinzia Signorini, Italy
Mithun Sinha, USA
Carla Tatone, Italy
Frank Thévenod, Germany
Shane Thomas, Australia
Carlo Tocchetti, Italy
Angela Trovato Salinaro, Jamaica
Paolo Tucci, Italy
Rosa Tundis, Italy
Giuseppe Valacchi, Italy
Jeannette Vasquez-Vivar, USA
Daniele Vergara, Italy
Victor M. Victor, Spain
László Virág, Hungary
Natalie Ward, Australia
Philip Wenzel, Germany
Anthony R. White, Australia
Georg T. Wondrak, USA
Michal Wozniak, Poland
Sho-ichi Yamagishi, Japan
Liang-Jun Yan, USA
Guillermo Zalba, Spain
Jacek Zielonka, USA
Mario Zoratti, Italy

# Contents

Hindawi
Oxidative Medicine and Cellular Longevity
Volume 2018, Article ID 7612172, 3 pages
https://doi.org/10.1155/2018/7612172

*Editorial*

# Mechanisms and Disease Pathogenesis Underlying Metal-Induced Oxidative Stress

**Pan Chen**,[1] **Julia Bornhorst**,[2] **M. Diana Neely**,[3] **and Daiana S. Avila**[4]

[1]*Department of Molecular Pharmacology, Albert Einstein College of Medicine, Bronx, NY, USA*
[2]*Department of Food Chemistry, Institute of Nutritional Science, University of Potsdam, Nuthetal, Germany*
[3]*Department of Pediatrics, Vanderbilt University Medical Center, Nashville, TN, USA*
[4]*Graduation Program in Biochemistry, Federal Pampa University, Uruguaiana, RS, Brazil*

Correspondence should be addressed to Pan Chen; pan.chen@einstein.yu.edu

Received 29 August 2018; Accepted 30 August 2018; Published 18 September 2018

Copyright © 2018 Pan Chen et al. This is an open access article distributed under the Creative Commons Attribution License, which permits unrestricted use, distribution, and reproduction in any medium, provided the original work is properly cited.

Metals are involved in almost all aspects of human life today: some are essential for maintenance of cell physiological activities and others are important industrial materials. Over half of the elements (23) with known physiological functions in humans are metals (12), including iron, zinc, copper, and manganese. While the deficiency of some metals may cause pathological conditions (such as iron-deficiency anemia and restless legs syndrome), excess exposure to metals can be toxic and can contribute to human diseases, including cancer, hepatic diseases, and neurodegenerative diseases (such as Alzheimer's, Parkinson's, and Huntington's diseases). Metals such as mercury and lead that are widely used in modern industry do not have any known physiological function in human; however, they are potent neurodevelopmental toxicants. Nowadays, increasing environmental exposures and fortification of food sources with various metallic compounds are causing growing concerns that imbalances in metal content and excess exposure in particular may contribute to the etiology of various human diseases.

Oxidative stress is a fundamental molecular mechanism underlying metal-induced toxicity. Most metals are redox-active, especially transition metals, such as iron, copper, manganese, and zinc. They can undergo redox cycling reactions resulting in the production of reactive oxygen/nitrogen species (RONS). For example, in Fenton's reaction, iron reacts with hydrogen peroxide to produce hydroxyl free radicals, one of the most reactive RONS molecules. Excess intracellular RONS eventually disrupts the intracellular redox state and energy production resulting in oxidative stress, which manifests itself in the modification of cellular biomolecules, such as DNA, lipids and proteins, the dysfunction of mitochondrial respiration, protein folding, DNA repair processes, endoplasmic reticulum (ER) stress, inflammation, autophagy, and/or apoptosis. These cellular phenotypes are frequently observed in the pathogenesis of human diseases.

Despite recent advances in biomedical sciences, the exact mechanisms underlying metal-associated cellular toxicity is in most cases not fully established. The understanding and knowledge of the mechanisms underlying metal-induced toxicities is of paramount importance for the development of antidotes for metal intoxication. This special issue includes papers that explore causative links between metals and human diseases (including cancer and neurological disorders), establish molecular mechanisms underlying metal-induced oxidative stress in the pathogenesis of these diseases, and identify molecular compounds with protective effects against these metals.

Neurodevelopmental- and neurodegenerative disease-associated metal toxicities are of great concern for the industrialized modern world, and several different metals including those that play a role in normal cellular physiology have been implicated to have adverse effects on neurodevelopment or to play a role in the pathogenesis of neurodegenerative or both.

Iron is present in several metalloproteins and, at physiological concentrations, plays a role in enzyme catalysis and in cellular functions such as oxygen transport, mitochondrial respiration, DNA, neurotransmitter, and myelin biosynthesis;

however, excess iron has been associated with the pathogenesis of several neurodegenerative diseases, including Alzheimer's and Parkinson's diseases. R. M. Uranga and G. A. Salvador have reviewed the toxic effects of iron overload on the brain and the interaction of this metal with the amyloid $\beta$ peptide. The authors conclude that excess iron results in oxidative stress. They postulate that the exploration of downstream targets of the iron-induced ROS and their role in CNS pathogenesis will allow us to shed light on mechanisms underlying neurodegeneration and the development of therapeutic tools.

Cadmium which has no known physiological function has been described as a serious hazard to human health by the International Agency for Research on Cancer. H. R. Marini et al. set out to assess the effects of chronic cadmium exposure on the mouse hippocampus and to explore the potential protective effects of polydeoxyribonucleotide, an adenosine A2A receptor agonist. They report a cadmium-induced decline of spatial memory and learning, a significant decrease of BDNF expression, an increase in mTOR expression, neuronal loss, and brain edema. Coadministration of the adenosine A2A receptor agonist polydeoxyribonucleotide ameliorated all of those cadmium-induced effects. The authors conclude from this and their previous studies and findings reported by other groups that the cadmium-induced expression of mTOR in the CNS observed here is the result of cadmium-increased ROS production and oxidative stress.

Mercury, another metal which has no biological function, is a well-established central nervous system toxicant. W. A. B. Aragão et al. investigated the effects of a chronic relatively low-dose oral mercury chloride ($HgCl_2$) exposure on the rat hippocampal campus. They report a 17-fold increase in hippocampal mercury levels in exposed animals over the baseline levels observed in the control group, suggesting that this metal is efficiently transported across the blood-brain barrier. They observed significant impairments in short- and long-term memory including cognitive impairment. They hypothesize that the elevated oxidative stress observed in the hippocampus led to cytotoxicity and apoptosis, affecting both astrocytes and neurons in the hippocampus.

Aside from its well established neurotoxicity, mercury has also been implicated in cancer. In cancer, abnormal cell growth is traditionally viewed to result from various genetic mutations; however, more recent studies support the hypothesis that the epigenetic regulations (such as DNA methylation, histone modification, transcription, and DNA repair) and especially of promoters also play an important role. In their review, R. Zefferino et al. propose a multistep pathway by which mercury promotes cancer development. Based on their study and other groups' studies, they propose that mercury in an initial step causes an imbalance in the cellular redox equilibrium by interfering with the activity of selenocysteine antioxidant enzymes and other sulfhydryl-containing proteins. This mercury-induced prooxidative state in turn results in the inhibition of gap junction-mediated intercellular communication and a proinflammatory cytokine release, both of which isolate cells from their tissue-specific homeostasis promoting excessive proliferation and inhibiting the immune system's defense of such inappropriate proliferation.

Copper-based Casiopeinas are a group of metal-based antineoplastic drugs designed to have lower generalized toxicity as compared to the alternative drugs cisplatin or doxorubicin. However, these drugs have shown significant cardiac toxicities in canine and rodent models. C. Silva-Platas et al. designed their studies to assess potential mechanisms underlying this cardiomyocyte toxicity of this group of drugs. They observed that in isolated hearts perfused with Casiopeinas, contractile function was inhibited and ATP levels were significantly reduced. Heart mitochondria isolated from Casiopeina-treated animals showed a reduction in mitochondrial membrane potential and calcium retention capacity. In cultured cardiomyocytes, Casiopeinas induced proapoptotic caspases and apoptosis. The authors conclude that the mitochondria are the main target of Casiopeina-induced cardiomyocyte toxicity, where these drugs impair mitochondrial respiratory chain function and induce energetic failure, events that typically result in oxidative stress.

Manganese (Mn) is an essential trace element and acts as a cofactor in enzymes, such as Mn superoxide dismutase thus playing a role in the protection against oxidative stress. However, excessive exposure to this metal is associated with cytotoxicity typically resulting from Mn-induced oxidative stress. L. Li and X. Yang have reviewed current studies addressing the connection between Mn and metabolic disorders that have become a significant health concern in the last decade. These disorders include type 2 diabetes mellitus (T2DM), obesity, insulin resistance, atherosclerosis, nonalcoholic fatty liver disease (NAFLD), and hepatic steatosis which share a common pathology involving the generation of excessive levels of reactive oxygen species (ROS), elevated oxidative stress, and inflammation.

Lead is a ubiquitous pollutant and commonly used in industries; therefore, contamination is common. Even low levels of lead can lead to significant physiological changes. Occupational exposure to this metal has thus to be constantly monitored to ensure a safe working environment for the workers. The study of M. Dobrakowski et al. assessed a cohort of 36 males exposed to lead for 36–44 days. As expected, blood lead levels were increased after their exposure; in addition, small changes of calcium, magnesium, zinc, and copper levels were also observed. The authors further report no change in the activities of catalase and superoxide dismutase and no elevation of malondialdehyde levels, a marker of oxidative stress; however, there was a 46% increase in serum lipid hydroperoxides, another manifestation of oxidative stress targeting lipids.

Metal poisoning is an increasing concern in our modern industrialized world. While environmental regulations need to be regularly updated with additional studies concerning the toxicities of metals, intoxication of humans will remain a serious health hazard at least for the nearer future. Antidotes for metal intoxication are rare, and there is an urgent need to develop therapeutic drugs to counteract metal poisoning. The elucidation of the mechanism underlying metal toxicities will be of a great value to the development of effective metal antidotes. Every study in this issue concludes that

oxidative stress is indeed an important metal-induced effect and is the cause that ultimately leads to dysfunction of cellular mechanisms and/or cell death in the model system examined. The mechanism by which a metal induces oxidative stress and the downstream targets of the oxidative stress should be evaluated using a combination of oxidative stress measures so that an "oxidative stress signature" phenotype can be established. It is the hope that such mechanistic analysis and knowledge will be able to support the successful development of therapeutics for the treatment of metal poisonings.

## Conflicts of Interest

The editors declare that they have no conflicts of interest regarding the publication of this Special Issue.

*Pan Chen*
*Julia Bornhorst*
*M. Diana Neely*
*Daiana S. Avila*

Hindawi
Oxidative Medicine and Cellular Longevity
Volume 2018, Article ID 4285694, 9 pages
https://doi.org/10.1155/2018/4285694

*Research Article*

# Neuroprotective Effects of Polydeoxyribonucleotide in a Murine Model of Cadmium Toxicity

**Herbert R. Marini**,[1] **Domenico Puzzolo**,[2] **Antonio Micali**,[2] **Elena Bianca Adamo**,[2] **Natasha Irrera**,[1] **Antonina Pisani**,[2] **Giovanni Pallio**,[1] **Vincenzo Trichilo**,[1] **Consuelo Malta**,[2] **Alessandra Bitto**,[1] **Francesco Squadrito**,[1] **Domenica Altavilla**,[2] **and Letteria Minutoli**[1]

[1]*Department of Clinical and Experimental Medicine, University of Messina, Messina, Italy*
[2]*Department of Biomedical and Dental Sciences and Morphofunctional Imaging, University of Messina, Messina, Italy*

Correspondence should be addressed to Antonio Micali; amicali@unime.it

Received 23 April 2018; Accepted 31 July 2018; Published 29 August 2018

Academic Editor: Daiana S. Avila

Copyright © 2018 Herbert R. Marini et al. This is an open access article distributed under the Creative Commons Attribution License, which permits unrestricted use, distribution, and reproduction in any medium, provided the original work is properly cited.

Cadmium (Cd) is a harmful heavy metal, which causes severe brain damage and neurotoxic effects. Polydeoxyribonucleotide (PDRN) stimulates adenosine $A_{2A}$ receptor, thus contrasting several deleterious mechanisms in course of tissue damages. We aimed to investigate the possible neuroprotective effect of PDRN in a murine model of Cd-induced brain toxicity. Male C57 BL/6J mice were treated as follows: vehicle (0.9% NaCl, 1 ml/kg/day), PDRN (8 mg/kg/day), $CdCl_2$ (2 mg/kg/day), and $CdCl_2$ + PDRN. Animals were tested with the Morris water maze test to assess spatial memory and learning. After 14 days of treatment, brains were processed to evaluate the presence of edema in the cerebral tissue, the expression of mammalian target of rapamycin kinase (mTOR) and brain-derived neurotrophic factor (BDNF), and the morphological behavior of the hippocampal structures. After $CdCl_2$ administration, the escape latency was high, protein expression of BDNF was significantly decreased if compared to controls, mTOR levels were higher than normal controls, and brain edema and neuronal damages were evident. The coadministration of $CdCl_2$ and PDRN significantly diminished the escape latency, increased BDNF levels, and decreased protein expression of mTOR. Furthermore, brain edema was reduced and the structural organization and the number of neurons, particularly in the CA1 and CA3 hippocampal areas, were improved. In conclusion, a functional, biochemical, and morphological protective effect of PDRN against Cd induced toxicity was demonstrated in mouse brain.

## 1. Introduction

Cadmium (Cd) is an extremely toxic metal with no known necessary function in the human body. It represents serious hazard to human health, as stated by the International Agency for Research on Cancer [1]. Major sources of Cd are food, cigarette smoke, and recharged nickel-cadmium batteries [2]. Foods as cereals, vegetables, nuts and pulses, starchy roots, potatoes, and meat products are the main source of Cd exposure for the nonsmoking population [3].

Several reports studied Cd toxicity in the brain as a whole or in its specific regions. In particular, Cd can experimentally induce neurotoxic effects either *in vitro* or *in vivo*. In fact, damages referred to Cd challenge were observed in cortical and trigeminal neurons [4, 5], in anterior pituitary cells [6], in glioma and neuroblastoma cells [7], and in nerve-glial cell cultures [8]. Neurotoxic effects were also described in neonatal mouse [9] and in adult rat brain [10] and in diabetic rat optic nerve experimentally exposed to Cd [11].

To date, the pathophysiological mechanism of Cd brain toxicity is not completely defined, even if reactive oxygen species (ROS) generation probably plays a crucial role in the detrimental neurotoxic cascade triggered by Cd [12]. Specifically, under these conditions ROS can promote an exaggerated inflammatory response characterized by increased cytokine expression and intercellular adhesion molecule-1 (ICAM-1) upregulation [13], particularly through the activation of nuclear factor-$\kappa$B (NF-$\kappa$B) [13].

Moreover, a peculiar role in neurotoxic damage following Cd exposure is played by mitogen-activated protein kinases (MAPKs) [12] able to promote apoptosis [14], as well as by Akt/mammalian target of rapamycin (mTOR) signaling pathway activation, which controls neuron proliferation, growth, and survival [15, 16].

An impaired neurogenesis, with strongly reduced neuronal differentiation and axonogenesis, was observed as a result of Cd-induced neurotoxicity; therefore, neuronal death occurred [17].

So far, in the brain of mammals, an intricate crosstalk underlying both neuroinflammation and neurogenesis provides many possible molecular targets; they might be harmfully impacted by Cd but also, on other side, by suitable therapeutic approaches to counteract Cd-induced neurotoxic effects [17, 18].

Among the neurotrophic factors that support differentiation [19], maturation [20], and survival of neurons [21], the brain-derived neurotrophic factor (BDNF) has neuroprotective effects under adverse conditions, such as glutamatergic stimulation, neuroinflammation, cerebral ischemia, hypoglycemia, and neurotoxicity [22].

Adenosine $A_{2A}$ receptor (ADORA2A) plays a crucial role in many physiological responses and pathological conditions [23]. However, it is still unclear if the role of ADORA2A in the control of neuroprotection is mostly due to the different homeostatic roles of these receptors related with the control of metabolism, of neuron-glial communication, of neuroinflammation, or of the control of action of growth factors [23].

ADORA2A is colocalized with BDNF in the brain, and the functional interaction between ADORA2A stimulation and BDNF action has been proposed [24]. Experimental data indicate that ADORA2A activation is a crucial requisite for the functioning of neurotrophic receptors at synapses. This has been shown for the facilitatory actions of BDNF on synaptic transmission [25, 26] typically on prolonged potentiation at the CA1 area of the hippocampus [27].

Interestingly, a high prevalence of brain function disorders, including cognitive and behavioral impairments, has been associated with mTOR signaling disturbances [28]; in particular, mTOR activation was related to two major signaling pathways, Ras-ERK and PI3K-Akt, that essentially control neuron survival, differentiation, and proliferation in response to extracellular signals [29]. So far, extracellular messengers linked to mTOR activation may involve the adenosine pathway through ADORA2A modulation in response to systemic inflammation [30].

Polydeoxyribonucleotide (PDRN) is the active fraction extracted from trout spermatozoa used for tissue repair [31]; acting through stimulation of ADORA2A, it can well contrast several harmful mechanisms observed in pathological conditions of low tissue perfusion [31–35].

A positive role of PDRN on Cd-induced structural changes of the blood-testis barrier was already demonstrated, suggesting that it may have a positive effect against Cd-induced structural lesions on gametogenesis [36].

In light of this background, PDRN effects in the brain of mice exposed to Cd chloride ($CdCl_2$) were investigated to better elucidate the role of this adenosine agonist.

## 2. Materials and Methods

*2.1. Experimental Protocol.* All procedures complied with the standards for care and use of animal subjects indicated by the Guide for the Care and Use of Laboratory Animals (Institute of Laboratory Animal Resources, National Academy of Sciences, Bethesda, MD, USA); they were carried out also in accordance with Directive 2010/63/EU on the protection of animals used for scientific experiments [37, 38]. Fifty-six male adult C57 BL/6J mice (25–30 g), obtained from Charles River Laboratories Italia srl (Calco, Italy), were provided a standard diet ad libitum with free access to tap water under a 12 h light/dark cycle. They were divided into four groups: (i) animals administered with a vehicle solution consisting in 0.9% NaCl (1 ml/kg, ip, daily), indicated as "control + vehicle animals," (ii) animals administered with PDRN (8 mg/kg, ip daily), indicated as "control + PDRN animals," (iii) animals challenged with $CdCl_2$ plus with the vehicle as above (2 mg/kg, ip, daily), indicated as "$CdCl_2$ + vehicle animals," and (iv) animals challenged with $CdCl_2$ (2 mg/kg, ip, daily) and treated with PDRN (8 mg/kg, ip, daily), immediately following $CdCl_2$ administration, indicated as "$CdCl_2$ + PDRN animals."

*2.2. Drugs.* $CdCl_2$ was purchased from Sigma-Aldrich Srl (Milan, Italy) and diluted to the requested concentration in 0.9% NaCl. PDRN was donated by Mastelli Srl (Sanremo, Italy). All chemicals and reagents were of commercially available reagent grades.

*2.3. Assessment of Cognitive Performance.* To assess spatial memory and learning, animals were tested with the Morris water maze (MWM) test [39]. The test was performed in a round white pool (diameter 80 cm and depth 55 cm). The pool was filled to a depth of 30 cm with water made opaque with white nontoxic water-based tempura paint. Pool temperature was maintained at $22 \pm 0.5^{\circ}$C by adding warm water. The escape platform was a 25 $cm^2$ plexiglas square, placed in the center of one quadrant of the pool, 15 cm from the pool's edge, and submerged 1 cm below the water surface. The mouse was gently placed in the water pool between the quadrants, facing the wall of the pool changing the order every day during each trial. The mice were given four trial sessions each day for five consecutive days, with an intertrial interval of 15 min. Escape latency time (ELT), that is, the time taken by the animal to move from the starting quadrant to find the hidden platform in the target quadrant, was recorded in each trial, and the average time, expressed in seconds (s), for each day was calculated. If the mouse failed to find the platform within 60 s, it was guided gently onto the platform and allowed to remain there for 20 s. Significant decrease in ELT from that of the first session was considered as successful learning. During all trials, the experimenter always stood in the same position. All trials were performed between 9.00 and 16.00 h in a sound dampened room.

*2.4. Brain Collection.* The experiments lasted 14 days, until the mice were sacrificed with an ip overdose of ketamine and xylazine (100/20 mg/kg, resp.) and then subjected to decapitation. Their skulls were quickly opened, and the

brains were extracted on ice and washed with cold phosphate-buffered saline (PBS). The brains of 14 animals for each group were divided as follows: seven brains were used for histological study. From the other seven brains, one half was stored at −80°C for Western blot analysis, and one half was used for edema evaluation.

*2.5. Evaluation of Brain Edema.* To evaluate the extent of edema, brain sections from each group of animals were assayed for water content using wet weight/dry weight. Freshly dissected tissue samples of the hippocampus were weighed on aluminum foil, dried for 24 h at 105°C, and reweighed as previously described [40]. The percentage of water was calculated as follows: water content (%) = (wet weight − dry weight)/wet weight × 100.

*2.6. Histological Evaluation.* Brains were immediately fixed in 4% paraformaldehyde in 0.2 M phosphate buffer solution (PBS), dehydrated in graded ethanol, cleared in xylene, and embedded in paraffin (Paraplast, Supplies SPI, West Chester, PA, USA). 5 $\mu$m coronal sections, cut with a RM2125 RT microtome (Leica Instruments, Nußloch, Germany), were cleared with xylene, rehydrated in ethanol, and stained with hematoxylin and eosin (H&E). Histological identification of nervous structures was made according to the atlas of Franklin and Paxinos [41], and the slides were photographed with a Nikon Ci-L (Nikon Instruments, Tokyo, Japan) light microscope; the images were taken with a digital camera Nikon Ds-Ri2 and processed to the final magnification of 800x.

*2.7. Morphometric Evaluation.* Five not serial sections per animal were evaluated for each group. Two experienced investigators, blinded to the experimental group of each animal, independently performed cell counting. The results gave an intraobserver and interobserver variation less than 5%. For hippocampal neurons counts, a region of interest (unit area (UA)) of 0.1 $mm^2$ (316 × 316 $\mu$m) in both the CA1 and CA3 regions was selected for each section; the cells overlapping the left and the bottom boundaries were counted, whereas the cells that touched the right and top boundaries were not included in the evaluation. Criteria for neurons to be counted were well-defined cytoplasm, clearly visible nucleus, and evident nucleolus.

*2.8. Determination of Protein Content.* Total cellular proteins were extracted in a lysis buffer composed of 25 mM Tris-HCl pH 7.4, 1.0 mM ethylene glycol tetraacetic acid (EGTA), 1.0 mM ethylenediaminetetraacetic acid (EDTA), and 0.5 mM phenyl methylsulphonyl fluoride, added with protease and phosphatase inhibitors (100 mM $Na_3VO_4$, aprotinin, leupeptin, and pepstatin (10 $\mu$g/ml each)). After centrifugation of the cell lysate for 15′ at 13000 rpm, the protein concentration was determined from the supernatant by Bio-Rad protein assay (Bio-Rad, Richmond, CA, USA).

*2.9. Malondialdehyde (MDA) and Glutathione (GSH) Determination.* MDA content was determined in all experimental groups with a colorimetric commercial kit (Lipid Peroxidation Assay kit, cat number 437634; Calbiochem-Novabiochem Corp, Darmstadt, Germany), as previously described [42], and expressed in nmol/mg protein. GSH content was also determined in all experimental groups according to the method of Gong et al. [43].

*2.10. Determination of BDNF and mTOR by Western Blot Analysis.* The supernatant was diluted with Laemmli buffer. Protein samples, denatured in reducing buffer (62 mM Tris-HCl pH 6.8, 10% glycerol, 2% SDS, 5% beta-mercaptoethanol, and 0.003% bromophenol blue), were separated by electrophoresis on SDS polyacrylamide gel (6% or 10%), for approximately 1 h. The separated proteins were moved to a PVDF membrane in a transfer buffer (39 mM glycine, 48 mM Tris-HCl (pH 8.3), and 20% methanol) at 200 mA for 1 h. The reaction was blocked with 5% nonfat dry milk in TBS-0.1% Tween-20 for 1 h at room temperature. Membranes were washed three times for 10 min each in TBS-0.1% Tween-20 and incubated with primary antibodies for mTOR (1 : 500 in TBS-0.1% Tween-20; Cell Signaling, Beverly, MA, USA) and BDNF (1 : 1000 in TBS-0.1% Tween-20; Abcam, Cambridge, UK). The following day, the membranes were washed three times for 10 min in TBS-0.1% Tween-20 and were incubated with a specific peroxidase-conjugated secondary antibody (1 : 10.000; KPL, USA) for 1 h at room temperature. After further washings, the membranes were analyzed by enhanced chemiluminescence (KPL, USA). Protein signals were quantified by scanning densitometry with a Bio Image Analysis system (C-DiGit Blot Scanner with Image Studio software), and the results were expressed as relative integrated intensity compared to controls. $\alpha$-Tubulin (Cell Signaling Technology, Beverly, MA, USA) was used to confirm equal protein loading and blotting.

*2.11. Statistical Analysis.* Primary outcome measures were assessment of cognitive performance and neuron morphology. The statistical significance of differences among groups was performed with the ANOVA comparison test, followed by the Bonferroni post hoc test. The MedCalc 12.2.1.0 statistical software (MedCalc Software, Ostend, Belgium) was used. A $p$ value $\leq 0.05$ was considered statistically significant. Values are provided as mean ± standard deviation (SD).

## 3. Results

*3.1. Effects of PDRN on MDA and GSH Content.* The levels of MDA were significantly increased in Cd-challenged mice. The coadministration of $CdCl_2$ and PDRN significantly decreased the levels of MDA in brains (Table 1). On the contrary, a significant decrease in the activity of GSH was observed in Cd-challenged mice. The treatment with PDRN significantly increased GSH levels in brains of Cd-treated mice (Table 1).

*3.2. Effects of PDRN on BDNF and mTOR Brain Expression.* The expression of BDNF was observed in the brain of control mice treated with vehicle or PDRN (Figure 1(a)). $CdCl_2$ caused a marked reduction on BDNF brain expression in mice (Figure 1(a)). Conversely, in mice treated with PDRN, the brain levels of BDNF were significantly higher than in the vehicle-treated $CdCl_2$ group (Figure 1(a)).

Table 1: Malondialdehyde (MDA) and glutathione (GSH) content in mice exposed to cadmium chloride ($CdCl_2$; 2 mg/kg ip) plus vehicle, as compared to mice exposed to $CdCl_2$ (2 mg/kg ip) plus PDRN (8 mg/kg/day ip) or to control mice treated with vehicle or PDRN alone.

| Group | MDA (nmol/mg protein) | GSH ($\mu$mol/g tissue) |
|---|---|---|
| Control + vehicle | $0.13 \pm 0.04$ | $66 \pm 5$ |
| Control + PDRN | $0.12 \pm 0.06$ | $69 \pm 6$ |
| $CdCl_2$ + vehicle | $0.81 \pm 0.31^a$ | $47 \pm 7^a$ |
| $CdCl_2$ + PDRN | $0.20 \pm 0.09^b$ | $64 \pm 3^b$ |

All the values are expressed as mean ± SD, $n = 7$ animals for each group. [a]$p < 0.05$ versus both controls; [b]$p < 0.05$ versus $CdCl_2$ + vehicle.

Low expression of mTOR was observed in the brain of control mice treated with vehicle or PDRN (Figure 1(b)). A higher expression of mTOR was detected in $CdCl_2$-treated animals (Figure 1(b)). mTOR expression was significantly reduced after PDRN administration if compared to mice treated with $CdCl_2$ alone (Figure 1(b)).

*3.3. Brain Edema Assessment.* No differences in brain water content were observed in both controls of hippocampal tissue (Figure 2). $CdCl_2$ challenge caused brain edema in the mouse hippocampus (Figure 2). PDRN treatment showed a significant reduction of brain edema when compared to $CdCl_2$-treated animals (Figure 2).

*3.4. Administration of PDRN Counteracts $CdCl_2$-Induced Neuronal Changes.* In both control groups of mice, CA1 and CA3 hippocampal regions showed normal organization (Figures 3(a), A1, A2, and 3b, B1, B2). In contrast, CA1 and CA3 regions of $CdCl_2$-challenged mice showed evident neuronal loss with degenerating pyramidal cells and interstitial edema (Figure 3(c), C1, C2). PDRN administration significantly reduced neuronal morphological changes in both CA1 and CA3 regions (Figure 3(d), D1, D2). The morphometric analysis showed a significant reduction of neurons in both the CA1 and CA3 regions in $CdCl_2$-challenged mice, which was normalized when PDRN was coadministered (Figure 3(e)).

*3.5. PDRN Enhances Cognitive Performance.* In both controls, a gradual shortening in ELT was observed along the five-consecutive-day trials (Table 2). $CdCl_2$ administration significantly increased ELT when compared with both control groups (Table 2). On the contrary, PDRN administration significantly reduced the time spent by mice to find the platform (Table 2).

## 4. Discussion

Oxidative stress is strongly related to neuroinflammatory mechanisms, so that it is particularly difficult to exert neuroprotective effects on the brain. In addition, glial activation involving astrocytes, microglial cells, and/or reactive mediators and/or growth factors are also hallmarks of inflammatory reaction [44]. This justifies the research strategies that rely on multiple mechanisms involving antiradical scavenging activity and antiapoptotic mechanisms, resulting in increased neuronal proliferation.

Neurotoxic effects may play a key role in the systemic toxic consequences of Cd exposure [45]. Therefore, the mechanism of Cd neurotoxicity should be better clarified, and measures should be taken to reduce Cd exposure in the general population to minimize the risk of adverse human health effects [46]. In this context, we previously demonstrated a positive effect of PDRN, an ADORA2A, which was demonstrated on Cd-induced damages of the blood-testis barrier, suggesting that it should also counteract the role of Cd as an endocrine disruptor [36].

Therefore, our data represent novel findings on the effects of PDRN on the brain, since few information on the molecular pathways involved are currently available.

Indeed, in our *in vivo* experimental model, we observed that mice challenged with $CdCl_2$ alone showed a significant increase of MDA and a decrease of GSH; on the contrary, PDRN administration protected mice against oxidative stress, thus confirming the harmful role of Cd in triggering the lipid peroxidation pathways [36].

Furthermore, an increased expression of mTOR in $CdCl_2$-challenged mice was demonstrated, whereas PDRN administration significantly reduced mTOR expression. This feature strongly suggests that Cd-induced neuronal toxicity is related to induction of ROS, which, in turn, leads to oxidative stress. In fact, it has been recently shown that Cd induces ROS generation in a time- and concentration-dependent manner in PC12 and SH-SY5Y cells [47], causing apoptosis of neuronal cells, particularly via activation of MAPKs and mTOR signaling pathways [12, 14–16, 47].

Accordingly, we observed that PDRN administration significantly increased BDNF levels in mice. It has been shown that BDNF *in vivo* can rescue different types of neurons from ischemic, traumatic, and toxic brain injury [48]. Recent evidences indicate that the protective effect of BDNF in hippocampal neurons against toxicity is mostly mediated by the PI3K and the Ras/MAPK signaling pathways and involves a long-term change in protein synthesis [29].

Moreover, the role of serine/threonine protein kinase mTOR was also considered [49]. In particular, it has been suggested that mTOR affects the translational control of proteins necessary for the formation and functional maturation of dendritic spines [50]. Moreover, it has been proposed that the neuroprotective effect of BDNF is mediated by autophagy through the PI3K/Akt/mTOR pathway [51]. Our results also show that PDRN administration resulted in a significant reduction of brain edema when compared to the water content of $CdCl_2$-treated animals. These effects may be strictly linked with previous explored molecular pathways because it has been suggested that ROS, cytokine overproduction, and neurotrophin reduction are strongly related to brain edema formation in animals challenged with neurotoxic agents [40, 52, 53]. Furthermore, in humans, acute Cd toxicity led to brain intracellular accumulation of the metal with consequent cell dysfunction, blood-brain barrier disruption, and even lethal cerebral edema [54]. It is likely that PDRN can also reinforce the detoxification mechanisms, such as antioxidant systems

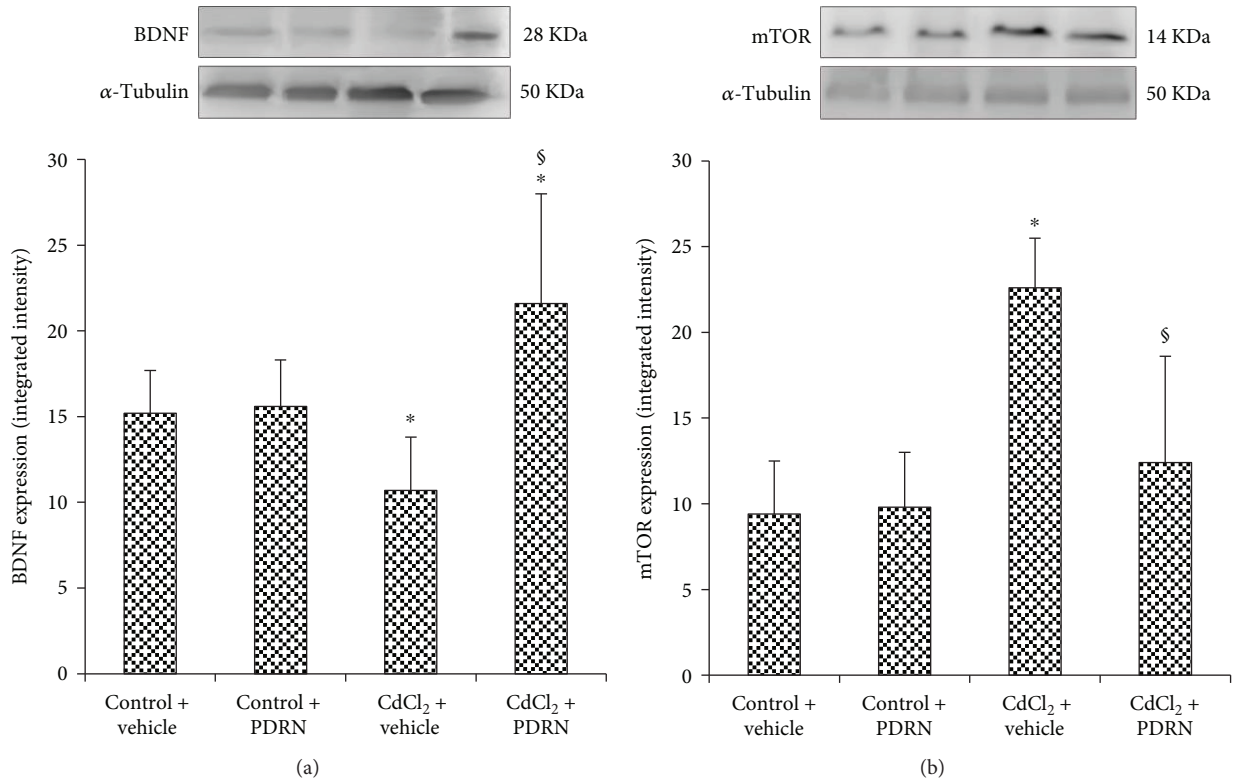


Figure 1: Representative Western blot analysis of BDNF (a) and mTOR (b) in brains of controls and $CdCl_2$- (2 mg/kg ip) challenged mice treated with vehicle or PDRN (8 mg/kg ip), respectively. $^*p < 0.05$ versus both controls; $^§p < 0.05$ versus $CdCl_2$ + vehicle. Bars indicate mea n ± SD of 7 experiments.

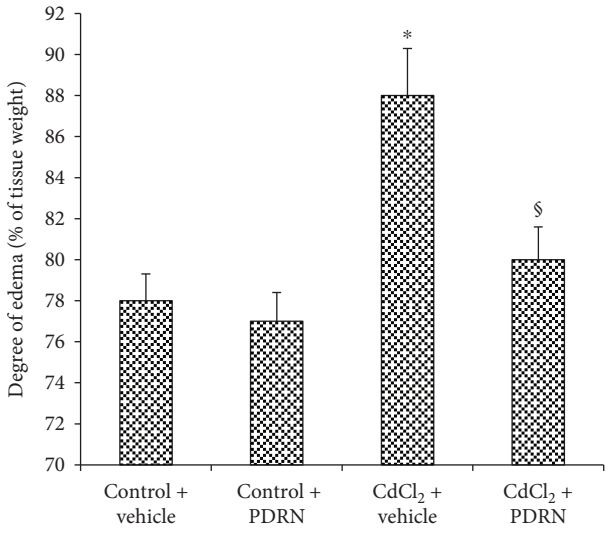


Figure 2: Brain edema evaluated through water content in the hippocampus of controls and $CdCl_2$ (2 mg/kg ip) challenged mice treated with vehicle or PDRN (8 mg/kg ip), respectively. $^*p < 0.05$ versus both controls; $^§p < 0.05$ versus $CdCl_2$ + vehicle. Bars indicate mean ± SD of 7 experiments.

through the induction of protective macromolecules (heat shock proteins, etc.), production of specific metal inclusion bodies or binding proteins, and biotransformation reactions (methylation, conjugation, etc.) localized in the choroid plexus [17]. Accordingly, ADORA2A was highly expressed in the choroid plexus [55].

The biochemical and molecular patterns correlated very well with the histological analysis. In fact, following $CdCl_2$ administration, we observed a significant neuronal loss in both CA1 and CA3 areas, which are susceptible to Cd-induced neurotoxic injury [56]. In contrast, PDRN administration showed significant neuroprotective effects, with a normal number of neurons/UA and structural organization.

Finally, the positive effects of PDRN treatment were also supported in our model by the evidence of a good protection against the behavioral changes that accompanied Cd administration. In fact, PDRN injection significantly improved ELT in mice tested with MWM following $CdCl_2$ challenge. This observation could have a strong translational impact considering that Cd causes learning disabilities and hyperactivity in environmentally exposed children [17] and neurological disorders, such as amyotrophic lateral sclerosis [57], Parkinsonism [58], and Parkinson's and Alzheimer's disease [59], in occupationally exposed subjects.

Taken together, our data suggest that adenosine receptor manipulation/modulation is a pertinent avenue of research for novel strategies in order to modulate neuroinflammatory signal into the brain in diseases characterized by impaired immune response induced by toxic agents.

Moreover, in light of our results, we feel that new environmental research on Cd should take aim at the role of neurotoxicity in causing the health effects following Cd exposure.

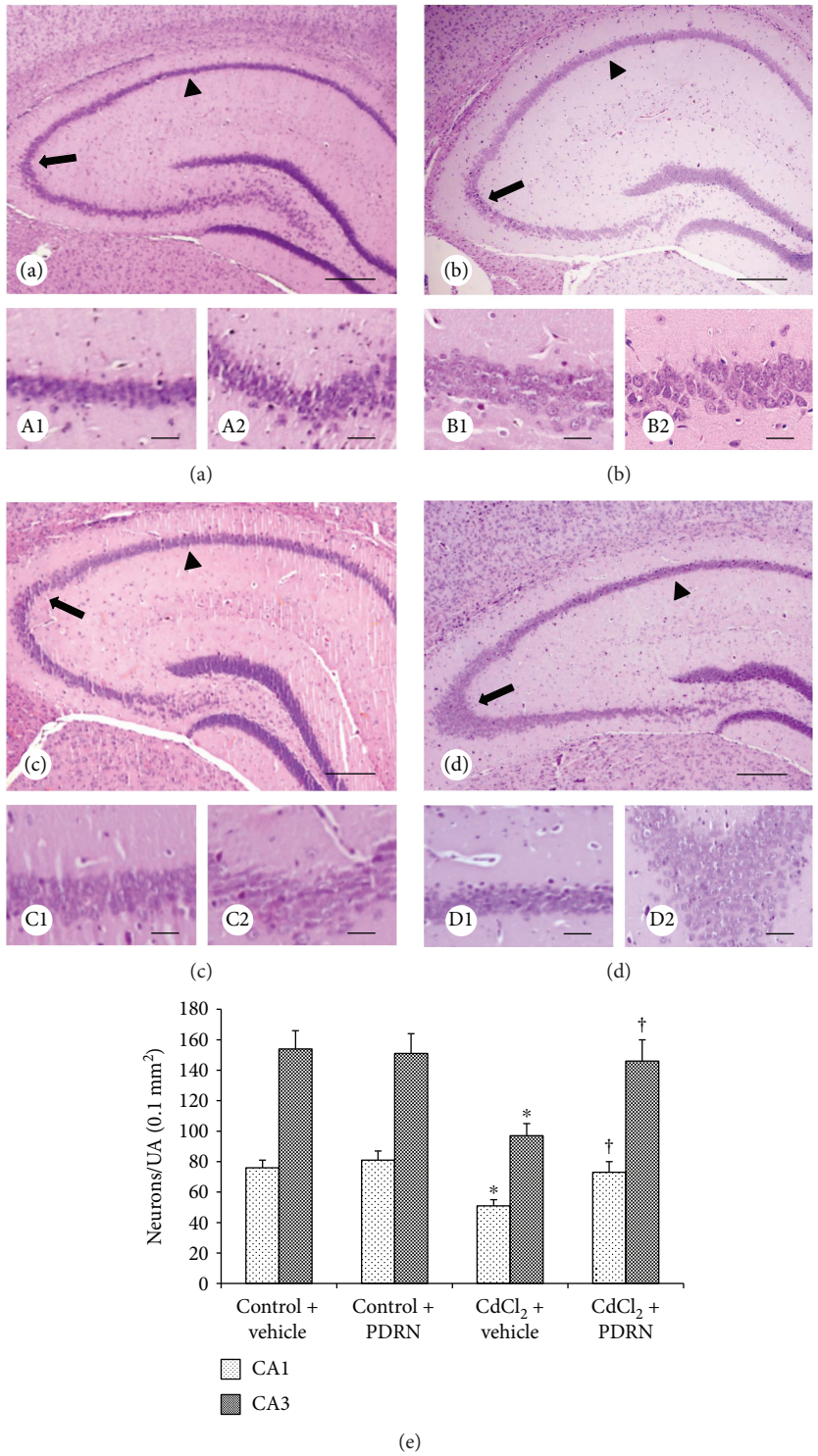


Figure 3: Structural organization of the hippocampus from mice of control plus vehicle (0.9% NaCl, 1 ml/kg/day ip), control plus PDRN (8 mg/kg/day ip), $CdCl_2$ (2 mg/kg/day ip) plus vehicle, and $CdCl_2$ plus PDRN (HE stain). (a, A1, A2, b, B1, B2) In both control plus vehicle and control plus PDRN-treated mice, the normal morphology of the nervous tissue of the hippocampus, particularly in CA1 (arrowhead) and CA3 (arrow) areas, is evident. (c, C1, C2) In $CdCl_2$ plus vehicle-treated mice, neuronal loss and mild edema of the nervous tissue of the hippocampus, particularly in CA1 (arrowhead) and CA3 (arrow) areas, are evident. (d, D1, D2) In $CdCl_2$ plus PDRN-treated mice, the hippocampus and CA1 (arrowhead) and CA3 (arrow) areas in particular show a well-preserved neuronal architecture. (e) Quantitative evaluation of neurons in both CA1 and CA3 regions in the different groups of mice. $^*p < 0.05$ versus both controls; $^\dagger p < 0.05$ versus $CdCl_2$ plus vehicle (scale bar: a, b, c, d = 500 $\mu$m; A1, A2, B1, B2, C1, C2, D1, D2 = 50 $\mu$m).

Table 2: Results obtained from the escape latency time (the time to reach the platform in seconds) evaluated with the Morris water maze test in mice exposed to cadmium chloride ($CdCl_2$; 2 mg/kg/day ip) plus vehicle, as compared to control mice treated with vehicle or PDRN alone or to mice exposed to $CdCl_2$ (2 mg/kg/day ip) plus PDRN (8 mg/kg/day ip).

| Group | Day 1 | Day 2 | Day 3 | Day 4 | Day 5 |
|---|---|---|---|---|---|
| Control + vehicle | 36 ± 2 | 31 ± 3 (13.4%)[a] | 19 ± 2 (47.3%)[a,b] | 14 ± 3 (61.2%)[a,b,c] | 11 ± 2 (69.5%)[a,b,c,d] |
| Control + PDRN | 34 ± 3 | 32 ± 3 (5.9%) | 18 ± 4 (47.1%)[b] | 15 ± 2 (55.9%)[a,b,c] | 12 ± 3 (64.8%)[a,b,c,d] |
| $CdCl_2$ + vehicle | 38 ± 3 | 34 ± 4 (10.5%)[a] | 27 ± 3 (28.9%) [a,b,e] | 22 ± 3 (42.1%) [a,b,c,e] | 20 ± 4 (47.3%)[a,b,c,e] |
| $CdCl_2$ + PDRN | 33 ± 4 | 32 ± 4 (3.1%) | 20 ± 2 (39.4%) [b,f] | 14 ± 4 (57.6%)[a,b,c,f] | 12 ± 2 (63.7%)[a,b,c,f] |

All the values are expressed as mean ± SD, $n = 14$ animals for each group. [a]$p < 0.05$ versus day 1 of the same group; [b]$p < 0.05$ versus day 2 of the same group; [c]$p < 0.05$ versus day 3 of the same group; [d]$p < 0.05$ versus day 4 of the same group; [e]$p < 0.05$ versus both controls at the same day; [f]$p < 0.05$ versus $CdCl_2$ + vehicle at the same day.

Both short- and long-duration epidemiological studies are required to determine the optimal doses of antioxidant products and dietary supplements alone and in combination, to provide safe and effective therapeutic strategies against Cd toxicity. In this context, PDRN, an agonist of ADORA2A, might offer a structural model for the production of new analog compounds (cosmeceuticals, nutraceuticals, and/or phytochemicals) that, properly combined with good agricultural practice to minimize Cd contamination in food crops and animals, could also provide a definite strategy to prevent and counteract severe damages in Cd-induced brain toxicity.

## Abbreviations

$CdCl_2$: Cadmium chloride
ROS: Reactive oxygen species
HE: Hematoxylin and eosin
MAPK: Mitogen-activated protein kinase
MDA: Malondialdehyde
GSH: Glutathione
mTOR: Mammalian target of rapamycin kinase
BDNF: Brain-derived neurotrophic factor
ADORA2A: Adenosine receptor $A_{2A}$
PDRN: Polydeoxyribonucleotide.

## Data Availability

The data used to support the findings of this study are included within the article.

## Disclosure

The paper was published as an abstract in the Proceedings of the Italian Society of Pharmacology, 38th National Meeting, 2017.

## Conflicts of Interest

The authors declare no actual or potential competing financial interests.

## Acknowledgments

The investigation was granted by a departmental funding. The authors thank Mister Sebastiano Brunetto of the Department of Biomedical Sciences, University of Messina, for his dedicated technical expertise.

## References

[1] ATSDR, *Agency for Toxic Substance and Disease Registry*, U.S. Toxicological Profile for Cadmium, Department of Health and Humans Services, Public Health Service, Centers for Disease Control, Atlanta, 2012.

[2] L. Järup and A. Akesson, "Current status of cadmium as an environmental health problem," *Toxicology and Applied Pharmacology*, vol. 238, no. 3, pp. 201–208, 2009.

[3] R. Chunhabundit, "Cadmium exposure and potential health risk from foods in contaminated area, Thailand," *Toxicological Research*, vol. 32, no. 1, pp. 65–72, 2016.

[4] E. López, S. Figueroa, M. J. Oset-Gasque, and M. P. González, "Apoptosis and necrosis: two distinct events induced by cadmium in cortical neurons in culture," *British Journal of Pharmacology*, vol. 138, no. 5, pp. 901–911, 2003.

[5] S. S. Habeebu, Y. Liu, J. D. Park, and C. D. Klaassen, "Strain differences in the toxicity of cadmium to trigeminal ganglia in mice," *Toxicology and Applied Pharmacology*, vol. 177, no. 3, pp. 200–207, 2001.

[6] A. H. Poliandri, J. P. Cabilla, M. O. Velardez, C. C. Bodo, and B. H. Duvilanski, "Cadmium induces apoptosis in anterior pituitary cells that can be reversed by treatment with antioxidants," *Toxicology and Applied Pharmacology*, vol. 190, no. 1, pp. 17–24, 2003.

[7] W. Wätjen and D. Beyersmann, "Cadmium-induced apoptosis in C6 glioma cells: influence of oxidative stress," *BioMetals*, vol. 17, no. 1, pp. 65–78, 2004.

[8] N. Sugawara, K. Aoshima, and M. Kasuya, "Effect of cadmium chloride and Cd-metallothionein on the nervous tissue culture," *Toxicology Letters*, vol. 16, no. 1-2, pp. 95–101, 1983.

[9] W. S. Webster and A. A. Valois, "The toxic effects of cadmium on the neonatal mouse CNS," *Journal of Neuropathology and Experimental Neurology*, vol. 40, no. 3, pp. 247–257, 1981.

[10] H. Carageorgiou, V. Tzotzes, C. Pantos, C. Mourouzis, A. Zarros, and S. Tsakiris, "In vivo and in vitro effects of cadmium on adult rat brain total antioxidant status, acetylcholinesterase, (Na+, K+)-ATPase and Mg2+-ATPase activities: protection by L-cysteine," *Basic & Clinical Pharmacology & Toxicology*, vol. 94, no. 3, pp. 112–118, 2004.

[11] N. Demir, G. Akkoyunlu, P. Yargicoglu, A. Agar, G. Tanriöver, and R. Demir, "Fiber structure of optic nerve in cadmium-exposed diabetic rats: an ultrastructural study," *The International Journal of Neuroscience*, vol. 113, no. 3, pp. 323–337, 2009.

[12] J. Liu, W. Qu, and M. B. Kadiiska, "Role of oxidative stress in cadmium toxicity and carcinogenesis," *Toxicology and Applied Pharmacology*, vol. 238, no. 3, pp. 209–214, 2009.

[13] E. M. Jeong, C. H. Moon, C. S. Kim et al., "Cadmium stimulates the expression of ICAM-1 via NF-κB activation in cerebrovascular endothelial cells," *Biochemical and Biophysical Research Communications*, vol. 320, no. 3, pp. 887–892, 2004.

[14] W. Qu, H. Ke, J. Pi et al., "Acquisition of apoptotic resistance in cadmium-transformed human prostate epithelial cells: Bcl-2 overexpression blocks the activation of JNK signal transduction pathway," *Environmental Health Perspectives*, vol. 115, no. 7, pp. 1094–1100, 2007.

[15] Y. Yuan, Y. Wang, F. F. Hu et al., "Cadmium activates reactive oxygen species-dependent AKT/mTOR and mitochondrial apoptotic pathways in neuronal cells," *Biomedical and Environmental Sciences*, vol. 29, no. 2, pp. 117–126, 2016.

[16] L. Chen, B. Xu, L. Liu et al., "Cadmium induction of reactive oxygen species activates the mTOR pathway, leading to neuronal cell death," *Free Radical Biology & Medicine*, vol. 50, no. 5, pp. 624–632, 2011.

[17] B. Wang and Y. Du, "Cadmium and its neurotoxic effects," *Oxidative Medicine and Cellular Longevity*, vol. 2013, Article ID 898034, 12 pages, 2013.

[18] N. E. Al Omairi, O. K. Radwan, Y. A. Alzahrani, and R. B. Kassab, "Neuroprotective efficiency of Mangifera indica leaves extract on cadmium-induced cortical damage in rats," *Metabolic Brain Disease*, vol. 33, no. 4, pp. 1121–1130, 2018.

[19] D. K. Binder and H. E. Scharfman, "Brain-derived neurotrophic factor," *Growth Factors*, vol. 22, no. 3, pp. 123–131, 2009.

[20] A. Acheson, J. C. Conover, J. P. Fandl et al., "A BDNF autocrine loop in adult sensory neurons prevents cell death," *Nature*, vol. 374, no. 6521, pp. 450–453, 1995.

[21] E. J. Huang and L. F. Reichardt, "Neurotrophins: roles in neuronal development and function," *Annual Review of Neuroscience*, vol. 24, no. 1, pp. 677–736, 2001.

[22] P. C. Maisonpierre, M. M. le Beau, R. Espinosa III et al., "Human and rat brain-derived neurotrophic factor and neurotrophin-3: gene structures, distributions, and chromosomal localizations," *Genomics*, vol. 10, no. 3, pp. 558–568, 1991.

[23] C. V. Gomes, M. P. Kaster, A. R. Tomé, P. M. Agostinho, and R. A. Cunha, "Adenosine receptors and brain diseases: neuroprotection and neurodegeneration," *Biochimica et Biophysica Acta (BBA) - Biomembranes*, vol. 1808, no. 5, pp. 1380–1399, 2011.

[24] S. J. Jeon, S. Y. Rhee, J. H. Ryu et al., "Activation of adenosine A2A receptor up-regulates BDNF expression in rat primary cortical neurons," *Neurochemical Research*, vol. 36, no. 12, pp. 2259–2269, 2011.

[25] M. J. Diógenes, C. C. Fernandes, A. M. Sebastião, and J. A. Ribeiro, "Activation of adenosine A2A receptor facilitates brain-derived neurotrophic factor modulation of synaptic transmission in hippocampal slices," *Journal of Neuroscience*, vol. 24, no. 12, pp. 2905–2913, 2004.

[26] M. T. Tebano, A. Martire, R. L. Potenza et al., "Adenosine A(2A) receptors are required for normal BDNF levels and BDNF-induced potentiation of synaptic transmission in the mouse hippocampus," *Journal of Neurochemistry*, vol. 104, no. 1, pp. 279–286, 2008.

[27] B. M. Fontinha, M. J. Diógenes, J. A. Ribeiro, and A. M. Sebastião, "Enhancement of long-term potentiation by brain-derived neurotrophic factor requires adenosine A2A receptor activation by endogenous adenosine," *Neuropharmacology*, vol. 54, no. 6, pp. 924–933, 2008.

[28] S. C. Borrie, H. Brems, E. Legius, and C. Bagni, "Cognitive dysfunctions in intellectual disabilities: the contributions of the Ras-MAPK and PI3K-AKT-mTOR pathways," *Annual Review of Genomics and Human Genetics*, vol. 18, no. 1, pp. 115–142, 2017.

[29] R. J. Shaw and L. C. Cantley, "Ras, PI(3)K and mTOR signalling controls tumour cell growth," *Nature*, vol. 441, no. 7092, pp. 424–430, 2006.

[30] Y. W. Liu, T. Yang, L. Zhao et al., "Activation of adenosine 2A receptor inhibits neutrophil apoptosis in an autophagy-dependent manner in mice with systemic inflammatory response syndrome," *Scientific Reports*, vol. 6, no. 1, article 33614, 2016.

[31] D. Altavilla, A. Bitto, F. Polito et al., "Polydeoxyribonucleotide (PDRN): a safe approach to induce therapeutic angiogenesis in peripheral artery occlusive disease and in diabetic foot ulcers," *Cardiovascular & Hematological Agents in Medicinal Chemistry*, vol. 7, no. 4, pp. 313–321, 2009.

[32] L. Minutoli, S. Arena, G. Bonvissuto et al., "Activation of adenosine A2A receptors by polydeoxyribonucleotide increases vascular endothelial growth factor and protects against testicular damage induced by experimental varicocele in rats," *Fertility and Sterility*, vol. 95, no. 4, pp. 1510–1513, 2011.

[33] D. Altavilla, F. Squadrito, F. Polito et al., "Activation of adenosine A2A receptors restores the altered cell-cycle machinery during impaired wound healing in genetically diabetic mice," *Surgery*, vol. 149, no. 2, pp. 253–261, 2011.

[34] L. Minutoli, P. Antonuccio, F. Squadrito et al., "Effects of polydeoxyribonucleotide on the histological damage and the altered spermatogenesis induced by testicular ischaemia and reperfusion in rats," *International Journal of Andrology*, vol. 35, no. 2, pp. 133–144, 2012.

[35] L. Minutoli, S. Arena, P. Antonuccio et al., "Role of inhibitors of apoptosis proteins in testicular function and male fertility: effects of polydeoxyribonucleotide administration in experimental varicocele," *BioMed Research International*, vol. 2015, Article ID 248976, 9 pages, 2015.

[36] F. Squadrito, A. Micali, M. Rinaldi et al., "Polydeoxyribonucleotide, an adenosine-A2A receptor agonist, preserves blood testis barrier from cadmium-induced injury," *Frontiers in Pharmacology*, vol. 7, 2017.

[37] https://grants.nih.gov/grants/olaw/guide-for-the-care-and-use-of-laboratory-animals.pdf.

[38] http://ec.europa.eu/environment/chemicals/lab_animals/legislation_en.htm.

[39] C. V. Vorhees and M. T. Williams, "Morris water maze: procedures for assessing spatial and related forms of learning and memory," *Nature Protocols*, vol. 1, no. 2, pp. 848–858, 2006.

[40] L. Minutoli, H. Marini, M. Rinaldi et al., "A dual inhibitor of cyclooxygenase and 5-lipoxygenase protects against kainic acid-induced brain injury," *Neuromolecular Medicine*, vol. 17, no. 2, pp. 192–201, 2015.

[41] K. B. J. Franklin and G. Paxinos, *The Mouse Brain in Stereotaxic Coordinates*, Elsevier, Amsterdam, 3rd edition, 2007.

[42] L. Minutoli, A. Micali, A. Pisani et al., "Research article flavocoxid protects against cadmium-induced disruption of the blood-testis barrier and improves testicular damage and germ cell impairment in mice," *Toxicological Sciences*, vol. 148, no. 1, pp. 311–329, 2015.

[43] P. Gong, F. Chen, X. Liu, X. Gong, J. Wang, and Y. Ma, "Protective effect of caffeic acid phenethyl ester against cadmium-induced renal damage in mice," *The Journal of Toxicological Sciences*, vol. 37, no. 2, pp. 415–425, 2012.

[44] R. Ientile, M. Currò, and D. Caccamo, "Transglutaminase 2 and neuroinflammation," *Amino Acids*, vol. 47, no. 1, pp. 19–26, 2015.

[45] M. Rinaldi, A. Micali, H. Marini et al., "Cadmium, organ toxicity and therapeutic approaches: a review on brain, kidney and testis damage," *Current Medicinal Chemistry*, vol. 24, no. 35, pp. 3879–3893, 2017.

[46] M. Rizwan, S. Ali, M. Adrees et al., "A critical review on effects, tolerance mechanisms and management of cadmium in vegetables," *Chemosphere*, vol. 182, pp. 90–105, 2017.

[47] L. Chen, L. Liu, Y. Luo, and S. Huang, "MAPK and mTOR pathways are involved in cadmium-induced neuronal apoptosis," *Journal of Neurochemistry*, vol. 105, no. 1, pp. 251–261, 2008.

[48] M. G. Lykissas, A. K. Batistatou, K. A. Charalabopoulos, and A. E. Beris, "The role of neurotrophins in axonal growth, guidance, and regeneration," *Current Neurovascular Research*, vol. 4, no. 2, pp. 143–151, 2007.

[49] M. Laplante and D. M. Sabatini, "mTOR signaling in growth control and disease," *Cell*, vol. 149, no. 2, pp. 274–293, 2012.

[50] N. Takei and H. Nawa, "mTOR signaling and its roles in normal and abnormal brain development," *Frontiers in Molecular Neuroscience*, vol. 7, 2014.

[51] S.-D. Chen, C.-L. Wu, W.-C. Hwang, and D.-I. Yang, "More insight into BDNF against neurodegeneration: anti-apoptosis, anti-oxidation, and suppression of autophagy," *International Journal of Molecular Sciences*, vol. 18, no. 3, 2017.

[52] H. Marini, D. Altavilla, M. Bellomo et al., "Modulation of IL-1 $\beta$ gene expression by lipid peroxidation inhibition after kainic acid-induced rat brain injury," *Experimental Neurology*, vol. 188, no. 1, pp. 178–186, 2004.

[53] H. Marini, C. Costa, M. Passaniti et al., "Levetiracetam protects against kainic acid-induced toxicity," *Life Sciences*, vol. 74, no. 10, pp. 1253–1264, 2004.

[54] J. P. Provias, C. A. Ackerley, C. Smith, and L. E. Becker, "Cadmium encephalopathy: a report with elemental analysis and pathological findings," *Acta Neuropathologica*, vol. 88, no. 6, pp. 583–586, 1994.

[55] J. H. Mills, D. G. Kim, A. Krenz, J. F. Chen, and M. S. Bynoe, "A2A adenosine receptor signaling in lymphocytes and the central nervous system regulates inflammation during experimental autoimmune encephalomyelitis," *Journal of Immunology*, vol. 188, no. 11, pp. 5713–5722, 2012.

[56] S. WANG, P. HU, H. WANG et al., "Effects of Cd(2+) on AMPA receptor-mediated synaptic transmission in rat hippocampal CA1 area," *Toxicology Letters*, vol. 176, no. 3, pp. 215–222, 2008.

[57] S. Bar-Sela, S. Reingold, and E. D. Richter, "Amyotrophic lateral sclerosis in a battery-factory worker exposed to cadmium," *International Journal of Occupational and Environmental Health*, vol. 7, no. 2, pp. 109–112, 2001.

[58] B. Okuda, Y. Iwamoto, H. Tachibana, and M. Sugita, "Parkinsonism after acute cadmium poisoning," *Clinical Neurology and Neurosurgery*, vol. 99, no. 4, pp. 263–265, 1997.

[59] M. Chin-Chan, J. Navarro-Yepes, and B. Quintanilla-Vega, "Environmental pollutants as risk factors for neurodegenerative disorders: Alzheimer and Parkinson diseases," *Frontiers in Cellular Neuroscience*, vol. 9, 2015.

Hindawi
Oxidative Medicine and Cellular Longevity
Volume 2018, Article ID 7878050, 11 pages
https://doi.org/10.1155/2018/7878050

*Research Article*

# Hippocampal Dysfunction Provoked by Mercury Chloride Exposure: Evaluation of Cognitive Impairment, Oxidative Stress, Tissue Injury and Nature of Cell Death

**Walessa Alana Bragança Aragão,[1] Francisco Bruno Teixeira,[1] Nathalia Carolina Fernandes Fagundes,[1] Rafael Monteiro Fernandes,[1] Luanna Melo Pereira Fernandes,[2] Márcia Cristina Freitas da Silva,[1] Lilian Lund Amado,[3] Fernanda Espírito Santo Sagica,[4] Edivaldo Herculano Correa Oliveira,[4] Maria Elena Crespo-Lopez,[5] Cristiane Socorro Ferraz Maia,[2] and Rafael Rodrigues Lima[1]**

[1]*Laboratory of Functional and Structural Biology, Institute of Biological Sciences, Federal University of Pará, Belém, PA, Brazil*
[2]*Laboratory of Pharmacology of Inflammation and Behavior, Institute of Health Sciences, Federal University of Pará, Belém, PA, Brazil*
[3]*Laboratory of Ecotoxicology, Institute of Biological Sciences, Federal University of Pará, Belém, PA, Brazil*
[4]*Laboratory of Tissue Culture and Cytogenetics, Evandro Chagas Institute, Ananindeua, PA, Brazil*
[5]*Laboratory of Molecular Pharmacology, Institute of Biological Sciences, Federal University of Pará, Belém, PA, Brazil*

Correspondence should be addressed to Rafael Rodrigues Lima; rafalima@ufpa.br

Received 22 November 2017; Revised 31 January 2018; Accepted 21 February 2018; Published 10 April 2018

Academic Editor: Julia Bornhorst

Copyright © 2018 Walessa Alana Bragança Aragão et al. This is an open access article distributed under the Creative Commons Attribution License, which permits unrestricted use, distribution, and reproduction in any medium, provided the original work is properly cited.

Mercury (Hg) is a highly toxic metal, which can be found in its inorganic form in the environment. This form presents lower liposolubility and lower absorption in the body. In order to elucidate the possible toxicity of inorganic Hg in the hippocampus, we investigated the potential of low doses of mercury chloride ($HgCl_2$) to promote hippocampal dysfunction by employing a chronic exposure model. For this, 56 rats were exposed to $HgCl_2$ (0.375 mg/kg/day) via the oral route for 45 days. After the exposure period, the animals were submitted to the cognitive test of fear memory. The hippocampus was collected for the measurement of total Hg levels, analysis of oxidative stress, and evaluation of cytotoxicity, apoptosis, and tissue injury. It was observed that chronic exposure to inorganic Hg promotes an increase in mercury levels in this region and damage to short- and long-term memory. Furthermore, we found that this exposure model provoked oxidative stress, which led to cytotoxicity and cell death by apoptosis, affecting astrocytes and neurons in the hippocampus. Our study demonstrated that inorganic Hg, even with its low liposolubility, is able to produce deleterious effects in the central nervous system, resulting in cognitive impairment and hippocampal damage when administered for a long time at low doses in rats.

## 1. Introduction

Mercury (Hg) represents the third most toxic element on the planet, according to the US Government Agency for Toxic Substances and Disease Registry [1]. Three forms of Hg can occur in the environment: organic Hg, elemental Hg, and inorganic Hg [2].

Organic Hg is one of the most toxic substances, with the highest number of studies dealing with their effects on human health [2–5]. It is known that organic Hg has a high

capacity to cross cellular membranes. After ingestion, it can pass through the blood-brain barrier and be metabolized to inorganic Hg, which is therefore present at low doses in the central nervous system (CNS) [1, 2, 6].

Human populations throughout the world are chronically exposed to different species of Hg compounds [7–10]. Amazonian populations, for example, are exposed to Hg vapor due to the use of this metal in artisanal processes and small-scale gold mining [7, 8]. Additionally, because of the contaminated environment, populations living downstream of the mining areas or near dams (large-scale projects that may concentrate Hg in the environment) are exposed to both organic and inorganic mercury [8, 10]. The latter exposure is predominantly via the oral route due to contaminated food (mainly piscivorous fish) [11]. Once inside the human body, cells of CNS origin are able to accumulate organic mercury and partially transform it to inorganic mercury [6].

Although the additional effects of Hg intoxication (such as cardiovascular alterations and genotoxicity) are still being described, neurological symptoms are the main deleterious consequences of intoxication by this metal. These include alterations of motor coordination, progressive deterioration of visual and tactile senses, and paralysis, among others. Recent studies in both animals and humans also point to altered cognitive function, especially in memory and learning performance, caused by Hg exposure [12, 13].

The hippocampus is responsible for consolidating two types of memory, storage and recall of events. One of the memory types is aversive memory, related to emotions and reactions of fear and alertness, presenting the hippocampus and amygdala as regulatory areas [14]. The biochemical events occur at neural transmission routes, in which the hippocampus represents an area of huge importance in cognitive and behavioral analysis [14].

In the hippocampus, previous studies verified the presence of increased levels of Hg in the neural parenchyma after chronic exposure to $HgCl_2$ [15], showing that Hg presents less tropism for the hippocampus when compared to the motor cortex. However, the tropism was sufficient to provoke a mnemonic dysfunction.

Based on this, we selected the cerebral hippocampal area for other analyses, aiming to study whether chronic exposure to inorganic Hg is capable of generating cognitive alterations and/or biochemical modulation, tissue damage, and cell death in the hippocampus of adult rats.

## 2. Materials and Methods

*2.1. Ethics Statement.* Experiments followed the protocol approved by the Ethics Committee on the use of animals (CEUA, Federal University of Pará, Protocol BIO139-13). They are in accordance with the NIH Guide for the Care and Use of Laboratory Animals and national law for laboratory experimentation [16].

*2.2. Animals and Experimental Groups.* Male Wistar rats ($n = 56$; 90 days old) from the Federal University of Pará (UFPA) animal facility were kept in collective cages (five animals per cage). The climate and light-controlled room was provided via a 12 h reverse light/dark cycle (lights on 7:00 a.m.), and animals received food and water ad libitum. Distilled water or $HgCl_2$ (0.375 mg/kg/day; $n = 20$ per group) was orally administered by gavage over a period of 45 days, according to a procedure previously described by Teixeira et al. [15]. Animals were weighed weekly for $HgCl_2$ dose adjustment.

*2.3. Behavioral Assay: Step-Down Inhibitory Avoidance.* After 24 h of $HgCl_2$ or distilled water administration, animals ($n = 14$ per group) were taken to the behavioral test room for 1 h (acclimation), with controlled noise levels and illumination (12 lux). The step-down inhibitory avoidance apparatus (EP104R, Insight, Brazil) consists of an acrylic box ($50 \times 25 \times 25$ cm) with parallel stainless steel bars (1 mm in diameter), a floor connected to an electrical stimulator, and a secure platform (7 cm wide × 2.5 cm high) situated against the left wall.

Briefly, the animals were placed in the platform and were free to explore the apparatus for 3 minutes in a habituation session. Twenty-four hours later, the training session was conducted in which each animal was reintroduced to the secure place and the latency of stepping down onto the floor with all four paws was recorded (cut-off 180 s). Immediately after the animal step-down response onto the grid floor, a foot shock of 0.4 mA for 1 s was performed. In the sequence, the rats were removed from the inhibitory avoidance equipment, and after 1.5 h and 24 h, they were subjected to the short- and long-term memory test sessions, respectively [17].

*2.4. Mercury Levels in the Hippocampus.* To validate the exposure to $HgCl_2$ and tissue levels compatible with the dose/time of administration, after the behavioral test, the animals ($n = 7$ per group) were euthanized and each hippocampus sample was weighed (0.5 g maximum of wet weight) in a sample digestion bottle. Then, 1 mL of distilled water, 2 mL of nitric acid-perchloric acid with $HNO_3$-$HClO_4$ (equal proportions), and 5 mL of sulfuric acid ($H_2SO_4$) were sequentially added, followed by heat treatment on a hot plate (200–230°C) for 30 min. Total Hg content in the samples was estimated by wet digestion, reduction, and cold vapor atomic absorption spectrometry (CVAAS) (semi-automated mercury analyzer, model Hg-201, Sanso Seisakusho Co. Ltd., Tokyo, Japan). The circulation-open airflow system was performed as previously described by Suzuki et al. [18]. The detection limit of the equipment for total Hg determination was $0.001\ mg{\cdot}kg^{-1}$, and the limit of quantification was $0.010\ mg{\cdot}kg^{-1}$. The results of the analyses of the samples were expressed in $\mu g/g$. The obtained data were tabulated and later submitted to the inferential statistical treatment. The detailed methodology of this analysis is described in a previously published work [15].

*2.5. Oxidative Stress.* For this analysis, seven animals per group were euthanized by cervical dislocation. The hippocampus was collected and processed for biochemical assays. These animals were not submitted to the inhibitory avoidance equipment. The parameters evaluated were antioxidant capacity against peroxyl radicals (ACAP), evaluated

through reactive oxygen species (ROS) determination in tissue samples treated or not with a peroxyl radical generator, by fluorimeter [19]; lipid peroxidation (LPO, using malondialdehyde—MDA—as an indicator); and nitrite levels (an indirect marker of nitric oxide production) by spectrophotometry, as previously described [20, 21]. For total protein evaluation, the method proposed by Bradford was used [22]. The results were expressed as percentages of the control groups.

*2.6. Assessment and Quantification of Cytotoxicity and Apoptosis.* In these assessments, animals ($n = 7$ per group) were euthanized by cervical dislocation and the hippocampus was dissected and treated with collagenase at a concentration of 2 mg/mL and 4 mg/mL and stored at 37°C for 20 minutes and 40 minutes, respectively, in order to dissociate the tissues (these animals were not submitted to inhibitory avoidance equipment). Thereafter, 100 mL of solution containing the isolated cells was added to 96-well microplates with 100 $\mu$L of the CytoTox-Glo™ Cytotoxicity Assay. This assay uses a luminogenic peptide substrate to measure dead-cell protease activity or Caspase-Glo® 3/7 Assay Systems, a luminescent assay to measure caspase-3/7 activities (Promega, The Netherlands). Readings were performed in a GloMax® (Promega, The Netherlands) according to the manufacturer's recommendations. The quantification results were expressed as percentages of relative fluorescence units (RFU) or relative light units (RLU) relative to the control group, for cytotoxicity and apoptosis, respectively.

*2.7. Histological Evaluation*

*2.7.1. Perfusion and Histological Procedures.* After behavioral assays, the remaining animals ($n = 7$ per group) were deeply anesthetized with ketamine hydrochloride (90 mg/kg, i.p.) and xylazine hydrochloride (10 mg/kg, i.p.), and transcardially perfused with heparinized 0.9% saline solution followed by 4% paraformaldehyde in 0.2 M phosphate buffer. Surgical manipulation was performed only after both the corneal and the paw withdraw reflexes were abolished. Brains were removed from the skull and postfixed for 6 h in Bouin solution. After postfixation, the brain tissue was embedded in paraplast (Monoject Scientific, Athy, Ireland) and sectioned on a microtome at 7 $\mu$m thick and mounted in silanized slides. The coronal sections containing the anterior hippocampus were located at −3.60 mm posterior to Bregma [23].

*2.7.2. Immunohistochemistry.* Sections of 7 $\mu$m were submitted to immunohistochemistry analysis. The immunohistochemical procedures were described in our previous investigations [23, 24]. Briefly, the slides were dewaxed in xylol and hydrated at increasing concentrations of ethanol. Antigenic recovery was performed with citrate buffer at pH 6.0. In order to improve labeling intensity, sections were treated with 0.2 M boric acid (pH 9.0), previously heated to 65°C for 25 min. The temperature was maintained constant over the treatment period. Sections were kept at room temperature for 20 min to decrease the temperature and incubated under constant agitation in a 1% hydrogen peroxide solution in methanol for 20 min. The sections were rinsed in 0.05% PBS/Tween (Sigma Company, USA) solution for 5 min three times and incubated with 10% normal horse serum (NeuN) and goat serum (GFAP) in PBS for 1 h. Without further rinsing, sections were incubated overnight with the primary antibody in PBS, NeuN (1 : 500, Miliporere, USA) and GFAP (1 : 1000, Sigma, USA), rinsed in PBS/Tween solution for 5 min (3 times), and incubated with biotinylated horse anti-mouse (NeuN antibody) and goat anti-rabbit (GFAP), secondary antibodies (Vector Laboratories, USA) diluted at 1 : 500 in PBS for 2 h. As a negative control, normal serum, rather than primary antibody, was used in some sections.

Sections were rinsed again for 5 min (three times) and incubated in the avidin-biotin-peroxidase complex (ABC Kit, Vector Laboratories, USA) for 2 h. Sections were rinsed four times (5 min each) and revealed with diaminobenzidine (DAB). After the DAB reaction, sections were rinsed twice (5 min each) in 0.1 M PB, dehydrated, and cover-slipped with Entellan (Merck, Germany). For more details of this methodology, see [25, 26].

*2.7.3. Morphometric Analyses.* For this quantification, a graticule (1 $mm^2$) attached to the eyepiece (objective 40x, Nikon, Eclipse E200, USA) was used to count three fields per section and three sections per animal in CA1, CA3, and hilus, as described previously [17] and illustrated in Figure 1. NeuN-positive cells corresponding to mature neurons and GFAP-positive cells corresponding to astrocytes were counted. Illustrative images from all experimental groups were obtained with a digital camera (Moticam 2500, USA) attached to a microscope (Nikon, Eclipse 50i, USA).

*2.8. Statistical Analysis.* All values were tabulated and expressed as mean ± SEM ($n = 14$ animals per group in behavioral test and $n = 7$ per group in other analysis) and analyzed for normality using the Shapiro-Wilk test. To analyze body weight, we performed the one-way ANOVA test for repeated measures. Statistical comparisons between groups were performed using the Student's $t$-test. Values of $p \leq 0.05$ were considered statistically significant. GraphPad Prism 5.0 (San Diego, CA, USA) software was used to perform statistical analyses.

The methods are summarized in Figure 1.

## 3. Results

*3.1. Chronic $HgCl_2$ Exposure Did Not Alter the Body Weight in Rats.* After 45 days of $HgCl_2$ exposure, the body weight of control (278.1 ± 2.08 g) and $HgCl_2$-exposed animals (281.3 ± 3.00 g) did not differ statistically ($p = 0.38$), as illustrated in Figure 2.

*3.2. $HgCl_2$ Exposure in Rats Displays Cognitive Deficits.* Chronic exposure by inorganic Hg during adult life impairs both short- and long-term memory in the inhibitory avoidance task Figure 3. These results were represented by a reduction in the step-down latency after 1.5 h training session in the animals exposed to Hg (5.60 ± 1.10 s) when compared to control (77.60 ± 22.48 s; $p < 0.0001$), as well

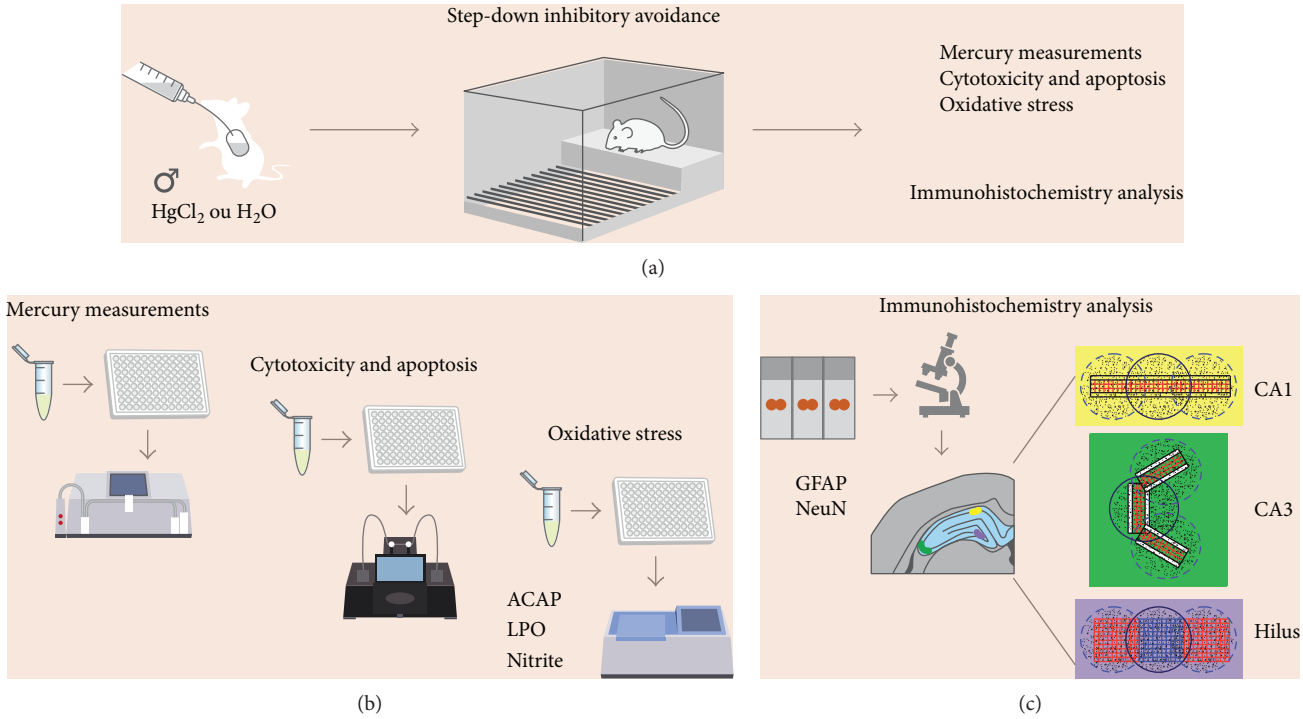


Figure 1: Sample description and experimental stages. Description of the sample and model of exposure to $HgCl_2$; step-down inhibitory avoidance test; division of experimental groups and animal destinations for each stage of analysis (a); total Hg measurement assay, evaluation and quantification of cytotoxicity and apoptosis, and oxidative balance assays (b); immunohistochemistry and morphometric analysis (c).

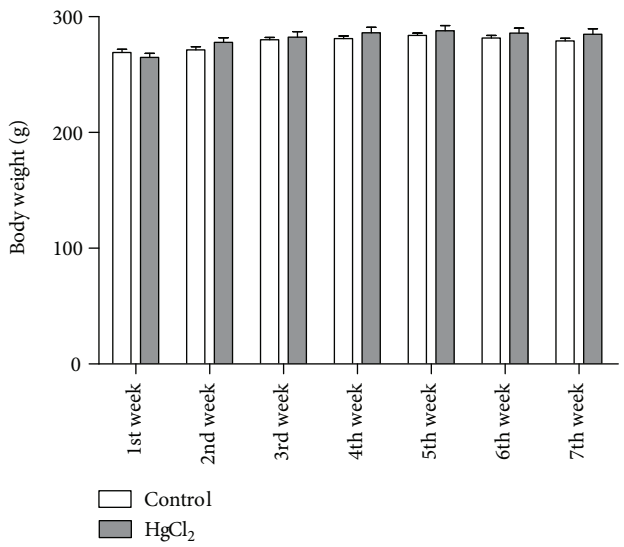


Figure 2: The effects of chronic exposure to $HgCl_2$ on body weight of adult Wistar rats (g). Results are expressed as mean ± standard error after the two-way ANOVA analysis.

as after the 24 h training session, in which the exposed animals (9.30 ± 1.77 s) presented lower values when compared to control (93.11 ± 22.20 s; $p < 0.0001$).

*3.3. Analysis of Total Hg Levels Revealed the Presence of Metal in the Hippocampus after Chronic Exposure to $HgCl_2$ in Rats.* The Hg levels in the hippocampus of control animals (0.0024 ± 0.0008 $\mu$g/g) differ significantly from exposed animals (0.0404 ± 0.0026 $\mu$g/g; $p < 0.0001$). Figure 4 displays the Hg levels in the hippocampus of rats after 45 days of intoxication, in $\mu$g/g.

*3.4. Chronic $HgCl_2$ Exposure Reduces Antioxidant Capacity against Peroxyl Radicals and Increases Nitrite Levels and Lipid Peroxidation in the Hippocampus of Rats.* The $HgCl_2$ exposure decreases the antioxidant capacity against peroxyl radicals in the hippocampus of exposed animals (41.76 ± 7.68%) when compared to control animals (100 ± 16.01%; $p = 0.0035$; Figure 5(a)). Moreover, the chronic exposure with $HgCl_2$ increased levels of prooxidant parameters, as evidenced by the increased levels of malondialdehyde (lipid peroxidation) in exposed animals (140.1 ± 6.08%), in comparison with the control group (100 ± 7.57%; $p = 0.0028$; Figure 5(b)). The same situation was registered in nitrite levels ($HgCl_2$ = 200.9 ± 9.98%, control = 100 ± 7.25%; $p = 0.0003$; Figure 5(c)).

*3.5. Chronic $HgCl_2$ Exposure Led to Cytotoxicity and Cell Death by Apoptosis.* The $HgCl_2$ chronic exposure induced cytotoxicity in the hippocampus of exposed animals (121.9 ± 3.39% RFU) when compared to the control animals (100 ± 0.39% RFU; $p = 0.0028$; Figure 6(a)). Besides, the induction of apoptosis was increased in exposed animals (268.1 ± 21.00% RLU) when compared to control (100 ± 4.29% RLU; $p < 0.0001$; Figure 6(b)).

*3.6. Chronic $HgCl_2$ Exposure Reduces the Number of Astrocytes in the Hippocampus.* The $GFAP^+$ cells in the hippocampus were affected by chronic $HgCl_2$ exposure, as indicated by a

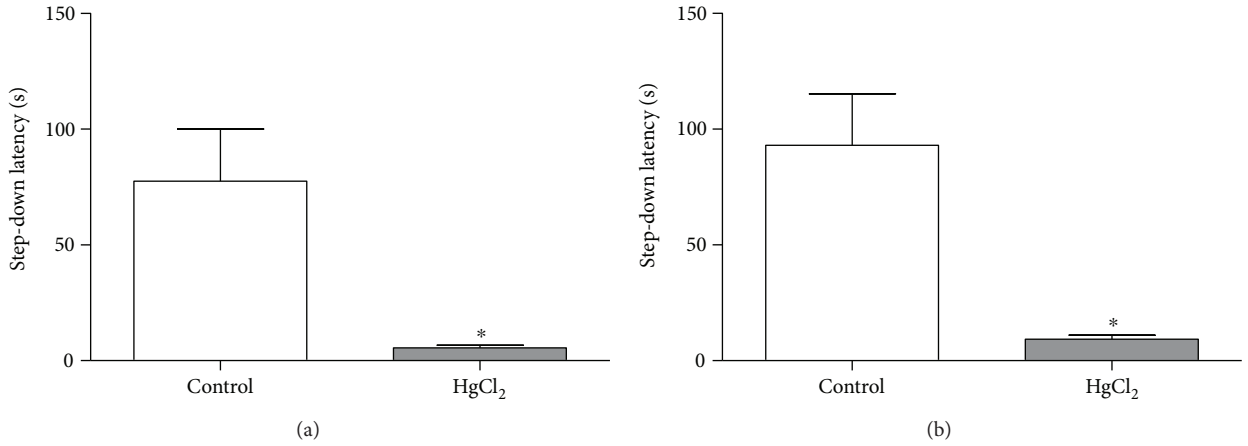


FIGURE 3: The effects of $HgCl_2$ exposure (0.375 mg/kg/day) for 45 days on the short- and long-term memory of male Wistar rats evaluated in step-down inhibitory avoidance. The results are expressed as the mean ± SEM of the (a) latency to step down in seconds (1.5 h) and (b) latency to step down in seconds (24 h). $^*p < 0.05$ compared to the control group (Student's *t*-test).

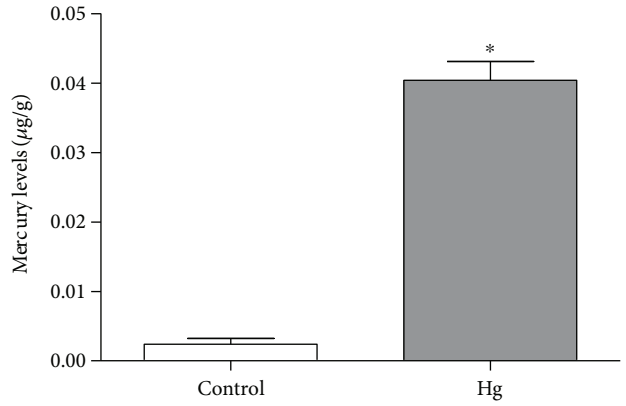


FIGURE 4: The effects of $HgCl_2$ administration (0.375 mg/kg/day) for 45 days on the levels of Hg ($\mu$g/g) in the hippocampus of male Wistar rats. The results are expressed as the mean ± SEM. $^*p < 0.05$ compared to the control group (Student's *t*-test).

significant reduction in cell density in all of the regions evaluated: CA1 (control 50.20 ± 7.29 cells/field; $HgCl_2$ = 25.00 ± 2.64 cells/field; $p = 0.043$), CA3 (control 74.75 ± 10.64 cells/field; $HgCl_2$ = 31.00 ± 12.50 cells/field; $p = 0.044$), and hilus (control 76.00 ± 3.50 cells/field; $HgCl_2$ = 50.00 ± 4.04 cells/field; $p = 0.003$) (Figure 7).

*3.7. Chronic $HgCl_2$ Exposure Induces Neuronal Loss in the Hippocampus.* The quantification for $NeuN^+$ cells showed that chronic $HgCl_2$ exposure induced a significant neuronal loss in three of the analyzed regions: CA1 (control 163.3 ± 7.43 cells/field; $HgCl_2$ = 127.8 ± 5.97 cells/field; $p = 0.0070$), CA3 (control 177.5 ± 4.48 cells/field; $HgCl_2$ = 99.60 ± 8.38 cells/field; $p = 0.0001$), and hilus (control 167.5 ± 6.71 cells/field; $HgCl_2$ = 123.8 ± 6.25 cells/field; $p = 0.0021$), as illustrated in Figure 8.

## 4. Discussion

This study shows that long-term chronic exposure to $HgCl_2$ in adult rats promotes cognitive impairment, triggering oxidative stress and cell death in the hippocampus. This metal presents a low liposolubility, which disfavors its passage through the blood-brain barrier, especially in adults, with a few investigations described in the literature about the effects in the CNS [1, 2]. Unfortunately, scarce information is available about inorganic mercury burden in chronically exposed populations because epidemiological studies usually analyzed the total mercury content and not that of the different mercury species [8].

Even in this scenario, we chose to administer $HgCl_2$ by intragastric gavage based on the fact that it represents an important form of intoxication by this metal [27, 28], reaching the systemic circulation and possibly crossing the blood-brain barrier and elevating the levels of Hg in neural parenchyma [15].

Models of chronic exposure to inorganic mercury are relatively uncommon in the literature, although the oral route was already shown to be an important route of chronic exposure to inorganic mercury [10, 11, 29]. Exposure to 0.8 mg/kg of inorganic mercury in a similar model did not cause obvious symptoms of toxicity in both pregnant rats and their pups (no movement disorder for adults and average body weight of newborns no less than 85% of controls). In this study, we used less than a half of that dose, characterizing an exposure to a relatively low concentration.

In this study, the analysis of total Hg levels revealed the presence of Hg in the hippocampus of chronically exposed rats to $HgCl_2$, demonstrating that, despite its low liposolubility, inorganic Hg crossed the blood-brain barrier and deposited in the nervous tissue, even at relatively low oral doses. This fact indicates the possibility of exposure to $HgCl_2$ during a prolonged period causing neurotoxic effects.

Hence, the Hg levels found were able to promote deficits in the short- and long-term memory tasks, evidenced by the inhibitory avoidance paradigm. In this trial, the animals were induced to learn and memorize an event through a noxious stimulus (electric shock). This test contains elements which cause a conflict in the motor response initiated by the animal, which previously held a noxious stimulus (walking on the grid and receiving an electric shock) [30].

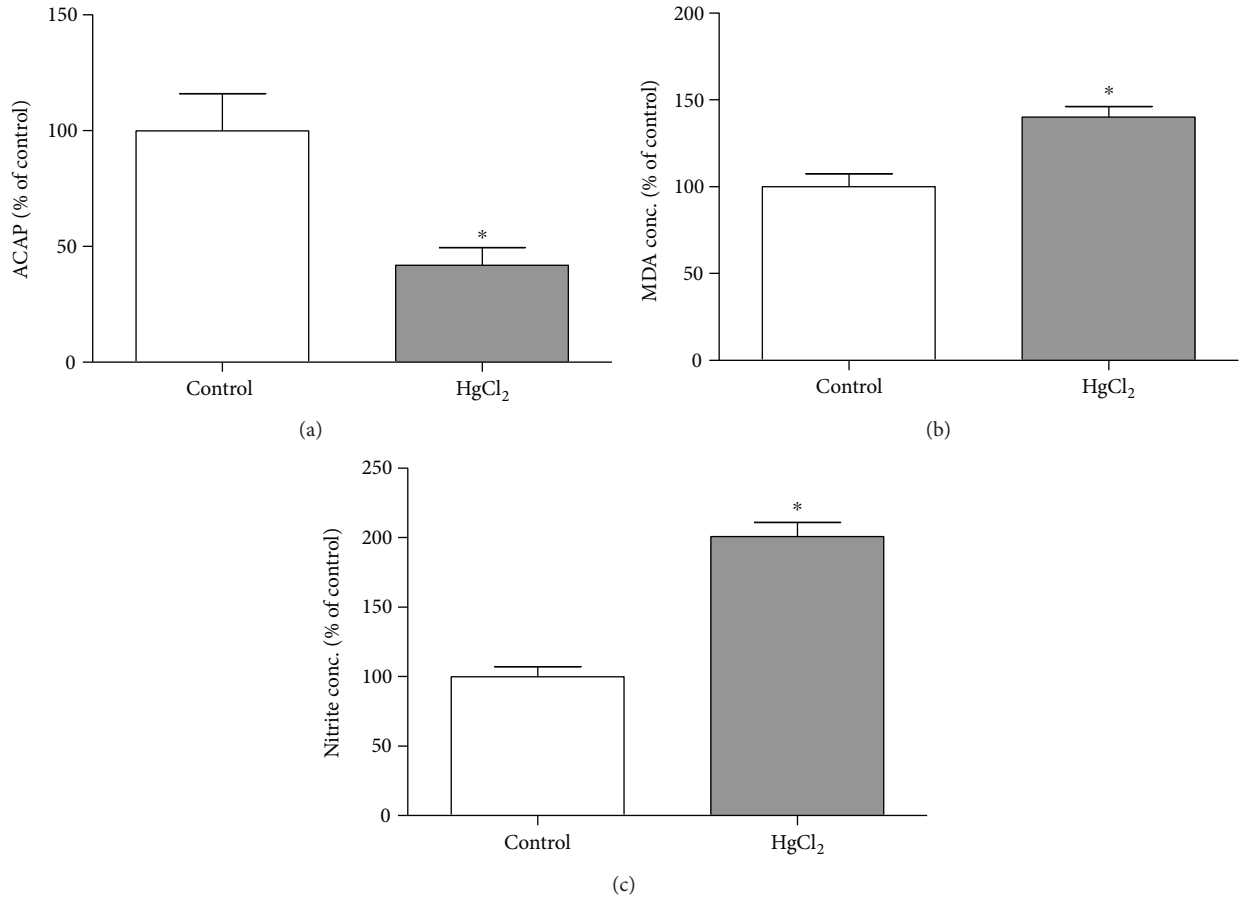


FIGURE 5: The effects of chronic exposure with $HgCl_2$ on oxidative stress in the hippocampus of adult Wistar rats. The results are expressed as mean ± standard error of the (a) percentages of the fluorescence unit area difference of the generated curves of the same sample with and without ABAP in comparison to the control group; (b) percentages of milligram per malondialdehyde protein in relation to the control group; and (c) percentages of milligram per nitrite protein in relation to the control group. $^*p < 0.05$ compared to the control group (Student's *t*-test).

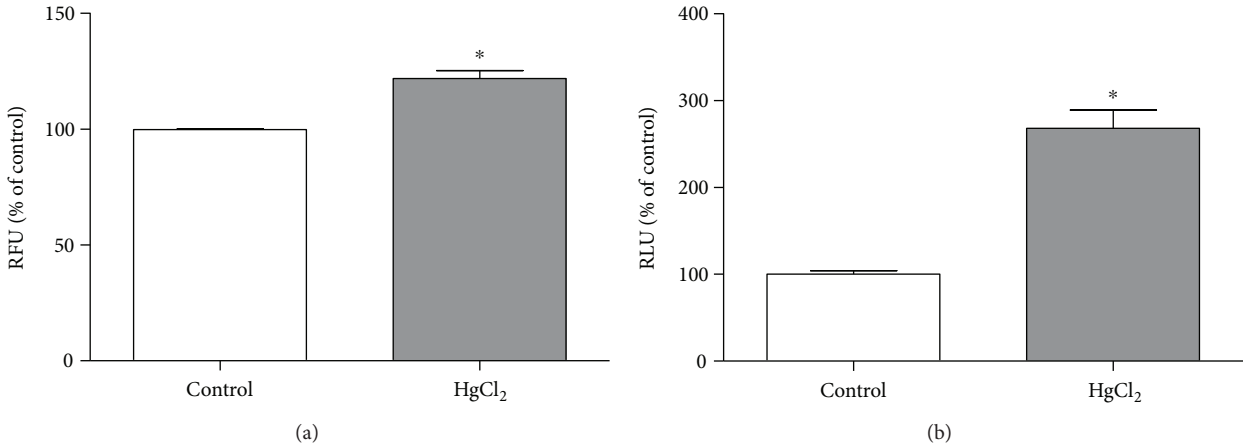


FIGURE 6: The effects of $HgCl_2$ administration (0.375 mg/kg/day) for 45 days on cytotoxicity in the hippocampus of male Wistar rats evaluated in CytoTox-Glo reagent systems and apoptosis evaluated in ApoTox-Glo® reagent systems (Promega). The results are expressed as the mean ± SEM of the (a) relative fluorescence units (RFU) for cytotoxicity and (b) relative light units (RLU) for apoptosis. $^*p < 0.05$ compared to the control group (Student's *t*-test).

Mello-Carpes et al. [31] have reported that occupational doses of $HgCl_2$ after 60 days of exposure display deficits on the long-term memory in rats, evaluated 24 h after the training session. Our study went beyond such results, in which we investigated the short-term memory in the same paradigm. It is important to consider that the inhibitory

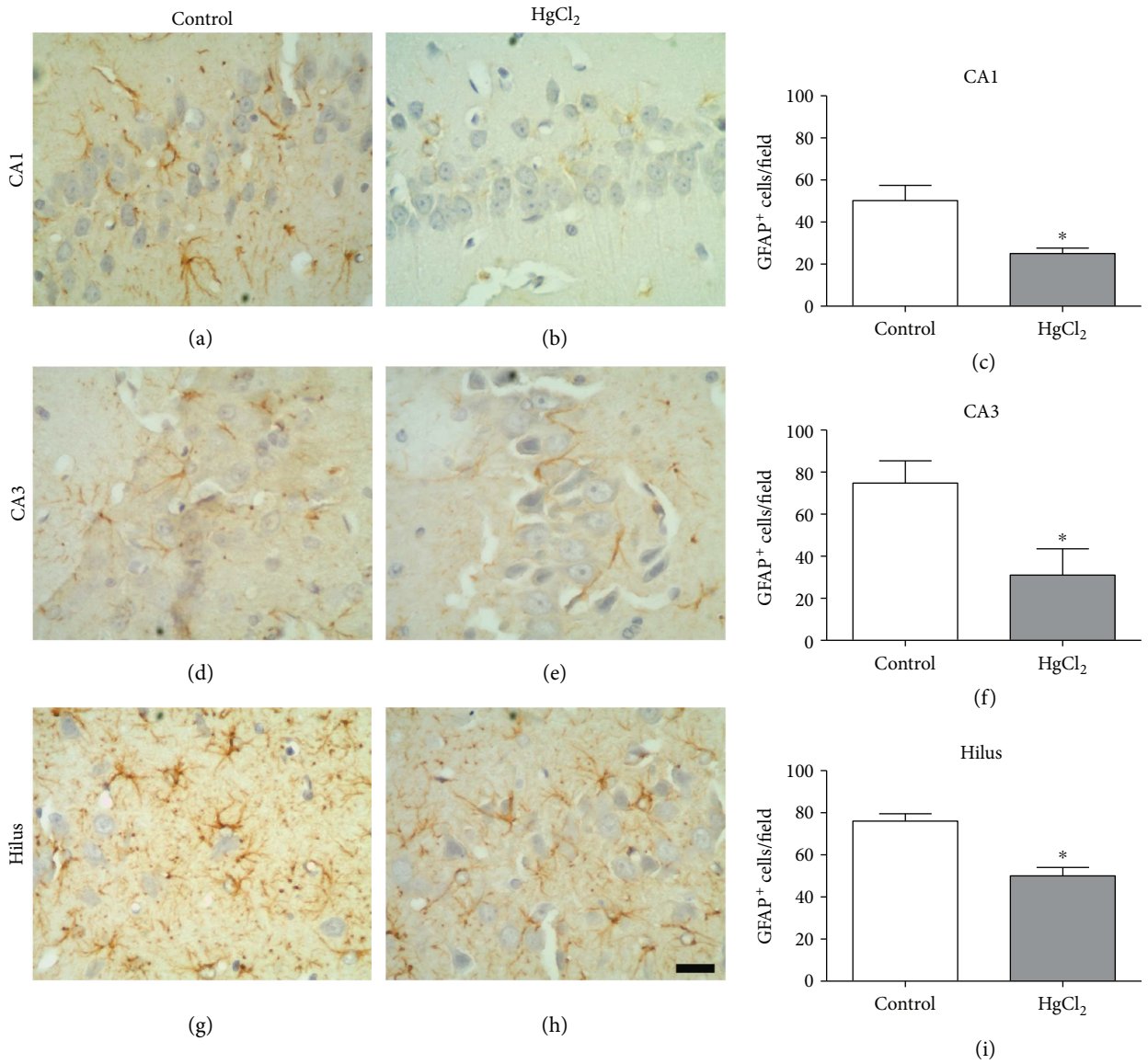


Figure 7: The effects of chronic exposure to $HgCl_2$ on astrocyte density ($GFAP^+$ cells) in the CA1 (a–c), CA3 (d–f), and hilus (g–i) of the hippocampus of adult Wistar rats. Results are expressed as mean ± standard error of the number of cells counted per field in each region (c, f, g). $^*p < 0.05$ compared to the control group (Student's $t$-test). Scale bar: 20 $\mu$m.

avoidance test is an essential behavioral assay to evaluate memory function connected to the hippocampus [24, 31, 32].

Inhibitory avoidance memory, a type of fear memory, is formed in the hippocampus, with involvement of the basolateral amygdala [33]. In the hippocampus, especially in the dorsal hippocampus (posterior segment), the regions associated with a fear memory are dorsal CA1 and CA3 [34]. In this investigation, we analyzed the hippocampus as an anatomic region of choice for measurements of the levels of Hg, oxidative stress, and cell death.

Hg presents toxic effects in the CNS, resulting in changes in neurotransmission [34], deficiencies in neuronal differentiation [35], damage to cellular DNA [36, 37], changes in the cytoskeleton [35], variations in intracellular $Ca^{2+}$ concentrations [38], and the production of reactive oxygen species (ROS) by configuring the mechanism of oxidative stress [39].

Thus, Hg-induced neurotoxicity is related to the overproduction of reactive oxygen and nitrogen species and/or a reduction of the antioxidant defense system [40–44]. It was demonstrated that chronic exposure to inorganic Hg promoted increased levels of malondialdehyde (MDA) and nitrites and decreased total antioxidant capacity by promoting oxidative stress in the hippocampus, similar to the results reported by Rizzetti et al., which evidenced the increase in MDA in the brain and plasma [45].

Our results of lipid peroxidation in the hippocampus after inorganic mercury exposure indicated that the

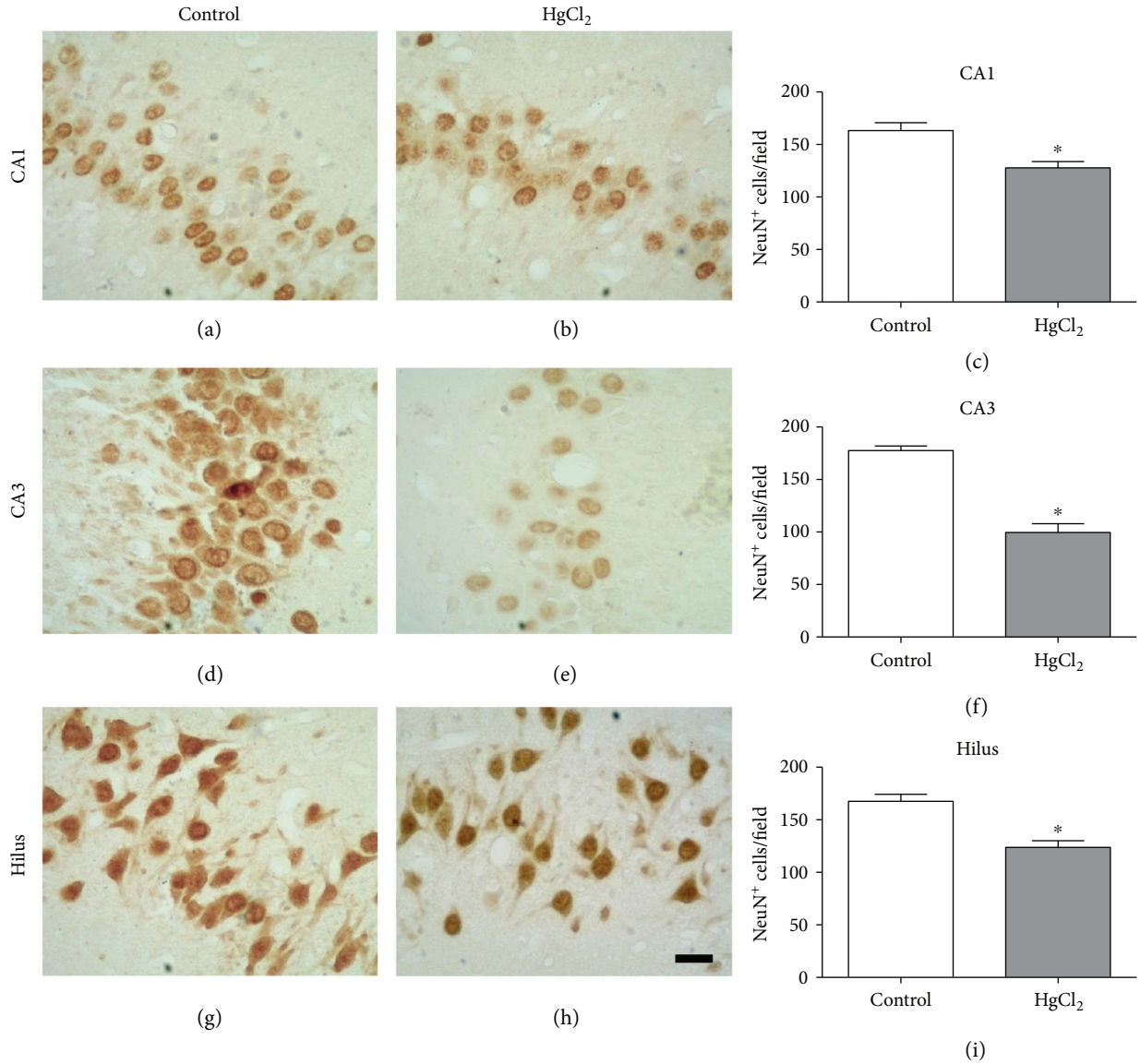


Figure 8: The effects of chronic exposure to $HgCl_2$ on neuron density ($NeuN^+$ cells) in the CA1 (a–c), CA3 (d–f), and hilus (g–i) of the hippocampus of adult Wistar rats. Results are expressed as mean ± standard error of the number of cells counted per field in each region (c, f, g). $^*p < 0.05$ compared to the control group (Student's $t$-test). Scale bar: 20 $\mu$m.

neurotoxicity induced by Hg is due to the overproduction of free radicals and products of lipid peroxidation. This is confirmed by the concomitant decrease in total antioxidant capacity, by ACAP analysis. The ability of Hg to inhibit antioxidant enzymes such as glutathione peroxidase, glutathione reductase, superoxide dismutase, and catalase is already known because of its ability to form free and protein-free complexes, which may decrease or inhibit enzymatic activity [40, 43]. A recent study by our group revealed that Hg can modulate the ACAP of salivary glands, as it is a sensitive parameter to mercurial exposure [27].

The levels of Hg present in the hippocampus, associated with decreased antioxidant capacity and increased prooxidant factors, led us to evaluate the presence of cell death caused by cytotoxicity and the induction of apoptosis in the hippocampus. The chronic exposure to inorganic Hg in our model promoted cytotoxicity and apoptosis induction.

Similar results have been described based on *in vitro* studies, in which the inorganic Hg in cultured astrocytes and neurons promoted cell death by cytotoxicity in both cell types. This process is not associated with apoptotic mechanisms, even after prolonged exposure to the metal [46]. However, in our research, we show that both mechanisms of cell death can be triggered and occur concurrently.

In an animal experimentation model at a dose of 0.4 mg/kg, cell death by apoptosis, triggered by inorganic Hg, may occur from acute exposure, with an increase in caspase-3 activation and oxidative stress [40]. This occurs

by an increase in the level of lipid peroxidation and inhibition of nitrite and the enzymatic antioxidant system. This decrease in antioxidant treatment could be represented by the decrease in the activity of superoxide dismutase, catalase, glutathione peroxidase, and glutathione reductase in the CNS [40]. These events are involved in neurotoxicity induced by Hg in the brain areas, thus increasing cytosolic $Ca^{2+}$ levels, and therefore acting in a mechanism of cell death, which involves necrosis and the induction of apoptosis [40, 47, 48]. From our results, we can infer that $HgCl_2$ can induce the decrease in both cell density and cytotoxicity by apoptosis, in adult organisms, with the processes occurring simultaneously in the hippocampus.

Chronic exposure to $HgCl_2$ promotes tissue changes in the CA1, CA3, and hilus hippocampal areas, revealed by our immunohistochemical analyses. GFAP is the main protein constituent of the astrocyte cytoskeleton, thus being an important tissue marker [49]. The reduction of immunostaining in $GFAP^+$ cell populations due to the neurotoxicity of $HgCl_2$ found in our work points to a disorder of the mnemonic neural processes, since these cells belonging to the glia are auxiliary to the neurons and act in metabolic processes, in synaptic transmission, and in local homeostasis [50]. Previous studies have reported the increased susceptibility of astrocytes to inorganic Hg toxicity compared to neurons [51, 52]. This fact agrees with the study of Allen et al. [53], which indicates that the neurotoxicity is due to a deficiency of the astrocytic activity in the maintenance of metabolic pathways and interactions with neurons.

The reduction of neuronal cells in the hippocampal areas analyzed demonstrated the occurrence of the events of cell death caused by chronic exposure to $HgCl_2$. The mechanisms involved in this process may be cytotoxicity or apoptosis, which in turn can be triggered by oxidative stress, as demonstrated in this study. This is in agreement with the results of Lohren et al. [46] which proved the inorganic Hg cytotoxicity in astrocytes and neurons, even though the occurrence of apoptotic processes was not observed. Another factor associated with this reduction of neuronal cells may be a notable reduction in their replacement due to the reduction of neurogenesis and gliogenesis [54].

Thus, inorganic Hg reaches and is deposited in the hippocampus. This accumulation promotes the increase of nitric oxide and other ROS levels, affecting membrane lipids and causing lipid peroxidation. The necrosis and apoptosis processes kill cells, both neurons and astrocytes. Finally, the decrease in the number of cells is the main cause of cognitive changes. The results presented in this study indicate the need for social measures and environmental policies aimed at determining the problem of Hg intoxication in populations living in contaminated regions.

In conclusion, chronic exposure to inorganic Hg during adulthood promotes cognitive disorders related to decreased cell density in the hippocampus, oxidative stress, cytotoxicity, and apoptosis induction.

## Conflicts of Interest

None of the authors has any conflict of interests.

## Authors' Contributions

Walessa Alana Bragança Aragão and Francisco Bruno Teixeira contributed equally to this work.

## References


[1] K. M. Rice, E. M. Walker Jr., M. Wu, C. Gillette, and E. R. Blough, "Environmental mercury and its toxic effects," *Journal of Preventive Medicine and Public Health*, vol. 47, no. 2, pp. 74–83, 2014.

[2] R. A. Bernhoft, "Mercury toxicity and treatment: a review of the literature," *Journal of Environmental and Public Health*, vol. 2012, Article ID 460508, 10 pages, 2012.

[3] P. Holmes, K. A. James, and L. S. Levy, "Is low-level environmental mercury exposure of concern to human health?," *Science of The Total Environment*, vol. 408, no. 2, pp. 171–182, 2009.

[4] S. Kothari, D. Kruse, R. Karimi et al., "High mercury seafood consumption associated with fatigue at specialty medical clinics on Long Island, NY," *Preventive Medicine Reports*, vol. 2, pp. 798–802, 2015.

[5] R. C. Marques, J. V. Bernardi, M. P. Cunha, and J. G. Dorea, "Impact of organic mercury exposure and home delivery on neurodevelopment of Amazonian children," *International Journal of Hygiene and Environmental Health*, vol. 219, no. 6, pp. 498–502, 2016.

[6] J. J. Berzas Nevado, R. C. Rodríguez Martín-Doimeadios, M. Jiménez Moreno, J. L. Martins do Nascimento, A. M. Herculano, and M. E. Crespo-López, "Mercury speciation analysis on cell lines of the human central nervous system to explain genotoxic effects," *Microchemical Journal*, vol. 93, no. 1, pp. 12–16, 2009.

[7] M. E. Crespo-López, A. M. Herculano, T. C. Corvelo, and J. L. Do Nascimento, "Mercury and neurotoxicity," *Revue Neurologique*, vol. 40, no. 7, pp. 441–447, 2005.

[8] J. J. Berzas Nevado, R. C. Rodríguez Martín-Doimeadios, F. J. Guzmán Bernardo et al., "Mercury in the Tapajós River basin, Brazilian Amazon: a review," *Environment International*, vol. 36, no. 6, pp. 593–608, 2010.

[9] F. Ruggieri, C. Majorani, F. Domanico, and A. Alimonti, "Mercury in children: current state on exposure through human biomonitoring studies," *International Journal of Environmental Research and Public Health*, vol. 14, no. 12, p. 519, 2017.

[10] G. P. F. Arrifano, R. C. R. Martín-Doimeadios, M. Jiménez-Moreno et al., "Large-scale projects in the amazon and human exposure to mercury: the case-study of the Tucuruí dam," *Ecotoxicology and Environmental Safety*, vol. 147, pp. 299–305, 2018.

[11] R. C. Rodríguez Martín-Doimeadios, J. J. Berzas Nevado, F. J. Guzmán Bernardo et al., "Comparative study of mercury speciation in commercial fishes of the Brazilian Amazon," *Environmental Science and Pollution Research International*, vol. 1, pp. 1–6, 2014.

[12] L. K. R. Leão, A. M. Herculano, C. Maximino et al., "*Mauritia flexuosa* L. protects against deficits in memory acquisition and oxidative stress in rat hippocampus induced by methylmercury exposure," *Nutritional Neuroscience*, vol. 20, no. 5, pp. 297–304, 2017.

[13] A. L. Milioni, B. V. Nagy, A. L. Moura, E. C. Zachi, M. T. Barboni, and D. F. Ventura, "Neurotoxic impact of mercury

on the central nervous system evaluated by neuropsychological tests and on the autonomic nervous system evaluated by dynamic pupillometry," *NeuroToxicology*, vol. 59, pp. 263–269, 2017.

[14] M. R. Drew and K. A. Huckleberry, "Modulation of aversive memory by adult hippocampal neurogenesis," *Neurotherapeutics*, vol. 14, no. 3, pp. 646–661, 2017.

[15] F. B. Teixeira, R. M. Fernandes, P. M. Farias-Junior et al., "Evaluation of the effects of chronic intoxication with inorganic mercury on memory and motor control in rats," *International Journal of Environmental Research and Public Health*, vol. 11, no. 12, pp. 9171–9185, 2014.

[16] Udo Albus, *Guide for the Care and Use of Laboratory Animals*, National Research Council of the National Academies, Washington, DC, 2011.

[17] A. C. Oliveira, M. C. Pereira, L. N. Santana et al., "Chronic ethanol exposure during adolescence through early adulthood in female rats induces emotional and memory deficits associated with morphological and molecular alterations in hippocampus," *Journal of Psychopharmacology*, vol. 29, no. 6, pp. 712–724, 2015.

[18] T. Suzuki, H. Akagi, K. Akimura et al., *Manual of Analyzes of Mercury*, Ministry of the Environment, Japan, 2004.

[19] L. L. Amado, M. L. Garcia, P. B. Ramos et al., "A method to measure total antioxidant capacity against peroxyl radicals in aquatic organisms: application to evaluate microcystins toxicity," *Science of The Total Environment*, vol. 407, no. 6, pp. 2115–2123, 2009.

[20] H. Esterbauer and K. H. Cheeseman, "[42] Determination of aldehydic lipid peroxidation products: malonaldehyde and 4-hydroxynonenal," *Methods in Enzymology*, vol. 186, pp. 407–421, 1990.

[21] L. C. Green, S. R. Tannenbaum, and P. Goldman, "Nitrate synthesis in the germfree and conventional rat," *Science*, vol. 212, no. 4490, pp. 56–58, 1981.

[22] M. M. Bradford, "A rapid and sensitive method for the quantitation of microgram quantities of protein utilizing the principle of protein-dye binding," *Analytical Biochemistry*, vol. 72, no. 1-2, pp. 248–254, 1976.

[23] A. F. Silva, M. S. Aguiar, O. S. Carvalho et al., "Hippocampal neuronal loss, decreased GFAP immunoreactivity and cognitive impairment following experimental intoxication of rats with aluminum citrate," *Brain Research*, vol. 1491, pp. 23–33, 2013.

[24] G. B. Oliveira, A. Fontes Ede Jr, S. de Carvalho et al., "Minocycline mitigates motor impairments and cortical neuronal loss induced by focal ischemia in rats chronically exposed to ethanol during adolescence," *Brain Research*, vol. 1561, pp. 23–34, 2014.

[25] R. R. Lima, J. Guimaraes-Silva, J. L. Oliveira et al., "Diffuse axonal damage, myelin impairment, astrocytosis and inflammatory response following microinjections of NMDA into the rat striatum," *Inflammation*, vol. 31, no. 1, pp. 24–35, 2008.

[26] R. R. Lima, L. N. Santana, R. M. Fernandes et al., "Neurodegeneration and glial response after acute striatal stroke: histological basis for neuroprotective studies," *Oxidative Medicine and Cellular Longevity*, vol. 2016, Article ID 3173564, 15 pages, 2016.

[27] L. O. Bittencourt, B. Puty, S. Charone et al., "Oxidative biochemistry disbalance and changes on proteomic profile in salivary glands of rats induced by chronic exposure to methylmercury," *Oxidative Medicine and Cellular Longevity*, vol. 2017, Article ID 5653291, 15 pages, 2017.

[28] C. C. Bridges and R. K. Zalups, "Mechanisms involved in the transport of mercuric ions in target tissues," *Archives of Toxicology*, vol. 91, no. 1, pp. 63–81, 2017.

[29] A. Szász, B. Barna, Z. Gajda, G. Galbács, M. Kirsch-Volders, and M. Szente, "Effects of continuous low-dose exposure to organic and inorganic mercury during development on epileptogenicity in rats," *Neurotoxicology*, vol. 23, no. 2, pp. 197–206, 2002.

[30] E. Atucha and B. Roozendaal, "The inhibitory avoidance discrimination task to investigate accuracy of memory," *Frontiers in Behavioral Neuroscience*, vol. 9, p. 60, 2015.

[31] P. B. Mello-Carpes, W. Barros, S. Borges et al., "Chronic exposure to low mercury chloride concentration induces object recognition and aversive memories deficits in rats," *International Journal of Developmental Neuroscience*, vol. 31, no. 7, pp. 468–472, 2013.

[32] T. Karl, R. Pabst, and S. von Horsten, "Behavioral phenotyping of mice in pharmacological and toxicological research," *Experimental and Toxicologic Pathology*, vol. 55, no. 1, pp. 69–83, 2003.

[33] I. Izquierdo, C. R. Furini, and J. C. Myskiw, "Fear memory," *Physiological Reviews*, vol. 96, no. 2, pp. 695–750, 2016.

[34] M. S. Fanselow and H. W. Dong, "Are the dorsal and ventral hippocampus functionally distinct structures?," *Neuron*, vol. 65, no. 1, pp. 7–19, 2010.

[35] M. C. Chan, E. Bautista, I. Alvarado-Cruz, B. Quintanilla-Vega, and J. Segovia, "Inorganic mercury prevents the differentiation of SH-SY5Y cells: amyloid precursor protein, microtubule associated proteins and ROS as potential targets," *Journal of Trace Elements in Medicine and Biology*, vol. 41, pp. 119–128, 2017.

[36] M. E. Crespo-Lopez, A. Costa-Malaquias, E. H. Oliveira et al., "Is low non-lethal concentration of methylmercury really safe? A report on genotoxicity with delayed cell proliferation," *PLoS One*, vol. 11, no. 9, article e0162822, 2016.

[37] M. E. Crespo-Lopez, A. Lima de Sa, A. M. Herculano, R. Rodriguez Burbano, and J. L. Martins do Nascimento, "Methylmercury genotoxicity: a novel effect in human cell lines of the central nervous system," *Environment International*, vol. 33, no. 2, pp. 141–146, 2007.

[38] T. L. Limke, J. J. Bearss, and W. D. Atchison, "Acute exposure to methylmercury causes Ca2+ dysregulation and neuronal death in rat cerebellar granule cells through an M3 muscarinic receptor-linked pathway," *Toxicological Sciences*, vol. 80, no. 1, pp. 60–68, 2004.

[39] N. Ercal, H. Gurer-Orhan, and N. Aykin-Burns, "Toxic metals and oxidative stress part I: mechanisms involved in metal-induced oxidative damage," *Current Topics in Medicinal Chemistry*, vol. 1, no. 6, pp. 529–539, 2001.

[40] A. E. Abdel Moneim, "The neuroprotective effect of berberine in mercury-induced neurotoxicity in rats," *Metabolic Brain Disease*, vol. 30, no. 4, pp. 935–942, 2015.

[41] S. Ceccatelli, E. Dare, and M. Moors, "Methylmercury-induced neurotoxicity and apoptosis," *Chemico-Biological Interactions*, vol. 188, no. 2, pp. 301–308, 2010.

[42] E. Fonfria, M. T. Vilaro, Z. Babot, E. Rodriguez-Farre, and C. Sunol, "Mercury compounds disrupt neuronal glutamate transport in cultured mouse cerebellar granule cells," *Journal of Neuroscience Research*, vol. 79, no. 4, pp. 545–553, 2005.

[43] L. L. Gutierrez, N. G. Mazzotti, A. S. Araujo et al., "Peripheral markers of oxidative stress in chronic mercuric chloride intoxication," *Brazilian Journal of Medical and Biological Research*, vol. 39, no. 6, pp. 767–772, 2006.

[44] T. Sumathi, C. Shobana, J. Christinal, and C. Anusha, "Protective effect of *Bacopa monniera* on methyl mercury-induced oxidative stress in cerebellum of rats," *Cellular and Molecular Neurobiology*, vol. 32, no. 6, pp. 979–987, 2012.

[45] D. A. Rizzetti, F. Fernandez, S. Moreno et al., "Egg white hydrolysate promotes neuroprotection for neuropathic disorders induced by chronic exposure to low concentrations of mercury," *Brain Research*, vol. 1646, pp. 482–489, 2016.

[46] H. Lohren, L. Blagojevic, R. Fitkau et al., "Toxicity of organic and inorganic mercury species in differentiated human neurons and human astrocytes," *Journal of Trace Elements in Medicine and Biology*, vol. 32, pp. 200–208, 2015.

[47] S. H. Kim and R. P. Sharma, "Mercury-induced apoptosis and necrosis in murine macrophages: role of calcium-induced reactive oxygen species and p38 mitogen-activated protein kinase signaling," *Toxicology and Applied Pharmacology*, vol. 196, no. 1, pp. 47–57, 2004.

[48] A. Nakaizumi, T. Horie, T. Kida et al., "Nitric oxide potentiates TNF-$\alpha$-induced neurotoxicity through suppression of NF-$\kappa$B," *Cellular and Molecular Neurobiology*, vol. 32, no. 1, pp. 95–106, 2012.

[49] O. Sveinsson, L. Herrman, and M. A. Hietala, "Heroin-induced acute myelopathy with extreme high levels of CSF glial fibrillar acidic protein indicating a toxic effect on astrocytes," *BMJ Case Reports*, vol. 2017, 2017.

[50] R. M. Ransohoff and M. A. Brown, "Innate immunity in the central nervous system," *The Journal of Clinical Investigation*, vol. 122, no. 4, pp. 1164–1171, 2012.

[51] J. S. Charleston, R. L. Body, R. P. Bolender, N. K. Mottet, M. E. Vahter, and T. M. Burbacher, "Changes in the number of astrocytes and microglia in the thalamus of the monkey Macaca fascicularis following long-term subclinical methylmercury exposure," *Neurotoxicology*, vol. 17, no. 1, pp. 127–138, 1996.

[52] R. H. Garman, B. Weiss, and H. L. Evans, "Alkylmercurial encephalopathy in the monkey (*Saimiri sciureus* and *Macaca arctoides*): a histopathologic and autoradiographic study," *Acta Neuropathologica*, vol. 32, no. 1, pp. 61–74, 1975.

[53] J. W. Allen, G. Shanker, K. H. Tan, and M. Aschner, "The consequences of methylmercury exposure on interactive functions between astrocytes and neurons," *Neurotoxicology*, vol. 23, no. 6, pp. 755–759, 2002.

[54] F. T. Crews, M. A. Collins, C. Dlugos et al., "Alcohol-induced neurodegeneration: when, where and why?," *Alcoholism, Clinical and Experimental Research*, vol. 28, no. 2, pp. 350–364, 2004.

Hindawi
Oxidative Medicine and Cellular Longevity
Volume 2018, Article ID 7580707, 11 pages
https://doi.org/10.1155/2018/7580707

*Review Article*

# The Essential Element Manganese, Oxidative Stress, and Metabolic Diseases: Links and Interactions

**Longman Li**[1] **and Xiaobo Yang**[1,2]

[1]*Department of Occupational Health and Environmental Health, School of Public Health, Guangxi Medical University, Nanning, Guangxi, China*
[2]*Center for Genomic and Personalized Medicine, Guangxi Medical University, Nanning, Guangxi, China*

Correspondence should be addressed to Xiaobo Yang; yangx@gxmu.edu.cn

Received 25 October 2017; Revised 10 February 2018; Accepted 12 March 2018; Published 5 April 2018

Academic Editor: Pan Chen

Copyright © 2018 Longman Li and Xiaobo Yang. This is an open access article distributed under the Creative Commons Attribution License, which permits unrestricted use, distribution, and reproduction in any medium, provided the original work is properly cited.

Manganese (Mn) is an essential element that is involved in the synthesis and activation of many enzymes and in the regulation of the metabolism of glucose and lipids in humans. In addition, Mn is one of the required components for Mn superoxide dismutase (MnSOD) that is mainly responsible for scavenging reactive oxygen species (ROS) in mitochondrial oxidative stress. Both Mn deficiency and intoxication are associated with adverse metabolic and neuropsychiatric effects. Over the past few decades, the prevalence of metabolic diseases, including type 2 diabetes mellitus (T2MD), obesity, insulin resistance, atherosclerosis, hyperlipidemia, nonalcoholic fatty liver disease (NAFLD), and hepatic steatosis, has increased dramatically. Previous studies have found that ROS generation, oxidative stress, and inflammation are critical for the pathogenesis of metabolic diseases. In addition, deficiency in dietary Mn as well as excessive Mn exposure could increase ROS generation and result in further oxidative stress. However, the relationship between Mn and metabolic diseases is not clear. In this review, we provide insights into the role Mn plays in the prevention and development of metabolic diseases.

## 1. Introduction

Manganese (Mn) is an essential element in the human body that is mainly obtained from food and water. Mn is absorbed through the gastrointestinal tract and then transported to organs enriched in the mitochondria (in particular the liver, pancreas, and pituitary) where it is rapidly concentrated [1]. Furthermore, Mn is involved in the synthesis and activation of many enzymes (e.g., oxidoreductases, transferases, hydrolases, lyases, isomerases, and ligases); metabolism of glucose and lipids; acceleration in the synthesis of protein, vitamin C, and vitamin B; catalysis of hematopoiesis; regulation of the endocrine; and improvement in immune function [2]. Moreover, Mn metalloenzymes including arginase, glutamine synthetase, phosphoenolpyruvate decarboxylase, and Mn superoxide dismutase (MnSOD) also contribute to the metabolism processes listed above and reduce oxidative stress against free radicals (Figure 1).

However, environmental or occupational Mn overexposure is harmful to human health, especially in at-risk populations such as miners, welders, and steel makers. According to data from the Mineral Commodity Summaries released by the US Geological Survey in 2016, South Africa, China, and Australia accounted for 67% of the total Mn mined (18 million tons) in the world in 2015. Mn ore mining and its processing cause air and water pollution, threatening the health of workers and general populations residing near factories through oral ingestion and inhalation as well as dermally and intravenously. Acute Mn exposure can lead to manganism, and chronic Mn exposure causes an extrapyramidal syndrome with features resembling those found in Parkinson's disease and postencephalitic parkinsonism [3].

The prevalence of metabolic diseases, including type 2 diabetes mellitus (T2DM), obesity, insulin resistance, atherosclerosis, hyperlipidemia, nonalcoholic fatty liver disease (NAFLD), and hepatic steatosis, has increased dramatically

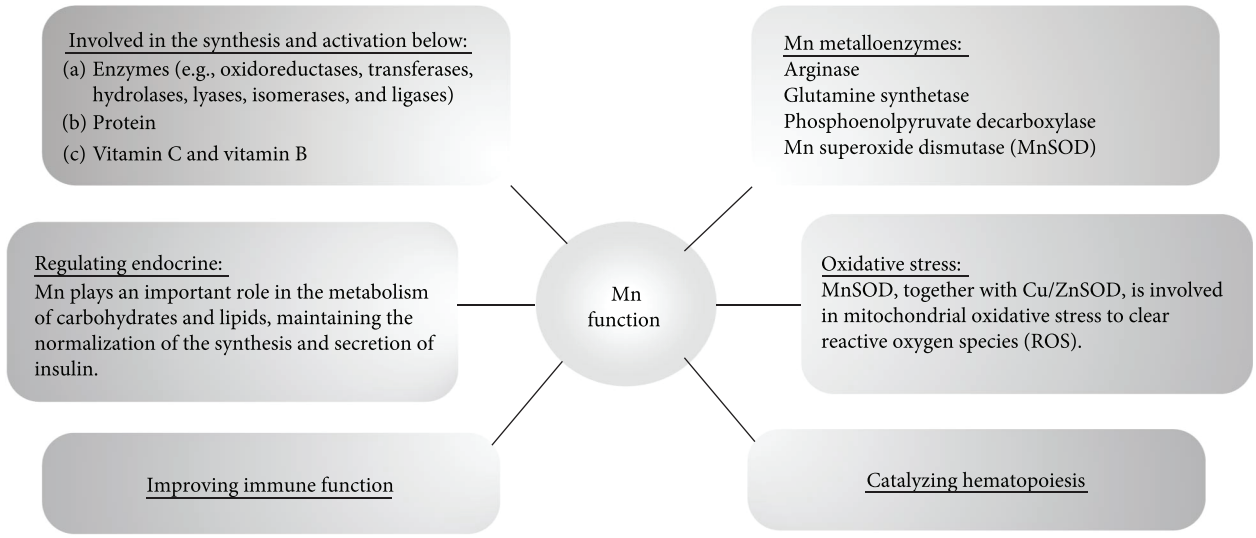


Figure 1: Physiological roles of Mn.

over the past few decades [4]. These metabolic disorders are usually caused by the clustering of metabolic syndrome (MetS). The criteria for identifying MetS include three of five markers: abdominal obesity, impaired carbohydrate metabolism, high blood pressure, and dyslipidemia, including elevated levels of triglycerides and decreased levels of high-density lipoprotein (HDL) [5]. In addition, many studies have shown that metabolic diseases are associated with oxidative stress and inflammation [6–12].

Mn is a component or activator of some enzymes, mostly antioxidants, and plays an important role in metabolisms of carbohydrates and lipids, even in maintaining the normalization of the synthesis and secretion of insulin as well. Therefore, Mn may have protective effects on the occurrence of MetS [13].

Importantly, Mn is a required component of MnSOD for reducing mitochondrial oxidative stress. Mitochondria are the major place where physiological and pathological cellular reactive oxygen species (ROS) are produced. When excessive ROS accumulate abnormally, it would contribute to the oxidative damage found in several neuropathological conditions related to enhanced glucocorticoid expression, which plays an important role in regulating the biosynthesis and metabolism of carbohydrates, lipids, and proteins [14]. Additionally, MnSOD is the primary antioxidant that scavenges superoxide formed within the mitochondria and protects against oxidative stress [15, 16]. If mitochondria are impaired or dysfunctional, ROS production will be further increased and will exacerbate the oxidative stress in mitochondria [17] (Figure 2).

Nevertheless, research in molecular biology or population related to the role of Mn in procession of metabolic diseases via mitochondrial oxidative stress is limited and inconsistent. Mn deficiency and intoxication are both associated with adverse metabolic and neuropsychiatric effects [18, 19]. Experimentally induced Mn deficiency caused a number of detrimental effects, such as impaired growth, poor bone formation and skeletal defects, reduced fertility and birth defects, abnormal glucose tolerance, and altered lipid and carbohydrate metabolism in both animals and humans [2]. By inhibiting mitochondrial complex I and II respiration as well as inducing permeability transition, excessive Mn accumulated in mitochondria could disrupt mitochondrial homeostasis and cause mitochondrial dysfunction [20–22]. In the study about metabolic gene polymorphisms and susceptibility to occupational chronic manganism, it has been found that individuals with homozygote polymorphism (L/L) of the cytochrome P450 2D6L gene (*CYP2D6L*) might decrease the risk of chronic manganism compared with the wild type (Wt/Wt) [23].

In this review, we summarize current hypotheses and research to explore the relationship between Mn and metabolic diseases and reveal how Mn affects the metabolism in both molecular biology and population studies.

## 2. Mn and Metabolic Syndrome

The prevalence of MetS is increasing throughout the world [24]. Recently, criteria to define MetS have been steeped in controversy, but MetS is generally defined by five components: central obesity, raised triglycerides, reduced HDL-cholesterol, raised blood pressure, and raised fasting plasma glucose [25]. The most important role of MetS is to help identify high-risk individuals of both T2DM and cardiovascular disease (CVD) [25].

Oxidative stress is a common risk factor for the pathogenesis of MetS components. Insulin resistance is generally accepted as the first level of metabolic changes in patients with MetS, while the state of chronic low-level inflammation and oxidative stress are second-level abnormalities [26]. Oxidative stress has been associated with all the individual components of MetS and with the onset of cardiovascular complications in subjects with MetS [26–29].

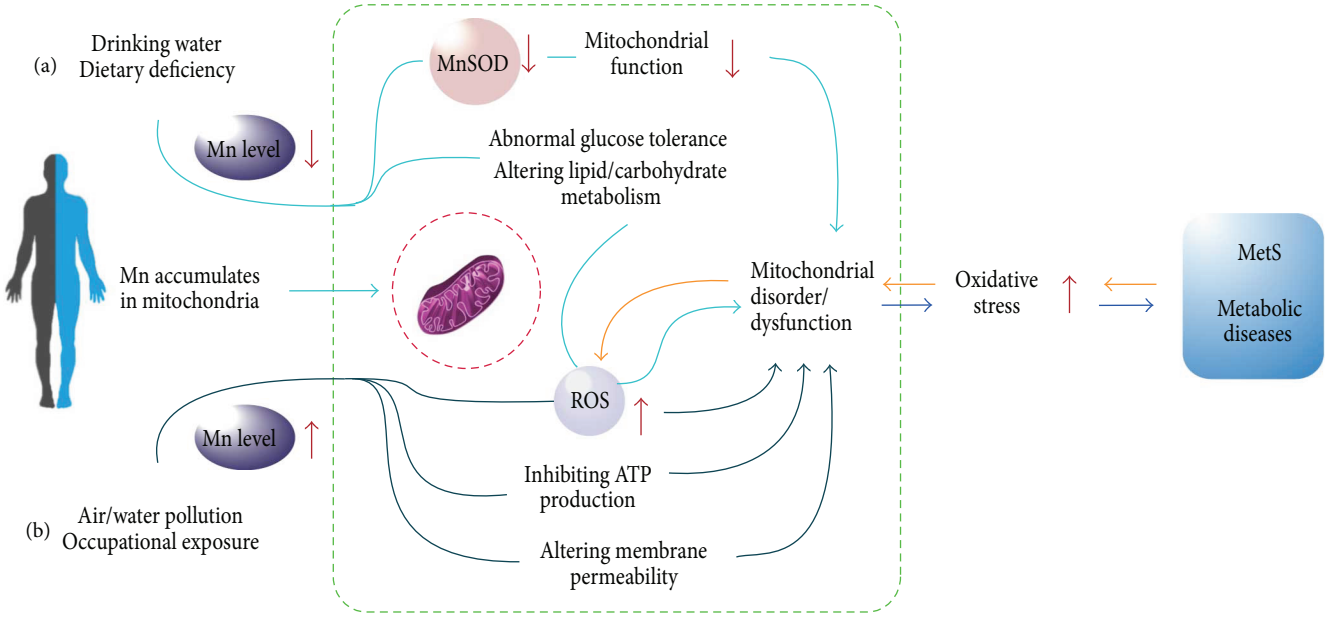


Figure 2: The mechanisms of Mn in metabolic diseases via oxidative stress. (a) Mn deficiency will cause a number of detrimental effects, such as impaired growth, poor bone formation and skeletal defects, reduced fertility and birth defects, abnormal glucose tolerance, and altered lipid and carbohydrate metabolism in both animals and humans. Therefore, Mn deficiency might lead to mitochondrial dysfunction or disorder via decreasing MnSOD level and altering lipid and carbohydrate metabolism. (b) Mn overloaded may disrupt normal mitochondrial function by increasing mitochondrial ROS, inhibiting ATP production, and altering membrane permeability; further result in mitochondrial dysfunction or disorder; and finally cause MetS or metabolic diseases. Excessive ROS and oxidative stress would lead to MetS or metabolic diseases directly. If MetS or metabolic diseases happen, it will in turn increase ROS production and oxidative stress and accelerate mitochondrial dysfunction or disorder.

So far, a few researches explore the association between Mn and MetS (Table 1). Higher Mn intake was associated with decreased risk of MetS in men but increased risk in women; Chinese researchers also found that Mn intake was inversely associated with MetS components including abdominal obesity and hypertriacylglycerolaemia in men, but positively associated with low HDL-cholesterol in both men and women [30]. In Korean women with MetS, dietary Mn intake was significantly lower than that of the healthy control group; the same result was also found in women subjects with high blood pressure only [31]. Moreover, another Chinese study indicated that daily intake of Mn was lower in individuals with a higher number of MetS components and a lower risk of developing MetS in the second, third, and highest quintiles of Mn intake compared to the lowest quintile, adjusted for age, sex, and energy intake [32]. However, blood and urine Mn concentrations were not significantly associated with MetS [5, 33].

However, these epidemiologic studies did not consider potential confounding factors, such as changing dietary habits of patients based on their nutritional knowledge about the MetS components, and did not exclude the MetS patients who have accepted therapy. That might be the main causes of previous data showing an inverted relation between Mn intake and risk for MetS. Besides, it is difficult to confirm the association between dietary intake and MetS risk, because the bioavailability of dietary nutrients would be influenced by some factors, for instance, characteristics of the food source, interactions with other dietary factors, cooking conditions, and various subject characteristics.

## 3. Mn and Type 2 Diabetes Mellitus/ Insulin Resistance

T2DM accounts for over 90% of global diabetes cases compared to type 1 diabetes. T2DM is characterized by hyperglycemia caused by insulin resistance and/or abnormal insulin secretion, either of which may predominate [34].

Several pathogenic pathways activated in diabetes such as ROS, which are generated by high glucose levels, are responsible for metabolic abnormalities and chronic complications [35]. Moreover, oxidative stress can result in impaired islet beta cell function, cause insulin resistance, and finally lead to T2DM and obesity [7, 8]. Normalizing levels of mitochondrial ROS prevents three pathways of hyperglycaemic damage including glucose-induced activation of protein kinase C, formation of advanced glycation end-products, sorbitol accumulation, and NF$\kappa$B activation [36]. Mitochondrial dysfunction has divergent, cell type-dependent effects on insulin action [37] and has been proposed to induce insulin resistance through ectopic lipid accumulation secondary to reduced $\beta$-oxidation, which impairs insulin signaling [38, 39]. In heterozygous MnSOD knockout mice, the MnSOD protein decreased by approximately 70% in muscle and fat, and glucose tolerance was already impaired after feeding these mice a standard chow [40]. Recent studies using

Table 1: The studies of Mn and MetS.

| Reference | Country | Study design | Sample size | Data source/ sample type | Results | |
|---|---|---|---|---|---|---|
| [30] | China | The 5th Chinese National Nutrition and Health Survey (2010–2012) | 2111 | Questionnaire of dietary Mn intake | Men | A decreased risk of MetS with higher Mn intake. |
| | | | | | Women | An increased risk of MetS with higher Mn intake. |
| | | | | | MetS components | Mn intake was inversely associated with abdominal obesity and hypertriacylglycerolaemia in men, but positively associated with low HDL-cholesterol in both men and women. |
| [31] | Korea | The Korea National Health and Nutrition Examination Survey (2007–2008) | 5136 | Questionnaire of dietary Mn intake | Men | No difference |
| | | | | | Women/MetS components | The women subjects with high blood pressure showed significantly lower intake of Mn than did control subjects. |
| [32] | China | Cross-sectional study | Cases: 221 Controls: 329 | Questionnaire of dietary Mn intake | Men/women | A lower risk of developing MetS in the second, third, and highest quintiles of Mn intake with respect to the lowest quintile after adjusting age, sex, and energy intake. |
| | | | | | MetS components | Daily intake of Mn was decreased with the increasing number of MetS components. |
| [5] | Poland | Cross-sectional study | 313 (men aged 50–75 years) | Serum (Mn level) | Significant positive correlations (Mn–BMI, Mn–abdominal circumference, Mn–waist-to-hip ratio, Mn–insulin, Mn–HOMA-IR), but no correlation with MetS. | |
| [33] | Korea | The Korea National Health and Nutrition Examination Survey (2008) | 1405 | Whole blood (Mn level) | No difference | |
| | | | | Urine (Mn level) | No difference | |

transgenic mice that overexpress MnSOD showed protection against diabetic complications, for example, diabetic cardiomyopathy [41], retinopathy [42, 43], and neuropathy [44], while also improving the viability of islet cell transplantation [45]. Therefore, it is very important to maintain the normal function of mitochondrial oxidative stress to prevent the development of T2DM and insulin resistance.

In a study on Zucker rats, a higher mean plasma Mn level in the diabetic fatty group was related to enhanced oxidative stress in diabetes and obesity [46]. Researchers have shown that Mn treatment can increase insulin secretion to improve glucose tolerance under conditions of dietary stress [47], reduce oxidative stress (ROS) and NADPH oxidase [48], and lower the risk of endothelial dysfunction in diabetes [48, 49]. A study on nonobese diabetic mice also found that Mn porphyrin catalytic antioxidant (MnP) treatment slightly enhanced glucose oxidation and reduced fatty acid oxidation [50]. Not only dietary Mn deficiency but also acute Mn exposure in rats can cause decreased plasma insulin levels, rapid hyperglycemia, and hypoinsulinemia, followed by a reactionary hypoglycemia, supporting evidences that the effects of Mn on carbohydrate metabolism may be due to a direct effect on insulin release and gluconeogenesis [51, 52]. A biochemical assessment in male rats' plasma samples showed that $MnO_2$ micro- and nanoparticles after injection of subchronic doses significantly increased plasma glucose and cholesterol levels [53].

Several epidemiologic studies have reported direct associations between Mn level and T2DM, although it remains unclear whether Mn plays a positive or negative role (Table 2). Current research suggests that the blood Mn level is significantly increased in T2DM patients [54, 55], while some showed decreased levels [3, 56–59] or even no difference in Mn levels compared to the controls [60]. A case-control study of 3228 participants in China indicated a U-shaped association between plasma Mn and T2DM, with both low and high levels of plasma Mn associated with higher odds of newly diagnosed T2DM [61]. Some research has found a positive correlation between urinary Mn level and T2DM [56, 59]. However, urinary Mn levels of coke oven workers were associated with hyperglycemia risk but not with diabetes risk, which might be due to the small sample size of diabetes and the relatively young population; researchers also found that the concentrations of urinary Mn in the occupational population were higher than those in the general population [62, 63]. Moreover, results were inconsistent in some studies concerning the Mn concentration in the samples of scalp hair, tears, and lymphocytes among individuals with T2DM [56, 59, 64–66].

## 4. Mn and Obesity

Over the last several decades, obesity, defined as excessive fat accumulation, has become an increasingly prevalent

Table 2: The epidemiologic studies of Mn level in T2DM, obesity, and atherosclerosis.

| Reference | Country | Disease | Study design | Sample size | Sample type | Results of Mn level in cases |
|---|---|---|---|---|---|---|
| [3] | Korean | T2DM | Cross-sectional study | 3996 | Whole blood | Decreased |
| [54] | Mexico | T2DM | Cross-sectional study | 76 | Serum<br>Urine | Increased<br>No different |
| [55] | Turkey | T2DM | Hospital-based case-control study | Cases: 200<br>Controls: 50 | Serum | Increased |
| [56] | Pakistan | T2DM | Cross-sectional study | Diabetes: 257<br>Healthy: 166 | Whole blood<br>Urine<br>Scalp hair | Decreased<br>Increased<br>Decreased |
| [57] | Egypt | T2DM | Hospital-based case-control study | Cases: 40<br>Controls: 36 | Serum | Decreased |
| [58] | Italy | T2DM | Case-control study | Cases: 68<br>Controls: 59 | Whole blood | Decreased |
| [59] | Pakistan | T2DM | Hospital-based case-control study | Cases with their infants: 76<br>Healthy with their infants: 68 | Whole blood<br>Urine<br>Scalp hair | Decreased<br>Increased<br>Decreased |
| [60] | Czech Republic | T2DM | Cross-sectional study | 1069 (aged 61–100 years) | Whole blood | No different |
| [61] | China | T2DM | Case-control study | Cases: 1614<br>Controls: 1614 | Plasma | U-shaped association |
| [62] | China | T2DM | Cross-sectional study | 1493 (coke oven workers) | Urine | Increased association with hyperglycemia risk but not with diabetes risk |
| [64] | Pakistan, Ireland | T2DM | Case-control study | Cases: 145<br>Controls: 177 | Scalp hair | Decreased |
| [65] | Austria | T2DM | Hospital-based case-control study | Cases: 53<br>Controls: 50 | Lymphocyte | Decreased |
| [66] | Italy | T2DM | Case-control study | Cases: 47<br>Controls: 50 | Tear | Increased |
| [5] | Poland | Obesity | Cross-sectional study | 313 (men aged 50–75 years) | Serum | Increased |
| [83] | Spain | Obesity | Cross-sectional study | 340 | Plasma | Increased association with the consumption of dairy products |
| [30] | China | Obesity | Cross-sectional study | 2111 | None | Higher Mn intake (e.g., >5.12 mg/d) was associated with a reduced risk of abdominal obesity and hypertriacylglycerolaemia among men. |
| [84] | Turkey | Obesity | Hospital-based case-control study | Cases: 57<br>Controls: 48 (children aged 6–17 years) | Serum | Increased |
| [85] | Turkey | Obesity | Prospective observational study | Cases: 34<br>Controls: 33 (children) | Serum | No different |
| [86] | USA | Obesity | Cross-sectional study | 5404 (children and adolescents aged 6–19 years) | Serum | Increased |
| [60] | Czech Republic | Atherosclerosis | Cross-sectional study | 1069 (aged 61–100 years) | Whole blood | Increased |
| [102] | Pakistan | Atherosclerosis | Case-control study | Cases: 90<br>Controls: 90 (aged 30–62 years) | Blood | Increased |

metabolic disease [67, 68] that is associated with increased risk of developing T2DM, cardiovascular disease, and NAFLD. Oxidative stress and production of ROS have been linked to the development of insulin resistance, T2DM, and obesity [7, 8, 69], suggesting a potential role for ROS in the pathogenesis of these disorders. In mouse 3T3-L1 mature adipocytes, there is an increased generation of superoxide and higher expression of antioxidant enzymes, potentially to help balance cellular ROS [70, 71]. In the presence of high ROS production, the antioxidant capacity of adipose tissue is also impaired in mouse models of obesity, and antioxidants such as SOD mimetics exert beneficial effects in metabolic diseases associated with obesity [72–75].

Compared with those fed a normal diet, rats fed a high fat-cholesterol diet had a significant decrease in MnSOD activity [76]. It has been shown that MnSOD deletion in mouse adipocytes triggers an adaptive stress response that activates mitochondrial biogenesis and enhanced mitochondrial fatty acid oxidation, thereby preventing diet-induced obesity and insulin resistance [77]. On the other hand, inflammation and excess triglyceride storage induced in obesity mice would raise epididymal adipocyte MnSOD [78]. In mouse studies, manganese [III] tetrakis [5,10,15,20]-benzoic acid porphyrin (MnTBAP), a nonpeptidic mimic of MnSOD, significantly reduced excess body weight and serum superoxide anion generation [79], ameliorated preexisting obesity, and improved insulin action by reducing caloric intake [80]. However, regarding the effect of MnTBAP on adiposity mice and in vivo insulin action, the evidences were conflicting. One suggested a preventive effect on the development of systemic insulin resistance and diabetes after high-fat diet, while the other was not [75, 81].

The concentrations of Mn in the liver, small intestine, and bone of obese mice were significantly lower than those in lean mice [82]. The cross-sectional epidemiological survey has found that plasma Mn was directly correlated with the consumption of dairy products [83]. Higher Mn intake (e.g., >5.12 mg/d) was associated with reduced risk of abdominal obesity and hypertriacylglycerolaemia among men in China [30]. Poland researchers have found that plasma Mn concentration was significantly higher in obese men aged 50–75 years [5]. Nevertheless, the data about blood Mn level in obese children are not consistent [84, 85]. The US National Health and Nutrition Examination Survey 2011–2014, performed with 5404 children and adolescents aged 6–19 years, revealed that the highest blood Mn concentration was associated with obesity and overweight [86].

## 5. Mn and Atherosclerosis

Atherosclerosis is the disease of the arterial wall, characterized by cholesterol accumulation, and culminates in potentially life-threatening conditions, such as heart attack, stroke, and angina [87]. Recent evidence suggests that atherosclerosis is a chronic inflammatory disease of the blood vessel wall [88–90]. Oxidized low-density lipoprotein (oxLDL) and endothelium dysfunction play a key role in the pathogenesis of atherosclerosis [91, 92]. Accumulation of oxLDL in the arterial wall is a characteristic feature of disease progression [88].

Previous studies have demonstrated that the roles of oxLDL and endothelium dysfunction are closely related to the imbalance of oxidative stress and inflammation in the pathogenic process of atherosclerosis [9, 10, 93, 94]. Mitochondrial DNA damage may result from reactive species production in vascular tissues and may in turn be an early event in the initiation of atherosclerotic lesions [95]. MnSOD was reported to reduce the oxLDL-induced apoptosis of macrophages [87, 96], protect against endothelial dysfunction [97, 98], and inhibit the oxidation of LDL by endothelial cells [9]. Furthermore, the association of decreased activity of MnSOD with atherogenesis has suggested that analysis of Mn content in the vascular wall matrix may be one of prospective methods for the diagnosis of early stages of atherosclerosis [99].

Several studies indicated that Mn supplementation could reduce high glucose-induced monocyte adhesion to endothelial cells and endothelial dysfunction and also lower blood levels of ICAM-1 and cholesterol [48, 49], elicit anti-inflammatory effects in endothelial cells [100], and potentially prevent or delay the progression of atherosclerosis. Little is known about the Mn concentration in atherosclerosis patient samples. It has been observed that the difference between the Mn contents of normal and atherosclerotic aortic tissue was not significant [101]. However, in epidemiologic studies, higher blood Mn levels were found in senior citizens aged 61–100 years with atherosclerosis compared to those without [60]. The same result was found in individuals aged 30–62 years [102].

## 6. Mn and Nonalcoholic Fatty Liver Disease

NAFLD, characterized by excess triglyceride (TG) accumulation in the absence of excessive alcohol intake, is the most common chronic liver disease and associated with MetS, obesity, and T2DM [103, 104]. This disease can progress to inflammatory nonalcoholic steatohepatitis (NASH), fibrosis, cirrhosis, and end-stage liver injury in humans [105, 106]. NASH, defined as a necroinflammatory disorder with fatty infiltration of hepatocytes, may progress to fibrosis and lead to cirrhosis [105]. Moreover, nonalcoholic steatosis is the first step in the pathogenesis of NASH linked to mitochondrial dysfunction and oxidative stress [11, 12, 107–109]. Rat histopathological observations suggest that nonpeptidyl mimics of MnSOD may help in the prevention and treatment of NASH in humans [79, 110]. However, few researchers have focused on the association between Mn concentration and NAFLD. In an in vitro NAFLD model established in human SMMC-7721 cells, Mn concentration did not significantly change in oleic acid-induced hepatic steatosis cells compared to the control [111].

## 7. Conclusions

Metabolic diseases are affected by dietary habits, the environment, and genes independently and through their interactions. They are complex diseases caused by multiple etiologies.

Intracellular homeostasis of Mn is associated with some metals. The Mn concentration also affects the absorption and metabolism of other metals. For example, Mn competes for iron (Fe) transporters by inhibiting divalent metal transporter 1 (DMT1) binding with Fe and disrupting the homeostasis of cesium (Cs), cobalt (Co), lead (Pb), mercury (Hg), nickel (Ni), and zinc (Zn) in cells [112]. Researchers have found that Fe depletion increases uptake and potentiates Mn-induced apoptosis, indicated by increased terminal deoxynucleotidyl transferase-mediated dUTP nick end labeling (TUNEL) staining of rat olfactory bulb and human SH-SY5Y cells [113]. Thus, low Fe levels could result in greater absorbance and accumulation of Mn, further influencing its toxicity [114, 115]. Moreover, Mn, copper (Cu), and Zn also competitively combined with SOD in oxidative stress. Alternatively, Mn exposure leads to increased Cu levels and decreased Fe and Ca levels in *Caenorhabditis elegans* (*C. elegans*) [116]. Therefore, studies about mixtures of metals are needed to better clarify how they crosstalk in metabolic diseases.

MnSOD plays a key role in mitochondrial oxidative stress, while the MnSOD Val16Ala polymorphism (rs4880) could result in reduced MnSOD activity and less efficient transport of MnSOD into the mitochondrial matrix [117, 118]. Both the MnSOD gene and levels of Mn could affect the activity of MnSOD [119]. Moreover, Mn supplementation enhanced MnSOD activity and protected against T2DM and its complications [47, 49]. Consequently, it is very important to systematically analyze whether the association with the risk of metabolic diseases and Mn levels is modified by genetic variation in MnSOD, Cu/ZnSOD, and related genes associated with Mn uptake, transport, metabolism, and excretion, such as DMT1, transferrin receptor (TfR), and soluble carrier family (SLC).

Several vitamins are antioxidative compounds, for example, vitamin C, vitamin D3, vitamin E, and $\beta$-carotene. The human-derived Caco-2 cell study indicated that expression of the SLC30A10 gene, as well as its encoded protein, the Zn and Mn transporter ZnT10, was augmented by vitamin D3 treatment [120]. MnSOD activity was significantly increased with high doses (30 and 100 mg/kg) of vitamin E after 4 and 6 weeks [121]. Thus, it is worth considering whether there is a causal relationship between Mn level and vitamin levels in the process of oxidation.

Previous researches have had small sample sizes, were designed primarily as cross-sectional and case-control studies, and lack large sample prospective studies. Therefore, a cohort study is urgently needed to confirm the causality between Mn and metabolic diseases, especially in occupational Mn-exposed workers [122]. In addition, by using a biological model study, for example, zebrafish and *C. elegans* [123, 124], we can further verify the effects of Mn and the combined action of various metals on metabolic diseases that were found in previous epidemiologic studies.

In summary, Mn is both a toxic and an essential trace element involved in human health and development. In the current literature, research supports a view that a U-shaped association exists between Mn, either deficiency in dietary Mn or excessive Mn exposure, and increased ROS generation as well as oxidative stress, which might affect the occurrence of metabolic diseases further, although it remains inadequate in molecular and epidemiological data on disease patients, especially among Mn workers.

## Conflicts of Interest

The authors declare that there is no conflict of interest regarding the publication of this article.

## Acknowledgments

This work was supported by the National Natural Science Foundation of China (Grant no. 81472962), the Fok Ying Tong Education Foundation's Young Teacher Award (Grant no. 141118), and the National Natural Science Foundation of Guangxi (Grant no. 2017GXNSFGA198003).

## References

[1] Q. Deng, J. Liu, Q. Li et al., "Interaction of occupational manganese exposure and alcohol drinking aggravates the increase of liver enzyme concentrations from a cross-sectional study in China," *Environmental Health*, vol. 12, no. 1, p. 30, 2013.

[2] J. L. Aschner and M. Aschner, "Nutritional aspects of manganese homeostasis," *Molecular Aspects of Medicine*, vol. 26, no. 4-5, pp. 353–362, 2005.

[3] E. S. Koh, S. J. Kim, H. E. Yoon et al., "Association of blood manganese level with diabetes and renal dysfunction: a cross-sectional study of the Korean general population," *BMC Endocrine Disorders*, vol. 14, no. 1, p. 24, 2014.

[4] R. Stegemann and D. A. Buchner, "Transgenerational inheritance of metabolic disease," *Seminars in Cell & Developmental Biology*, vol. 43, pp. 131–140, 2015.

[5] I. Rotter, D. Kosik-Bogacka, B. Dołęgowska, K. Safranow, A. Lubkowska, and M. Laszczyńska, "Relationship between the concentrations of heavy metals and bioelements in aging men with metabolic syndrome," *International Journal of Environmental Research and Public Health*, vol. 12, no. 12, pp. 3944–3961, 2015.

[6] D. Liu, L. Liu, Z. Hu, Z. Song, Y. Wang, and Z. Chen, "Evaluation of the oxidative stress–related genes *ALOX5*, *ALOX5AP*, *GPX1*, *GPX3* and *MPO* for contribution to the risk of type 2 diabetes mellitus in the Han Chinese population," *Diabetes and Vascular Disease Research*, 2018.

[7] M. Johns, R. Fyalka, J. A. Shea et al., "SR-135, a peroxynitrite decomposing catalyst, enhances $\beta$-cell function and survival in B6D2F1 mice fed a high fat diet," *Archives of Biochemistry and Biophysics*, vol. 577-578, pp. 49–59, 2015.

[8] D. S. Fernandez-Twinn and S. E. Ozanne, "Early life nutrition and metabolic programming," *Annals of the New York Academy of Sciences*, vol. 1212, no. 1, pp. 78–96, 2010.

[9] X. Fang, N. L. Weintraub, C. D. Rios et al., "Overexpression of human superoxide dismutase inhibits oxidation of low-density lipoprotein by endothelial cells," *Circulation Research*, vol. 82, no. 12, pp. 1289–1297, 1998.

[10] M. Glover, V. Y. Hebert, K. Nichols et al., "Overexpression of mitochondrial antioxidant manganese superoxide dismutase (MnSOD) provides protection against AZT- or

3TC-induced endothelial dysfunction," *Antiviral Research*, vol. 111, pp. 136–142, 2014.

[11] B. Fromenty, M. A. Robin, A. Igoudjil, A. Mansouri, and D. Pessayre, "The ins and outs of mitochondrial dysfunction in NASH," *Diabetes & Metabolism*, vol. 30, no. 2, pp. 121–138, 2004.

[12] K. Mehta, D. H. Van Thiel, N. Shah, and S. Mobarhan, "Nonalcoholic fatty liver disease: pathogenesis and the role of antioxidants," *Nutrition Reviews*, vol. 60, no. 9, pp. 289–293, 2002.

[13] M. Korc, "Manganese action on pancreatic protein synthesis in normal and diabetic rats," *American Journal of Physiology-Gastrointestinal and Liver Physiology*, vol. 245, no. 5, pp. G628–G634, 1983.

[14] E. Martin-Montañez, J. Pavia, L. J. Santin et al., "Involvement of IGF-II receptors in the antioxidant and neuroprotective effects of IGF-II on adult cortical neuronal cultures," *Biochimica et Biophysica Acta (BBA) - Molecular Basis of Disease*, vol. 1842, no. 7, pp. 1041–1051, 2014.

[15] S. Munusamy and L. A. MacMillan-Crow, "Mitochondrial superoxide plays a crucial role in the development of mitochondrial dysfunction during high glucose exposure in rat renal proximal tubular cells," *Free Radical Biology & Medicine*, vol. 46, no. 8, pp. 1149–1157, 2009.

[16] J. Azadmanesh and G. Borgstahl, "A review of the catalytic mechanism of human manganese superoxide dismutase," *Antioxidants*, vol. 7, no. 2, 2018.

[17] L. I. Rachek, S. I. Musiyenko, S. P. LeDoux, and G. L. Wilson, "Palmitate induced mitochondrial deoxyribonucleic acid damage and apoptosis in l6 rat skeletal muscle cells," *Endocrinology*, vol. 148, no. 1, pp. 293–299, 2007.

[18] J. L. Greger, "Nutrition versus toxicology of manganese in humans: evaluation of potential biomarkers," *Neurotoxicology*, vol. 20, no. 2-3, pp. 205–212, 1999.

[19] "Manganese deficiency in humans: fact or fiction?," *Nutrition Reviews*, vol. 46, no. 10, pp. 348–352, 1988.

[20] E. A. Malecki, "Manganese toxicity is associated with mitochondrial dysfunction and DNA fragmentation in rat primary striatal neurons," *Brain Research Bulletin*, vol. 55, no. 2, pp. 225–228, 2001.

[21] K. V. R. Rao and M. D. Norenberg, "Manganese induces the mitochondrial permeability transition in cultured astrocytes," *Journal of Biological Chemistry*, vol. 279, no. 31, pp. 32333–32338, 2004.

[22] K. Sriram, G. X. Lin, A. M. Jefferson et al., "Mitochondrial dysfunction and loss of Parkinson's disease-linked proteins contribute to neurotoxicity of manganese-containing welding fumes," *FASEB Journal*, vol. 24, no. 12, pp. 4989–5002, 2010.

[23] Y. X. Zheng, P. Chan, Z. F. Pan et al., "Polymorphism of metabolic genes and susceptibility to occupational chronic manganism," *Biomarkers*, vol. 7, no. 4, pp. 337–346, 2002.

[24] E. S. Ford, C. Li, L. C. McGuire, A. H. Mokdad, and S. Liu, "Intake of dietary magnesium and the prevalence of the metabolic syndrome among U.S. adults," *Obesity*, vol. 15, no. 5, pp. 1139–1146, 2007.

[25] M. A. Cornier, D. Dabelea, T. L. Hernandez et al., "The metabolic syndrome," *Endocrine Reviews*, vol. 29, no. 7, pp. 777–822, 2008.

[26] K. E. Wellen and G. S. Hotamisligil, "Inflammation, stress, and diabetes," *Journal of Clinical Investigation*, vol. 115, no. 5, pp. 1111–1119, 2005.

[27] S. Furukawa, T. Fujita, M. Shimabukuro et al., "Increased oxidative stress in obesity and its impact on metabolic syndrome," *Journal of Clinical Investigation*, vol. 114, no. 12, pp. 1752–1761, 2004.

[28] J. F. Keaney Jr., M. G. Larson, R. S. Vasan et al., "Obesity and systemic oxidative stress: clinical correlates of oxidative stress in the Framingham Study," *Arteriosclerosis, Thrombosis, and Vascular Biology*, vol. 23, no. 3, pp. 434–439, 2003.

[29] M. Pinzani, F. Marra, and V. Carloni, "Signal transduction in hepatic stellate cells," *Liver*, vol. 18, no. 1, pp. 2–13, 1998.

[30] B. Zhou, X. Su, D. Su et al., "Dietary intake of manganese and the risk of the metabolic syndrome in a Chinese population," *British Journal of Nutrition*, vol. 116, no. 5, pp. 853–863, 2016.

[31] M. K. Choi and Y. J. Bae, "Relationship between dietary magnesium, manganese, and copper and metabolic syndrome risk in Korean adults: the Korea National Health and Nutrition Examination Survey (2007-2008)," *Biological Trace Element Research*, vol. 156, no. 1–3, pp. 56–66, 2013.

[32] Y. Li, H. Guo, M. Wu, and M. Liu, "Serum and dietary antioxidant status is associated with lower prevalence of the metabolic syndrome in a study in Shanghai, China," *Asia Pacific Journal of Clinical Nutrition*, vol. 22, no. 1, pp. 60–68, 2013.

[33] S. Y. Rhee, Y. C. Hwang, J. T. Woo et al., "Blood lead is significantly associated with metabolic syndrome in Korean adults: an analysis based on the Korea National Health and Nutrition Examination Survey (KNHANES), 2008," *Cardiovascular Diabetology*, vol. 12, no. 1, p. 9, 2013.

[34] P. Zimmet, K. G. M. M. Alberti, and J. Shaw, "Global and societal implications of the diabetes epidemic," *Nature*, vol. 414, no. 6865, pp. 782–787, 2001.

[35] F. Giacco and M. Brownlee, "Oxidative stress and diabetic complications," *Circulation Research*, vol. 107, no. 9, pp. 1058–1070, 2010.

[36] T. Nishikawa, D. Edelstein, X. L. du et al., "Normalizing mitochondrial superoxide production blocks three pathways of hyperglycaemic damage," *Nature*, vol. 404, no. 6779, pp. 787–790, 2000.

[37] S. D. Martin, S. Morrison, N. Konstantopoulos, and S. L. McGee, "Mitochondrial dysfunction has divergent, cell type-dependent effects on insulin action," *Molecular Metabolism*, vol. 3, no. 4, pp. 408–418, 2014.

[38] B. B. Lowell and G. I. Shulman, "Mitochondrial dysfunction and type 2 diabetes," *Science*, vol. 307, no. 5708, pp. 384–387, 2005.

[39] K. Morino, K. F. Petersen, S. Dufour et al., "Reduced mitochondrial density and increased IRS-1 serine phosphorylation in muscle of insulin-resistant offspring of type 2 diabetic parents," *Journal of Clinical Investigation*, vol. 115, no. 12, pp. 3587–3593, 2005.

[40] K. L. Hoehn, A. B. Salmon, C. Hohnen-Behrens et al., "Insulin resistance is a cellular antioxidant defense mechanism," *Proceedings of the National Academy of Sciences of the United States of America*, vol. 106, no. 42, pp. 17787–17792, 2009.

[41] X. Shen, S. Zheng, N. S. Metreveli, and P. N. Epstein, "Protection of cardiac mitochondria by overexpression of MnSOD reduces diabetic cardiomyopathy," *Diabetes*, vol. 55, no. 3, pp. 798–805, 2006.

[42] H. Goto, T. Nishikawa, K. Sonoda et al., "Endothelial MnSOD overexpression prevents retinal VEGF expression

in diabetic mice," *Biochemical and Biophysical Research Communications*, vol. 366, no. 3, pp. 814–820, 2008.

[43] R. A. Kowluru, V. Kowluru, Y. Xiong, and Y. S. Ho, "Overexpression of mitochondrial superoxide dismutase in mice protects the retina from diabetes-induced oxidative stress," *Free Radical Biology & Medicine*, vol. 41, no. 8, pp. 1191–1196, 2006.

[44] A. M. Vincent, J. W. Russell, K. A. Sullivan et al., "SOD2 protects neurons from injury in cell culture and animal models of diabetic neuropathy," *Experimental Neurology*, vol. 208, no. 2, pp. 216–227, 2007.

[45] S. Bertera, M. L. Crawford, A. M. Alexander et al., "Gene transfer of manganese superoxide dismutase extends islet graft function in a mouse model of autoimmune diabetes," *Diabetes*, vol. 52, no. 2, pp. 387–393, 2003.

[46] M. Navarro-Alarcon, F. J. Ruiz-Ojeda, R. M. Blanca-Herrera, and A. Agil, "Antioxidant activity of melatonin in diabetes in relation to the regulation and levels of plasma Cu, Zn, Fe, Mn, and Se in Zucker diabetic fatty rats," *Nutrition*, vol. 29, no. 5, pp. 785–789, 2013.

[47] S. H. Lee, H. A. Jouihan, R. C. Cooksey et al., "Manganese supplementation protects against diet-induced diabetes in wild type mice by enhancing insulin secretion," *Endocrinology*, vol. 154, no. 3, pp. 1029–1038, 2013.

[48] E. Burlet and S. K. Jain, "Manganese supplementation increases adiponectin and lowers ICAM-1 and creatinine blood levels in Zucker type 2 diabetic rats, and downregulates ICAM-1 by upregulating adiponectin multimerization protein (DsbA-L) in endothelial cells," *Molecular and Cellular Biochemistry*, vol. 429, no. 1-2, pp. 1–10, 2017.

[49] E. Burlet and S. K. Jain, "Manganese supplementation reduces high glucose-induced monocyte adhesion to endothelial cells and endothelial dysfunction in Zucker diabetic fatty rats," *Journal of Biological Chemistry*, vol. 288, no. 9, pp. 6409–6416, 2013.

[50] M. M. Delmastro-Greenwood, T. Votyakova, E. Goetzman et al., "Mn porphyrin regulation of aerobic glycolysis: implications on the activation of diabetogenic immune cells," *Antioxidants & Redox Signaling*, vol. 19, no. 16, pp. 1902–1915, 2013.

[51] D. Baly, B. Lonnerdal, and C. Keen, "Effects of high doses of manganese on carbohydrate homeostasis," *Toxicology Letters*, vol. 25, no. 1, pp. 95–102, 1985.

[52] L. S. Hurley, C. L. Keen, and D. L. Baly, "Manganese deficiency and toxicity: effects on carbohydrate metabolism in the rat," *Neurotoxicology*, vol. 5, no. 1, pp. 97–104, 1984.

[53] Z. Mousavi, M. Hassanpourezatti, P. Najafizadeh, S. Rezagholian, M. S. Rhamanifar, and N. Nosrati, "Effects of subcutaneous injection $MnO_2$ micro- and nanoparticles on blood glucose level and lipid profile in rat," *Iranian Journal of Medical Sciences*, vol. 41, no. 6, pp. 518–524, 2016.

[54] C. R. Flores, M. P. Puga, K. Wrobel, M. E. Garay Sevilla, and K. Wrobel, "Trace elements status in diabetes mellitus type 2: possible role of the interaction between molybdenum and copper in the progress of typical complications," *Diabetes Research and Clinical Practice*, vol. 91, no. 3, pp. 333–341, 2011.

[55] S. Ekin, N. Mert, H. Gunduz, and I. Meral, "Serum sialic acid levels and selected mineral status in patients with type 2 diabetes mellitus," *Biological Trace Element Research*, vol. 94, no. 3, pp. 193–202, 2003.

[56] T. G. Kazi, H. I. Afridi, N. Kazi et al., "Copper, chromium, manganese, iron, nickel, and zinc levels in biological samples of diabetes mellitus patients," *Biological Trace Element Research*, vol. 122, no. 1, pp. 1–18, 2008.

[57] M. Badran, R. Morsy, H. Soliman, and T. Elnimr, "Assessment of trace elements levels in patients with type 2 diabetes using multivariate statistical analysis," *Journal of Trace Elements in Medicine and Biology*, vol. 33, pp. 114–119, 2016.

[58] G. Forte, B. Bocca, A. Peruzzu et al., "Blood metals concentration in type 1 and type 2 diabetics," *Biological Trace Element Research*, vol. 156, no. 1–3, pp. 79–90, 2013.

[59] H. I. Afridi, T. G. Kazi, N. Kazi et al., "Status of essential trace metals in biological samples of diabetic mother and their neonates," *Archives of Gynecology and Obstetrics*, vol. 280, no. 3, pp. 415–423, 2009.

[60] J. Rambousková, A. Krsková, M. Slavíková et al., "Trace elements in the blood of institutionalized elderly in the Czech Republic," *Archives of Gerontology and Geriatrics*, vol. 56, no. 2, pp. 389–394, 2013.

[61] Z. Shan, S. Chen, T. Sun et al., "U-shaped association between plasma manganese levels and type 2 diabetes," *Environmental Health Perspectives*, vol. 124, no. 12, pp. 1876–1881, 2016.

[62] B. Liu, W. Feng, J. Wang et al., "Association of urinary metals levels with type 2 diabetes risk in coke oven workers," *Environmental Pollution*, vol. 210, pp. 1–8, 2016.

[63] W. Feng, X. He, M. Chen et al., "Urinary metals and heart rate variability: a cross-sectional study of urban adults in Wuhan, China," *Environmental Health Perspectives*, vol. 123, no. 3, pp. 217–222, 2015.

[64] H. I. Afridi, T. G. Kazi, D. Brabazon, S. Naher, and F. N. Talpur, "Comparative metal distribution in scalp hair of Pakistani and Irish referents and diabetes mellitus patients," *Clinica Chimica Acta*, vol. 415, pp. 207–214, 2013.

[65] C. Ekmekcioglu, C. Prohaska, K. Pomazal, I. Steffan, G. Schernthaner, and W. Marktl, "Concentrations of seven trace elements in different hematological matrices in patients with type 2 diabetes as compared to healthy controls," *Biological Trace Element Research*, vol. 79, no. 3, pp. 205–219, 2001.

[66] A. Cancarini, J. Fostinelli, L. Napoli, M. E. Gilberti, P. Apostoli, and F. Semeraro, "Trace elements and diabetes: assessment of levels in tears and serum," *Experimental Eye Research*, vol. 154, pp. 47–52, 2017.

[67] C. L. Ogden, M. D. Carroll, and K. M. Flegal, "Prevalence of obesity in the United States," *JAMA*, vol. 312, no. 2, pp. 189-190, 2014.

[68] C. P. Kovesdy, S. L. Furth, C. Zoccali, and on behalf of the World Kidney Day Steering Committee, "Obesity and kidney disease: hidden consequences of the epidemic," *American Journal of Nephrology*, vol. 45, no. 3, pp. 283–291, 2017.

[69] N. Bashan, J. Kovsan, I. Kachko, H. Ovadia, and A. Rudich, "Positive and negative regulation of insulin signaling by reactive oxygen and nitrogen species," *Physiological Reviews*, vol. 89, no. 1, pp. 27–71, 2009.

[70] P. H. Ducluzeau, M. Priou, M. Weitheimer et al., "Dynamic regulation of mitochondrial network and oxidative functions during 3T3-L1 fat cell differentiation," *Journal of Physiology and Biochemistry*, vol. 67, no. 3, pp. 285–296, 2011.

[71] T. Kojima, T. Norose, K. Tsuchiya, and K. Sakamoto, "Mouse 3T3-L1 cells acquire resistance against oxidative stress as the adipocytes differentiate via the transcription factor FoxO," *Apoptosis*, vol. 15, no. 1, pp. 83–93, 2010.

[72] A. R. Subauste and C. F. Burant, "Role of FoxO1 in FFA-induced oxidative stress in adipocytes," *American Journal of Physiology-Endocrinology and Metabolism*, vol. 293, no. 1, pp. E159–E164, 2007.

[73] H. Kobayashi, M. Matsuda, A. Fukuhara, R. Komuro, and I. Shimomura, "Dysregulated glutathione metabolism links to impaired insulin action in adipocytes," *American Journal of Physiology-Endocrinology and Metabolism*, vol. 296, no. 6, pp. E1326–E1334, 2009.

[74] K. C. Coate and K. W. Huggins, "Consumption of a high glycemic index diet increases abdominal adiposity but does not influence adipose tissue pro-oxidant and antioxidant gene expression in C57BL/6 mice," *Nutrition Research*, vol. 30, no. 2, pp. 141–150, 2010.

[75] K. M. Pires, O. Ilkun, M. Valente, and S. Boudina, "Treatment with a SOD mimetic reduces visceral adiposity, adipocyte death, and adipose tissue inflammation in high fat-fed mice," *Obesity*, vol. 22, no. 1, pp. 178–187, 2014.

[76] S. H. Ko, J. H. Park, S. Y. Kim, S. W. Lee, S. S. Chun, and E. Park, "Antioxidant effects of spinach (Spinacia oleracea L.) supplementation in hyperlipidemic rats," *Preventive Nutrition and Food Science*, vol. 19, no. 1, pp. 19–26, 2014.

[77] Y. H. Han, M. Buffolo, K. M. Pires, S. Pei, P. E. Scherer, and S. Boudina, "Adipocyte-specific deletion of manganese superoxide dismutase protects from diet-induced obesity through increased mitochondrial uncoupling and biogenesis," *Diabetes*, vol. 65, no. 9, pp. 2639–2651, 2016.

[78] S. Krautbauer, K. Eisinger, M. Neumeier et al., "Free fatty acids, lipopolysaccharide and IL-1$\alpha$ induce adipocyte manganese superoxide dismutase which is increased in visceral adipose tissues of obese rodents," *PLoS One*, vol. 9, no. 1, article e86866, 2014.

[79] A. Laurent, C. Nicco, J. Tran van Nhieu et al., "Pivotal role of superoxide anion and beneficial effect of antioxidant molecules in murine steatohepatitis," *Hepatology*, vol. 39, no. 5, pp. 1277–1285, 2004.

[80] J. R. Brestoff, T. Brodsky, A. Z. Sosinsky et al., "Manganese [III] tetrakis [5,10,15,20]-benzoic acid porphyrin reduces adiposity and improves insulin action in mice with pre-existing obesity," *PLoS One*, vol. 10, no. 9, article e0137388, 2015.

[81] N. Houstis, E. D. Rosen, and E. S. Lander, "Reactive oxygen species have a causal role in multiple forms of insulin resistance," *Nature*, vol. 440, no. 7086, pp. 944–948, 2006.

[82] M. L. Kennedy, M. L. Failla, and J. C. Smith Jr., "Influence of genetic obesity on tissue concentrations of zinc, copper, manganese and iron in mice," *Journal of Nutrition*, vol. 116, no. 8, pp. 1432–1441, 1986.

[83] C. Sanchez, M. Lopez-Jurado, P. Aranda, and J. Llopis, "Plasma levels of copper, manganese and selenium in an adult population in southern Spain: influence of age, obesity and lifestyle factors," *Science of the Total Environment*, vol. 408, no. 5, pp. 1014–1020, 2010.

[84] Y. Cayir, A. Cayir, M. I. Turan et al., "Antioxidant status in blood of obese children: the relation between trace elements, paraoxonase, and arylesterase values," *Biological Trace Element Research*, vol. 160, no. 2, pp. 155–160, 2014.

[85] M. E. Tascilar, I. T. Ozgen, A. Abaci, M. Serdar, and O. Aykut, "Trace elements in obese Turkish children," *Biological Trace Element Research*, vol. 143, no. 1, pp. 188–195, 2011.

[86] Y. Fan, C. Zhang, and J. Bu, "Relationship between selected serum metallic elements and obesity in children and adolescent in the U.S.," *Nutrients*, vol. 9, no. 12, 2017.

[87] V. A. Shatrov and B. Brune, "Induced expression of manganese superoxide dismutase by non-toxic concentrations of oxidized low-density lipoprotein (oxLDL) protects against oxLDL-mediated cytotoxicity," *Biochemical Journal*, vol. 374, no. 2, pp. 505–511, 2003.

[88] R. Ross, "Atherosclerosis—an inflammatory disease," *New England Journal of Medicine*, vol. 340, no. 2, pp. 115–126, 1999.

[89] A. J. Lusis, "Atherosclerosis," *Nature*, vol. 407, no. 6801, pp. 233–241, 2000.

[90] L. Hegyi, S. J. Hardwick, R. C. M. Siow, and J. N. Skepper, "Macrophage death and the role of apoptosis in human atherosclerosis," *Journal of Hematotherapy & Stem Cell Research*, vol. 10, no. 1, pp. 27–42, 2001.

[91] D. P. Hajjar and M. E. Haberland, "Lipoprotein trafficking in vascular cells. Molecular Trojan horses and cellular saboteurs," *Journal of Biological Chemistry*, vol. 272, no. 37, pp. 22975–22978, 1997.

[92] J. W. Heinecke, "Oxidants and antioxidants in the pathogenesis of atherosclerosis: implications for the oxidized low density lipoprotein hypothesis," *Atherosclerosis*, vol. 141, no. 1, pp. 1–15, 1998.

[93] J. Steppan, D. Nyhan, and D. E. Berkowitz, "Development of novel arginase inhibitors for therapy of endothelial dysfunction," *Frontiers in Immunology*, vol. 4, p. 278, 2013.

[94] M. Feletou and P. M. Vanhoutte, "Endothelial dysfunction: a multifaceted disorder (The Wiggers Award Lecture)," *American Journal of Physiology-Heart and Circulatory Physiology*, vol. 291, no. 3, pp. H985–H1002, 2006.

[95] S. W. Ballinger, C. Patterson, C. A. Knight-Lozano et al., "Mitochondrial integrity and function in atherogenesis," *Circulation*, vol. 106, no. 5, pp. 544–549, 2002.

[96] R. Kinscherf, R. Claus, M. Wagner et al., "Apoptosis caused by oxidized LDL is manganese superoxide dismutase and p53 dependent," *FASEB Journal*, vol. 12, no. 6, pp. 461–467, 1998.

[97] F. Jiang, Y. Guo, D. Salvemini, and G. J. Dusting, "Superoxide dismutase mimetic M40403 improves endothelial function in apolipoprotein(E)-deficient mice," *British Journal of Pharmacology*, vol. 139, no. 6, pp. 1127–1134, 2003.

[98] M. Ohashi, M. S. Runge, F. M. Faraci, and D. D. Heistad, "MnSOD deficiency increases endothelial dysfunction in ApoE-deficient mice," *Arteriosclerosis, Thrombosis, and Vascular Biology*, vol. 26, no. 10, pp. 2331–2336, 2006.

[99] A. P. Lozhkin, T. B. Biktagirov, V. A. Abdul'yanov et al., "Manganese in atherogenesis: detection, origin, and a role," *Biochemistry (Moscow) Supplement Series B: Biomedical Chemistry*, vol. 5, no. 2, pp. 158–162, 2011.

[100] Q. Zhou, M. Einert, H. Schmitt et al., "MnTBAP increases BMPR-II expression in endothelial cells and attenuates vascular inflammation," *Vascular Pharmacology*, vol. 84, pp. 67–73, 2016.

[101] S. Mendis, "Magnesium, zinc, and manganese in atherosclerosis of the aorta," *Biological Trace Element Research*, vol. 22, no. 3, pp. 251–256, 1989.

[102] A. Ilyas and M. H. Shah, "Multivariate statistical evaluation of trace metal levels in the blood of atherosclerosis patients in comparison with healthy subjects," *Heliyon*, vol. 2, no. 1, article e00054, 2016.

[103] K. Cusi, "Role of insulin resistance and lipotoxicity in non-alcoholic steatohepatitis," *Clinics in Liver Disease*, vol. 13, no. 4, pp. 545–563, 2009.

[104] E. Fabbrini, S. Sullivan, and S. Klein, "Obesity and nonalcoholic fatty liver disease: biochemical, metabolic, and clinical implications," *Hepatology*, vol. 51, no. 2, pp. 679–689, 2010.

[105] P. Angulo, "Nonalcoholic fatty liver disease," *New England Journal of Medicine*, vol. 346, no. 16, pp. 1221–1231, 2002.

[106] A. E. Feldstein, A. Canbay, M. E. Guicciardi, H. Higuchi, S. F. Bronk, and G. J. Gores, "Diet associated hepatic steatosis sensitizes to Fas mediated liver injury in mice," *Journal of Hepatology*, vol. 39, no. 6, pp. 978–983, 2003.

[107] D. Pessayre, A. Mansouri, and B. Fromenty, "V. Mitochondrial dysfunction in steatohepatitis," *American Journal of Physiology-Gastrointestinal and Liver Physiology*, vol. 282, no. 2, pp. G193–G199, 2002.

[108] H. Jaeschke, G. J. Gores, A. I. Cederbaum, J. A. Hinson, D. Pessayre, and J. J. Lemasters, "Mechanisms of hepatotoxicity," *Toxicological Sciences*, vol. 65, no. 2, pp. 166–176, 2002.

[109] S. Chitturi and G. C. Farrell, "Etiopathogenesis of nonalcoholic steatohepatitis," *Seminars in Liver Disease*, vol. 21, no. 1, pp. 27–42, 2001.

[110] A. Rezazadeh and R. Yazdanparast, "Prevention of nonalcoholic steatohepatitis in rats by two manganese-salen complexes," *Iranian Biomedical Journal*, vol. 18, no. 1, pp. 41–48, 2014.

[111] S. Wang, X. Kuang, Z. Fang, Z. Huang, and P. Shi, "Effect of oleic acid on the levels of eight metal ions in human hepatoma SMMC-7721 cells," *Biological Trace Element Research*, vol. 159, no. 1–3, pp. 445–450, 2014.

[112] P. Chen, S. Chakraborty, S. Mukhopadhyay et al., "Manganese homeostasis in the nervous system," *Journal of Neurochemistry*, vol. 134, no. 4, pp. 601–610, 2015.

[113] Y. A. Seo, Y. Li, and M. Wessling-Resnick, "Iron depletion increases manganese uptake and potentiates apoptosis through ER stress," *NeuroToxicology*, vol. 38, pp. 67–73, 2013.

[114] V. A. Fitsanakis, N. Zhang, M. J. Avison, K. M. Erikson, J. C. Gore, and M. Aschner, "Changes in dietary iron exacerbate regional brain manganese accumulation as determined by magnetic resonance imaging," *Toxicological Sciences*, vol. 120, no. 1, pp. 146–153, 2011.

[115] E. A. Smith, P. Newland, K. G. Bestwick, and N. Ahmed, "Increased whole blood manganese concentrations observed in children with iron deficiency anaemia," *Journal of Trace Elements in Medicine and Biology*, vol. 27, no. 1, pp. 65–69, 2013.

[116] S. Angeli, T. Barhydt, R. Jacobs, D. W. Killilea, G. J. Lithgow, and J. K. Andersen, "Manganese disturbs metal and protein homeostasis in *Caenorhabditis elegans*," *Metallomics*, vol. 6, no. 10, pp. 1816–1823, 2014.

[117] S. Shimoda-Matsubayashi, H. Matsumine, T. Kobayashi, Y. Nakagawa-Hattori, Y. Shimizu, and Y. Mizuno, "Structural dimorphism in the mitochondrial targeting sequence in the human manganese superoxide dismutase gene: a predictive evidence for conformational change to influence mitochondrial transport and a study of allelic association in Parkinson's disease," *Biochemical and Biophysical Research Communications*, vol. 226, no. 2, pp. 561–565, 1996.

[118] A. Sutton, H. Khoury, C. Prip-Buus, C. Cepanec, D. Pessayre, and F. Degoul, "The Ala16Val genetic dimorphism modulates the import of human manganese superoxide dismutase into rat liver mitochondria," *Pharmacogenetics*, vol. 13, no. 3, pp. 145–157, 2003.

[119] G. Bresciani, I. B. M. Cruz, J. A. de Paz, M. J. Cuevas, and J. González-Gallego, "The MnSOD Ala16Val SNP: relevance to human diseases and interaction with environmental factors," *Free Radical Research*, vol. 47, no. 10, pp. 781–792, 2013.

[120] T. Claro da Silva, C. Hiller, Z. Gai, and G. A. Kullak-Ublick, "Vitamin $D_3$ transactivates the zinc and manganese transporter SLC30A10 via the vitamin D receptor," *The Journal of Steroid Biochemistry and Molecular Biology*, vol. 163, pp. 77–87, 2016.

[121] M. Hajiani, F. Razi, A. Golestani et al., "Time- and dose-dependent differential regulation of copper-zinc superoxide dismutase and manganese superoxide dismutase enzymatic activity and mRNA level by vitamin E in rat blood cells," *Redox Report*, vol. 17, no. 3, pp. 101–107, 2012.

[122] Y. Lv, Y. Zou, J. Liu et al., "Rationale, design and baseline results of the Guangxi manganese-exposed workers healthy cohort (GXMEWHC) study," *BMJ Open*, vol. 4, no. 7, article e005070, 2014.

[123] Z. Xia, J. Wei, Y. Li et al., "Zebrafish *slc30a10* deficiency revealed a novel compensatory mechanism of Atp2c1 in maintaining manganese homeostasis," *PLoS Genetics*, vol. 13, no. 7, article e1006892, 2017.

[124] P. Chen, M. R. DeWitt, J. Bornhorst et al., "Age- and manganese-dependent modulation of dopaminergic phenotypes in a *C. elegans DJ-1* genetic model of Parkinson's disease," *Metallomics*, vol. 7, no. 2, pp. 289–298, 2015.

Hindawi
Oxidative Medicine and Cellular Longevity
Volume 2018, Article ID 8949450, 13 pages
https://doi.org/10.1155/2018/8949450

*Research Article*

# Ex Vivo Cardiotoxicity of Antineoplastic Casiopeinas Is Mediated through Energetic Dysfunction and Triggered Mitochondrial-Dependent Apoptosis

**Christian Silva-Platas,[1] César A. Villegas,[1] Yuriana Oropeza-Almazán,[1] Mariana Carrancá,[1] Alejandro Torres-Quintanilla,[1] Omar Lozano,[1] Javier Valero-Elizondo,[1] Elena C. Castillo,[1,2] Judith Bernal-Ramírez,[1] Evaristo Fernández-Sada,[1] Luis F. Vega,[1] Niria Treviño-Saldaña,[1] Héctor Chapoy-Villanueva,[1] Lena Ruiz-Azuara,[3] Carmen Hernández-Brenes,[2,4] Leticia Elizondo-Montemayor,[1,2] Carlos E. Guerrero-Beltrán,[1] Karla Carvajal,[5] María E. Bravo-Gómez,[6] and Gerardo García-Rivas[1,2]**

[1]*Cátedra de Cardiología y Medicina Vascular, Escuela de Medicina, Tecnológico de Monterrey, 64849 Monterrey, NL, Mexico*
[2]*Centro de Investigación Biomédica, Hospital Zambrano Hellion, Tecnológico de Monterrey, 66278 San Pedro Garza García, NL, Mexico*
[3]*Departamento de Química Inorgánica, Facultad de Química, Universidad Nacional Autónoma de México, 04510 Mexico City, Mexico*
[4]*Escuela de Ingeniería y Ciencias, Tecnológico de Monterrey, 64849 Monterrey, NL, Mexico*
[5]*Laboratorio de Nutrición Experimental, Instituto Nacional de Pediatría, 04530 Mexico City, Mexico*
[6]*Departamento de Toxicología, Facultad de Medicina, Universidad Nacional Autónoma de México, 04510 Mexico City, Mexico*

Correspondence should be addressed to Gerardo García-Rivas; gdejesus@itesm.mx

Received 31 August 2017; Revised 23 December 2017; Accepted 23 January 2018; Published 25 March 2018

Academic Editor: Daiana S. Avila

Copyright © 2018 Christian Silva-Platas et al. This is an open access article distributed under the Creative Commons Attribution License, which permits unrestricted use, distribution, and reproduction in any medium, provided the original work is properly cited.

Casiopeinas are a group of copper-based antineoplastic molecules designed as a less toxic and more therapeutic alternative to cisplatin or Doxorubicin; however, there is scarce evidence about their toxic effects on the whole heart and cardiomyocytes. Given this, rat hearts were perfused with Casiopeinas or Doxorubicin and the effects on mechanical performance, energetics, and mitochondrial function were measured. As well, the effects of Casiopeinas-triggered cell death were explored in isolated cardiomyocytes. Casiopeinas III-Ea, II-gly, and III-ia induced a progressive and sustained inhibition of heart contractile function that was dose- and time-dependent with an $IC_{50}$ of $1.3 \pm 0.2$, $5.5 \pm 0.5$, and $10 \pm 0.7\,\mu M$, correspondingly. Myocardial oxygen consumption was not modified at their respective $IC_{50}$, although ATP levels were significantly reduced, indicating energy impairment. Isolated mitochondria from Casiopeinas-treated hearts showed a significant loss of membrane potential and reduction of mitochondrial $Ca^{2+}$ retention capacity. Interestingly, Cyclosporine A inhibited Casiopeinas-induced mitochondrial $Ca^{2+}$ release, which suggests the involvement of the mitochondrial permeability transition pore opening. In addition, Casiopeinas reduced the viability of cardiomyocytes and stimulated the activation of caspases 3, 7, and 9, demonstrating a cell death mitochondrial-dependent mechanism. Finally, the early perfusion of Cyclosporine A in isolated hearts decreased Casiopeinas-induced dysfunction with reduction of their toxic effect. Our results suggest that heart cardiotoxicity of Casiopeinas is similar to that of Doxorubicin, involving heart mitochondrial dysfunction, loss of membrane potential, changes in energetic metabolites, and apoptosis triggered by mitochondrial permeability.

## 1. Introduction

The search for cancer treatments has generated novel discoveries of underlying carcinogenesis mechanisms, including discoveries in cardiovascular research, given that many of the targets explored in tumors play critical roles in the heart. The collective efforts of cardiovascular and cancer researchers along with that of clinical researchers are needed to understand how to safely translate such efforts from the laboratory bench to the patients. For instance, anthracyclines such as Doxorubicin (Doxo) can generate heart failure (HF) and left ventricular dysfunction in a dose-dependent manner [1]. Anthracyclines produce cardiac toxicity by increasing myofibrillar disarray and mitochondrial dysfunction [2]. Moreover, Doxo induces reactive oxygen species (ROS) production in the heart via redox cycling of the drug at complex I of the electron transport chain [3]. Therefore, prior work supports the idea that mitochondria are a primary target of both acute and chronic Doxo-induced cardiotoxicity.

Casiopeinas (Cas) are recently developed copper-containing drugs that have shown promising results as chemotherapeutic agents in animal models, as well as in clinical trials [4, 5]. Nevertheless, Cas have shown acute toxicity in a canine model, including cardiac arrhythmias (i.e., bradycardia, heart block, and ventricular arrhythmias) and systolic dysfunction [6]. Cas toxicity has also been related to the inhibition of energy metabolism with changes in glycolytic and oxidative phosphorylation fluxes [7–9]. Experiments in rat hearts have shown that Cas markedly depress contractility and reduce ATP and phosphocreatine (PCr) pools [10]; however, the precise mechanisms behind these responses are still not well understood. Recently, *in vitro* experiments with isolated cardiac mitochondria have shown that Cas increased the oxygen consumption rate at basal respiration and depolarized mitochondrial membrane potential, suggesting that Cas act as mitochondrial uncouplers [8]. In addition, the immunosuppressant cyclosporine A (CsA) inhibited Cas-induced mitochondrial swelling and depolarization, proposing the involvement of the permeability transition pore opening (MPT) [8]. Highlighting its importance, the MPT opening has been associated with matrix swelling and the release of small proapoptotic proteins, such as cytochrome c and oxidative damage of protein or lipids [9, 11]. These changes might be responsible for the inhibitory effect on the electron transport chain in rat heart mitochondria [8] and the Cas-triggered apoptosis observed in neoplastic cells and tumors [12]. In the present study, we aimed to integrate the Cas cardiotoxicity known effects, which include potential impairment of energy metabolism, mitochondrial dysfunction, and MPT involvement, into a whole-heart model, in order to better understand the mechanisms underlying the heart tissue contractile dysfunction and apoptosis. Furthermore, the study explored CsA perfusion as a novel strategy to reduce the toxic effects of Cas in the whole-heart rat model. The proposed mechanisms for Cas were also studied in isolated cardiomyocytes and compared to the effects with Doxo.

## 2. Materials and Methods

*2.1. Animal Use.* All procedures involving animals and their care were performed in accordance with the animal care guidelines of the National Institutes of Health, USA (2011 edition). All procedures were approved by the animal use and care committee of Tecnológico de Monterrey Medical School (protocol number 2011-Re-017).

*2.2. Ex Vivo Heart Experiments.* Male Wistar rats (250–300 g) were injected with heparin ($10^3$ U·kg$^{-1}$, i.p.) 20 minutes prior to anesthesia with pentobarbital (100 mg·kg$^{-1}$, i.p.). When bilateral corneal reflex was absent, the heart was excised through an abdominal approach. Then, the ascending aorta was visualized and cut and the heart was placed in a cardioplegic solution. To avoid ischemia, the time between cutting the diaphragm to placing the heart in the solution was less than 60 seconds. The hearts were mounted in accordance with the Langendorff model and perfused at a constant flow (12 ml·min$^{-1}$) with a Krebs-Henseleit buffer as previously described [13]. A latex balloon connected to a pressure transducer filled with saline solution was inserted into the left ventricle after establishing autonomous contraction. The pulmonary artery was cannulated and connected to a closed chamber using a Clark-type oxygen electrode (Yellow Springs Instruments, Yellow Springs, Ohio) to measure myocardial oxygen consumption ($MVO_2$) in the coronary effluent. The rate of $MVO_2$ was calculated as the difference between the concentration in the K-H buffer before (100%) and after perfusion. Data Trax software (WPI, Sarasota, Florida) was used for continuous recording of the heart rate (HR), left ventricular pressure (LVP), $MVO_2$, and maximum positive and negative derivative of left ventricular pressure (±dP/dt). The baseline was established during 10–15 minutes of K-H perfusion. Each concentration of Cas or Doxo remained in the heart for 30 min. Hearts in the control group were perfused with K-H buffer during the whole experimental time. Rate pressure product ($RPP = HR \times LVP$) and cardiac efficiency ($CE = RPP \times MVO_2$) were calculated as previously reported [14].

*2.3. Cell Fractionation and Sample Preparation.* To measure the energetic metabolites ATP, phosphocreatine (PCr), and aconitase activity at the end of the perfusion protocols, samples were prepared as follows: the hearts were removed from the perfusion system by cutting the aorta and immediately flash-frozen with liquid $N_2$, weighed, and stored at −80°C. Afterward, the hearts were homogenized in ice-cold buffer containing 250 mM sucrose, 10 mM HEPES, and 1 mM EDTA (pH 7.4). For enzymatic determination, aliquots of the homogenate were immediately frozen in liquid nitrogen and stored at −80°C. Quantification of ATP and PCr was carried out in a HPLC system with a dual-pump gradient (Waters Chromatography, Toronto, Canada) as previously described [15].

To measure mitochondrial oxygen consumption, mitochondrial membrane potential, and $Ca^{2+}$ uptake, cytochrome c samples were prepared as follows: after perfusion, heart tissue from the left ventricle was minced and homogenized

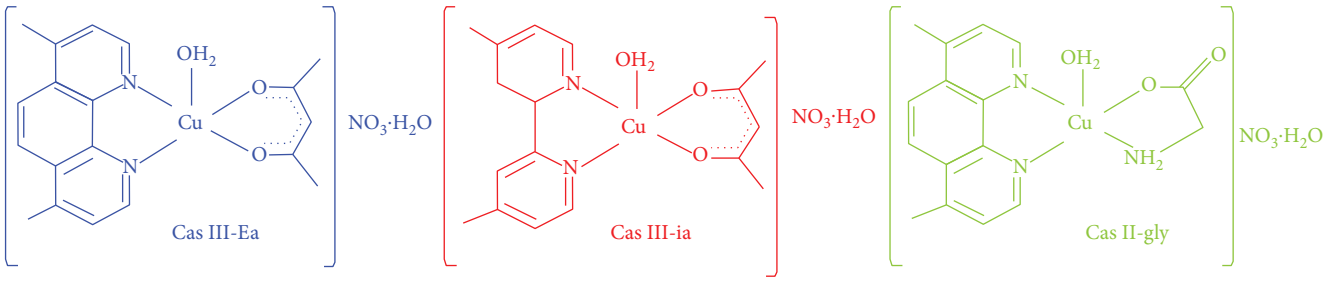


Figure 1: Structures of Cas III-Ea, III-ia, and II-gly.

in cold mitochondrial isolation medium (in mM: 125 KCl, 1 EDTA, and 10 HEPES-HCl; pH 7.3). The mitochondrial fraction was obtained by differential centrifugation using the protease Nagarse, as previously described [16]. Mitochondrial oxygen consumption was measured using a Clark-type oxygen electrode. The experiments were carried out in respiration assay medium containing 125 KCl, 10 HEPES-HCl, and 3 $KH_2PO_4$ (in mM) with pH 7.3. State 4 respiration was measured in the presence of 10 mM glutamate-malate, and state 3 respiration was evaluated after addition of 100 $\mu$M ADP. Maximal respiration was determined with 0.08 $\mu$M of carbonyl cyanide m-chlorophenyl hydrazine (CCCP) [17]. The mitochondrial membrane potential was measured by fluorometry using 5 $\mu$M safranine [13]. Mitochondrial $Ca^{2+}$ uptake was determined with the metalochromic indicator, Arsenazo III, or calcium green 5N (5N-CG) [18, 19], using a medium containing 50 $\mu$M Arsenazo or 10 $\mu$M 5N-CG, 10 mM succinate plus rotenone (0.1 $\mu g \cdot ml^{-1}$), 200 $\mu$M ADP, and 0.25 $\mu$g oligomycin A. Pulses of 10 nmol $Ca^{+2}$ were added every 3 minutes to reach a $Ca^{+2}$ release due to MPT opening. Mitochondrial cytochrome c quantification from Cas-treated hearts was performed using Western blot analysis as described previously [11]. The blots were developed with Luminata crescendo substrate (Merck Millipore, Darmstadt, Germany) and detected with VisionWorks LS-UVP Chimio System (BioSpectrum 415 Imaging System, Cambridge, UK).

*2.4. Cardiomyocytes Experiments.* Ventricular cardiomyocytes were obtained from male Wistar rats (250–300 g) by digestion with collagenase type II as previously described [20]. Cells were washed in Tyrode solution (mM): 130 NaCl, 5.4 KCl, 0.4 $NaH_2PO_4$, 0.5 $MgCl_2$, 25 HEPES, and 5 glucose with pH 7.4. After isolation, cells were cultivated at a density of $3.2 \times 10^3$ viable cells/well in 96-well plates pretreated with laminin in M-199 medium supplemented in mM with 5 taurine, 5 creatine, 2 L-carnitine, 2.5 sodium pyruvate, and penicillin-streptomycin at 100 $U \cdot ml^{-1}$ and 100 $\mu g \cdot ml^{-1}$, respectively, at 37°C, with 5% $CO_2$ and 95% air. After incubation for three hours, varying concentrations of Cas were tested in triplicate, exposing the myocytes during 24 hours to each treatment. At the end of the incubation period, the cytotoxicity of Cas was measured using the Alamar Blue viability test (Life Technologies, Carlsbad, CA, USA). Release of cytoplasmic lactate dehydrogenase (LDH) was determined using CytoTox-ONE homogeneous membrane integrity kit (Promega Madison, WI, USA). The activity of caspases 3/7 and caspase 9 was measured in cell lysates using caspase-Glo 3/7 and caspase-Glo 9 test luminescent assay (Promega, Madison, WI, USA), respectively. The cardiomyoblast cell line H9c2 (ATCC CRL-1446) was maintained using standard procedures in DMEM supplemented with 10% fetal bovine serum prior to the oxidative stress experiments.

*2.5. Oxidative Stress Markers.* Mitochondrial aconitase activity was measured in isolated heart homogenates by spectrophotometry as previously described [8]. Membrane lipid peroxidation was detected by the TBARS assay using thiobarbituric acid-reactive species as reported by Silva-Platas et al. [8]. Free thiol content was determined by Ellman's reagent, 5,5′-dithiobis(2-nitrobenzoic acid) (DTNB) as previously reported [8]. Thiol groups in the adenine nucleotide translocase were measured by eosin 5-maleimide interaction (EMA) with cysteine residues susceptible to oxidative stress or oxidizing agents [21] and followed by SDS/PAGE electrophoresis. Adenine nucleotide translocase measurement was performed using primary antibody anti-adenine nucleotide translocase (Abcam, MA, USA). The protein bands were detected with secondary HRP conjugated antibody, and the blots were developed as described above. Experiments for anion superoxide production were performed in intact cardiomyoblasts using the fluorescent probe MitoSOX (Molecular Probes) in the flow cytometer. H9c2 cells were loaded with MitoSOX during 15 min at 37°C with a cell density of 100,000 cells/mL (final concentration of MitoSOX 5 $\mu$M). Afterwards, the cells were subjected to Cas III-Ea treatment (4 or 20 $\mu$M); DOXO (5 $\mu$M) and Antimycin A (10 $\mu$g/mL) were used as positive controls. Finally, the cells were washed and analyzed on a FACSCanto II (BD Biosciences). FACS data was analyzed using FlowJo version 10.0 (Tree Star).

*2.6. Chemicals.* All chemical reagents were acquired from Sigma-Aldrich (St. Louis, MO, USA), unless otherwise specified. Casiopeina II-gly [Aqua(4,7-dimethyl-1,10-phenanthroline)(glycinate)copper(II)nitrate], Casiopeina III-ia [Aqua(4,4-dimethyl-2,2′bipyridine)(acetylacetonate)copper(II) nitrate], and Casiopeina III-Ea [Aqua(4,7-dimethyl-1,10-phenanthroline)(acetylacetonate)copper(II)nitrate] were synthesized following the synthesis as formerly described [22]. The Cas are referred to as III-Ea, III-ia, and II-gly, respectively. The detailed chemical structure of Cas is shown in Figure 1.

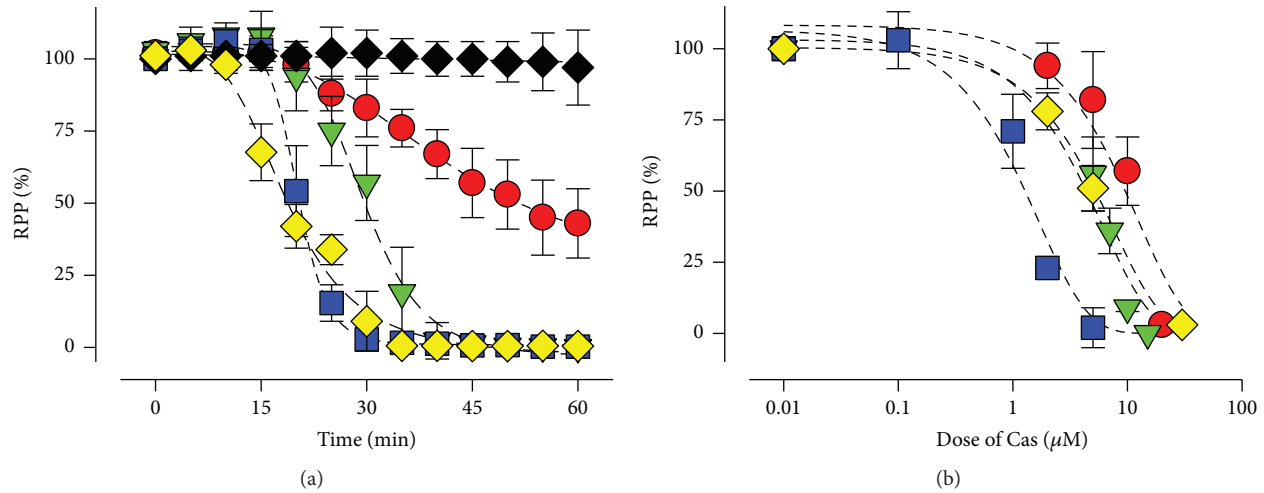


Figure 2: Cas affect contractility on isolated rat hearts. Cas were perfused at 5 $\mu$M for 60 minutes (a) or in a dose-dependent manner (b). The blue squares indicate III-Ea, green triangles indicate II-gly, and red circles indicate III-ia. Black rhombuses indicate control and yellow rhombuses indicate Doxo treatment. Values are mean ± SEM. ($n = 5$ experiments at least for each treatment).

*2.7. Statistical Analyses of Data.* All data were expressed as mean ± SEM. Data were analyzed by ANOVA followed by Dunnett's or Tukey's multiple comparisons test when appropriate using SigmaPlot 10 (Systat Software Inc., Germany) or GraphPad Prism 5 (V.5.01; La Jolla, CA, USA). A $p$ value $< 0.05$ was considered statistically significant.

## 3. Results

*3.1. Cas Inhibit Cardiac Function in a Time- and Dose-Dependent Manner.* To assess the effect of Cas on cardiac function, isolated rat hearts were perfused with equimolar concentrations (5 $\mu$M) of III-Ea, III-ia, II-gly, and Doxo. The progress of the RPP on III-Ea perfused hearts was gradually reduced 48% and 97% from the baseline values at 20 and 30 min, respectively (Figure 2(a)). III-Ea and II-gly showed a similar time-dependent inhibitory effect on RPP; however, the inhibitory effect of III-ia was 2.3-fold slower than that of III-Ea. Remarkably, III-Ea exhibited a $t_{0.5}$ similar to that of Doxo (Table 1). III-Ea, II-gly, and III-ia induced a dose-dependent progressive and sustained inhibition of RPP, with a half-maximal inhibitory concentration ($IC_{50}$) of 1.3 ± 0.2, 5.5 ± 0.5, and 10 ± 0.7 $\mu$M, respectively (Figure 2(b)). II-gly presented a similar $IC_{50}$ to Doxo, and surprisingly, III-Ea showed 3.8-fold more potent effect on RPP than Doxo did (Table 1). As seen in Supplemental Figure 1, the heart rate (HR) was not affected by treatment with III-ia, II-gly, or III-Ea, while Doxo-treatment significantly reduced the HR by 24%. At $IC_{50}$ for RPP, III-ia, III-Ea, and Doxo decreased cardiac efficiency (CE) by 48%, 47%, and 55%, respectively, whereas II-gly lightly impaired CE, causing only a 23% drop (Table 2). In our experimental conditions, all Cas affected the contraction rate (+dP/dt) in a similar manner (≈43%). Furthermore, −dP/dt was inhibited around 70–79%, suggesting a more profound impact on relaxation over contraction.

Table 1: Dose- and time-dependent parameters of hearts treated with Cas.

| | Cas III-ia ($n = 6$) | Cas II-gly ($n = 7$) | Cas III-Ea ($n = 8$) | Doxo ($n = 5$) |
|---|---|---|---|---|
| $IC_{50}$ ($\mu$M) | $10 \pm 0.7^{a,b,c}$ | $5.5 \pm 0.5^{b,d}$ | $1.3 \pm 0.2^{a,b,d}$ | $5 \pm 0.3^{c,d}$ |
| $t_{0.5}$ (min) | $49 \pm 0.8^{a,b,c}$ | $29 \pm 1.0^{d}$ | $21 \pm 5.0^{d}$ | $18.6 \pm 4.0^{d}$ |

The time for half-inhibition ($t_{0.5}$) at 5 $\mu$M and the half-maximal inhibitory concentration ($IC_{50}$) at 30 min of Cas-treated hearts. Values are mean ± SEM. $p < 0.05$ versus [a]Doxo, [b]II-gly, [c]III-Ea, and [d]III-ia ($n = 5$ experiments at least for each treatment).

*3.2. Cas Impair Energetic Metabolism.* It is well known that under normal conditions, the relationship between RPP and $MVO_2$ should be linear, given that any increase in cardiac contractility should be accompanied by a proportional increase in $MVO_2$ (ATP production in control conditions). Figure 3(a) displays this linear relationship between RPP and $MVO_2$. Interestingly, Cas-treated hearts showed a reduced slope, thus evidencing an apparent inefficient coupling between contraction and $O_2$ consumption. III-ia, III-Ea, and Doxo required, respectively, a 1.45-, 1.47-, and 1.8-fold additional $MVO_2$ to generate the same contractile force compared to the control hearts. Nevertheless, II-gly had a RPP/$MVO_2$ ratio similar to the control. There were no changes in $MVO_2$ with III-ia, III-Ea, or Doxo treatments; however, a 37%, 56%, and 74% decrease, respectively, in ATP content was observed (Figures 3(b) and 3(c)). Thus, III-ia, III-Ea, and Doxo act similarly to CCCP (a mitochondrial uncoupler), which stimulates $MVO_2$ by uncoupling ATP synthesis from the mitochondrial electron transport [23]. III-ia and Doxo also decreased PCr levels. Furthermore, the PCr/ATP ratio was augmented only in II-gly-treated hearts (Figure 3(d)), showing a PCr accumulation, which might point to inability of the myofibrillar creatine kinase system to rephosphorylate ADP.

Table 2: Effect of Cas on cardiac efficiency, contraction, and relaxation rates.

| | Control ($n = 9$) | Cas III-ia ($n = 6$) | Cas II-gly ($n = 7$) | Cas III-Ea ($n = 8$) | Doxo ($n = 5$) |
|---|---|---|---|---|---|
| Cardiac efficiency (RPP · $MVO_2^{-1}$) | $6.2 \pm 0.25$ | $3.2 \pm 0.4^*$ | $4.8 \pm 0.81$ | $3.3 \pm 0.2^*$ | $2.8 \pm 0.1^*$ |
| +dP/dt × 1000 (mmHg·s$^{-1}$) | $4.2 \pm 0.41$ | $2.4 \pm 0.20^*$ | $2.0 \pm 0.13^*$ | $2.4 \pm 0.23^*$ | $2.1 \pm 0.23^*$ |
| −dP/dt × 1000 (mmHg·s$^{-1}$) | $-3.3 \pm 0.22$ | $-1.0 \pm 0.16^*$ | $-0.7 \pm 0.09^*$ | $-0.8 \pm 0.13^*$ | $-0.8 \pm 0.18^*$ |

Rat hearts were treated with Cas or Doxo at the $IC_{50}$. CE: cardiac efficiency; RPP: rate-pressure product; $MVO_2$: myocardial oxygen consumption; +dP/dt: contraction rate; −dP/dt: relaxation rate. Values are mean ± SEM. $^*p < 0.05$ versus control ($n = 5$ experiments at least for each treatment).

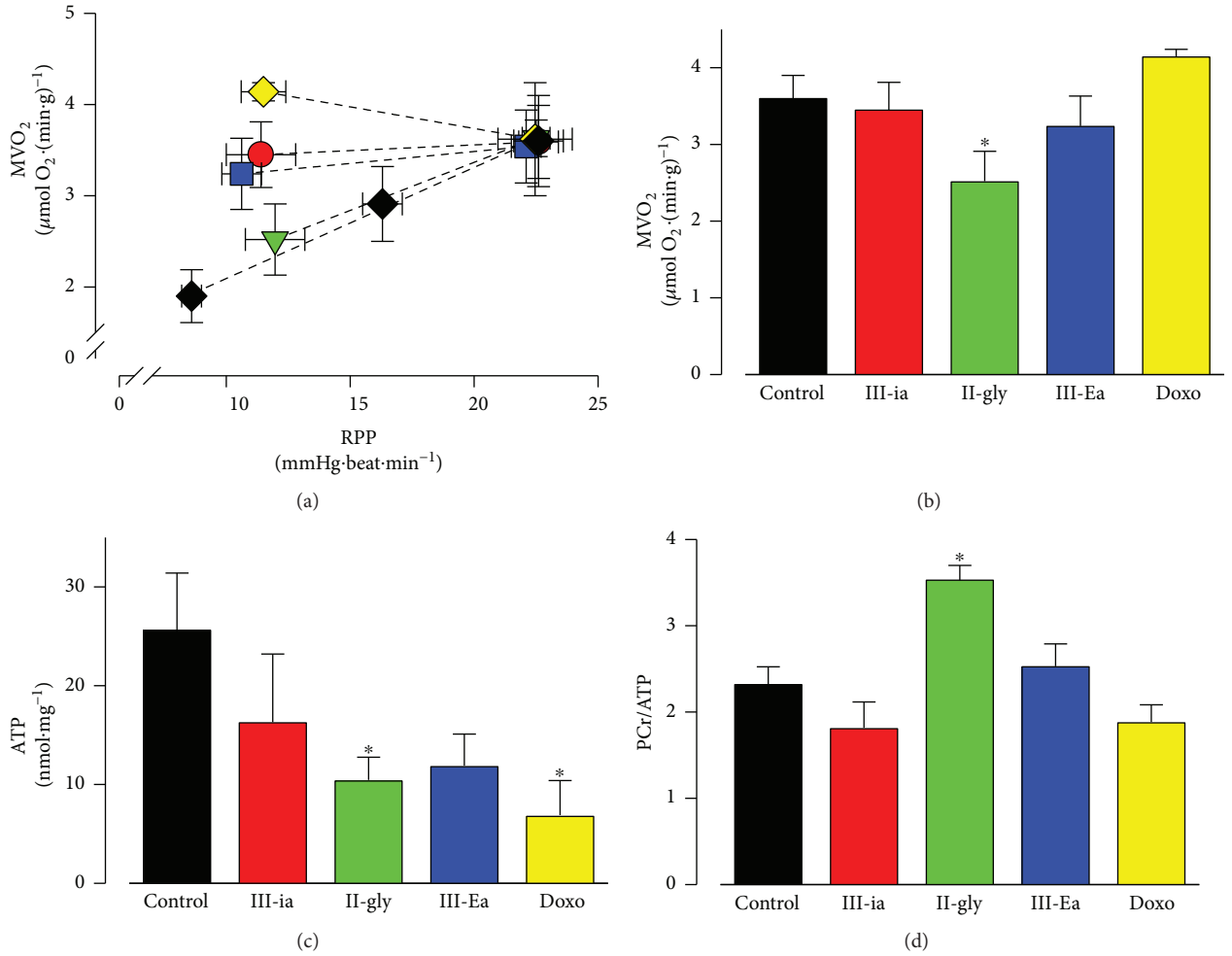


Figure 3: Cas impair oxygen consumption and energetic metabolites. Isolated rat hearts were used to measure the effect of Cas $IC_{50}$ and Doxo (5 $\mu$M) on mechanical (RPP) and metabolic coupling (oxygen consumption ($MVO_2$) relationship) (a), $MVO_2$ (b), ATP content (c), and myocardial PCr/ATP ratio (d). Values are mean ± SEM. $^*p < 0.05$ versus control ($n = 5$ experiments at least for each treatment).

*3.3. Cas Uncouple Mitochondrial Respiratory Chain and Induce Permeability Transition Pore.* To explore the effect of Cas on mitochondrial function, the respiratory activities of mitochondria isolated from Cas-treated hearts were measured. NADH-linked respiratory rate was determined using malate/glutamate as a substrate (Table 3). Mitochondria from II-gly- and III-ia-treated hearts exhibited a 77% and 78% decrease in the state 3 respiration rates, respectively. Consistently, an 82% and 87% reduction in maximal respiration was revealed, respectively, suggesting a potent inhibition of the respiratory chain. On the other hand, a moderate inhibitory effect on maximal mitochondrial respiration and an increased state 4 respiration rate was shown in mitochondria from III-Ea-treated hearts compared to III-ia- and II-gly-treated ones. However, the respiratory control ratio was depressed in mitochondria from hearts treated with III-Ea, indicating an uncoupling effect. In addition, to determine whether a Cas-induced MPT opening was evident, mitochondrial $Ca^{2+}$ retention capacity experiments were performed. As shown in Figures 4(a) and 4(b), the mitochondrial $Ca^{2+}$ retention capacity of III-Ea-treated hearts decreased by 50.5%, while that of II-gly decreased by

Table 3: Mitochondrial respiratory activity from Cas-treated hearts.

| | Control ($n = 5$) | Cas III-ia ($n = 3$) | Cas II-gly ($n = 3$) | Cas III-Ea ($n = 3$) | Doxo ($n = 4$) |
|---|---|---|---|---|---|
| State 3 respiration (nmol O $min^{-1}{\cdot}mg^{-1}$) | 86.17 ± 7.5 | 18.5 ± 0.6* | 20.2 ± 7.3* | 37.3 ± 2.7* | 25 ± 8.8* |
| State 4 respiration (nmol O $min^{-1}{\cdot}mg^{-1}$) | 25.5 ± 4.4 | 15.6 ± 2.6 | 13.0 ± 5.0 | 24.5 ± 5.4 | 18 ± 2.0 |
| Max. respiration (nmol O $min^{-1}{\cdot}mg^{-1}$) | 90.1 ± 9.0 | 12.3 ± 2.6* | 16.5 + 3.0* | 48.3 ± 5.7* | 25 ± 15.1* |
| Respiratory control | 4.1 ± 0.7 | 1.3 ± 0.1* | 1.6 ± 0.3* | 1.5 ± 0.2* | 1 ± 0.3* |

Values are mean ± SEM. *$p < 0.05$ versus control.

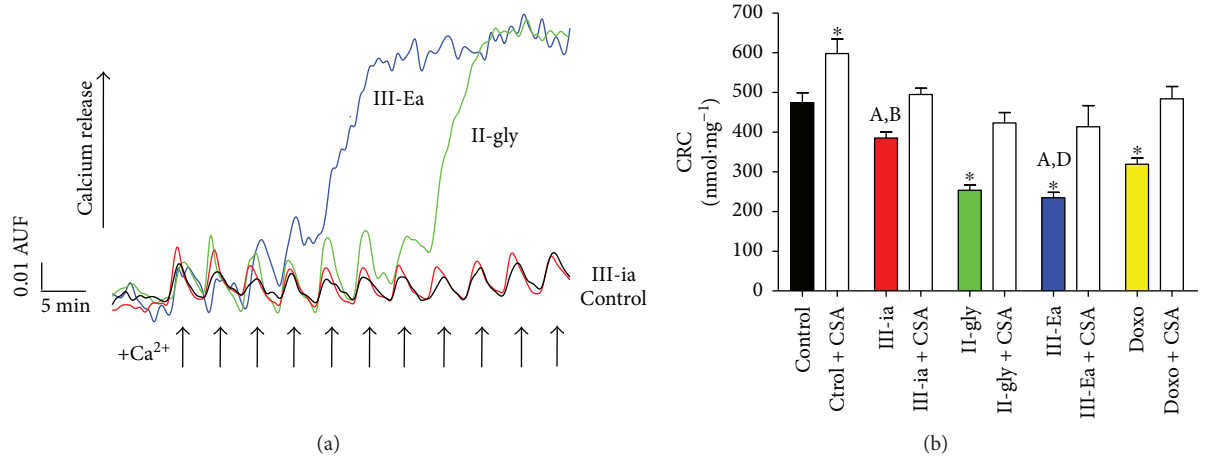


Figure 4: Cas treatments induce MPT opening. (a) Representative recording of $Ca^{2+}$ retention capacity (CRC) experiment with isolated mitochondria from $IC_{50}$ Cas-treated and Doxo (5 $\mu$M) hearts and (b) semiquantitative analysis of mitochondrial CRC in the presence of CsA (0.5 $\mu$M). Arrows indicate 10 $\mu$M pulses of $Ca^{2+}$. Values are mean ± SEM. *$p < 0.05$ versus control; $p < 0.05$ versus (A) Doxo, (B) II-gly, and (D) III-ia ($n = 5$ animals for each treatment, exception Doxo groups ($n = 3$)).

46.5% compared with the control. A protective effect of CsA (*in vitro* addition) treatment was also evident, as shown in Figure 4(b). CsA significantly protected Cas and Doxo effects. Mitochondria from III-Ea-treated hearts in the presence of CsA showed a 1.8-fold delay in the opening of MPT. In mitochondria treated by III-ia, II-gly, and Doxo, CsA demonstrated a protective effect of 28%, 60%, and 51%, respectively.

*3.4. Effect of Cas on Mitochondrial ROS and TBARS Production.* Mitochondrial activity, aconitase activity, and TBARS content were measured in isolated hearts to determine the role of oxidative damage of Cas in triggering mitochondrial dysfunction. In the ex vivo heart, only III-ia decreased aconitase activity, an effect that was also observed in the Doxo-treated hearts (Figure 5(b)). Thiol groups and specific thiol groups in adenine nucleotide translocase from mitochondria isolated from Cas-treated hearts were measured. As shown in Figure 5(a), there was no increase in lipid peroxidation, nor in thiol oxidation (data not shown) with the Cas treatments (Figure 5(a)) when compared with the control. In addition, mitochondrial anion superoxide production was measured using the MitoSOX probe. Histograms of flow cytometry analysis (Supplemental Figure 2A) showed a 9-fold increase in mean intensity in cells treated acutely with Antimycin A (a well-known mitochondrial inhibitor and inducer of anion superoxide production) and a 4-fold increase with Doxo. However, there was no change in the anion superoxide production in intact cells with III-Ea treatment at 4 or 20 $\mu$M, suggesting that mitochondrial ROS production is not significant in III-Ea cell injury (Supplemental Figure 2B). On the other hand, there was a twofold increase in the oxidation state of adenine nucleotide translocase thiol groups with the III-Ea treatments (Figure 5(c)), an effect previously reported in isolated mitochondria [8]. It has been shown that o-phenanthroline, in addition to $Cu^{+2}$, interacts directly with adenine nucleotide translocase inducing a cytosolic-conformational state, which inhibits ADP/ATP translocation and rises MPT opening [15]. In III-Ea, $Cu^{+2}$ is coordinated with 4,7-dimethyl-1,10-phenanthroline. It thus seems that the interaction with adenine nucleotide translocase, which increased the thiol group oxidation and the MPT opening, does not require ROS production and oxidative damage. In summary, the observed effects of Cas in the isolated heart model were not strong enough to induce significant phospholipid or protein damage.

*3.5. Cas Trigger Mitochondrial Apoptosis.* To assess the effect of Cas on cardiomyocyte viability, we cultured adult rat ventricular myocytes with different concentrations of Cas (0–1000 $\mu$M) and examined cell death after a 24 h treatment using the Alamar blue assay. As shown in Supplemental

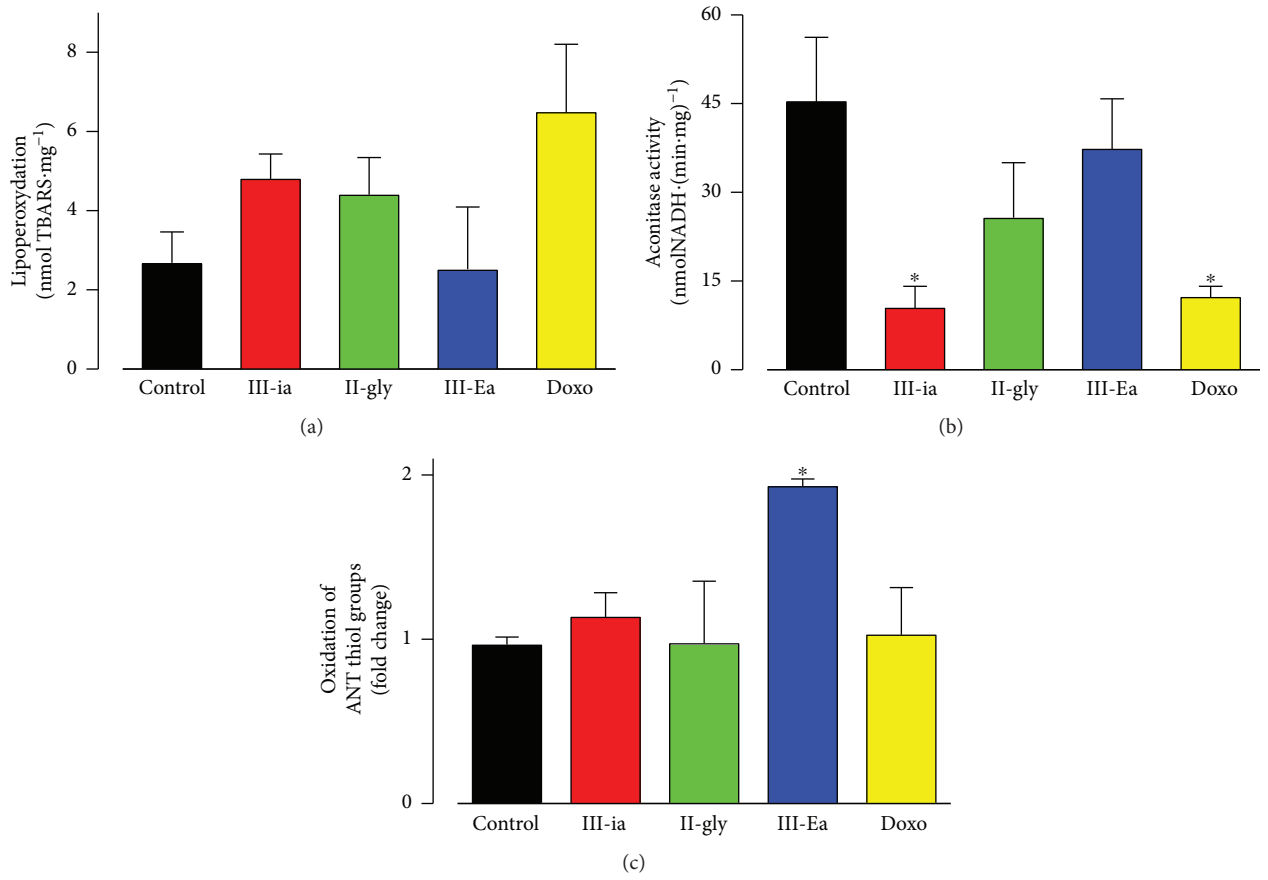


Figure 5: Effect of Cas on isolated heart on TBARS content (a), aconitase activity (b), and ANT/thiols groups (c) on mitochondria from $IC_{50}$ Cas-treated and Doxo (5 $\mu$M) hearts. Values are mean ± SEM. $^*p < 0.05$ versus control ($n = 5$ animals for each treatment, except for Doxo group ($n = 3$)).

Figure 3, III-Ea, II-gly, and III-ia induced significant cytotoxic effects in a dose-dependent manner, with a $LD_{50}$ of $2 \pm 0.4$, $2 \pm 0.5$, and $7 \pm 1.7$ $\mu$M, respectively, indicating a 3-fold higher toxicity of III-Ea and II-gly compared to III-ia. These results are consistent with previous quantitative structure-activity relationship (QSAR) studies [4]. Likewise, $IC_{50}$ from III-Ea was 5-fold higher than that of Doxo ($10 \pm 0.5$ $\mu$M). At its $IC_{50}$, Cas induced diverse cytotoxic effects and cell death mechanisms, evidenced by different release levels of LDH, a marker of necrosis (Figure 6(a)). Doxo and II-gly produced a 4.7- and 3.5-fold increase in LDH release, respectively, compared to the control. On the other hand, activity of caspases 3 and 7 increased ~4-fold for III-ia and II-gly treatments, compared to Doxo or the control. Interestingly, the significant increases in caspase 3 and 7 activities observed for III-ia and II-gly treatments correlated directly with reduction of cytochrome c from the mitochondria, suggesting the activation of a mitochondria-dependent apoptosis pathway ($p < 0.5$) (Figure 6(d)). However, for caspase 9, only II-gly caused a 1.7-fold significant ($p < 0.05$) increase in activity (Figure 6(c)).

*3.6. Early Perfusion of CsA in Isolated Hearts Ameliorates the Cas Effect due to MPT Opening.* To prove the role of MPT opening on the Cas-mediated cardiotoxicity, experiments were performed in the whole-heart model treated with CsA. As previously described, 1 $\mu$M CsA was perfused during 10 minutes, then 10 $\mu$M III-Ea was perfused while recording the left ventricular pressure to calculate the RPP and evaluate mechanical performance. As expected, the perfusion of III-Ea resulted in a decline of contractility ($t_{0.5}$ of 9.65 min). However, treatments with the perfusion of CsA prior to III-Ea perfusion resulted in a significant reduction in contractile dysfunction (Figure 7(a)). RPP analyses showed a significantly protective effect ($t_{0.5}$ of 11.98 min, $p = 0.035$, $n = 4$) exerted by CsA with respect to the cardiotoxicity observed for III-Ea alone (Figure 7(b)). Results from functionality of heart-isolated mitochondria at the end of perfusion treatments are shown in Figures 7(c), 7(d), and 7(e). A representative recording of membrane potential (Figure 7(c)) showed the depolarization of mitochondria after the addition of 10 $\mu$M $Ca^{+2}$, from III-Ea-treated hearts; however, mitochondria from CsA-III-Ea-treated hearts remained polarized similar to mitochondria from untreated hearts. Calcium retention capacity analyses indicated that mitochondria from CsA-III-Ea-treated hearts tolerated 69% more calcium than mitochondria from III-Ea hearts ($226 \pm 13$ versus $133 \pm 14$ nmol·mg$^{-1}$, $p = 0.03$, $n = 4$). Hence, the uncoupling of contractility and energetics in the hearts treated with III-Ea was observed to be partly dependent on MPT opening.

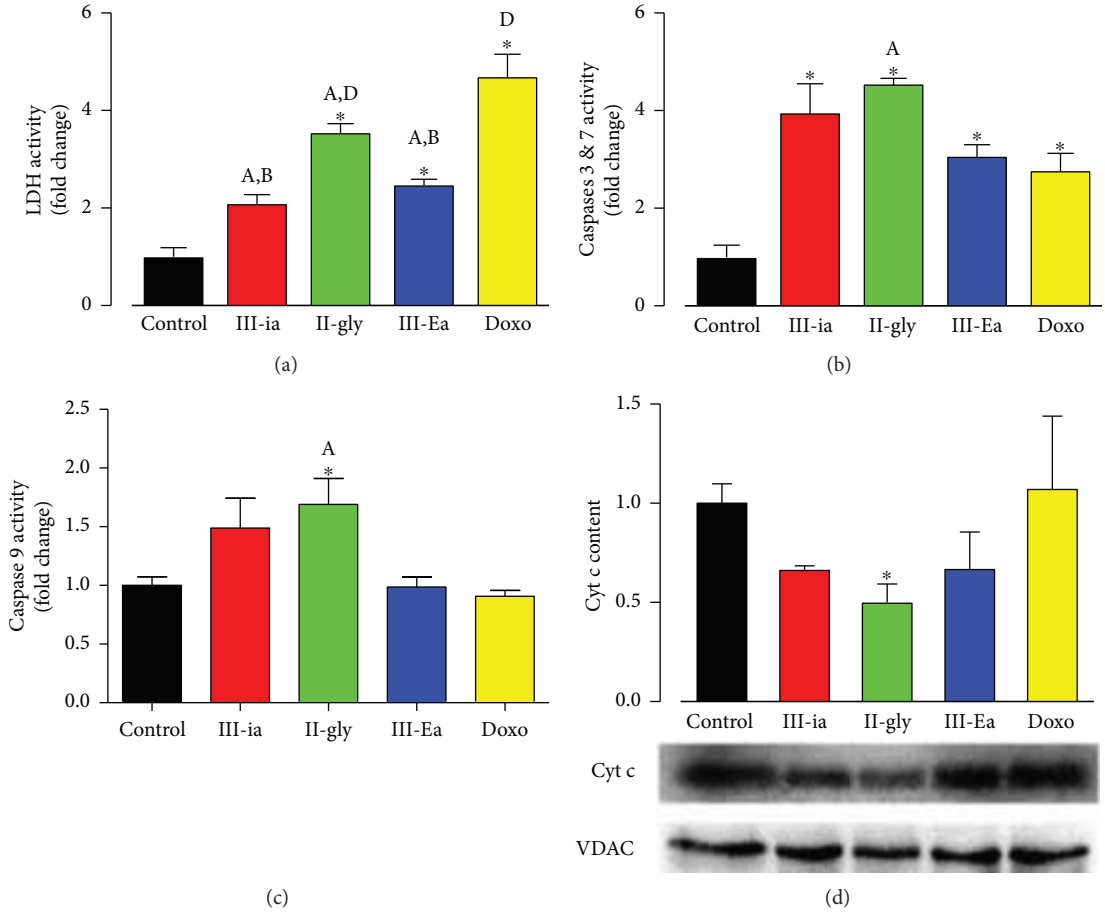


Figure 6: Cas trigger mitochondrial cell death. Panels (a–c) shows LDH, caspase 3/7 and caspase 9 activities on isolated cardiomyocytes treated with Cas at its $IC_{50}$ (in $\mu$M: III-ia (7), II-gly (2), III-Ea (2), and Doxo (10)). Panel (d) shows cytochrome c content by Western blot analysis in heart mitochondria after Cas-perfusion for 30 minutes in the ex vivo hearts at its $IC_{50}$ (in $\mu$M: III-ia (10), II-gly (5.5), III-Ea (1.3), and Doxo (5)). Values are mean ± SEM. $^*p < 0.05$ versus control; $p < 0.05$ versus (A) Doxo, (B) II-gly, and (D) III-ia ($n = 5$ experiments for each treatment, except for panel (d) (3 animals for group)).

## 4. Discussion

In recent years, more powerful and specific drugs have been developed to treat cancer. Unfortunately, several highly effective antineoplastic drugs have reported cardiotoxicity as a side effect, including Doxo and trastuzumab, a recombinant humanized antibody [2, 24, 25]. The use of Doxo as an antineoplastic drug has been mostly hampered by some adverse cardiovascular events such as hypertension, ventricular dysfunction, and HF [1, 26]. The onset of these adverse cardiovascular events might take place early or be delayed up to two decades after the conclusion of cancer treatment [1, 27]. Noteworthy, novel chemotherapeutic agents such as Cas have shown more potent antitumoral activity than Doxo [28]. For instance, the reduction of the volume of subcutaneous tumors in nude mice achieved by III-ia was 81% [29] while that of Doxo was 20% [30]. However, in cellular and isolated mitochondrial models, Cas have shown a remarkable cytotoxic effect [8]. In this regard, as an attempt to determine the potential cardiotoxicity of Cas (ex vivo) and its underlying mechanisms, this work examined the acute cardiotoxicity of Cas treatments in ex vivo heart and isolated cardiomyocytes. Our experimental results have shown that 1-10 $\mu$M of Cas decline cardiac metabolism and contractility. These events are dose- and time-dependent at similar or lower concentrations than Doxo [1]. Similarly, as previously observed in mice and *in vitro* experiments, III-Ea and II-gly (with phenanthroline substituents) were 7- and 2-fold more potent inhibitors of cardiac contractility, respectively, compared to III-ia (with bipyridine as a ligand) [4]. These results suggest that a decrease in cardiotoxicity and a slower effect on RPP could be attributable to the absence of the third benzene ring in bipyridines. Both ligands in III-Ea, phenanthroline and acetylacetonate, render the compound more permeable than II-gly, whose second ligand is glycinate instead of acetylacetonate, and more permeable than III-ia, whose imine ligand is dipyridine. In both, the whole-heart model and in adult rat cardiomyocytes, III-Ea and II-gly exhibited a lower $IC_{50}$ for RPP and cell viability compared to III-ia. Yet, III-Ea showed a lower $IC_{50}$ than II-gly in the whole-heart model. This might be resultant to the length of the second carbon ligand (acetylacetonate) that also facilitates the early decline of contractility by interrupting the ATP supply. Previous experiments in cardiac mitoplasts compared to intact

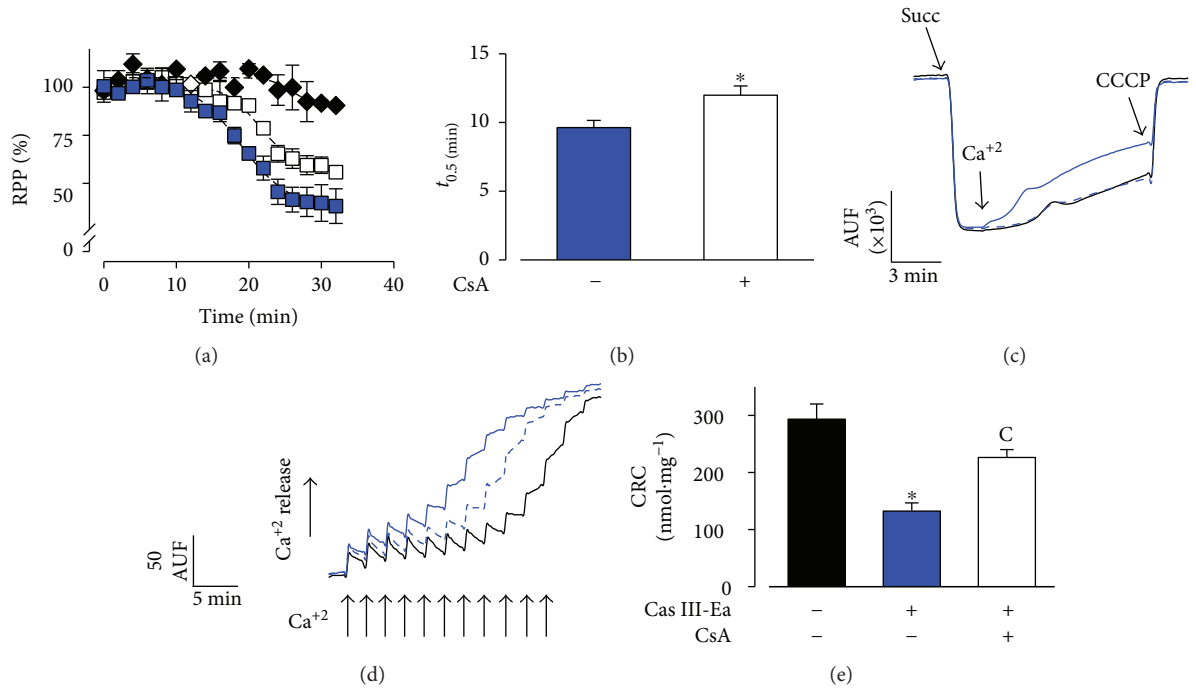


FIGURE 7: Early perfusion of CsA in isolated hearts ameliorates the Cas effect due to MPT opening. RPP is shown in (a). The decline in contractility due to the perfusion (20 min) of 10 $\mu$M III-Ea alone is presented as the blue trace. The early perfusion (10 min) of 1 $\mu$M CsA (white squares) delays the decline in contractility due to the subsequent perfusion with III-Ea. The control trace is presented as the black trace. Analysis of the traces is presented as the time for half inhibition ($t_{0.5}$) (b). Experiments in isolated mitochondria prepared from these hearts at the end of perfusion. Representative recording of membrane potential (c) and $Ca^{2+}$ retention capacity (d). Semiquantitative analysis of mitochondrial CRC (e). Mitochondria from III-Ea-treated hearts are represented as a blue solid line, mitochondria from CsA-Cas III-Ea hearts as a blue dot line, and untreated hearts as a black solid line. Arrows indicates succinate (10 mM), CCCP (0.08 $\mu$M), or 10 $\mu$M pulses of $Ca^{2+}$ addition. Values are mean ± SEM. $^*p < 0.05$ versus control; $p < 0.05$ versus (C) III-Ea ($n = 4$ animals for each treatment).

mitochondria indicated that phenanthroline ligands might accelerate copper transport and cause intracellular and mitochondrial damage [8]. This effect might be accredited to the hydrophobicity of the substituents, which rises passive uptake of copper [22]. Thus, the phenanthroline ligands of III-Ea and II-gly might act as carriers in the cellular membrane transport of copper compounds. On the other hand, the uncoupling effect on mitochondria might depend on the acetylacetonate or glycinate ligand. These substituents in metal coordination compounds have shown an acidic-dissociable acetyl group with a pKa ≈ 6, which corresponds to an electron-withdrawing moiety. This dissociation could stabilize the anionic species through delocalization of the charge over its structure [31]. Subsequently, protonated III-Ea and II-gly could move from the intermembrane space into the mitochondrial matrix, dissociate, and then diffuse back in their ionized form to the intermembrane space, where they might be protonated again, repeating the cycle. However, an acidic-dissociable acetyl group is not enough to account for a mitochondrial uncoupling effect. In addition to the Cas geometric arrangement, the hydrophobicity of phenanthroline is required to transport protons across the inner membrane, possibly through adenine nucleotide translocase, dissipating the membrane potential required for the ATP synthesis (Table 3). Therefore, Cas III-ia, without a phenanthroline substituent, is not prone to produce mitochondrial membrane depolarization and MPT opening (Figure 4). On the other hand, a reactive acetylacetonate ligand, as observed in III-ia and III-Ea, can potentially contribute to the reduction potential of the copper center as a decisive factor in ROS-production. From an experimental point of view, a previous report from our group observed that III-ia induced a twofold decrease in $\alpha$-ketoglutarate dehydrogenase activity compared with III-Ea [8]. Besides, there was no mitochondrial ROS production by III-Ea. These conflicting results could indicate that III-Ea remains preferentially at the mitochondrial inner membrane (interacting with MPT components, such as the adenine nucleotide translocase) instead of the mitochondrial matrix interacting with soluble enzymes such as $\alpha$-ketoglutarate dehydrogenase. However, the molecular mechanism by which the glycinate ligand in II-gly contributes to mitochondrial dysfunction is unclear. II-gly shows a lower depolarizing effect than III-Ea but a similar effect on mitochondrial inhibition as that of III-ia. A II-gly-reduced effect on mitochondrial inhibition might be synergized with the uncoupling effect of the phenanthroline ligand, producing a toxic Cas. In this regard, production of ROS by a Fenton-like reaction consuming reducing metabolites [32] or by generation of stable copper-GSH (reduced glutathione) compounds [12, 32] are the previously

described mechanisms of II-gly- and III-ia-induced injury. The reactions in both mechanisms lead to membrane damage and lipid peroxidation [32]. Nevertheless, our experiments in cardiac tissue and cardiomyoblasts indicate that oxidative stress is not enough to completely explain Cas cardiotoxicity. In fact, there is strong evidence that Cas cardiotoxicity arises from ROS-independent mechanisms, such as impairment of cellular energetics, which compromises the cardiomyocyte ability to generate adequate contraction-relaxation cycles. Perhaps the high activity of antioxidant enzymes and the levels of GSH within the heart provide a strong antioxidant defense system against the consequent oxidative stress injury [33]. In brief, our results point to the mitochondria as the main target for Cas cardiotoxicity, impairing oxidative phosphorylation and inducing energetic failure in the whole heart. These findings correlate with the mitochondrial dysfunction observed in mitochondria isolated from Cas-treated hearts. An acute uncoupling effect, collapsing the mitochondrial membrane potential, was the most consistent effect of Cas at both, the whole-heart and the mitochondrial levels. Mitochondria isolated from Cas-treated hearts presented limited ability to conduct ADP-coupled oxidative phosphorylation, given the lower respiratory control (Table 3 and Figure 7(c)). Whole hearts showed induction of the MPT opening, which generated a disruption of the membrane potential and an uncoupling of the respiratory chain, resulting in an increased $MVO_2$. In this context, it has been demonstrated that mitochondrial uncouplers induce apoptosis in several cell types [34], supporting the idea that Cas-induced mitochondrial uncoupling causes membrane permeabilization. Increased permeability to protons of the mitochondrial membrane could occur in circumstances of extensive and nonspecific membrane damage, such as those implicated in protein oxidation due to excessive ROS production [35]. Our results did elicit a significant prooxidant action on adenine nucleotide translocase thiol groups in the hearts during III-Ea treatment, although not entirely due to mitochondrial ROS production. Hence, Cas might play a direct role in mitochondrial permeability and mitochondrial-triggered apoptosis. Accordingly, Silva-Platas et al. [8] have observed III-Ea-induced MPT opening and extensive mitochondrial membrane depolarization and swelling [9]. Mitochondrial swelling has been associated with the release of cytochrome c and cell death, particularly in cardiomyocytes [11, 18, 36]. It has been shown that apoptosis induction by Cas acting as uncouplers or MPT openers might be achieved via cytochrome c release followed by the activation of caspases [37, 38]. In accordance, we found that cytochrome c was decreased in mitochondria isolated from Cas-treated hearts (Figure 6(d)), indicating its release out of the mitochondria. On this point, Nakagawa et al. observed that cytochrome c can be released out of the mitochondria via the MPT, which in turn is induced by $Ca^{2+}$, without the involvement of proapoptotic proteins like Bax [39]. We found no significant changes in Bax (data not shown), probably due to the early stages of apoptosis in the Cas-treated hearts. It is also noteworthy that our experiments did not include *in vivo* models, which can alter or change the way Cas exert their effects.

As formerly reported, Cas binding to plasma proteins prompts their different availability between ex vivo and *in vitro* conditions [40], just as has been observed with Doxo [41]. On the other hand, while pharmacokinetics, elimination time, and distribution of Cas are only partially understood [6, 40], the defined therapeutic dose is still a source of debate. However, in the current ex vivo study, there were no plasma proteins such as albumin, which has been found to bind near 80% of the Cas dose [42]. Therefore, a 5-fold higher *in vivo* dose would be needed to achieve current $IC_{50}$ cardiotoxic levels using an acute dose, while it is completely unclear during chronic exposure.

Currently, monitoring and reducing cardiotoxicity of cancer drugs is of the utmost priority. With respect to Cas, the mechanism underlying their cardiac side effects appears to involve the MPT opening, which produces an energetic debacle. Our results demonstrated that the early perfusion of CsA, prior to the exposure to Cas, ameliorated the decline in contractility in isolated rat hearts. MPT opening was the protection mechanism involved, which was also evidenced by the functionality of mitochondria isolated from the perfused hearts. Features of MPT opening and mitochondrial-triggered apoptosis are consistent with previous reports of Doxo-induced cardiomyocyte toxicity [26, 43], in which the CsA effect was also reported to be cardioprotective in the rat heart in a dose-dependent form [37]. In this context, pharmacological inhibition of the MPT opening improved cardiac function by reducing heart injury in animal models and in patients [16, 44]. Also, pretreatment with carvedilol delayed death in Cas-treated dogs [6] acting similarly as CsA, by reducing the MPT opening and the release of cytochrome c [45]. Moreover, the use of CsA has been found to increase the chemosensitivity in non-small lung cancer cells resistant to epidermal growth factor receptor tyrosine kinase inhibitors [46] and cisplatin-resistant ovarian cancer [47]. These effects occur mainly by augmenting STAT3 inhibition in tumor cells. In conclusion, we determined Cas-mediated cardiotoxicity in an acute setting and demonstrated that III-Ea is the most cardiotoxic Cas, since it compromised adenine nucleotide translocase thiol groups, increased the MPT opening, and uncoupled the mitochondrial energetic function of cardiac mechanical performance. The early perfusion of CsA ameliorated the decline in contractility, demonstrating the involvement of MPT opening in III-Ea cardiotoxicity. Further work implicates designing subacute or longer-term studies to fully understand the magnitude and complexity of Cas cardiotoxicity and more thoroughly to elucidate the molecular pathophysiology during a chronic exposure. Our results contribute with new scientific knowledge by identifying a possible mechanism involved in Cas-induced cardiac side effects, which is crucial to the further improvement of more potent and efficacious cancer therapies with less cardiotoxicity.

## Conflicts of Interest

The authors declare that they have no conflicts of interest.

## Authors' Contributions

Christian Silva-Platas, César A. Villegas, and Yuriana Oropeza-Almazán contributed equally to this work.

## Acknowledgments

This work was partially supported by the Endowed Chair in Cardiology, Tecnológico de Monterrey grant 0020CAT131 as well as CONACYT, México, grants 151136 and 256577 (Gerardo García-Rivas), and Xignus Research Foundation, Red Temática Farmoquímicos, CONACYT supported the publication. César A. Villegas, Evaristo Fernández-Sada, Niria Treviño-Saldaña, and Alejandro Torres-Quintanilla were supported by CONACYT MSc scholarships. Elena C. Castillo, Héctor Chapoy-Villanueva, and Omar Lozano were supported by a postdoctoral Fellowship from CONACYT. The authors thank Jesús R. Garza, M.D., for his exceptional technical assistance. The authors also thank Drs. Julio Altamirano and Noemí García for their helpful discussion.

## Supplementary Materials

*Supplementary 1*. Figure 1: heart rate (HR) was not affected by the Cas treatment. HR was measured in rat heart perfused with Cas at 5 $\mu$M. Values are mean ± SEM. $^{*}p < 0.05$ versus control ($n = 5$ experiments at least for each treatment).

*Supplementary 2*. Figure 2: anion superoxide production in the myoblast cell line H9c2 exposed to ($\mu$M) Doxorubicin (5), III-Ea (4 and 20), and Antimycin A (10 $\mu$g/mL) using the fluorescent probe MitoSOX and flow cytometry. The representative histogram of the MitoSOX signal is presented in A, and the mean fluorescence intensity is calculated and compared in B. $^{*}p < 0.05$, $n = 3$.

*Supplementary 3*. Figure 3: dose-dependent effect of Cas (0–1000 $\mu$M) on cardiomyocyte viability. Values are mean ± SEM ($n = 5$ experiments at least for each treatment).

## References

[1] R. G. Schwartz, W. B. McKenzie, J. Alexander et al., "Congestive heart failure and left ventricular dysfunction complicating doxorubicin therapy. Seven-year experience using serial radionuclide angiocardiography," *The American Journal of Medicine*, vol. 82, no. 6, pp. 1109–1118, 1987.

[2] A. Colombo, C. Cipolla, M. Beggiato, and D. Cardinale, "Cardiac toxicity of anticancer agents," *Current Cardiology Reports*, vol. 15, no. 5, p. 362, 2013.

[3] J. H. Doroshow and K. J. Davies, "Redox cycling of anthracyclines by cardiac mitochondria. II. Formation of superoxide anion, hydrogen peroxide, and hydroxyl radical," *The Journal of Biological Chemistry*, vol. 261, no. 7, pp. 3068–3074, 1986.

[4] M. E. Bravo-Gomez, J. C. Garcia-Ramos, I. Gracia-Mora, and L. Ruiz-Azuara, "Antiproliferative activity and QSAR study of copper(II) mixed chelate [Cu(N–N)(acetylacetonato)]$NO_3$ and [Cu(N–N)(glycinato)]$NO_3$ complexes, (Casiopeínas®)," *Journal of Inorganic Biochemistry*, vol. 103, no. 2, pp. 299–309, 2009.

[5] C. Trejo-Solis, D. Jimenez-Farfan, S. Rodriguez-Enriquez et al., "Copper compound induces autophagy and apoptosis of glioma cells by reactive oxygen species and JNK activation," *BMC Cancer*, vol. 12, no. 1, p. 156, 2012.

[6] M. Leal-Garcia, L. Garcia-Ortuno, L. Ruiz-Azuara, I. Gracia-Mora, J. Luna-Delvillar, and H. Sumano, "Assessment of acute respiratory and cardiovascular toxicity of casiopeinas in anaesthetized dogs," *Basic & Clinical Pharmacology & Toxicology*, vol. 101, no. 3, pp. 151–158, 2007.

[7] A. Marin-Hernandez, J. C. Gallardo-Perez, S. Y. Lopez-Ramirez et al., "Casiopeina II-gly and bromo-pyruvate inhibition of tumor hexokinase, glycolysis, and oxidative phosphorylation," *Archives of Toxicology*, vol. 86, no. 5, pp. 753–766, 2012.

[8] C. Silva-Platas, C. E. Guerrero-Beltran, M. Carranca et al., "Antineoplastic copper coordinated complexes (Casiopeinas) uncouple oxidative phosphorylation and induce mitochondrial permeability transition in cardiac mitochondria and cardiomyocytes," *Journal of Bioenergetics and Biomembranes*, vol. 48, no. 1, pp. 43–54, 2016.

[9] A. Marin-Hernandez, I. Gracia-Mora, L. Ruiz-Ramirez, and R. Moreno-Sanchez, "Toxic effects of copper-based antineoplastic drugs (Casiopeinas®) on mitochondrial functions," *Biochemical Pharmacology*, vol. 65, no. 12, pp. 1979–1989, 2003.

[10] L. Hernandez-Esquivel, A. Marin-Hernandez, N. Pavon, K. Carvajal, and R. Moreno-Sanchez, "Cardiotoxicity of copper-based antineoplastic drugs casiopeinas is related to inhibition of energy metabolism," *Toxicology and Applied Pharmacology*, vol. 212, no. 1, pp. 79–88, 2006.

[11] F. Correa, V. Soto, and C. Zazueta, "Mitochondrial permeability transition relevance for apoptotic triggering in the post-ischemic heart," *The International Journal of Biochemistry & Cell Biology*, vol. 39, no. 4, pp. 787–798, 2007.

[12] A. I. Valencia-Cruz, L. I. Uribe-Figueroa, R. Galindo-Murillo et al., "Whole genome gene expression analysis reveals casiopeína-induced apoptosis pathways," *PLoS One*, vol. 8, no. 1, article e54664, 2013.

[13] G. de Jesus Garcia-Rivas, A. Guerrero-Hernandez, G. Guerrero-Serna, J. S. Rodriguez-Zavala, and C. Zazueta, "Inhibition of the mitochondrial calcium uniporter by the oxo-bridged dinuclear ruthenium amine complex ($Ru_{360}$) prevents from irreversible injury in postischemic rat heart," *The FEBS Journal*, vol. 272, no. 13, pp. 3477–3488, 2005.

[14] E. Fernandez-Sada, C. Silva-Platas, C. A. Villegas et al., "Cardiac responses to $\beta$-adrenoceptor stimulation is partly dependent on mitochondrial calcium uniporter activity," *British Journal of Pharmacology*, vol. 171, no. 18, pp. 4207–4221, 2014.

[15] N. Garcia, E. Martinez-Abundis, N. Pavon, F. Correa, and E. Chavez, "Copper induces permeability transition through Its interaction with the adenine nucleotide translocase," *Cell Biology International*, vol. 31, no. 9, pp. 893–899, 2007.

[16] G. J. García-Rivas, K. Carvajal, F. Correa, and C. Zazueta, "$Ru_{360}$, a specific mitochondrial calcium uptake inhibitor, improves cardiac post-ischaemic functional recovery in rats *in vivo*," *British Journal of Pharmacology*, vol. 149, no. 7, pp. 829–837, 2006.

[17] F. Correa, N. García, G. García, and E. Chávez, "Dehydroepiandrosterone as an inducer of mitochondrial permeability transition," *The Journal of Steroid Biochemistry and Molecular Biology*, vol. 87, no. 4-5, pp. 279–284, 2003.

[18] C. Silva-Platas, N. Garcia, E. Fernandez-Sada et al., "Cardiotoxicity of acetogenins from *Persea americana* occurs through the mitochondrial permeability transition pore and caspase-dependent apoptosis pathways," *Journal of Bioenergetics and Biomembranes*, vol. 44, no. 4, pp. 461–471, 2012.

[19] Y. Oropeza-Almazán, E. Vázquez-Garza, H. Chapoy-Villanueva, G. Torre-Amione, and G. García-Rivas, "Small interfering RNA targeting mitochondrial calcium uniporter improves cardiomyocyte cell viability in hypoxia/reoxygenation injury by reducing calcium overload," *Oxidative Medicine and Cellular Longevity*, vol. 2017, Article ID 5750897, 13 pages, 2017.

[20] B. C. Willis, A. Salazar-Cantu, C. Silva-Platas et al., "Impaired oxidative metabolism and calcium mishandling underlie cardiac dysfunction in a rat model of post-acute isoproterenol-induced cardiomyopathy," *American Journal of Physiology-Heart and Circulatory Physiology*, vol. 308, no. 5, pp. H467–H477, 2015.

[21] N. Garcia, N. Pavon, and E. Chavez, "The effect of *N*-ethylmaleimide on permeability transition as induced by carboxyatractyloside, agaric acid, and oleate," *Cell Biochemistry and Biophysics*, vol. 51, no. 2-3, pp. 81–87, 2008.

[22] M. E. Bravo-Gómez, S. Dávila-Manzanilla, J. Flood-Garibay et al., "Secondary ligand effects on the cytotoxicity of several Casiopeína's group II compounds," *Journal of the Mexican Chemical Society*, vol. 56, pp. 85–92, 2012.

[23] J. Fuchs, P. Veit, and G. Zimmer, "Uncoupler- and hypoxia-induced damage in the working rat heart and its treatment. II. Hypoxic reduction of aortic flow and its reversal," *Basic Research in Cardiology*, vol. 80, no. 3, pp. 231–240, 1985.

[24] D. B. Sawyer, C. Zuppinger, T. A. Miller, H. M. Eppenberger, and T. M. Suter, "Modulation of anthracycline-induced myofibrillar disarray in rat ventricular myocytes by neuregulin-1$\beta$ and anti-erbB2: potential mechanism for trastuzumab-induced cardiotoxicity," *Circulation*, vol. 105, no. 13, pp. 1551–1554, 2002.

[25] Z. V. Varga, P. Ferdinandy, L. Liaudet, and P. Pacher, "Drug-induced mitochondrial dysfunction and cardiotoxicity," *American Journal of Physiology-Heart and Circulatory Physiology*, vol. 309, no. 9, pp. H1453–H1467, 2015.

[26] Y. Octavia, C. G. Tocchetti, K. L. Gabrielson, S. Janssens, H. J. Crijns, and A. L. Moens, "Doxorubicin-induced cardiomyopathy: from molecular mechanisms to therapeutic strategies," *Journal of Molecular and Cellular Cardiology*, vol. 52, no. 6, pp. 1213–1225, 2012.

[27] Z. Heger, N. Cernei, J. Kudr et al., "A novel insight into the cardiotoxicity of antineoplastic drug doxorubicin," *International Journal of Molecular Sciences*, vol. 14, no. 12, pp. 21629–21646, 2013.

[28] L. Ruiz-Azuara and M. E. Bravo-Gomez, "Copper compounds in cancer chemotherapy," *Current Medicinal Chemistry*, vol. 17, no. 31, pp. 3606–3615, 2010.

[29] F. Carvallo-Chaigneau, C. Trejo-Solis, C. Gomez-Ruiz et al., "Casiopeina III-ia induces apoptosis in HCT-15 cells in vitro through caspase-dependent mechanisms and has antitumor effect in vivo," *Biometals*, vol. 21, no. 1, pp. 17–28, 2008.

[30] T. Watanabe, T. Tsuruo, M. Naito, and N. Kokubu, "Regression of established tumors expressing P-glycoprotein by combinations of adriamycin, cyclosporin derivatives, and MRK-16 antibodies," *Journal of the National Cancer Institute*, vol. 89, no. 7, pp. 512–518, 1997.

[31] K. L. Haas and K. J. Franz, "Application of metal coordination chemistry to explore and manipulate cell biology," *Chemical Reviews*, vol. 109, no. 10, pp. 4921–4960, 2009.

[32] R. Alemon-Medina, J. L. Munoz-Sanchez, L. Ruiz-Azuara, and I. Gracia-Mora, "Casiopeína II-gly induced cytotoxicity to HeLa cells depletes the levels of reduced glutathione and is prevented by dimethyl sulfoxide," *Toxicology In Vitro*, vol. 22, no. 3, pp. 710–715, 2008.

[33] P. Li, J. Jia, D. Zhang, J. Xie, X. Xu, and D. Wei, "*In vitro* and *in vivo* antioxidant activities of a flavonoid isolated from celery (*Apium graveolens* L. var. dulce)," *Food & Function*, vol. 5, no. 1, pp. 50–56, 2014.

[34] O. J. Stoetzer, A. Pogrebniak, R. Pelka-Fleischer, M. Hasmann, W. Hiddemann, and V. Nuessler, "Modulation of apoptosis by mitochondrial uncouplers: apoptosis-delaying features despite intrinsic cytotoxicity," *Biochemical Pharmacology*, vol. 63, no. 3, pp. 471–483, 2002.

[35] C. Vidau, R. A. Gonzalez-Polo, M. Niso-Santano et al., "Fipronil is a powerful uncoupler of oxidative phosphorylation that triggers apoptosis in human neuronal cell line SHSY5Y," *NeuroToxicology*, vol. 32, no. 6, pp. 935–943, 2011.

[36] S. Javadov and M. Karmazyn, "Mitochondrial permeability transition pore opening as an endpoint to initiate cell death and as a putative target for cardioprotection," *Cellular Physiology and Biochemistry*, vol. 20, no. 1-4, pp. 1–22, 2007.

[37] A. P. Halestrap, G. P. McStay, and S. J. Clarke, "The permeability transition pore complex: another view," *Biochimie*, vol. 84, no. 2-3, pp. 153–166, 2002.

[38] A. J. Kowaltowski, R. F. Castilho, and A. E. Vercesi, "Opening of the mitochondrial permeability transition pore by uncoupling or inorganic phosphate in the presence of $Ca^{2+}$ is dependent on mitochondrial-generated reactive oxygen species," *FEBS Letters*, vol. 378, no. 2, pp. 150–152, 1996.

[39] T. Nakagawa, S. Shimizu, T. Watanabe et al., "Cyclophilin D-dependent mitochondrial permeability transition regulates some necrotic but not apoptotic cell death," *Nature*, vol. 434, no. 7033, pp. 652–658, 2005.

[40] G. Vertiz, L. E. Garcia-Ortuno, J. P. Bernal et al., "Pharmacokinetics and hematotoxicity of a novel copper-based anticancer agent: casiopeina III-Ea, after a single intravenous dose in rats," *Fundamental & Clinical Pharmacology*, vol. 28, no. 1, pp. 78–87, 2014.

[41] J. Lao, J. Madani, T. Puertolas et al., "Liposomal doxorubicin in the treatment of breast cancer patients: a review," *Journal of Drug Delivery*, vol. 2013, Article ID 456409, 12 pages, 2013.

[42] I. Fuentes-Noriega, L. Ruiz-Ramírez, A. Tovar-Tovar, H. Rico-Morales, and I. García-Mora, "Development and validation of a liquid chromatographic method for Casiopeina IIIi® in rat plasma," *Journal of Chromatography B*, vol. 772, no. 1, pp. 115–121, 2002.

[43] P. Mukhopadhyay, M. Rajesh, S. Batkai et al., "Role of superoxide, nitric oxide, and peroxynitrite in doxorubicin-induced cell death in vivo and in vitro," *American Journal of Physiology-Heart and Circulatory Physiology*, vol. 296, no. 5, pp. H1466–H1483, 2009.

[44] G. J. Garcia-Rivas and G. Torre-Amione, "Abnormal mitochondrial function during ischemia reperfusion provides targets for pharmacological therapy," *Methodist DeBakey Cardiovascular Journal*, vol. 5, no. 3, pp. 2–7, 2009.

[45] A. P. Rolo, P. J. Oliveira, A. J. Moreno, and C. M. Palmeira, "Chenodeoxycholate induction of mitochondrial permeability transition pore is associated with increased membrane fluidity and cytochrome *c* release: protective role of carvedilol," *Mitochondrion*, vol. 2, no. 4, pp. 305–311, 2003.

[46] J. Shou, L. You, J. Yao et al., "Cyclosporine A sensitizes human non-small cell lung cancer cells to gefitinib through inhibition of STAT3," *Cancer Letters*, vol. 379, no. 1, pp. 124–133, 2016.

[47] T. Yu, Y. Yang, J. Zhang, H. He, and X. Ren, "Circumvention of cisplatin resistance in ovarian cancer by combination of cyclosporin A and low-intensity ultrasound," *European Journal of Pharmaceutics and Biopharmaceutics*, vol. 91, pp. 103–110, 2015.

Hindawi
Oxidative Medicine and Cellular Longevity
Volume 2018, Article ID 2850341, 12 pages
https://doi.org/10.1155/2018/2850341

*Review Article*

# Unraveling the Burden of Iron in Neurodegeneration: Intersections with Amyloid Beta Peptide Pathology

**Romina María Uranga**[1,2] **and Gabriela Alejandra Salvador**[1,2]

[1]*Instituto de Investigaciones Bioquímicas de Bahía Blanca, Universidad Nacional del Sur (UNS)-Consejo Nacional de Investigaciones Científicas y Técnicas, Bahía Blanca 8000, Argentina*
[2]*Departamento de Biología, Bioquímica y Farmacia, UNS, Bahía Blanca 8000, Argentina*

Correspondence should be addressed to Romina María Uranga; ruranga@criba.edu.ar
and Gabriela Alejandra Salvador; salvador@criba.edu.ar

Received 12 October 2017; Accepted 17 December 2017; Published 31 January 2018

Academic Editor: Daiana S. Avila

Copyright © 2018 Romina María Uranga and Gabriela Alejandra Salvador. This is an open access article distributed under the Creative Commons Attribution License, which permits unrestricted use, distribution, and reproduction in any medium, provided the original work is properly cited.

Iron overload is a hallmark of many neurodegenerative processes such as Alzheimer's, Parkinson's, and Huntington's diseases. Unbound iron accumulated as a consequence of brain aging is highly reactive with water and oxygen and produces reactive oxygen species (ROS) or free radicals. ROS are toxic compounds able to damage cell membranes, DNA, and mitochondria. Which are the mechanisms involved in neuronal iron homeostasis and in neuronal response to iron-induced oxidative stress constitutes a cutting-edge topic in metalloneurobiology. Increasing our knowledge about the underlying mechanisms that operate in iron accumulation and their consequences would shed light on the comprehension of the molecular events that participate in the pathophysiology of the abovementioned neurodegenerative diseases. In this review, current evidences about iron accumulation in the brain, the signaling mechanisms triggered by metal overload, as well as the interaction between amyloid $\beta$ (A$\beta$) and iron, will be summarized.

## 1. Introduction

Metals are widely distributed in biological systems and can be referred to as either "biometals" or "toxicological metals," according to whether they have functional or detrimental roles, respectively, to the organism. In the particular case of transition metals (which are defined as those elements that form at least one ion with a partially filled shell of electrons, e.g., iron, copper, and zinc), when at the appropriate concentration, they participate in the maintenance of normal cellular processes. As with many other substances, the dyshomeostasis of any metal ion, which results in levels outside the normal physiological range, can result in biological damage [1, 2].

Iron is one of the most abundant metals in the Earth's crust [3], and its presence since Earth surface oxygenation (the appearance of oxygen in the atmosphere) has made it possible for life to survive in the oxidative environment. Its high availability, together with its chemical properties, makes it a key component in energy-generating processes [3–6]. This metal, as part of several metalloproteins in the body, is crucial in sensing and transporting oxygen, transferring electrons, and catalyzing many reactions [7]. The biological functions of iron rely upon its chemical properties: it is able to dynamically and flexibly form several coordination complexes with organic ligands, and it has a favorable redox potential to switch between $Fe^{2+}$ (ferrous state) and $Fe^{3+}$ (ferric state). Important to note is the fact that iron bioavailability is limited in aerobic conditions because $Fe^{2+}$ is readily oxidized in solution to $Fe^{3+}$, which is insoluble at a physiological pH [8]. The molecular mechanisms of iron absorption, storage, and homeostasis have been further defined through the discovery of a number of genes and proteins in various iron-overload disorders in animal models and in humans [9].

## 2. Systemic and Brain Iron Metabolism

*2.1. Absorption.* A crucial event in iron homeostasis is absorption through diet. A dysregulation of dietary iron

absorption leads to iron overload or iron deficiency. Between 1 and 2 mg of dietary iron is absorbed in the duodenum per day, and this is counterbalanced with losses from sloughing of mucosal and skin cells, menstruation, and other blood losses [9].

In humans, body iron varies between 3 and 5 g and most of it (~80%) is distributed between hemoglobin from erythrocytes and developing erythroid cells. Significant amounts of iron are also found in myoglobin, and the excess of the metal is stored in the liver as well as the macrophages of the reticuloendothelial system [10].

There are two forms of dietary iron: the heme (a prosthetic group of several enzymes composed of protoporphyrin IX and a $Fe^{2+}$ ion) and the nonheme (ionic) forms (2/3 heme iron, 1/3 inorganic iron), both of which are absorbed at the apical surface of duodenal enterocytes via different mechanisms. Dietary heme (derived from myoglobin from red meat or blood hemoglobin) is transported across the apical membrane by an incompletely characterized pathway [4, 11, 12]. Heme iron absorption has been shown to be modulated by transporters formerly called heme carrier protein 1 (HCP1). However, the main physiological function of these transporters is folate transport. For this reason, these proteins in charge of heme iron absorption are now named proton-coupled folate transporter/HCP1 [4]. Once internalized in the enterocyte, heme iron is metabolized by heme oxygenase-1 (HO-1) which liberates $Fe^{2+}$. Nonheme iron exists mainly as $Fe^{3+}$, a nonbioavailable form which requires reduction in the intestinal lumen by ferric reductases before it can be transported across the apical membrane of the enterocytes by the divalent metal transporter 1 (DMT1) [8, 13, 14]. No matter where $Fe^{2+}$ comes from, that is, heme metabolization or nonheme reduction, it is either complexed with ferritin (storage) or transported across the basolateral membrane of the enterocyte into the bloodstream via the $Fe^{2+}$ transporter ferroportin (FPN) [8]. During efflux, $Fe^{2+}$ is oxidized again to $Fe^{3+}$ by the ferroxidase hephaestin [10, 15] which is thought to work together with FPN. Evidence indicates that ceruloplasmin, a plasma ferroxidase known to share significant homology with hephaestin, also participates in iron export from enterocytes and its binding to transferrin as well [16]. Once exported, iron is transported as a redox nonreactive form by transferrin (Tf) to tissues [17–19].

*2.2. Transport.* At any given time, relatively little of the iron in the body is in transit. As stated above, the transport of iron occurs via the serum transport protein Tf. Serum Tf is a glycoprotein of 80 kDa able to bind two $Fe^{3+}$ with high affinity, and, under physiological conditions, only 30% of the Tf is saturated with iron [20]. The Tf iron pool is highly dynamic: only a small part of it comes from diet-absorbed iron and most of it comes from continuously recycled iron from senescent red blood cells. Macrophages from the reticuloendothelial system metabolize heme from effete erythrocytes and release iron ($Fe^{2+}$) to the bloodstream through FPN in a process that involves reoxidation to $Fe^{3+}$ (catalyzed by ceruloplasmin) and binding to Tf.

Developing erythroid cells take $Fe^{3+}$ from plasma Tf. Tf releases iron within the cell in a process that involves interaction of Tf with cell surface receptors (TfR), internalization of the Tf-$Fe^{3+}$ complex in a vesicle (endosome), acidification of the endosome to pH 5.5 via a proton pump-mediated mechanism, release of $Fe^{3+}$ from Tf in low pH (Tf remains bound to TfR), reduction of $Fe^{3+}$ to $Fe^{2+}$ by a ferrireductase (Steap3), transport of $Fe^{2+}$ across the endosomal membrane by DMT1 to the cytosol, dissociation of the Tf-TfR complex (their affinity is drastically reduced after the release of iron), and secretion of the apo-Tf into the bloodstream to recapture $Fe^{3+}$ [9].

In the particular case of the brain, iron uptake occurs through the blood-brain barrier (BBB). Tf-$Fe^{3+}$ complex is picked up through TfR located at the surface of the cerebral capillary endothelium [21]. Neurons also express TfR, and a homolog Tf receptor named TfR2 is known to be expressed in dopaminergic neurons. Among the non-Tf bound iron uptake, it has been proposed to be incorporated in neurons by the proton-driven transporter DMT1 or another iron transporter [22]. However, under physiological conditions, this is still a matter of debate [23]. Upon uptake, FPN and DMT1 mediate the export of iron from endothelial abluminal membranes of BBB to the cerebral compartments [24]. In brain interstitial fluids, iron is bound to Tf and becomes available for neurons and neuroglia that express TfR [25].

It is worth mentioning that iron concentration varies in different areas of the brain according to the levels of TfR expression. This pattern is due to the uneven distribution of TfR in the cerebral endothelia. For example, the hippocampus and the striatum present the highest metal concentration, whereas the cortex and the brain stem contain the lowest iron levels [26].

Lactoferrin is another iron-binding protein involved in brain iron uptake via a specific receptor (lactoferrin receptor, LfR). LfR has been demonstrated to be expressed in blood vessels and nigral dopaminergic neurons [27], suggesting that this receptor may be related to iron incorporation in the brain [28]. Moreover, an increase in LfR in dopaminergic neurons has been reported in patients with Parkinson's disease (PD) compared to control subjects. Interestingly, the greater LfR expression, the higher dopaminergic neuron degeneration. Thus, the increase in LfR has been associated with iron accumulation in vulnerable neuronal populations [27, 29]. However, the exact mechanism by which iron is augmented in the brain of PD patients still remains unclear.

*2.3. Storage.* The main storage organ for iron is the liver. Hepatocytes accumulate this metal as ferritin or hemosiderin. Ferritin is composed of a protein coat and an iron core of hydrous ferric oxide containing variable amounts of phosphate [30]. Around 4,500 iron atoms can be reversibly stored within the protein coat in a soluble complex, thus preventing iron toxicity by sequestering it in a nontoxic form. Hemosiderin stores iron in a form very similar to that in ferritin, but the iron-protein complex is insoluble.

In the central nervous system, iron excretion is extremely low [31]. Until aging, the presence of iron in neurons is almost exclusively limited to its ferrous form [32, 33]. With increasing age, neurons from different brain areas raise their content of iron and ferritin. However, ferritin content in

neurons differs from that observed in oligodendrocytes, suggesting that neurons may have particular mechanisms for iron handling [34].

Mitochondrial ferritin (FtMt) is another iron storage protein. The amino acid sequence of FtMt shares high homology with H-chain ferritin indicating similar functions for both proteins [35]. It has been shown that FtMt expression is limited to tissues with high metabolic activity and oxygen consumption, among them, brain, testis, and heart [36, 37].

Neuromelanin, a dark pigment present in catecholaminergic neurons, is another iron-binding protein [38]. The exact role of neuromelanin in brain iron metabolism is still unknown, but its interaction with iron has been extensively studied in the parkinsonian *substantia nigra* [38–40]. As ferritin is mainly located in glia rather than neurons, it is possible that neuromelanin could regulate neuronal iron levels. Iron binding by neuromelanin may upregulate free radical formation [41] or may act as a hydroxyl radical scavenger [42, 43]. A recent proteomic study of neuromelanin isolated from human *substantia nigra* confirms its role in the homeostasis of neuronal iron [44]. In addition, diminished neuromelanin content in PD patients supports the function of this pigment in iron binding and the regulation of oxidative stress as well.

*2.4. Regulation of Systemic and Brain Iron.* Hepcidin, a liver-synthesized hormone, regulates the ferroportin-mediated transport of iron from enterocytes and macrophages to the bloodstream [45]. Hepcidin is able to bind to FPN and induce its phosphorylation and lysosomal degradation [30, 46]. Iron intake results in hepcidin accumulation with decreased iron absorption from diet. On the contrary, iron deficiency states promote a decrease in hepcidin levels, which stimulates duodenal iron absorption. Also, inflammatory states foster hepcidin accumulation and iron retention in macrophages. As hepcidin regulation is a complex mechanism, the discussion on the large number of proteins and transcription factors involved in this process goes beyond the aim of this review. It is worthy to note, however, that although the regulation of iron efflux by hepcidin is of great importance, the expression of FPN is also subjected to transcriptional and posttranscriptional control [10].

Several studies have shed light on the expression of hepcidin in different brain areas such as the cortex, the hippocampus, and the spinal cord [47, 48]. Both neurons and glial cells have been shown to express hepcidin in these brain regions. An increase in hepcidin levels has been demonstrated in the choroid plexus during inflammatory processes. Reinforcing the regulatory role of hepcidin in brain iron metabolism, it has been demonstrated that overexpression of this protein decreases FPN levels and provokes iron overload and, in consequence, neurodegeneration [47].

## 3. Iron and Oxidative Stress

In cells, iron concentration ranges between 0.2 and 1.5 $\mu$M and is weakly bound to low-molecular weight substrates. The ability of iron to change between 2+ and 3+ valency states with a redox potential compatible with the cellular environment renders it one of the most important metals in catalytic processes of oxidative biology [49, 50]. As stated above, the appearance of oxygen in the atmosphere made it possible for the organisms that adapted to those conditions to get 20 times more energy than that obtained from fermentative reactions [51]. However, the negative part of this issue is the continuous generation of reactive oxygen species (ROS) as normal by-products of metabolism. The redox equilibrium is essential for the physiology of the body, and since ROS first appeared, they have been involved in the regulatory mechanisms of synthesis and homeostasis of biomolecules, as well as many important processes of the organism [52]. Although small amounts of free radicals are produced in all metabolic processes (enzymatic reactions in the endoplasmic reticulum, microsomes, peroxisomes, or cytoplasm), the major generation of ROS emerges by incomplete reduction of dioxygen in the mitochondrial electron transport chain. In brief, the first radical formed from $O_2$ is the superoxide radical ($O_2^{\bullet}$), which is not itself very reactive but it is able to generate other dangerous species. The addition of a second electron to a superoxide radical results in the peroxide ion ($O_2^{2-}$). Peroxide is not a radical, and when protonated, it generates hydrogen peroxide ($H_2O_2$). The following reduction of hydrogen peroxide (through the metal-ion catalyzed Fenton reaction) produces the hydroxyl radical ($OH^{\bullet}$) which reacts rapidly with high affinity with almost every molecule found in living cells [51, 53–55]. Under normal conditions, ROS are rapidly detoxified by the cell, but under certain circumstances in which ROS production exceeds intracellular antioxidant defense, an increase in the steady state concentration of ROS is observed: a condition known as oxidative stress.

*In vitro* experiments have shown that cellular oxidative stress induced by iron overload is characterized by increased lipid peroxidation and protein and nucleic acid modifications [56–59]. The presence of a labile iron pool (LIP, redox-active iron bound to low affinity compounds and which determines the iron status of the cell) is the main contributor to oxidative stress during iron overload [60]. This destructive potential of iron has led to investigate its role in the pathophysiology of several neurodegenerative diseases associated to oxidative stress, and this is the main focus of this review.

## 4. Evidence of Iron Accumulation in the Brain

The increased human lifespan of today has had a significant impact on the development of neurodegenerative diseases in elderly people. Metalloneurobiology, a relatively new discipline, has become extremely important for establishing the role of transition metals in neuronal degeneration. Iron is required for usual metabolic processes, such as mitochondrial respiration and DNA synthesis, and it also plays a key role in the biosynthesis of neurotransmitters and myelin in the brain [51, 61]. Moreover, iron has been demonstrated to be necessary for the normal development of cognitive functions. In this regard, iron deficiency early in life has shown to cause learning and memory impairment in humans [62–64]. Additionally, it has been observed that this metal ion progressively accumulates in the brain during normal

aging [65]. However, this accumulation has also been related to the pathogenesis of several neurodegenerative disorders, such as PD and Alzheimer's disease (AD) [61]. In this connection, interesting studies have been conducted on *Octodon degus*. This Chilean rodent, widely utilized for modeling sporadic AD, has shown increased levels of redox-active metals (Fe, Cu, and Zn), specifically in the cortex and the hippocampus, the brain areas mainly affected in AD [66]. Indeed, increased iron in the *substantia nigra* of PD patients has been related to neurodegenerative mechanisms and, notably, clinical studies using iron chelators have shown to lower iron levels and improve the performance of early diagnosed PD patients [67].

In the abovementioned disorders, iron-induced oxidative stress, combined with defective antioxidant capacities, promotes neuronal death and neurodegeneration [4, 22, 68]. However, it is still uncertain whether the extensive brain iron accumulation is a primary cause of the pathogenic event, or just a consequence of a previous dysfunction [69, 70]. Interestingly, the diseases collectively known as neurodegeneration with brain iron accumulation (NBIA), all of which are characterized by iron accumulation in basal ganglia and mutations in proteins involved in iron traffic or metabolism, have shown clinical and molecular similarities with neurodegenerative diseases such as AD and PD [71–73]. Importantly, iron deposition has been reported to occur only in specific brain regions in patients with chronic neurodegenerative diseases [4, 68, 69, 74]. In the case of AD, iron accumulates mainly in the cerebral cortex and hippocampus, without a concomitant increase in ferritin normally observed in aging [74], thereby raising the risk of oxidative stress. Both neurodegenerative diseases present neuroinflammation as a triggering factor for neuronal death. A recent study reports that the inflammatory process related to neurodegeneration causes an increase in iron levels and ferritin in microglia and neurons as well [75]. Moreover, the release of iron from dying neurons, glial cells, and macrophages to the extracellular space has been postulated as a source of iron to be taken up by nonaffected neurons in a TfR-mediated pathway [75]. Tf-independent iron uptake has also been described. This pathway is known to induce ferritin expression to serve as an iron scavenger [76]. A balance between the expression levels of ferritin and ferroportin (which mediates neuronal iron excretion) has been reported in neurons that usually deal with large amounts of iron [75]. However, although there is strong evidence of a link between iron and neurodegeneration, further studies that correlate the temporal relationship need to be carried out. Most importantly and although in its infancy, the development of new living models makes it possible to observe the detailed and unambiguous molecular events occurring in the degenerative process urges.

## 5. Intersections between A$\beta$ and Iron in the Brain: Iron Chelation Therapies

It is well established that the pathological hallmarks of AD in the brain include abundant extracellular amyloid $\beta$ peptide (A$\beta$) plaques, intracellular neurofibrillary tangles of protein tau, and increased brain iron (in and around A$\beta$ plaques) [77, 78]. In this review, we focus particularly on A$\beta$ and iron interactions. The aggregation of A$\beta$ (which has been shown to be toxic to neurons) is known to be triggered by metals such as zinc, copper, and iron [79–82]. Therefore, metal dyshomeostasis may be an important factor leading to AD pathogenesis. Moreover, A$\beta$ has been demonstrated to bind zinc and iron, and more strongly, copper [83]. Therefore, these chelation characteristics of the peptide may account for the enrichment of these metal ions in A$\beta$ plaques [83].

Cumulative evidence suggests that A$\beta$ is the major cause of neurotoxicity and may significantly contribute to synaptic dysfunction in AD [84]. Iron accumulation in affected brain regions, as reported by *postmortem* and magnetic resonance imaging (MRI) studies [85–87], may also be responsible for the increased oxidative stress observed in AD [50, 88]. A$\beta$ has broadly been shown to bind iron [89]. This A$\beta$-iron interaction is through His6, His13, and His14 of A$\beta$ and is thought to be facilitated in a more reduced environment such as the brain due to the prevalence for the ferrous form of iron to bind A$\beta$ [50, 90]. Interestingly, a very recent study carried out on APP/PS1 mice has demonstrated that ferrous iron is an integral part of amyloid plaques and has provided evidence that (supporting previous *in vitro* studies) A$\beta$-induced reduction of iron is able to occur *in vivo* [91]. On the other hand, ROS generated through iron-aggregated A$\beta$ are toxic to neurons [92] and would partially contribute to the neurotoxicity present within the iron-enriched environment around senile plaques [93, 94]. Moreover, accumulated iron in neurofibrillary tangle-containing neurons and the neuritic processes adjoining senile plaques in AD [95] have been correlated with cognitive decline [96].

As iron homeostasis is so important in preventing cell oxidative damage, mechanisms to keep iron in the physiological concentration range have been evolutionarily incorporated to maintain optimal cell function [10]. The proteins required to regulate cellular iron homeostasis in the brain are quite the same as those used in the body's periphery: the iron response proteins (IRPs) 1 and 2 bind to their respective iron regulatory elements (IREs) in either the 3′-untranslated region (UTR) or 5′-UTR of an mRNA. Despite studies suggesting that iron nonspecifically coprecipitate with A$\beta$ in AD [50, 97], a role for iron in A$\beta$ metabolism and AD progression has been shown and, conversely, A$\beta$ seems to be involved in neuronal iron homeostasis. Not only has iron been demonstrated to bind to and accelerate A$\beta$ precipitation [90, 98] but it also regulates its generation from amyloid precursor protein (APP) (Figure 1). The aforementioned A$\beta$ plaques are mainly constituted by a 40–42-amino acid A$\beta$ peptide cleaved from the APP by $\beta$- and $\gamma$-secretases in the amyloidogenic pathway [83, 99]. Interestingly, intracellular iron levels have been reported to control APP translation via an IRE RNA stem loop in the 5′-UTR of the APP transcript. This APP IRE has been found to physiologically bind with IRP1, and not with IRP2 in human neural cells [100]. Therefore, increased

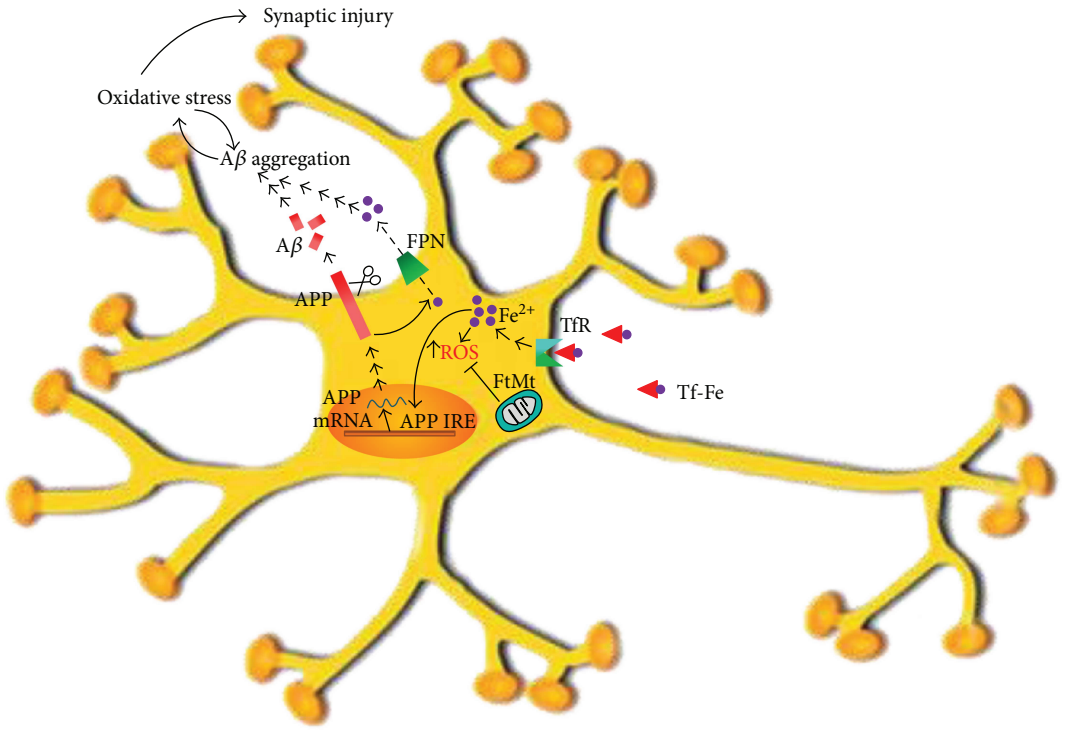


Figure 1: Iron and A$\beta$ interactions. Transferrin-bound iron is taken up by the neuron via a receptor- (TfR) mediated mechanism. An augmented pool of intracellular iron (mainly as $Fe^{2+}$) increases ROS production with the concomitant generation of oxidative stress. Mitochondrial ferritin is able to protect the neuron against iron-induced oxidative stress. Iron itself is able to induce APP expression through an APP IRE. Also, APP mediates iron export via FPN. An increased APP expression (due to an increased iron uptake) results in an increased A$\beta$ generation. Interestingly, iron is involved in A$\beta$ aggregation in a mechanism that generates oxidative stress, but it is also known that previous oxidative stress increases A$\beta$ aggregation. In this way, both A$\beta$ and iron participate in a vicious cycle known to culminate with synaptic oxidative injury.

cytosolic iron levels translationally upregulate APP expression [99, 100]. Interestingly, APP has been found to facilitate neuronal iron efflux through a mechanism that involves FPN [101, 102] (Figure 1). Hence, iron influx drives the translational expression of the neuronal APP, which, in turn, has a role in iron efflux. In this regard, intracellular iron retention has been reported in neuronal cultures and mouse models depleted of APP, and normal iron efflux has been observed to be restored when APP was either added extracellularly [101] or overexpressed [101, 103]. It is also worth noting that Down's syndrome-suffering children (who have increased APP expression) have been found to present anemia and a high risk of iron deficiency [50, 104, 105].

Another piece of evidence between the link of iron and A$\beta$ comes from the recently described neuroprotective role of FtMt. In neurons exposed to A$\beta$25-35, the overexpression of FtMt diminished the labile iron pool, decreased oxidative injury, and prevented cytochrome c release from mitochondria through the activation of the mitogen-activated protein kinase (MAPK) pathway, thus inhibiting neuronal apoptosis [106]. Moreover, an increased FtMt expression has been described in AD [107, 108].

In view of the crucial and multifactorial role of iron in AD progression, it is imperious to consider this metal in the therapeutic design. Metal chelation is one of the therapeutic strategies for AD [109]. The great challenge will be developing chelating drugs able to cross the BBB. It has been demonstrated that A$\beta$-insoluble aggregates are dissolved by metal chelators [110]. Moreover, the iron chelator desferrioxamine has shown to decelerate disease progression [111]. However, due to the size of desferrioxamine and the relative impermeability of the BBB to this drug, desferrioxamine has had limited success in the brain when administered peripherally [112]. Fortunately, smaller molecular compounds with chemical modifications have had promising results in preclinical trials [113, 114]. For instance, deferiprone has been approved for peripheral iron overload in thalassemia and in the neurodegenerative disease, Friedrich's ataxia [115]. Additionally, clioquinol derivatives have been used in clinical trials in AD patients, showing reduced A$\beta$ in cerebrospinal fluid, as well as improved cognitive performance [116]. A key point to take into account in the chelation therapy would be to restrain iron without generating a deficiency which would be as dangerous as the excess of the metal.

## 6. Signaling of Iron in the Central Nervous System

The activation or inactivation of specific signaling pathways is one of the multiple responses a neuron can give to oxidative stressors. The decision of living or dying in a certain cell

type will depend on several aspects of the stress (type, extent, and time of exposure) which will determine the signaling pathways that will result in being turned on and off. The sum of these aspects will define the cellular fate [117, 118]. In this respect, iron has been involved in the triggering of several protective and proapoptotic signaling pathways in neurons [119].

It has been demonstrated that synaptic endings are the sites where the first signs of neurodegenerative processes are likely to appear. It is well known that marked synapse loss, rather than neuronal death, occurs during the initial events of AD [119–121]. This fact might involve apoptotic cascades triggered locally at the synapse that might occur independently of gene transcription. It has been reported that morphological changes in the synapses precede A$\beta$ deposition [122]. Also, a decrease in synaptic markers has been observed in hippocampal neurons exposed to $Fe^{2+}$ [57]. Synaptic susceptibility to iron-induced oxidative stress has been largely shown [123–129], being that synaptic endings from senile animals are more vulnerable to $Fe^{2+}$ exposure than those isolated from adult animals [128]. Increased membrane lipid peroxidation, loss of selective permeability of plasma membrane, 4-hydroxynonenal (HNE) generation, impairment of membrane ion-motive ATPases, glucose and glutamate transport, and mitochondrial function have been reported to be constant observations of synaptosomal oxidative injury induced by iron exposure [123–129].

Regarding synaptic iron-triggered signaling, phosphatidylinositol 3-kinase (PI3K)/Akt pathway, a well-known survival-associated pathway, has been reported to be activated in synaptic endings of both adult and aged animals; the difference has been found mainly in the time frame of the activation, which varies with animal age [128]. One of the best known Akt substrates, glycogen synthase kinase 3$\beta$ (GSK3$\beta$), has been largely reported to be involved in metabolism, survival, gene expression, and cytoskeletal dynamics, and it is considered a crucial player for determining neuronal fate [130]. The phosphorylation (and inactivation) of synaptic GSK3$\beta$ has been shown to follow the same time pattern as Akt [128]. Extracellular signal-regulated kinases (ERK) 1/2, key components of stress-related cellular responses that have been involved in both survival and death, have been found to present different patterns of synaptic activation according to the age of animals. Moreover, the dependence of ERK1/2 activation on the PI3K pathway has also shown to be age-dependent [128].

Kuperstein and Yavin have described the effect of iron and A$\beta$ on ERK signaling in neuronal cultures [131]. Interestingly, a two-peaked activation of ERK has been shown: a rapid one (5 min) followed by a decline by 30 min and a second one (continuous up to 24 h) in which nuclear translocation of ERK is detected. Desferrioxamine, as well as antioxidant treatments, has shown to suppress ERK activation and nuclear translocation, resulting in a reduced apoptotic death. In the light of these observations, it can be concluded that ERK promotes iron-triggered damage. In extending these findings, it has also been demonstrated that the coexposure of neuronal cells to iron and A$\beta$ induces a decrease in Akt activity and Bad phosphorylation, and an increase in the activation of p38 and caspase-3 and caspase-9 [132]. It is important to highlight that there are many controversies about the effect of iron and A$\beta$ (each alone or combined) on cellular signaling cascades. Differences may be due to the specific experimental conditions (time of exposure, concentration of the metal or A$\beta$, and cellular type). The signaling lipid phosphatidic acid, produced by phospholipase D (PLD), has been also involved in the synaptic response induced by iron overload. Moreover, PLD1 and PLD2 activities have shown to be involved in the activation of protein kinase D (PKD) 1, ERK1/2, and protein kinase C (PKC) $\alpha/\beta$II in adult animals, but not in senile animals [133]. These molecular differences in the signaling reported in aged animals could account for the increased age-related synaptic susceptibility to iron and might also suggest that these signaling cascades pursue different goals in the synapses according to age. Indeed, PLD2 has been shown to be activated by oligomeric A$\beta$ in cultured neurons [134]. Moreover, A$\beta$ has been proven to fail in the suppression of long-term potentiation in PLD2-deficient mice hippocampal slices, suggesting that PLD2 is required for the synaptotoxic action of A$\beta$ [134]. Experiments carried out in a transgenic mouse model of AD (SwAPP) have also confirmed that PLD2 activity is increased and the ablation of its gene (*Pld2*) ameliorates memory deficits and protects the synapses [134]. These findings highlight the capital role of PLD in AD progression.

As mentioned, iron (alone or in combination with A$\beta$) is able to activate different signaling cascades. These signaling pathways are the molecular events necessary for the activation of several transcription factors which, by regulating the expression of specific genes, modulate the neuronal response to the injury. Extensive evidence links the transcription factors Forkhead box O (FoxO), nuclear factor- (NF-) $\kappa$B, and activator protein (AP) 1 to neuronal responses to oxidative stress [57, 135]. FoxO transcription factors have been shown to increase stress resistance and to extend lifespan in *Drosophila* [136]. Recent studies have demonstrated that phosphorylated FoxO3A translocates out of the nucleus in HT22 neurons in a PI3K/Akt-mediated mechanism after iron exposure [57]. Surprisingly, this defensive response to oxidative stress leads to downregulation of superoxide dismutase (SOD) 1 and 2 expression, so that the neuron responds to the oxidative injury via glutathione metabolism [57]. Interestingly, the neuron has been shown to respond to oligomeric A$\beta$ exposure with the same insulinomimetic signaling as it does upon iron exposure, although undetectable oxidative stress markers have been reported in the presence of A$\beta$ [137]. NF-$\kappa$B plays crucial roles in cellular resistance to oxidants and survival. The role of this transcription factor in the inhibition of apoptosis (by participating in the induction of antiapoptotic genes) has been well demonstrated [138]. As to iron and AD, NF-$\kappa$B has been associated with increased resistance of neurons to apoptosis induced by exposure to the metal ion [135]. The expression of this transcription factor has been found to be increased both in neurons and astrocytes in areas adjoining A$\beta$ plaques in patients with AD [139]. There is also evidence about A$\beta$-induced activation of NF-$\kappa$B in cultured neurons, and both protective and injurious roles of this transcription factor have

been reported [140–142]. For its part, AP-1, an essential transcription factor in cellular response to oxidative stress (as well as in other processes such as proliferation, differentiation, and survival), c-Jun-N-terminal kinase, and p38 (two stress-related MAPK which are upstream of AP-1 in the cascade) have also shown to be activated by oxidative stress [135]. Both MAPK, as well as AP-1, have been shown to be involved in physiological functions of the brain. Interestingly, c-Jun, a component of AP-1, has been recently attributed a dual role: it is able to mediate plasticity and repair mechanisms, but it is also thought to participate in neuronal death [143].

The role of free calcium in neuronal death induced by oxidative stress has been well documented [128, 144, 145]. Under physiological conditions, the intracellular calcium level is tightly controlled, and relatively small fluctuations in intracellular calcium concentration might cause neuronal deterioration and eventually lead to cell degeneration. Neuronal activity generates calcium signals that result in the transcription of genes that are crucial for synaptic plasticity and neuronal survival. It has also been demonstrated that calcium participates in the early events of iron-induced oxidative injury in synapses, but after long-term exposure to iron, the absence, as much as the excess of calcium, appears to be more deleterious to the synaptic endings than the damage induced by iron itself [128]. The exact mechanism by which calcium participates in synaptic injury is not clear. It seems that the activation of distinct signaling cascades downstream from key points of calcium entry at synapses has a major role in the neurodegenerative process. In the whole neuron, calcium released from intracellular stores has been linked to the stimulation of ERK and calcium-calmodulin-dependent protein kinases and cAMP response element-binding protein- (CREB-) dependent gene transcription [64]. The latter, a process known to be involved in synaptic plasticity, occurs through the calcium-induced calcium release, a compelling mechanism based on the calcium-dependent activation of calcium release channels, such as the ryanodine receptors (RyR) or the IP3 receptors (IP3R), and by which small and localized calcium signals can be amplified or propagated to the nucleus (also to the mitochondria) [64]. Interestingly, RyR activity has been shown to be redox sensitive, due to a few cysteine residues of the RyR protein [64, 146, 147]. For this reason, RyR, which have been proposed as redox sensors [64, 147], have attracted increasing attention in the research field of synaptic plasticity in hippocampal neurons [148, 149]. Work from Muñoz and colleagues has demonstrated that iron exposure of PC12 cells or hippocampal neurons leads to ROS generation and ERK activation through RyR-mediated calcium release. Both effects are clearly reduced by either mannitol (hydroxyl radical scavenger) or desferrioxamine (an iron chelator), indicating that iron-induced hydroxyl radicals are responsible for calcium release and ERK stimulation [150]. This is clear evidence of calcium and iron involvement in the events necessary for synaptic plasticity and supports the idea that increased iron concentration may cause neurodegeneration via excessive intracellular calcium [64].

## 7. Concluding Remarks

In this review, we summarize cutting-edge knowledge about iron and its involvement in neurodegenerative processes, in particular, AD. Vast evidence has demonstrated that iron is a clear generator of oxidative stress. Both iron and oxidative stress have been linked to A$\beta$ aggregation. However, the exact order in the molecular events that lead to the onset of AD still remains elusive. Exploring the brain's own iron homeostatic mechanisms and the signaling events involved in response to metal overload may shed light on several unclear aspects of the disease and may therefore lead straightaway to the development of a definite therapeutic tool.

## Abbreviations

HNE: 4-Hydroxynonenal
AD: Alzheimer's disease
APP: Amyloid precursor protein
BBB: Blood-brain barrier
DMT1: Divalent metal transporter 1
ERK: Extracellular signal-regulated kinases
FPN: Ferroportin
GSK3$\beta$: Glycogen synthase kinase
HCP1: Heme carrier protein 1
HO-1: Heme oxygenase-1
IRE: Iron regulatory elements
IRP: Iron response protein
LIP: Labile pool iron
LfR: Lactoferrin receptor
MRI: Magnetic resonance imaging
FtMt: Mitochondrial ferritin
NBIA: Neurodegeneration with brain iron accumulation
PD: Parkinson's disease
ROS: Reactive oxygen species
TfR: Transferrin receptor
Tf: Transferrin
UTR: Untranslated mRNA.

## Disclosure

Gabriela Alejandra Salvador and Romina María Uranga are research members of CONICET.

## Conflicts of Interest

The authors declare that they have no conflict of interest.

## Acknowledgments

The authors are grateful to translator Viviana Soler for her technical assistance in controlling the use of the English language in this review. The authors wish to thank Ms. Janice Warren for carefully reading and suggesting improvements to the manuscript. This work was supported by grants from the *Universidad Nacional del Sur* (PGI24B/179), the *Consejo Nacional de Investigaciones Científicas y Técnicas* (PIP-CONICET), and the *Agencia Nacional de Promoción Científica y Tecnológica* (PICT-2010-936, PICT2013-0987).

## References


[1] P. A. Adlard and A. I. Bush, "Metals and Alzheimer's disease," *Journal of Alzheimer's Disease*, vol. 10, no. 2-3, pp. 145–163, 2006.

[2] J. J. R. Fraústo da Silva and R. J. P. Williams, *The biological chemistry of the elements*, Oxford University Press, Oxford, 2001.

[3] K. A. Weber, L. A. Achenbach, and J. D. Coates, "Microorganisms pumping iron: anaerobic microbial iron oxidation and reduction," *Nature Reviews Microbiology*, vol. 4, no. 10, pp. 752–764, 2006.

[4] M. Farina, D. S. Avila, J. B. da Rocha, and M. Aschner, "Metals, oxidative stress and neurodegeneration: a focus on iron, manganese and mercury," *Neurochemistry Internationa*l, vol. 62, no. 5, pp. 575–594, 2013.

[5] J. F. Turrens, "Mitochondrial formation of reactive oxygen species," *The Journal of Physiology*, vol. 552, no. 2, pp. 335–344, 2003.

[6] G. Wachtershauser, "On the chemistry and evolution of the pioneer organism," *Chemistry & Biodiversity*, vol. 4, no. 4, pp. 584–602, 2007.

[7] P. Aisen, C. Enns, and M. Wessling-Resnick, "Chemistry and biology of eukaryotic iron metabolism," *The International Journal of Biochemistry & Cell Biology*, vol. 33, no. 10, pp. 940–959, 2001.

[8] G. Papanikolaou and K. Pantopoulos, "Iron metabolism and toxicity," *Toxicology and Applied Pharmacology*, vol. 202, no. 2, pp. 199–211, 2005.

[9] T. Ganz, "Systemic iron homeostasis," *Physiological Reviews*, vol. 93, no. 4, pp. 1721–1741, 2013.

[10] J. Wang and K. Pantopoulos, "Regulation of cellular iron metabolism," *Biochemical Journal*, vol. 434, no. 3, pp. 365–381, 2011.

[11] E. C. Theil, "Iron homeostasis and nutritional iron deficiency," *The Journal of Nutrition*, vol. 141, no. 4, pp. 724S–728S, 2011.

[12] A. R. West and P. S. Oates, "Mechanisms of heme iron absorption: current questions and controversies," *World Journal of Gastroenterol*, vol. 14, no. 26, pp. 4101–4110, 2008.

[13] H. Gunshin, B. Mackenzie, U. V. Berger et al., "Cloning and characterization of a mammalian proton-coupled metal-ion transporter," *Nature*, vol. 388, no. 6641, pp. 482–488, 1997.

[14] A. T. McKie, D. Barrow, G. O. Latunde-Dada et al., "An iron-regulated ferric reductase associated with the absorption of dietary iron," *Science*, vol. 291, no. 5509, pp. 1755–1759, 2001.

[15] K. Y. Yeh, M. Yeh, L. Mims, and J. Glass, "Iron feeding induces ferroportin 1 and hephaestin migration and interaction in rat duodenal epithelium," *American Journal of Physiology-Gastrointestinal and Liver Physiology*, vol. 296, no. 1, pp. G55–G65, 2009.

[16] N. E. Hellman and J. D. Gitlin, "Ceruloplasmin metabolism and function," *Annual Review of Nutrition*, vol. 22, no. 1, pp. 439–458, 2002.

[17] I. De Domenico, W. D. McVey, and J. Kaplan, "Regulation of iron acquisition and storage: consequences for iron-linked disorders," *Nature Reviews Molecular Cell Biology*, vol. 9, no. 1, pp. 72–81, 2008.

[18] R. E. Fleming and P. Ponka, "Iron overload in human disease," *The New England Journal of Medicine*, vol. 366, no. 4, pp. 348–359, 2012.

[19] E. Nemeth and T. Ganz, "Regulation of iron metabolism by hepcidin," *Annual Review of Nutrition*, vol. 26, no. 1, pp. 323–342, 2006.

[20] S. Puntarulo, "Iron, oxidative stress and human health," *Molecular Aspects of Medicine*, vol. 26, no. 4-5, pp. 299–312, 2005.

[21] M. W. Bradbury, "Transport of iron in the blood-brain-cerebrospinal fluid system," *Journal of Neurochemistry*, vol. 69, no. 2, pp. 443–454, 1997.

[22] M. T. Nunez, P. Urrutia, N. Mena, P. Aguirre, V. Tapia, and J. Salazar, "Iron toxicity in neurodegeneration," *Biometals*, vol. 25, no. 4, pp. 761–776, 2012.

[23] I. Pelizzoni, D. Zacchetti, C. P. Smith, F. Grohovaz, and F. Codazzi, "Expression of divalent metal transporter 1 in primary hippocampal neurons: reconsidering its role in non-transferrin-bound iron influx," *Journal of. Neurochemistry*, vol. 120, no. 2, pp. 269–278, 2012.

[24] W. Zheng and A. D. Monnot, "Regulation of brain iron and copper homeostasis by brain barrier systems: implication in neurodegenerative diseases," *Pharmacology & Therapeutics*, vol. 133, no. 2, pp. 177–188, 2012.

[25] J. Han, J. R. Day, J. R. Connor, and J. L. Beard, "Gene expression of transferrin and transferrin receptor in brains of control vs. iron-deficient rats," *Nutritional Neuroscience*, vol. 6, no. 1, pp. 1–10, 2003.

[26] R. Deane, W. Zheng, and B. V. Zlokovic, "Brain capillary endothelium and choroid plexus epithelium regulate transport of transferrin-bound and free iron into the rat brain," *Journal of Neurochemistry*, vol. 88, no. 4, pp. 813–820, 2004.

[27] B. A. Faucheux, N. Nillesse, P. Damier et al., "Expression of lactoferrin receptors is increased in the mesencephalon of patients with Parkinson disease," *Proceedings of the National Academy of Sciences of the United States of America*, vol. 92, no. 21, pp. 9603–9607, 1995.

[28] A. M. Snyder and J. R. Connor, "Iron, the substantia nigra and related neurological disorders," *Biochimica et Biophysica Acta (BBA) - General Subjects*, vol. 1790, no. 7, pp. 606–614, 2009.

[29] B. Leveugle, B. A. Faucheux, C. Bouras et al., "Cellular distribution of the iron-binding protein lactotransferrin in the mesencephalon of Parkinson's disease cases," *Acta Neuropathologica*, vol. 91, no. 6, pp. 566–572, 1996.

[30] E. C. Theil and K. N. Raymond, "Transition-metal storage, transport, and biomineralization," in *Bioinorganic Chemistry*, I. Bertini, H. B. Gray, S. J. Lippard and J. S. Valentine, Eds., pp. 1–35, University Science Books, Mill Valley, California, 1994.

[31] P. R. Dallman and R. A. Spirito, "Brain iron in the rat: extremely slow turnover in normal rats may explain long-lasting effects of early iron deficiency," *Journal of Nutrition*, vol. 107, no. 6, pp. 1075–1081, 1977.

[32] S. A. Benkovic and J. R. Connor, "Ferritin, transferrin, and iron in selected regions of the adult and aged rat brain," *The Journal of Comparative Neurology*, vol. 338, no. 1, pp. 97–113, 1993.

[33] D. Kaur, F. Yantiri, S. Rajagopalan et al., "Genetic or pharmacological iron chelation prevents MPTP-induced neurotoxicity in vivo: a novel therapy for Parkinson's disease," *Neuron*, vol. 37, no. 6, pp. 899–909, 2003.

[34] H. H. Andersen, K. B. Johnsen, and T. Moos, "Iron deposits in the chronically inflamed central nervous system and contributes to neurodegeneration," *Cellular and Molecular Life Sciences*, vol. 71, no. 9, pp. 1607–1622, 2014.

[35] B. Langlois d'Estaintot, P. Santambrogio, T. Granier et al., "Crystal structure and biochemical properties of the human mitochondrial ferritin and its mutant Ser144Ala," *Journal of Molecular Biology*, vol. 340, no. 2, pp. 277–293, 2004.

[36] G. Gao and Y. Z. Chang, "Mitochondrial ferritin in the regulation of brain iron homeostasis and neurodegenerative diseases," *Frontiers in Pharmacology*, vol. 5, p. 19, 2014.

[37] D. Finazzi and P. Arosio, "Biology of ferritin in mammals: an update on iron storage, oxidative damage and neurodegeneration," *Archives of Toxicology*, vol. 88, no. 10, pp. 1787–1802, 2014.

[38] H. Fedorow, F. Tribl, G. Halliday, M. Gerlach, P. Riederer, and K. L. Double, "Neuromelanin in human dopamine neurons: comparison with peripheral melanins and relevance to Parkinson's disease," *Progress in Neurobiology*, vol. 75, no. 2, pp. 109–124, 2005.

[39] G. Becker, J. Seufert, U. Bogdahn, H. Reichmann, and K. Reiners, "Degeneration of substantia nigra in chronic Parkinson's disease visualized by transcranial color-coded real-time sonography," *Neurology*, vol. 45, no. 1, pp. 182–184, 1995.

[40] V. M. Mann, J. M. Cooper, S. E. Daniel et al., "Complex I, iron, and ferritin in Parkinson's disease substantia nigra," *Annals of Neurology*, vol. 36, no. 6, pp. 876–881, 1994.

[41] M. B. Youdim, D. Ben-Shachar, and P. Riederer, "Is Parkinson's disease a progressive siderosis of substantia nigra resulting in iron and melanin induced neurodegeneration?," *Acta Neurologica Scandinavica*, vol. 80, no. S126, pp. 47–54, 1989.

[42] K. L. Double, L. Zecca, P. Costi et al., "Structural characteristics of human substantia nigra neuromelanin and synthetic dopamine melanins," *Journal of Neurochemistry*, vol. 75, no. 6, pp. 2583–2589, 2000.

[43] W. Korytowski, T. Sarna, and M. Zareba, "Antioxidant action of neuromelanin: the mechanism of inhibitory effect on lipid peroxidation," *Archives of Biochemistry and Biophysics*, vol. 319, no. 1, pp. 142–148, 1995.

[44] S. Plum, S. Steinbach, J. Attems et al., "Proteomic characterization of neuromelanin granules isolated from human *substantia nigra* by laser-microdissection," *Scientific Reports*, vol. 6, no. 1, article 37139, 2016.

[45] K. E. Finberg, "Regulation of systemic iron homeostasis," *Current Opinion in Hematology*, vol. 20, no. 3, pp. 208–214, 2013.

[46] C. Sennett, L. E. Rosenberg, and I. S. Mellman, "Transmembrane transport of cobalamin in prokaryotic and eukaryotic cells," *Annual Review of Biochemistry*, vol. 50, no. 1, pp. 1053–1086, 1981.

[47] S. M. Wang, L. J. Fu, X. L. Duan et al., "Role of hepcidin in murine brain iron metabolism," *Cellular and Molecular Life Sciences*, vol. 67, no. 1, pp. 123–133, 2010.

[48] R. Raha-Chowdhury, A. A. Raha, S. Forostyak, J. W. Zhao, S. R. W. Stott, and A. Bomford, "Expression and cellular localization of hepcidin mRNA and protein in normal rat brain," *BMC Neuroscience*, vol. 16, no. 1, p. 24, 2015.

[49] P. J. Urrutia, N. P. Mena, and M. T. Nunez, "The interplay between iron accumulation, mitochondrial dysfunction, and inflammation during the execution step of neurodegenerative disorders," *Frontiers in Pharmacology*, vol. 5, p. 38, 2014.

[50] B. X. Wong and J. A. Duce, "The iron regulatory capability of the major protein participants in prevalent neurodegenerative disorders," *Frontiers in Pharmacology*, vol. 5, p. 81, 2014.

[51] R. Crichton, *Iron Metabolism: From Molecular Mechanisms to Clinical Consequences*, John Wiley & Sons, 2009.

[52] P. D. Ray, B. W. Huang, and Y. Tsuji, "Reactive oxygen species (ROS) homeostasis and redox regulation in cellular signaling," *Cellular Signalling*, vol. 24, no. 5, pp. 981–990, 2012.

[53] J. M. McCord, "Iron, free radicals, and oxidative injury," *Seminars in Hematology*, vol. 35, no. 1, pp. 5–12, 1998.

[54] H. Fenton, "Oxidation of tartaric acid in presence of iron," *Journal of the Chemical Society, Transactions*, vol. 65, no. 0, pp. 899–910, 1894.

[55] F. Haber and J. Weiss, "The catalytic decomposition of hydrogen peroxide by iron salts," *Proceedings of the Royal Society A: Mathematical, Physical and Engineering Sciences*, vol. 147, no. 861, pp. 332–351, 1934.

[56] G. Rodríguez Diez, R. M. Uranga, M. V. Mateos, N. M. Giusto, and G. A. Salvador, "Differential participation of phospholipase $A_2$ isoforms during iron-induced retinal toxicity. Implications for age-related macular degeneration," *Neurochemistry International*, vol. 61, no. 5, pp. 749–758, 2012.

[57] R. M. Uranga, S. Katz, and G. A. Salvador, "Enhanced phosphatidylinositol 3-kinase (PI3K)/Akt signaling has pleiotropic targets in hippocampal neurons exposed to iron-induced oxidative stress," *Journal of Biological Chemistry*, vol. 288, no. 27, pp. 19773–19784, 2013.

[58] R. J. Ward, F. A. Zucca, J. H. Duyn, R. R. Crichton, and L. Zecca, "The role of iron in brain ageing and neurodegenerative disorders," *The Lancet Neurology*, vol. 13, no. 10, pp. 1045–1060, 2014.

[59] R. Crichton and R. J. Ward, *Metal-Based Neurodegeneration: From Molecular Mechanisms to Therapeutic Strategies*, John Wiley & Sons, 2014.

[60] N. E. Piloni, J. C. Perazzo, V. Fernandez, L. A. Videla, and S. Puntarulo, "Sub-chronic iron overload triggers oxidative stress development in rat brain: implications for cell protection," *Biometals*, vol. 29, no. 1, pp. 119–130, 2016.

[61] P. T. Lieu, M. Heiskala, P. A. Peterson, and Y. Yang, "The roles of iron in health and disease," *Molecular Aspects of Medicine*, vol. 22, no. 1-2, pp. 1–87, 2001.

[62] J. L. Beard and J. R. Connor, "Iron status and neural functioning," *Annual Review of Nutrition*, vol. 23, no. 1, pp. 41–58, 2003.

[63] B. T. Felt, J. L. Beard, T. Schallert et al., "Persistent neurochemical and behavioral abnormalities in adulthood despite early iron supplementation for perinatal iron deficiency anemia in rats," *Behavioural Brain Research*, vol. 171, no. 2, pp. 261–270, 2006.

[64] C. Hidalgo and M. T. Nunez, "Calcium, iron and neuronal function," *IUBMB Life*, vol. 59, no. 4, pp. 280–285, 2007.

[65] G. Bartzokis, T. A. Tishler, I. S. Shin, P. H. Lu, and J. L. Cummings, "Brain ferritin iron as a risk factor for age at onset in neurodegenerative diseases," *Annals of the New York Academy of Sciences*, vol. 1012, no. 1, pp. 224–236, 2004.

[66] N. Braidy, A. Poljak, C. Marjo et al., "Identification of cerebral metal ion imbalance in the brain of aging *Octodon degus*," *Frontiers in Aging Neuroscience*, vol. 9, p. 66, 2017.

[67] S. Genoud, B. R. Roberts, A. P. Gunn et al., "Subcellular compartmentalisation of copper, iron, manganese, and zinc in the Parkinson's disease brain," *Metallomics*, vol. 9, no. 10, pp. 1447–1455, 2017.

[68] D. B. Kell, "Towards a unifying, systems biology understanding of large-scale cellular death and destruction caused by poorly liganded iron: Parkinson's, Huntington's, Alzheimer's, prions, bactericides, chemical toxicology and others as examples," *Archives of Toxicology*, vol. 84, no. 11, pp. 825–889, 2010.

[69] H. Kumar, H. W. Lim, S. V. More et al., "The role of free radicals in the aging brain and Parkinson's disease: convergence and parallelism," *International Journal of Molecular Sciences*, vol. 13, no. 12, pp. 10478–10504, 2012.

[70] J. K. Andersen, "Oxidative stress in neurodegeneration: cause or consequence?," *Nature Reviews Neuroscience*, vol. 10, no. 7, pp. S18–S25, 2004.

[71] S. A. Schneider and K. P. Bhatia, "Excess iron harms the brain: the syndromes of neurodegeneration with brain iron accumulation (NBIA)," *Journal of Neural Transmission*, vol. 120, no. 4, pp. 695–703, 2013.

[72] S. A. Schneider, J. Hardy, and K. P. Bhatia, "Syndromes of neurodegeneration with brain iron accumulation (NBIA): an update on clinical presentations, histological and genetic underpinnings, and treatment considerations," *Movement Disorders*, vol. 27, no. 1, pp. 42–53, 2012.

[73] S. A. Schneider and K. P. Bhatia, "Syndromes of neurodegeneration with brain iron accumulation," *Seminars in Pediatric Neurology*, vol. 19, no. 2, pp. 57–66, 2012.

[74] J. R. Connor, B. S. Snyder, J. L. Beard, R. E. Fine, and E. J. Mufson, "Regional distribution of iron and iron-regulatory proteins in the brain in aging and Alzheimer's disease," *Journal of Neuroscience Research*, vol. 31, no. 2, pp. 327–335, 1992.

[75] M. S. Thomsen, M. V. Andersen, P. R. Christoffersen, M. D. Jensen, J. Lichota, and T. Moos, "Neurodegeneration with inflammation is accompanied by accumulation of iron and ferritin in microglia and neurons," *Neurobiology of Disease*, vol. 81, pp. 108–118, 2015.

[76] T. A. Rouault, "Iron metabolism in the CNS: implications for neurodegenerative diseases," *Nature Reviews Neuroscience*, vol. 14, no. 8, pp. 551–564, 2013.

[77] M. A. Smith, P. L. Harris, L. M. Sayre, and G. Perry, "Iron accumulation in Alzheimer disease is a source of redox-generated free radicals," *Proceedings of the National Academy of Sciences of the United States of America*, vol. 94, no. 18, pp. 9866–9868, 1997.

[78] M. A. Lovell, J. D. Robertson, W. J. Teesdale, J. L. Campbell, and W. R. Markesbery, "Copper, iron and zinc in Alzheimer's disease senile plaques," *Journal of the Neurological Sciences*, vol. 158, no. 1, pp. 47–52, 1998.

[79] C. S. Atwood, R. D. Moir, X. Huang et al., "Dramatic aggregation of Alzheimer abeta by Cu(II) is induced by conditions representing physiological acidosis," *Journal of Biological Chemistry*, vol. 273, no. 21, pp. 12817–12826, 1998.

[80] C. S. Atwood, X. Huang, R. D. Moir, R. E. Tanzi, and A. I. Bush, "Role of free radicals and metal ions in the pathogenesis of Alzheimer's disease," *Metal Ions in Biological System*, vol. 36, pp. 309–364, 1999.

[81] C. S. Atwood, R. C. Scarpa, X. Huang et al., "Characterization of copper interactions with alzheimer amyloid $\beta$ peptides: identification of an attomolar-affinity copper binding site on amyloid $\beta$1-42," *Journal of Neurochemistry*, vol. 75, no. 3, pp. 1219–1233, 2000.

[82] A. I. Bush, W. H. Pettingell, G. Multhaup et al., "Rapid induction of Alzheimer A$\beta$ amyloid formation by zinc," *Science*, vol. 265, no. 5177, pp. 1464–1467, 1994.

[83] C. S. Atwood, M. E. Obrenovich, T. Liu et al., "Amyloid-$\beta$: a chameleon walking in two worlds: a review of the trophic and toxic properties of amyloid-$\beta$," *Brain Research Reviews*, vol. 43, no. 1, pp. 1–16, 2003.

[84] B. R. Roberts, T. M. Ryan, A. I. Bush, C. L. Masters, and J. A. Duce, "The role of metallobiology and amyloid-$\beta$ peptides in Alzheimer's disease," *Journal of Neurochemistry*, vol. 120, no. Suppl 1, pp. 149–166, 2012.

[85] V. Antharam, J. F. Collingwood, J. P. Bullivant et al., "High field magnetic resonance microscopy of the human hippocampus in Alzheimer's disease: quantitative imaging and correlation with iron," *Neuroimage*, vol. 59, no. 2, pp. 1249–1260, 2012.

[86] M. F. Falangola, S. P. Lee, R. A. Nixon, K. Duff, and J. A. Helpern, "Histological co-localization of iron in Abeta plaques of PS/APP transgenic mice," *Neurochemical Research*, vol. 30, no. 2, pp. 201–205, 2005.

[87] C. R. Jack Jr, T. M. Wengenack, D. A. Reyes et al., "*In vivo* magnetic resonance microimaging of individual amyloid plaques in Alzheimer's transgenic mice," *Journal of Neuroscience*, vol. 25, no. 43, pp. 10041–10048, 2005.

[88] R. J. Castellani, P. I. Moreira, G. Liu et al., "Iron: the redox-active center of oxidative stress in Alzheimer disease," *Neurochemical Research*, vol. 32, no. 10, pp. 1640–1645, 2007.

[89] K. J. Barnham and A. I. Bush, "Metals in Alzheimer's and Parkinson's diseases," *Current Opinion in Chemical Biology*, vol. 12, no. 2, pp. 222–228, 2008.

[90] F. Bousejra-ElGarah, C. Bijani, Y. Coppel, P. Faller, and C. Hureau, "Iron(II) binding to amyloid-$\beta$, the Alzheimer's peptide," *Inorganic Chemistry*, vol. 50, no. 18, pp. 9024–9030, 2011.

[91] N. D. Telling, J. Everett, J. F. Collingwood et al., "Iron biochemistry is correlated with amyloid plaque morphology in an established mouse model of Alzheimer's disease," *Cell Chemical Biology*, vol. 24, no. 10, pp. 1205–1215.e3, 2017.

[92] B. Liu, A. Moloney, S. Meehan et al., "Iron promotes the toxicity of amyloid beta peptide by impeding its ordered aggregation," *Journal of Biological Chemistry*, vol. 286, no. 6, pp. 4248–4256, 2011.

[93] J. J. Gallagher, M. E. Finnegan, B. Grehan, J. Dobson, J. F. Collingwood, and M. A. Lynch, "Modest amyloid deposition is associated with iron dysregulation, microglial activation, and oxidative stress," *Journal of Alzheimer's Disease*, vol. 28, no. 1, pp. 147–161, 2012.

[94] M. D. Meadowcroft, J. R. Connor, M. B. Smith, and Q. X. Yang, "MRI and histological analysis of beta-amyloid plaques in both human Alzheimer's disease and APP/PS1 transgenic mice," *Journal of Magnetic Resonance Imaging*, vol. 29, no. 5, pp. 997–1007, 2009.

[95] C. Quintana, S. Bellefqih, J. Y. Laval et al., "Study of the localization of iron, ferritin, and hemosiderin in Alzheimer's disease hippocampus by analytical microscopy at the subcellular level," *Journal of Structural Biology*, vol. 153, no. 1, pp. 42–54, 2006.

[96] B. Ding, K. M. Chen, H. W. Ling et al., "Correlation of iron in the hippocampus with MMSE in patients with Alzheimer's disease," *Journal of Magnetic Resonance Imaging*, vol. 29, no. 4, pp. 793–798, 2009.

[97] S. Altamura and M. U. Muckenthaler, "Iron toxicity in diseases of aging: Alzheimer's disease, Parkinson's disease and atherosclerosis," *Journal of Alzheimer's Disease*, vol. 16, no. 4, pp. 879–895, 2009.

[98] C. Ha, J. Ryu, and C. B. Park, "Metal ions differentially influence the aggregation and deposition of Alzheimer's beta-amyloid on a solid template," *Biochemistry*, vol. 46, no. 20, pp. 6118–6125, 2007.

[99] J. T. Rogers, A. I. Bush, H. H. Cho et al., "Iron and the translation of the amyloid precursor protein (APP) and ferritin mRNAs: riboregulation against neural oxidative damage in Alzheimer's disease," *Biochemical Society Transactions*, vol. 36, no. 6, pp. 1282–1287, 2008.

[100] H. H. Cho, C. M. Cahill, C. R. Vanderburg et al., "Selective translational control of the Alzheimer amyloid precursor protein transcript by iron regulatory protein-1," *Journal of Biological Chemistry*, vol. 285, no. 41, pp. 31217–31232, 2010.

[101] J. A. Duce, A. Tsatsanis, M. A. Cater et al., "Iron-export ferroxidase activity of $\beta$-amyloid precursor protein is inhibited by zinc in Alzheimer's disease," *Cell*, vol. 142, no. 6, pp. 857–867, 2010.

[102] B. X. Wong, A. Tsatsanis, L. Q. Lim, P. A. Adlard, A. I. Bush, and J. A. Duce, "$\beta$-Amyloid precursor protein does not possess ferroxidase activity but does stabilize the cell surface ferrous iron exporter ferroportin," *PLoS. One*, vol. 9, no. 12, article e114174, 2014.

[103] L. Wan, G. Nie, J. Zhang, and B. Zhao, "Overexpression of human wild-type amyloid-$\beta$ protein precursor decreases the iron content and increases the oxidative stress of neuroblastoma SH-SY5Y cells," *Journal of Alzheimer's Disease*, vol. 30, no. 3, pp. 523–530, 2012.

[104] N. E. Dixon, B. G. Crissman, P. B. Smith, S. A. Zimmerman, G. Worley, and P. S. Kishnani, "Prevalence of iron deficiency in children with Down syndrome," *The Journal of Pediatrics*, vol. 157, no. 6, pp. 967–971.e1, 2010.

[105] A. Tenenbaum, S. Malkiel, I. D. Wexler, F. Levy-Khademi, S. Revel-Vilk, and P. Stepensky, "Anemia in children with down syndrome," *International Journal of Pediatrics*, vol. 2011, Article ID 813541, 5 pages, 2011.

[106] W. S. Wu, Y. S. Zhao, Z. H. Shi et al., "Mitochondrial ferritin attenuates $\beta$-amyloid-induced neurotoxicity: reduction in oxidative damage through the Erk/P38 mitogen-activated protein kinase pathways," *Antioxidants & Redox Signaling*, vol. 18, no. 2, pp. 158–169, 2013.

[107] L. Wang, H. Yang, S. Zhao et al., "Expression and localization of mitochondrial ferritin mRNA in Alzheimer's disease cerebral cortex," *PLoS. One*, vol. 6, no. 7, article e22325, 2011.

[108] H. Yang, H. Guan, M. Yang et al., "Upregulation of mitochondrial ferritin by proinflammatory cytokines: implications for a role in Alzheimer's disease," *Journal of Alzheimer's Disease*, vol. 45, no. 3, pp. 797–811, 2015.

[109] P. A. Adlard, R. A. Cherny, D. I. Finkelstein et al., "Rapid restoration of cognition in Alzheimer's transgenic mice with 8-hydroxy quinoline analogs is associated with decreased interstitial A$\beta$," *Neuron*, vol. 59, no. 1, pp. 43–55, 2008.

[110] R. A. Cherny, J. T. Legg, C. A. McLean et al., "Aqueous dissolution of Alzheimer's disease A$\beta$ amyloid deposits by biometal depletion," *Journal of Biological Chemistry*, vol. 274, no. 33, pp. 23223–23228, 1999.

[111] C. W. Ritchie, A. I. Bush, A. Mackinnon et al., "Metal-protein attenuation with iodochlorhydroxyquin (clioquinol) targeting A$\beta$ amyloid deposition and toxicity in Alzheimer disease: a pilot phase 2 clinical trial," *Archives of Neurology*, vol. 60, no. 12, pp. 1685–1691, 2003.

[112] D. R. Richardson, "Novel chelators for central nervous system disorders that involve alterations in the metabolism of iron and other metal ions," *Annals of the New York Academy of Sciences*, vol. 1012, no. 1, pp. 326–341, 2004.

[113] F. Molina-Holgado, A. Gaeta, P. T. Francis, R. J. Williams, and R. C. Hider, "Neuroprotective actions of deferiprone in cultured cortical neurones and SHSY-5Y cells," *Journal of Neurochemistry*, vol. 105, no. 6, pp. 2466–2476, 2008.

[114] J. R. Prasanthi, M. Schrag, B. Dasari et al., "Deferiprone reduces amyloid-$\beta$ and tau phosphorylation levels but not reactive oxygen species generation in hippocampus of rabbits fed a cholesterol-enriched diet," *Journal of Alzheimer's Disease*, vol. 30, no. 1, pp. 167–182, 2012.

[115] N. Boddaert, K. H. . le Quan Sang, A. Rotig et al., "Selective iron chelation in Friedreich ataxia: biologic and clinical implications," *Blood*, vol. 110, no. 1, pp. 401–408, 2007.

[116] L. Lannfelt, K. Blennow, H. Zetterberg et al., "Safety, efficacy, and biomarker findings of PBT2 in targeting A$\beta$ as a modifying therapy for Alzheimer's disease: a phase IIa, double-blind, randomised, placebo-controlled trial," *The Lancet Neurol.*, vol. 7, no. 9, pp. 779–786, 2008.

[117] A. Nunomura, P. Moreira, H. Lee et al., "Neuronal death and survival under oxidative stress in Alzheimer and Parkinson diseases," *CNS & Neurological Disorders Drug Targets*, vol. 6, no. 6, pp. 411–423, 2007.

[118] R. B. Petersen, A. Nunomura, H.g. Lee et al., "Signal transduction cascades associated with oxidative stress in Alzheimer's disease," *Journal of Alzheimer's Disease*, vol. 11, no. 2, pp. 143–152, 2007.

[119] G. A. Salvador, "Iron in neuronal function and dysfunction," *Biofactors*, vol. 36, no. 2, pp. 103–110, 2010.

[120] R. M. Koffie, B. T. Hyman, and T. L. Spires-Jones, "Alzheimer's disease: synapses gone cold," *Molecular Neurodegeneration*, vol. 6, no. 1, p. 63, 2011.

[121] R. Manyevitch, M. Protas, S. Scarpiello et al., "Evaluation Of metabolic and synaptic dysfunction hypotheses of Alzheimer's disease (Ad): a meta-analysis of Csf markers," *Current Alzheimer Research*, vol. 15, no. 2, pp. 164–181, 2018.

[122] S. T. DeKosky, S. W. Scheff, and S. D. Styren, "Structural correlates of cognition in dementia: quantification and assessment of synapse change," *Neurodegeneration*, vol. 5, no. 4, pp. 417–421, 1996.

[123] M. P. Mattson, J. N. Keller, and J. G. Begley, "Evidence for synaptic apoptosis," *Experimental Neurology*, vol. 153, no. 1, pp. 35–48, 1998.

[124] J. N. Keller, A. Germeyer, J. G. Begley, and M. P. Mattson, "17$\beta$-Estradiol attenuates oxidative impairment of synaptic $Na^+/K^+$-ATPase activity, glucose transport, and glutamate transport induced by amyloid $\beta$-peptide and iron," *Journal of Neuroscience Research*, vol. 50, no. 4, pp. 522–530, 1997.

[125] J. N. Keller, R. J. Mark, A. J. Bruce et al., "4-Hydroxynonenal, an aldehydic product of membrane lipid peroxidation, impairs glutamate transport and mitochondrial function in

synaptosomes," *Neuroscience*, vol. 80, no. 3, pp. 685–696, 1997.

[126] J. N. Keller, Z. Pang, J. W. Geddes et al., "Impairment of glucose and glutamate transport and induction of mitochondrial oxidative stress and dysfunction in synaptosomes by amyloid $\beta$-peptide: role of the lipid peroxidation product 4-hydroxynonenal," *Journal of Neurochemistry*, vol. 69, no. 1, pp. 273–284, 1997.

[127] R. M. Uranga, M. V. Mateos, N. M. Giusto, and G. A. Salvador, "Activation of phosphoinositide-3 kinase/Akt pathway by $FeSO_4$ in rat cerebral cortex synaptic endings," *Journal of Neuroscience Research*, vol. 85, no. 13, pp. 2924–2932, 2007.

[128] R. M. Uranga, N. M. Giusto, and G. A. Salvador, "Iron-induced oxidative injury differentially regulates PI3K/Akt/GSK3$\beta$ pathway in synaptic endings from adult and aged rats," *Toxicological Sciences*, vol. 111, no. 2, pp. 331–344, 2009.

[129] R. M. Uranga, N. M. Giusto, and G. A. Salvador, "Effect of transition metals in synaptic damage induced by amyloid beta peptide," *Neuroscience*, vol. 170, no. 2, pp. 381–389, 2010.

[130] A. R. Cole, "$GSK_3$ as a sensor determining cell fate in the brain," *Frontiers in Molecular Neuroscience*, vol. 5, p. 4, 2012.

[131] F. Kuperstein and E. Yavin, "ERK activation and nuclear translocation in amyloid-$\beta$ peptide- and iron-stressed neuronal cell cultures," *European Journal of Neuroscience*, vol. 16, no. 1, pp. 44–54, 2002.

[132] F. Kuperstein and E. Yavin, "Pro-apoptotic signaling in neuronal cells following iron and amyloid beta peptide neurotoxicity," *Journal of Neurochemistry*, vol. 86, no. 1, pp. 114–125, 2003.

[133] M. V. Mateos, N. M. Giusto, and G. A. Salvador, "Distinctive roles of PLD signaling elicited by oxidative stress in synaptic endings from adult and aged rats," *Biochimica et Biophysica Acta (BBA) - Molecular Cell Research*, vol. 1823, no. 12, pp. 2136–2148, 2012.

[134] T. G. Oliveira, R. B. Chan, H. Tian et al., "Phospholipase d2 ablation ameliorates Alzheimer's disease-linked synaptic dysfunction and cognitive deficits," *Journal of Neuroscience*, vol. 30, no. 49, pp. 16419–16428, 2010.

[135] G. A. Salvador and P. I. Oteiza, "Iron overload triggers redox-sensitive signals in human IMR-32 neuroblastoma cells," *Neurotoxicology*, vol. 32, no. 1, pp. 75–82, 2011.

[136] K. S. Lee, K. Iijima-Ando, K. Iijima et al., "JNK/FOXO-mediated neuronal expression of fly homologue of peroxiredoxin II reduces oxidative stress and extends life span," *Journal of Biological Chemistry*, vol. 284, no. 43, pp. 29454–29461, 2009.

[137] R. M. Uranga, N. P. Alza, M. A. Conde, S. S. Antollini, and G. A. Salvador, "Phosphoinositides: two-path signaling in neuronal response to oligomeric amyloid $\beta$ peptide," *Molecular Neurobiology*, vol. 54, no. 5, pp. 3236–3252, 2017.

[138] G. G. Mackenzie, G. A. Salvador, C. Romero, C. L. Keen, and P. I. Oteiza, "A deficit in zinc availability can cause alterations in tubulin thiol redox status in cultured neurons and in the developing fetal rat brain," *Free Radical Biology & Medicine*, vol. 51, no. 2, pp. 480–489, 2011.

[139] K. Terai, A. Matsuo, and P. L. McGeer, "Enhancement of immunoreactivity for NF-$\kappa$B in the hippocampal formation and cerebral cortex of Alzheimer's disease," *Brain Research*, vol. 735, no. 1, pp. 159–168, 1996.

[140] K. Z. Bourne, D. C. Ferrari, C. Lange-Dohna, S. Roßner, T. G. Wood, and J. R. Perez-Polo, "Differential regulation of BACE1 promoter activity by nuclear factor-$\kappa$B in neurons and glia upon exposure to $\beta$-amyloid peptides," *Journal of Neuroscience Research*, vol. 85, no. 6, pp. 1194–1204, 2007.

[141] P. Kuner, R. Schubenel, and C. Hertel, "$\beta$-amyloid binds to $p75^{NTR}$ and activates NF$\kappa$B in human neuroblastoma cells," *Journal of Neuroscience Research*, vol. 54, no. 6, pp. 798–804, 1998.

[142] L. Tan, P. Schedl, H. J. Song, D. Garza, and M. Konsolaki, "The *Toll*→NF$\kappa$B signaling pathway mediates the neuropathological effects of the human Alzheimer's A$\beta$42 polypeptide in *Drosophila*," *PLoS. One*, vol. 3, no. 12, article e3966, 2008.

[143] G. Raivich and A. Behrens, "Role of the AP-1 transcription factor c-Jun in developing, adult and injured brain," *Progress in Neurobiology*, vol. 78, no. 6, pp. 347–363, 2006.

[144] M. P. Mattson, "Calcium and neurodegeneration," *Aging Cell*, vol. 6, no. 3, pp. 337–350, 2007.

[145] U. Wojda, E. Salinska, and J. Kuznicki, "Calcium ions in neuronal degeneration," *IUBMB Life*, vol. 60, no. 9, pp. 575–590, 2008.

[146] C. Hidalgo, "Cross talk between $Ca^{2+}$ and redox signalling cascades in muscle and neurons through the combined activation of ryanodine receptors/$Ca^{2+}$ release channels," *Philosophical Transactions of the Royal Society B: Biological Sciences*, vol. 360, no. 1464, pp. 2237–2246, 2005.

[147] C. Hidalgo, P. Donoso, and M. A. Carrasco, "The ryanodine receptors Ca2+ release channels: cellular redox sensors?," *IUBMB Life*, vol. 57, no. 4-5, pp. 315–322, 2005.

[148] C. Hidalgo, M. A. Carrasco, P. Munoz, and M. T. Nunez, "A role for reactive oxygen/nitrogen species and iron on neuronal synaptic plasticity," *Antioxidants & Redox Signaling*, vol. 9, no. 2, pp. 245–255, 2007.

[149] F. Serrano and E. Klann, "Reactive oxygen species and synaptic plasticity in the aging hippocampus," *Ageing Research Reviews*, vol. 3, no. 4, pp. 431–443, 2004.

[150] P. Muñoz, G. Zavala, K. Castillo, P. Aguirre, C. Hidalgo, and M. T. Núñez, "Effect of iron on the activation of the MAPK/ERK pathway in PC12 neuroblastoma cells," *Biological Research*, vol. 39, no. 1, pp. 189-190, 2006.

Hindawi
Oxidative Medicine and Cellular Longevity
Volume 2017, Article ID 7028583, 6 pages
https://doi.org/10.1155/2017/7028583

*Review Article*

# Possible Mechanisms of Mercury Toxicity and Cancer Promotion: Involvement of Gap Junction Intercellular Communications and Inflammatory Cytokines

**Roberto Zefferino,[1] Claudia Piccoli,[2] Nunzia Ricciardi,[1] Rosella Scrima,[2] and Nazzareno Capitanio[2]**

[1]*Department of Medical and Surgical Sciences, University of Foggia, Via L. Pinto 1, 71122 Foggia, Italy*
[2]*Department of Clinical and Experimental Medicine, University of Foggia, Via L. Pinto 1, 71122 Foggia, Italy*

Correspondence should be addressed to Roberto Zefferino; roberto.zefferino@unifg.it

Received 28 July 2017; Accepted 29 November 2017; Published 21 December 2017

Academic Editor: Pan Chen

Copyright © 2017 Roberto Zefferino et al. This is an open access article distributed under the Creative Commons Attribution License, which permits unrestricted use, distribution, and reproduction in any medium, provided the original work is properly cited.

A number of observations indicate that heavy metals are able to alter cellular metabolic pathways through induction of a prooxidative state. Nevertheless, the outcome of heavy metal-mediated effects in the development of human diseases is debated and needs further insights. Cancer is a well-established DNA mutation-linked disease; however, epigenetic events are perhaps more important and harmful than genetic alterations. Unfortunately, we do not have reliable screening methods to assess/validate the epigenetic (promoter) effects of a physical or a chemical agent. We propose a mechanism of action whereby mercury acts as a possible promoter carcinogen. In the present contribution, we resume our previous studies on mercury tested at concentrations comparable with its occurrence as environmental pollutant. It is shown that Hg(II) elicits a prooxidative state in keratinocytes linked to inhibition of gap junction-mediated intercellular communication and proinflammatory cytokine production. These combined effects may on one hand isolate cells from tissue-specific homeostasis promoting their proliferation and on the other hand tamper the immune system defense/surveillance checkmating the whole organism. Since Hg(II) is not a mutagenic/genotoxic compound directly affecting gene expression, in a broader sense, mercury might be an example of an epigenetic tumor promoter or, further expanding this concept, a "metagenetic" effector.

## 1. Mechanisms of the Prooxidative Activity of Mercury

The cytotoxic effect of mercury in its divalent ionic form $Hg^{2+}$ has been linked to cellular oxidative stress by many authors [1–3]. The general belief is that given the well-known reactivity of $Hg^{2+}$ with thiols to form mercaptans this may result in depletion of the thiol-based antioxidant buffers constituted in cells mainly by glutathione. Consistent with this notion, increased GSSG/GSH ratio and $H_2O_2$ production have been repeatedly reported in literature in different cell phenotypes exposed to mercury-containing compounds.

Accordingly, our group found that exposure of cultured human keratinocytes (HK) to nanomolar concentrations of $HgCl_2$ for 24 h caused a 40% decrease of the fluorescence signal associated to the free thiol-reacting probe Alexa Fluor 594 C5 maleimide as assessed by confocal microscopy imaging [4]. Moreover, direct measurement of the reduced and oxidized glutathione resulted in a twofold increase of the relative amount of GSSG thus confirming the negative effect of $Hg^{2+}$ on the free thiol-based antioxidant cellular pool. Consistently, when the intracellular level of reactive oxygen species (ROS) was measured by the redox-sensitive fluorescent probe DCF, a fivefold increase of the signal was detectable by confocal microscopy in $Hg^{2+}$-treated HK as compared with untreated cells. Higher resolution of the imaged intracellular fluorescence revealed that the brighter signal was localized in the mitochondrial compartment. Similar results were attained with the superoxide anion-($O_2^{\bullet-}$) specific mitotropic probe MitoSOX. However, both

measurement of the mitochondrial respiratory chain activity as well as of the mitochondrial transmembrane potential ($\Delta\Psi_m$) (by the TMRE probe) did not show appreciable differences between untreated and $Hg^{2+}$-treated HK. Overall, these results suggest that the $HgCl_2$-mediated oxidative unbalance was likely due to depletion/impairment of the antioxidant buffering system rather than to increased ROS production at least of mitochondrial origin. However, it must be considered that the intracellular concentration of free thiol groups is estimated in the millimolar range, whereas the concentration of $HgCl_2$ was 5-6 order of magnitude lower. Even considering the small volume of the cell layer of HK in culture and all the $Hg^{2+}$ available in the medium, the amount of $Hg^{2+}$ was still largely substoichiometric with respect to the intracellular free thiol groups. This ruled out a direct involvement of $Hg^{2+}$ in the oxidative modification of the thiol-based redox buffering rather suggesting $Hg^{2+}$-mediated modification of specific catalytic reactions controlling the ROS homeostasis.

Evidences have been provided that mercury-containing compounds induce changes in the redox state of the sulphydrilic lateral chain of cysteines in the active site of several enzymes [5–8] with some of these possibly involved in the control of the balance between ROS production and ROS scavenging. Importantly, some antioxidant enzymes such as glutathione peroxidases and thioredoxin reductase contain a residue of selenocysteine in their active site [9]. The selenol group (-Se-H) exhibits a pKa about three unit lower than that of the -SH group (i.e, 5.2 versus 8.3) therefore largely existing at physiological pH in the dissociated and more nucleophilic form ($-Se^-$). Consequently, the selenol group displays a much higher reactivity toward $Hg^{2+}$ as compared with the thiol group. On this basis, we proposed that the prooxidant activity of $Hg^{2+}$ attainable at low concentration in HK is mainly mediated by its selective reaction with seleno enzymes involved in the "detoxification" of reactive oxygen species (see Figure 1).

To support our conclusion, there are a number of studies. In 2012, Branco et al. [10] observed in Zeabra-seabreams the histopathological alterations of $Hg^{2+}$ in the liver and kidney and correlated this effect to a reduction of thioredoxin reductase activity. Importantly, the coexposure of $Hg^{2+}$ and Se prevented both the organ lesions and the inhibition of the thioredoxin reductase.

Although data on the mechanisms mediating Hg0 neurotoxicity are scarce, existing evidence suggests that changes in the redox state of -SH-containing proteins plays a critical role [5–8]. However, based on the high affinity of $Hg^{2+}$ (derived from Hg0) for selenols [11], it is reasonable to suggest that selenoproteins could also mediate the neurotoxic effects observed after Hg0 exposure. Carvalho and coworkers [12] observed that the selenoprotein thioredoxin reductase (TrxR) is selectively inhibited by $Hg^{2+}$ and concluded that the significant potency of the mercurial to bind to the selenol group in the active site of TrxR represents a major molecular mechanism of its toxicity. Because of the probable interaction between $Hg^{2+}$ (derived from Hg0) and selenols in the CNS, the potential involvement of selenoproteins in the neurotoxicity elicited by Hg0 represents an important research field that deserves further attention. This is believed because (i) $Hg^{2+}$ toxicity is antagonized by selenium compounds [13, 14], (ii) $Hg^{2+}$, which is generated in the SNC after Hg0 oxidation, inhibits the activity of selenoproteins by interacting with their selenol group [12], and (iii) miners occupationally exposed to Hg0 had lower levels of plasma selenium when compared with control individuals [15].

## 2. Effect of Mecury on Gap Junction Intercellular Communication and Cytokine Release

Gap junctions play a central role in coordinating intercellular signal-transduction pathways to control tissue homeostasis. A family of transmembrane proteins, called connexins, assembles at the level of the plasma membrane to form exameric emichannels or connexons [16]; the docking of connexons of adjacent cells forms what is called gap junction. Opening of the gap junction allows the cytoplasm of the connected cells to establish a continuum whereby low molecular weight (<500 D) metabolites, messengers, and ions can freely flow following concentration gradients. The opening/closing of the gap junction "gates" is controlled by a number of post-translational covalent modifications linked to the activation of various signaling pathways [16]. To notice, the intercellular communication has been recently recognized to occur by different modalities consisting in nanotube connections and transfer of exosomic microvesicles between cells [17, 18]. In both cases, molecules with bio-signaling properties, genetic materials (like small RNAs), and even subcellular organelles were shown to be transferrable. The mechanisms controlling non gap junction-mediated intercellular communication are, however, yet to be fully elucidated. Deregulation of gap junctional intercellular communication is a common phenotype of cancer cells, and several lines of evidence support its involvement in the carcinogenesis process. The basic principle underlying this hypothesis is that functional isolation/segregation of a cell from the neighbor cellular environment promotes autonomous cell cycling not synchronized/regulated by the tissue biochemical cues. Once this condition becomes chronic, it primes/fosters the acquisition of a transformed phenotype. Concomitant genetic alterations can ultimately lead to cancer. Accordingly, many carcinogens, like environmental heavy-metal chemical pollutants, are known to negatively modulate GJIC though the molecular mechanism is still debated.

If an enhanced level of ROS is kept below a cytotoxic threshold, they serve as bio-signals to evoke cellular adaptation. Notably, many protein kinase/phosphatases are redox sensitive as well as transcription factors thus suggesting the occurrence of an interplay among several signaling pathways. In our previous studies, we reported that prooxidant conditioning of HK exposed to low concentration of $HgCl_2$ resulted in inhibition of the GJIC accompanied with altered electrophoretic migration of connexin 43 reported to be caused by phosphorylation of the protein. Importantly, cotreatment of HK with antioxidant or inhibitor of protein kinase C prevented completely the $Hg^{2+}$-mediated blockage

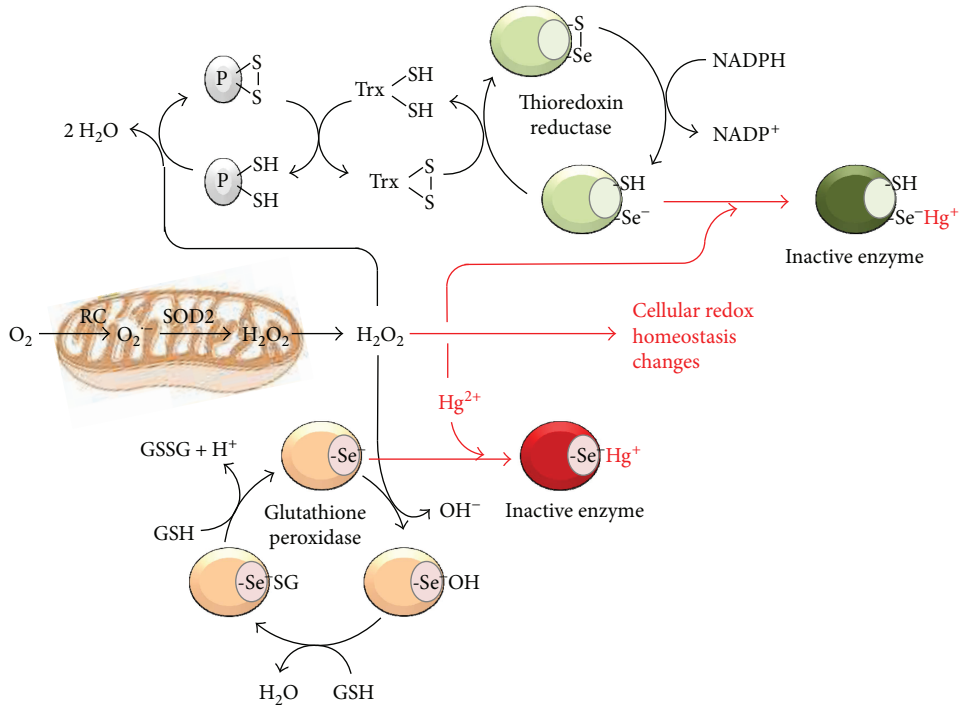


Figure 1: Proposed mechanism for the prooxidative action of Hg(II). Mercury ion ($Hg^{2+}$) is shown to bind to the dissociated form of the selenol ($-Se^-$) moiety of the catalytic selenocysteine residue of glutathione peroxidase and thioredoxin reductase thereby inactivating the enzymes; the result is an enhanced level of reactive oxygen species because of their lower inactivation. The catalytic cycles of the two antioxidant enzymes are also shown: glutathione peroxidase converts $H_2O_2$ in 2 $H_2O$ molecules at expense of 2 reduced glutathione molecules (GSH), which are oxidized to GSSG; thioredoxin reductase reduces oxidized thioredoxin (Txr) at the expense of NADPH thereby enabling reduced Txr to preserve the redox state of protein cysteines (P) from the $H_2O_2$-mediated oxidation. Mitochondria is illustrated as a major intracellular producer of ROS generated from electron leaks from the respiratory chain (RC) to $O_2$ to form the superoxide anion ($O_2^{\bullet -}$). This is further converted in $H_2O_2$ by the mitochondrial isoform of the superoxide dismutase ($SOD_2$).

of the GJIC [19]. On this basis, we proposed a mechanistic model whereby exposure of HK to $Hg^{2+}$ causes enhanced ROS production by inhibition of selenocysteine-containing antioxidant enzyme. This stimulates member of the protein kinase C family, proved to be redox sensitive, which in turn hampers/closes the GJIC by phosphorylating connexin 43. The physiological rationale of this adaptive mechanism to a prooxidative setting remains to be fully understood. However, it might be a protective mechanism evolutionary selected to limit the spread of potentially harmful species toward in-contact neighbor cells.

Recent studies have advanced our understanding that the regulation of immune responses is not only confined to immunocompetent cells. Upon stimulation, keratinocytes are capable of releasing various factors and expressing pattern recognition receptors (PRRs) that are significantly involved in the innate immune response. Indeed, in response to challenge with microbes or microbial-derived substances, the activation and nuclear translocation of NF-$\kappa$B and the production of nitric oxide (NO) and inflammatory cytokines occur in keratinocytes, in a TLR-dependent manner [20]. On this basis, we have investigated the impact of $Hg^{2+}$ on the LPS-mediated immune activation of HK. We found that nanomolar concentrations of $HgCl_2$ significantly reduced the release of TNF-$\alpha$ and IL-1$\beta$ in LPS-stimulated cells and that this effect was redox sensitive as it was abrogated by antioxidant cotreatment [21]. Although the mechanism linking mercury-mediated ROS accumulation to inhibition of cytokine production remains to be detailed, nevertheless our finding supports the long known immunosuppressive role of mercury compounds on immunocompetent cells [22].

## 3. Mercury as Cancer Promoter: a Sensu Lato Epigenetic Modifier

Epigenetics is defined as a complex of events leading to the control and regulation of gene expression without the involvement of any change in the genetic sequence. The processes, which can be altered in the epigenetic modification, include DNA methylation, histone modification, RNA regulation, DNA repair, transcription, RNA stability, alternative RNA splicing, protein degradation, gene copy number, and transposon activation. Pollutants such as heavy metals, as well as pharmaceuticals, hormones, nutrition, and behavior, can all modify the expression of genes. The pattern of the epigenetic alterations can be both transient and permanent to be transmitted to offsprings.

Epigenetic effects of heavy metals have been investigated extensively, particularly arsenic, cadmium, cobalt, chromium, nickel, and mercury. Regarding arsenic, numerous authors observed global hypomethylation, but also global and gene-specific hypermethylation particularly P53, plus

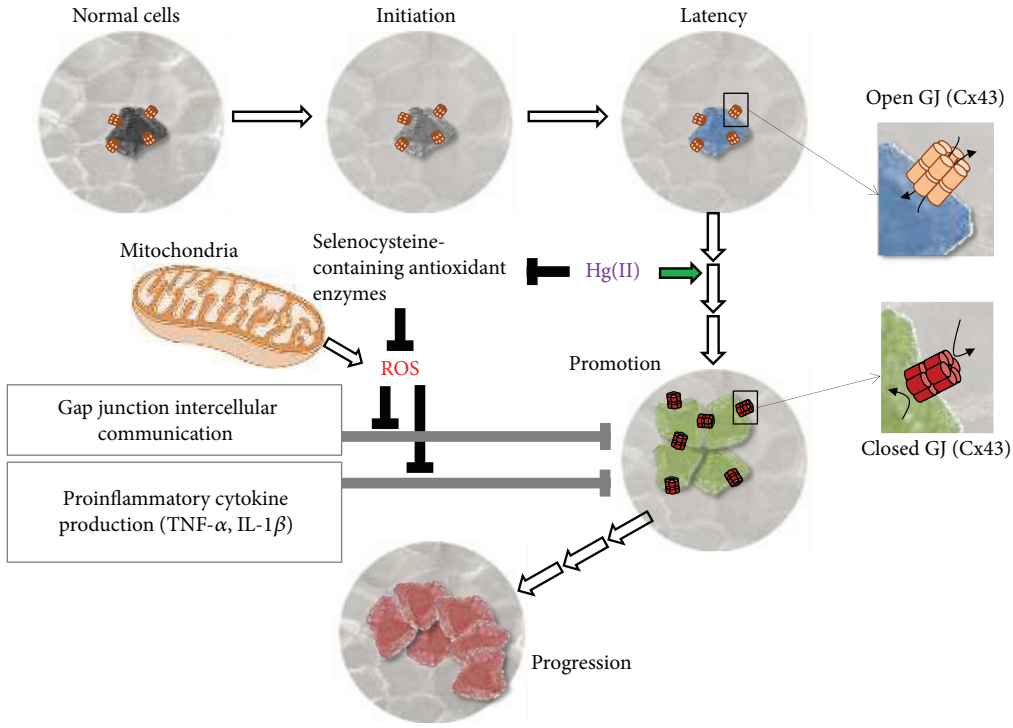


Figure 2: Proposed role of mercury as epigenetic/promoter carcinogen. The progressive multistep transformation of a normal cell to a cancer cell is shown schematically. The indicated phases (i.e., initiation → latency → promotion → progression) are those commonly accepted for cancer development. Mercury (Hg(II)) is indicated to act in the promotion phase by causing an unbalance in the reactive oxygen species (ROS) homeostasis accomplished by selective inhibition of selenocysteine antioxidant enzymes. Mitochondria are also shown as a major ROS generator. The Hg(II)-induced prooxidative state in turn would result in inhibition of the gap junction intercellular communication (GJIC) and of the proinflammatory cytokine release. Both mechanisms might on one hand isolate cells from tissue-specific homeostasis promoting their proliferation and on the other hand tamper the immune system defense/surveillance checkmating the whole organism. The Cx43-related open gap junction is shown as progressively closing in the transitions following the "latent" state.

histone modification (alkylation) and increment of miRNAs as miR-22 or decrement of miR-210 and miR-19a [23]. For cadmium, both global hypomethylation and hypermethylation have been reported depending on the exposure time [24–26]. For cobalt, the epigenetic effects published consisted enhanced oxidative stress, proinflammatory effects, and abnormal apoptosis [27]. It has been proved that chromium caused P16 and Gpt hypermethylation, as well as histone modifications as alkylation and phosphorylation [28]. Nickel was able to induce hypermethylation of ATF-1, HIF-1 gpt, Rb, and P16, and then histone modification as alkylation and phosphorylation [28–31]. Finally, mercury induced global hypomethylation and hypermethylation of the signaling G protein GTPase Rnd2 [32, 33].

In addition to the abovementioned modifications, dynamically controlling chromatin remodeling, gene transcription can also be indirectly modulated by the availability of metabolites functioning as substrates or effectors of epigenetic modifier enzymes as well as from microRNAs (miRNAs). This emerging notion let us to reconsider epigenetics in a broader sense including all the conditions directly or indirectly leading to acute or chronic modification of gene expression. In this acceptation, the intercellular communication may be considered an epigenetic process regulating gene expression. Indeed, the low molecular weight of the 22-nucleotide noncoding miRNAs enables them to be transferred through gap junction establishing an intercellular genetic cross-talk. The intercellular genetic communication is now emerging as an essential requirement for coordination of cell proliferation and differentiation and has an important role in many cellular processes [34].

A promoter carcinogen is by definition any agent able to determinate an uncontrolled proliferation. This action, in the opinion of several authors, including ourselves, would be linked to inhibition of GJIC. In fact, cells deprived by inhibitory control of neighboring cells start to proliferate. This aspect is, obviously, only one part of the complex and multistep carcinogenic process where microenvironmental factors play conditioning activities. In this context, the cytokine network might contribute to determine the destiny of cell towards the death or the survival. Accordingly, numerous observations proved a link between inflammation and cancer. If a substance apart from the inhibition of GJIC is also able to reduce the release of proinflammatory cytokines, its carcinogenic potency would result incremented.

In keeping the above defined concepts and on the basis of the evidences provided by our experimental work on HK, as well as by others, we hypothesize that mercury might be an epigenetic carcinogen. Indeed, Hg(II) fulfils both the capacity to induce an inhibition of the GJIC and that to induce immunosuppressive effects. This double mechanism of toxicity by Hg(II) might overcome the organism defences that exploit

inflammation to contrast the cell hyperproliferation. Both these Hg-mediated outcomes are linked to an upstream alteration of the intracellular redox tone likely caused by a specific inhibition of antioxidant enzymes containing selenocysteines (see scheme of Figure 2).

The "carcinogen as mutagen" has become a "default" paradigm. This is partly because the carcinogenicity of a compound is commonly assessed by the so-called "genotoxicity" in vitro assays and tests to evaluate whether epigenetic toxicology are lacking in the routine. Consequently, mercury has been classified in group 3 by IARC (International Agency Research Cancer) which means "not classifiable as to their carcinogenicity to humans" [35]. However, if a toxic compound inhibits the intercellular communication, it might potentially act as a cancer "promoter," although resulting nongenotoxic. In the case of the GJIC, the impact on it of chemical agent can be easily assessed as a number of protocols have been developed [36, 37]. Most notably, for some of these protocols measuring intercellular fluorescent dye transfer, either a specialized expertise or particular instrumentations, is required in making the setup of the assay easily accessible to every basic laboratory.

All together, the abovementioned considerations let us to conclude that *there is something more beyond the epigenetic effect*. Alyea et al. [38] stated that epigenetic effects caused by metals and toxic compounds always appear at low concentration, even below what they called no-observed-adverse-effect level (NOAEL), and then the authors concluded that the epigenome dynamic variability is not completely characterized. Thus, given the state of our current scientific knowledge, an epigenetic change cannot be contextualized as adverse in the absence of a phenotypic anchor. They concluded that more research is needed in this area to perform additional epigenetic studies that include apical end points with full-dose response curves, in order to gain a more comprehensive understanding of adverse health outcomes that could be causally linked to epigenetic changes. These conclusions are useful to approach in a new and unexpected way the epigenetic effect, trying to evaluate more critically where this event drives. It is known that cells, tissues, organs, apparatuses, and organisms are able to develop feedback mechanisms that counteract modifications induced by toxic substances. Hence, though it is useful to investigate canonical epigenetic modifications, it will be even more useful in the future to ask ourselves what links these epigenetic effects with other epigenetic effects that could be defined "beyond/after epigenetic effect" to differentiate them. Several authors as Alyea et al. [38] consider inhibition of intercellular communication, enhanced oxidative stress, proinflammatory effects, and abnormal apoptosis/survival as "bona fide" epigenetic effects. They could be also defined, in our opinion, in a single word as "metagenetic effects" using an ancient Greek prefix that means beyond.

## Abbreviations

GJIC: Gap junction intercellular communication
PKC: Protein kinase C
PKA: Protein kinase A
LPS: Lipopolysaccharide—endotoxin
IL-1$\beta$: Interleukin 1 beta
TNF-$\alpha$: Tumor necrosis factor alpha
NOAEL: No-observed-adverse-effect level.

## Data Access

The authors are available to share their data.

## Conflicts of Interest

The authors declare that they have no competing interests.

## Authors' Contributions

All authors read and approved the final manuscript.

## Acknowledgments

The authors would like to thank Professor Luigi Ambrosi for his scientific advices: these exceeded the limits and invested our lives, improving it and lighting up the path towards future challenges. Local grants are from the University of Foggia.

## References

[1] T. Syversen and P. Kaur, "The toxicology of mercury and its compounds," *Journal of Trace Elements in Medicine and Biology*, vol. 26, no. 4, pp. 215–226, 2012.

[2] E.-J. Park and K. Park, "Induction of reactive oxygen species and apoptosis in BEAS-2B cells by mercuric chloride," *Toxicology In Vitro*, vol. 21, no. 5, pp. 789–794, 2007.

[3] D. Grotto, J. Valentini, M. Fillion et al., "Mercury exposure and oxidative stress in communities of the Brazilian Amazon," *Science of the Total Environment*, vol. 408, no. 4, pp. 806–811, 2010.

[4] C. Piccoli, A. D'Aprile, R. Scrima, L. Ambrosi, R. Zefferino, and N. Capitanio, "Subcytotoxic mercury chloride inhibits gap junction intercellular communication by a redox- and phosphorylation-mediated mechanism," *Free Radical Biology & Medicine*, vol. 52, no. 5, pp. 916–927, 2012.

[5] J. Albrecht and E. Matyja, "Glutamate: a potential mediator of inorganic mercury neurotoxicity," *Metabolic Brain Disease*, vol. 11, no. 2, pp. 175–184, 1996.

[6] M. Aschner and J. L. Aschner, "Mercury neurotoxicity: mechanisms of blood-brain barrier transport," *Neuroscience and Biobehavioral Reviews*, vol. 14, no. 2, pp. 169–176, 1990.

[7] N. Brookes and D. A. Kristt, "Inhibition of amino acid transport and protein synthesis by $HgCl_2$ and methylmercury in astrocytes: selectivity and reversibility," *Journal of Neurochemistry*, vol. 53, no. 4, pp. 1228–1237, 1989.

[8] M. Yoshida, C. Watanabe, M. Kishimoto et al., "Behavioral changes in metallothionein-null mice after the cessation of long-term, low-level exposure to mercury vapor," *Toxicology Letters*, vol. 161, no. 3, pp. 210–218, 2006.

[9] H. Steinbrenner, B. Speckmann, and L. O. Klotz, "Selenoproteins: antioxidant selenoenzymes and beyond," *Archives of Biochemistry and Biophysics*, vol. 595, pp. 113–119, 2016.

[10] V. Branco, P. Ramos, J. Canário, J. Lu, A. Holmgren, and C. Carvalho, "Biomarkers of adverse response to mercury:

histopathology versus thioredoxin reductase activity," *Journal of Biomedicine and Biotechnology*, vol. 2012, Article ID 359879, 9 pages, 2012.

[11] C. Sasakura and K. T. Suzuki, "Biological interaction between transition metals (Ag, Cd and Hg), selenide/sulfide and selenoprotein P," *Journal of Inorganic Biochemistry*, vol. 71, no. 3-4, pp. 159–162, 1998.

[12] C. M. L. Carvalho, E. H. Chew, S. I. Hashemy, J. Lu, and A. Holmgren, "Inhibition of the human thioredoxin system. A molecular mechanism of mercury toxicity," *The Journal of Biological Chemistry*, vol. 283, no. 18, pp. 11913–11923, 2008.

[13] M. Farina, F. A. Soares, A. Feoli et al., "In vitro effects of selenite and mercuric chloride on liver thiobarbituric acid-reactive substances and non-protein thiols from rats: influences of dietary cholesterol and polyunsaturated and saturated fatty acids," *Nutrition*, vol. 19, no. 6, pp. 531–535, 2003.

[14] I. Yamamoto, "Effect of various amounts of selenium on the metabolism of mercuric chloride in mice," *Biochemical Pharmacology*, vol. 34, no. 15, pp. 2713–2720, 1985.

[15] A. B. Kobal, M. Horvat, M. Prezelj et al., "The impact of long-term past exposure to elemental mercury on antioxidative capacity and lipid peroxidation in mercury miners," *Journal of Trace Elements in Medicine and Biology*, vol. 17, no. 4, pp. 261–274, 2004.

[16] M. S. Nielsen, L. N. Axelsen, P. L. Sorgen, V. Verma, M. Delmar, and N. H. Holstein-Rathlou, "Gap junctions," *Comprehensive Physiology*, vol. 2, no. 3, pp. 1981–2035, 2012.

[17] S. Sisakhtnezhad and L. Khosravi, "Emerging physiological and pathological implications of tunneling nanotubes formation between cells," *European Journal of Cell Biology*, vol. 94, no. 10, pp. 429–443, 2015.

[18] J. M. Pitt, G. Kroemer, and L. Zitvogel, "Extracellular vesicles: masters of intercellular communication and potential clinical interventions," *The Journal of Clinical Investigation*, vol. 126, no. 4, pp. 1139–1143, 2016.

[19] R. Zefferino, A. Leone, S. Piccaluga, R. Cincione, and L. Ambrosi, "Mercury modulates interplay between IL-1$\beta$, TNF-$\alpha$, and gap junctional intercellular communication in keratinocytes: mitigation by lycopene," *Journal of Immunotoxicology*, vol. 5, no. 4, pp. 353–360, 2008.

[20] A. Pivarcsi, L. Kemény, and A. Dobozy, "Innate immune functions of the keratinocytes. A review," *Acta Microbiologica et Immunologica Hungarica*, vol. 51, no. 3, pp. 303–310, 2004.

[21] R. Zefferino, S. Piccaluga, M. Lasalvia, G. D'Andrea, M. Margaglione, and L. Ambrosi, "Role of tumour necrosis factor alpha and interleukin 1 beta in promoter effect induced by mercury in human keratinocytes," *International Journal of Immunopathology and Pharmacology*, vol. 19, Supplement 4, pp. 15–20, 2006.

[22] P. Moszczyński, "Mercury compounds and the immune system: a review," *International Journal of Occupational Medicine and Environmental Health*, vol. 10, no. 3, pp. 247–258, 1997.

[23] P. Intarasunanont, P. Navasumrit, S. Waraprasit et al., "Effects of arsenic exposure on DNA methylation in cord blood samples from newborn babies and in a human lymphoblast cell line," *Environmental Health*, vol. 11, no. 1, p. 31, 2012.

[24] S. Virani, K. M. Rentschler, M. Nishijo et al., "DNA methylation is differentially associated with environmental cadmium exposure based on sex and smoking status," *Chemosphere*, vol. 145, pp. 284–290, 2016.

[25] K. E. Pelch, E. J. Tokar, B. A. Merrick, and M. P. Waalkes, "Differential DNA methylation profile of key genes in malignant prostate epithelial cells transformed by inorganic arsenic or cadmium," *Toxicology and Applied Pharmacology*, vol. 286, no. 3, pp. 159–167, 2015.

[26] J. Brocato and M. Costa, "Basic mechanics of DNA methylation and the unique landscape of the DNA methylome in metal-induced carcinogenesis," *Critical Reviews in Toxicology*, vol. 43, no. 6, pp. 493–514, 2013.

[27] R. Magaye, J. Zhao, L. Bowman, and M. DING, "Genotoxicity and carcinogenicity of cobalt-, nickel- and copper-based nanoparticles," *Experimental and Therapeutic Medicine*, vol. 4, no. 4, pp. 551–561, 2012.

[28] J. Brocato and M. Costa, "10th NTES conference: nickel and arsenic compounds alter the epigenome of peripheral blood mononuclear cells," *Journal of Trace Elements in Medicine and Biology*, vol. 31, pp. 209–213, 2015.

[29] Q. Ke, T. Ellen, and M. Costa, "Nickel compounds induce histone ubiquitination by inhibiting histone deubiquitinating enzyme activity," *Toxicology and Applied Pharmacology*, vol. 228, no. 2, pp. 190–199, 2008.

[30] X. Zhou, Q. Li, A. Arita, H. Sun, and M. Costa, "Effects of nickel, chromate, and arsenite on histone 3 lysine methylation," *Toxicology and Applied Pharmacology*, vol. 236, no. 1, pp. 78–84, 2009.

[31] L. Ma, Y. Bai, H. Pu et al., "Histone methylation in nickel-smelting industrial workers," *PLoS One*, vol. 10, no. 10, article e0140339, 2015.

[32] J. Z. J. Maccani, D. C. Koestler, B. Lester et al., "Placental DNA methylation related to both infant toenail mercury and adverse neurobehavioral outcomes," *Environmental Health Perspectives*, vol. 123, no. 7, pp. 723–729, 2015.

[33] J. M. Goodrich, N. Basu, A. Franzblau, and D. C. Dolinoy, "Mercury biomarkers and DNA methylation among Michigan dental professionals," *Environmental and Molecular Mutagenesis*, vol. 54, no. 3, pp. 195–203, 2013.

[34] L. Zong, L. Zhou, Y. Hou et al., "Genetic and epigenetic regulation on the transcription of GABRB2: genotype-dependent hydroxymethylation and methylation alterations in schizophrenia," *Journal of Psychiatric Research*, vol. 88, pp. 9–17, 2017.

[35] http://monographs.iarc.fr/ENG/Classification/ClassificationsGroupOrder.pdf.

[36] I. V. Budunova and G. M. Williams, "Cell culture assays for chemicals with tumor-promoting or tumor-inhibiting activity based on the modulation of intercellular communication," *Cell Biology and Toxicology*, vol. 10, no. 2, pp. 71–116, 1994.

[37] J. E. Klaunig and Y. Shi, "Assessment of gap junctional intercellular communication," *Current Protocols in Toxicology*, 2009, Chapter 2, Unit 2.17.

[38] R. A. Alyea, N. P. Moore, M. J. LeBaron, B. B. Gollapudi, and R. J. Rasoulpour, "Is the current product safety assessment paradigm protective for epigenetic mechanisms?," *Journal of Pharmacological and Toxicological Methods*, vol. 66, no. 3, pp. 207–214, 2012.

Hindawi
Oxidative Medicine and Cellular Longevity
Volume 2017, Article ID 8763793, 9 pages
https://doi.org/10.1155/2017/8763793

*Research Article*

# The Effect of a Short-Term Exposure to Lead on the Levels of Essential Metal Ions, Selected Proteins Related to Them, and Oxidative Stress Parameters in Humans

**Michał Dobrakowski,[1] Marta Boroń,[2] Ewa Birkner,[1] Aleksandra Kasperczyk,[1] Ewa Chwalińska,[1] Grażyna Lisowska,[3] and Sławomir Kasperczyk[1]**

[1]*Department of Biochemistry, School of Medicine with the Division of Dentistry, Medical University of Silesia, Ul. Jordana 19, 41-808 Zabrze, Poland*
[2]*Institute of Occupational Medicine and Environmental Health in Sosnowiec, Ul. Kościelna 13, 41-200 Sosnowiec, Poland*
[3]*Department of Otorhinolaryngology and Laryngological Oncology, School of Medicine with the Division of Dentistry, Medical University of Silesia, Ul. Skłodowskiej 10, 41-800 Zabrze, Poland*

Correspondence should be addressed to Michał Dobrakowski; michal.dobrakowski@poczta.fm

Received 9 July 2017; Revised 7 October 2017; Accepted 13 November 2017; Published 13 December 2017

Academic Editor: Daiana S. Avila

Copyright © 2017 Michał Dobrakowski et al. This is an open access article distributed under the Creative Commons Attribution License, which permits unrestricted use, distribution, and reproduction in any medium, provided the original work is properly cited.

The present study was designed to explore the possible influence of subacute exposure to lead on the levels of selected essential metals, selected proteins related to them, and oxidative stress parameters in occupationally exposed workers. The study population included 36 males occupationally exposed to lead for 36 to 44 days. Their blood lead level at the beginning of the study was $10.7 \pm 7.67\,\mu$g/dl and increased to the level of $49.1 \pm 14.1\,\mu$g/dl at the end of the study. The levels of calcium, magnesium, and zinc increased significantly after lead exposure compared to baseline by 3%, 3%, and 8%, respectively, while the level of copper decreased significantly by 7%. The malondialdehyde (MDA) level and the activities of catalase (CAT) and superoxide dismutase (SOD) did not change due to lead exposure. However, the level of lipid hydroperoxides (LPH) in serum increased significantly by 46%, while the level of erythrocyte lipofuscin (LPS) decreased by 13%. The serum levels of essential metals are modified by a short-term exposure to lead in occupationally exposed workers. A short-term exposure to lead induces oxidative stress associated with elevated levels of LPH but not MDA.

## 1. Introduction

Lead is one of the ubiquitous pollutants and exposure to it is a global concern. Lead is commonly used in many industries, and its disposal has resulted in its accumulation in the environment [1, 2]. There is no known physiological value of lead, and there is no safe level of exposure to this xenobiotic. Even low blood lead levels ($<10\,\mu$g/dl) are believed to be associated with abnormalities in hematopoietic, nervous, and renal systems [3].

Occupational lead exposure occurs mainly through the respiratory tract. Approximately 30–40% of inhaled lead is absorbed into the bloodstream. 99% of circulating lead is bound to erythrocytes for approximately 30–35 days and is distributed into the tissues, such as the liver, renal cortex, blood vessels, brain, lungs, spleen, teeth, and bones, over the following 4–6 weeks. In adults, approximately 80–95% of absorbed lead is stored in bones [4].

There are many proposed mechanisms of toxic lead action. It has been established that lead induces oxidative stress by generation of reactive oxygen species (ROS) and impairment of antioxidant defenses, including enzymatic antioxidants, such as superoxide dismutase and catalase [5]. Besides, lead interferes with divalent cations, such as calcium (Ca), magnesium (Mg), iron (Fe), zinc (Zn), copper (Cu), and selenium (Se) [3, 6].

Essential metals are coactivators of several important enzymes, including antioxidant enzymes, and proteins which

are necessary for health maintenance [6, 7]. Therefore, their interactions with lead may affect various fundamental biological processes, including intra- and intercellular signaling, cell adhesion, protein folding and maturation, apoptosis, ionic transportation, enzyme regulation, and release of neurotransmitters [3]. On the other hand, micronutrients could influence lead's absorption, postexposure distribution, deposition, and excretion processes [1]. For example, it has been reported that a low calcium and iron diet results in increased susceptibility to lead toxicity by its increased absorption. Conversely, supplementation with zinc and iron has been shown to reduce intestinal absorption of lead [2]. Consequently, it is postulated that there are possible feedback loops between blood lead and essential metals [7].

The associations between concentration of lead and essential metals in the blood and oxidative stress intensity are not fully understood. Previous studies on this topic conducted on humans focused on occupational and environmental chronic lead exposure [6]. In this context, investigation of the effects of a short-term exposure to lead would provide more information. Therefore, the aim of the present study was to explore the possible influence of subacute exposure to lead on the levels of selected micro and macro elements, selected proteins related to them, and oxidative stress parameters in occupationally exposed workers.

## 2. Material and Methods

*2.1. Study Population.* The experimental setup has been approved by the Bioethics Committee of the Medical University of Silesia in Katowice No. KNW/0022/KB1/108/14.

The study population included 36 males occupationally exposed to lead for 36 to 44 days. All participants were recruited by an occupational medicine specialist during prophylactic medical examinations and provided informed consent to the study. Blood lead level (B-Pb) served as an exposure marker. Half of the workers were only environmentally exposed to lead before the study, while the second half had a history of an occupational exposure to lead. They had been exposed to lead several years before the study began. Periods of lead exposures in the past lasted for several months to several years. Additively, the exposed population was divided into pairs of subgroups based on smoking habits and a median of age and BMI. In the examined group, 5% and 3% of workers were diagnosed with hypertension and coronary artery disease, respectively, while none of them were diagnosed with diabetes and malignant neoplasm.

Subjects in the examined group worked in lead-zinc works in the southern region of Poland to perform periodic maintenance of blast furnaces and production lines. The mean concentration of lead in the air at the participants' workplaces was $0.083 \pm 0.12\,mg/m^3$. This mean concentration exceeds the Polish MAC level of $0.050\,mg/m^3$. Besides, examined subjects were exposed to negligible doses of zinc. The mean concentration of zinc in the air at the participants' workplaces was $0.15 \pm 0.13\,mg/m^3$. This value is much lower than the Polish MAC level of $5.0\,mg/m^3$.

Blood of all examined workers was drawn during prophylactic medical examinations at the beginning of the studied lead exposure for the first time and after a period of short-term exposure to lead for the second time. In the collected blood samples, the biochemical analysis included the activities of superoxide dismutase (SOD) and catalase (CAT) and the levels of essential metals, ceruloplasmin (CER), lipid hydroperoxides (LPH), malondialdehyde (MDA), and lipofuscin (LPS).

This study was supported by the Medical University of Silesia in Katowice (KNW-1-063/N/6/O).

*2.2. Laboratory Procedures*

*2.2.1. Blood Collection.* We followed the methods of Dobrakowski et al. [8]. To obtain whole blood, erythrocytes, and leukocytes, 14 ml of blood was drawn by venipuncture into tubes containing an EDTA solution as an anticoagulant. Immediately after blood sampling, 5 ml of whole blood was centrifuged. The plasma supernatant was removed. The sedimented erythrocytes were washed three times through centrifugation with 0.9% sodium chloride solution. Subsequently, the erythrocytes were lysed with bidistilled water. Finally, 10% (*v*/*v*) hemolysate was prepared. To isolate the leukocytes, 3 ml of the whole blood was layered over Histopaque-1077 (Sigma-Aldrich) in a 1 : 1 ratio and centrifuged for 30 min. Leukocytes (1.5 ml) were collected from the interface and washed three times through centrifugation with 0.9% sodium chloride solution. Finally, the lysate of leukocytes was prepared in 1.5 ml of bidistilled water.

*2.2.2. Determination of Lead and Essential Metal Concentrations.* The assessments of the PbB (wavelength 283.3 nm) and serum concentration of selenium (196.0 nm) were performed by graphite furnace atomic absorption spectrometry using an ICE 3400 instrument (Thermo Fisher Scientific, Waltham, MA, USA). The detection limits for PbB were 0.08 $\mu$g/dl and for Se 0.32 $\mu$g/dl. Data were shown in micrograms per deciliter ($\mu$g/dl). The assessments of the serum concentrations of magnesium (wavelength 285.2 nm), calcium (422.7 nm), iron (248.3 nm), zinc (213.9 nm), and copper (324.8 nm) were performed by air-acetylene flame atomic absorption spectrometry using an ICE 3300 instrument (Thermo Fisher Scientific, Waltham, MA, USA). The detection limits for Mg were 0.0022 mg/dl, for Ca 0.0037 mg/dl, for Fe 0.0043 mg/dl, for Zn 0.0033 mg/dl, and Cu 0.0045 mg/dl. Concentrations of Ca and Mg were shown in milligrams per deciliter (mg/dl); Fe, Zn, and Cu were shown in micrograms per deciliter ($\mu$g/dl). Coefficient of variation (CV) ranged 1.64–2.18%. The overall methods recovery were 95–105%. The laboratory met the requirements of proficiency tests (Lead and Multi-Element Proficiency–CDC in Atlanta). The ClinCal® Whole Blood Calibrator and ClinCal Serum Calibrator (Recipe, Germany) were used for calibration of the instrument and control materials. ClinCheck Whole Blood Control Levels I, II, and III and ClinCheck Serum Control Levels I and II were used for quality control.

*2.2.3. Determination of Superoxide Dismutase (SOD) Activity.* The method of Oyanagui [9] was used to measure the activity of SOD in serum, erythrocytes, and leukocytes. In this method, xanthine oxidase produces superoxide anions which

react with hydroxylamine forming nitric ions. These ions react with naphthalene diamine and sulfanilic acid generating a colored product. Concentration of this product is proportional to the amount of produced superoxide anions and negatively proportional to the activity of SOD. Absorbance was measured using an automated analyzer PerkinElmer at a wavelength of 550 nm. The enzymatic activity of SOD was expressed in nitric units. The isoenzymes of SOD, such as Mn-SOD and CuZn-SOD, were also indicated in leukocytes, using KCN as the inhibitor of the CuZn-SOD activity. The activity of SOD is equal to 1 nitric unit (NU) when it inhibits nitric ion production by 50%. Activity of SOD was expressed in NU/ml in serum, NU/mg of hemoglobin (Hb) in erythrocytes, and in NU/mg of protein (P) in leukocytes.

*2.2.4. Determination of Catalase (CAT) Activity.* Catalase activity in erythrocytes and leukocytes was measured by the method of Johansson and Borg [10] using an automated analyzer PerkinElmer. The method is based on the reaction of the enzyme with methanol in the presence of optimal concentrations of hydrogen peroxide. Formaldehyde produced is measured spectrophotometrically at 550 nm as a dye purpald. The activity of Cat-Px was expressed as U/mg P in leukocytes and as kU/g Hb in erythrocytes.

*2.2.5. Determination of Ceruloplasmin (CER) Concentration.* The CER concentration in serum was determined spectrophotometrically by Richterich [11], using the reaction with p-phenyl diamine. To 20 ml of serum (examined sample) and to the mixture of 20 ml of serum and 200 ml of sodium azide solution (control sample), 1 ml of p-phenylenediamine dihydrochloride in acetate buffer was added. After 15 minutes of incubation, to the examined sample, 200 ml of sodium azide solution was also added. After another 15 minutes of incubation, the absorbance was measured at a wavelength of 546 nm. The values shown were in mg/dl.

*2.2.6. Determination of Lipid Hydroperoxide (LPH) Concentration.* The concentration of lipid hydroperoxides in serum was assessed according to a method described by Södergren et al. [12]. This assay is based on the ferrous oxidation of xylenol orange following the addition of methanol and butylated hydroxytoluene (BHT). The presence of ferric ions induces a color change in xylenol orange that can be measured as the change in absorbance at 560 nm relative to blank samples containing triphenylphosphine in methanol. The assay was conducted in the Victor X3 (PerkinElmer, Waltham, MA, USA) automated analyzer, which was calibrated with hydrogen peroxide. The values corresponding to total lipid hydroperoxides were shown in $\mu$mol/l.

*2.2.7. Determination of Malondialdehyde (MDA) Concentration.* Malondialdehyde level was measured fluorometrically as a 2-thiobarbituric acid-reactive substance (TBARS) in serum according to Ohkawa et al. [13] with modifications. Samples were mixed with 8.1% sodium dodecyl sulfate, 20% acetic acid, and 0.8% 2-thiobarbituric acid. After vortexing, samples were incubated for 1 hour in 950°C and butanol-pyridine 15 : 1 ($v/v$) was added. The mixture was shaken for 10 minutes and then centrifuged. The butanol-pyridine layer was measured fluorometrically at 552 nm and 515 nm excitation (PerkinElmer, USA). TBARS values are expressed as malondialdehyde (MDA) equivalents. Tetraethoxypropane was used as the standard. Concentrations were given in $\mu$mol/l.

*2.2.8. Determination of Lipofuscin (LPS) Concentration.* The concentration of LPS was determined in serum and erythrocytes according to the method of Jain [14]. To the hemolysate, isopropanol and chloroform in a ratio of 3 : 2 ($v/v$) was added. Then, the sample was shaken for 2 minutes and after 30 minutes of incubation at 20°C was centrifuged. Fluorescence was measured in the clear supernatant using an LS45 spectrofluorometer PerkinElmer at a wavelength of 400 nm (absorbance) and 455 nm (emission). The values were presented in relative units (RU). The value of RU 100 corresponds to the fluorescence of a 0.1 mg/ml quinidine sulfate solution in sulfuric acid. The concentration of LPS was shown in RU/g Hb in erythrocytes and in RU/ml in serum.

*2.2.9. Statistical Analysis.* The statistical analysis was performed using the Statistica 9.1 PL software program. The statistical analyses included the means and standard deviations of the data. Shapiro-Wilk test was used to verify normality, and Levene's test was used to verify the homogeneity of variances. Statistical comparisons were made using the $t$-test, $t$-test with separate variance estimates, the Mann–Whitney $U$ test, or the chi-squared test. The Spearman nonparametric correlation was calculated. A value of $p < 0.05$ was considered to be significant.

## 3. Results

The mean age of the exposed population was $40.94 \pm 13.68$ years. Their PbB at the beginning of the study was $10.7 \pm 7.67$ $\mu$g/dl and increased to the level of $49.1 \pm 14.1$ $\mu$g/dl at the end of the study period (Table 1).

The levels of calcium, magnesium, and zinc increased significantly after lead exposure compared to baseline by 3%, 3%, and 8%, respectively, while the level of copper decreased significantly by 7% (Table 2).

Activities of CAT, SOD, and SOD isoenzymes did not change due to lead exposure. Analogically, the level of MDA, CER, and serum LPS did not differ when compared its values after lead exposure and at baseline. However, the level of serum LPH increased significantly by 46%, while the level of erythrocyte LPS decreased by 13% (Table 3).

The analysis of correlations showed negative correlations between the change of PbB level and changes of leukocyte SOD ($R = -0.58$) and Mn-SOD ($R = -0.55$) activities. Inverse correlations were also observed between the change of CuZn-SOD activity and the changes of MDA ($R = -0.34$) and LPH ($R = -0.37$) levels due to the studied lead exposure. Analogical correlation was found for leukocyte SOD and LPH ($R = -0.46$). Positive correlations were shown between the changes of LPH and MDA levels ($R = 0.78$) and between the change of serum LPS level and changes of the MDA ($R = 0.47$) and LPH levels ($R = 0.42$) (Table 4).

Table 1: Epidemiological data and blood lead levels (B-Pb) in the study population.

| | Mean | SD |
|---|---|---|
| Lead exposure duration (days) | 40 | 3.2 |
| Age (years) | 40.94 | 13.68 |
| BMI (kg/m$^2$) | 25.86 | 3.71 |
| Percentage of smokers (%) | 69% | — |
| B-Pb $_{\text{before exposure}}$ ($\mu$d/dl) | 10.7 | 7.67 |
| B-Pb $_{\text{after exposure}}$ ($\mu$d/dl) | 49.1 | 14.1 |

Table 2: The levels of essential metals in the examined population.

| | Before exposure | | After exposure | | Relative change (%) | $p$ value |
|---|---|---|---|---|---|---|
| | Mean | SD | Mean | SD | | |
| Ca (mg/dl) | 112.55 | 6.13 | 116.29 | 8.34 | 3 | 0.042 |
| Mg (mg/dl) | 2.09 | 0.19 | 2.14 | 0.19 | 3 | 0.045 |
| Se ($\mu$g/dl) | 69.94 | 9.55 | 74.59 | 9.83 | 7 | 0.060 |
| Fe ($\mu$g/dl) | 156.42 | 60.33 | 172.34 | 64.73 | 10 | 0.096 |
| Zn ($\mu$g/dl) | 92.40 | 9.02 | 99.58 | 15.48 | 8 | 0.008 |
| Cu ($\mu$g/dl) | 95.27 | 15.07 | 88.62 | 11.45 | −7 | 0.028 |

Comparisons between subgroups of workers exposed to lead before the study and workers without such exposure, smokers and non-smokers, younger and older workers, and workers with higher and lower BMI are presented in corresponding tables. Data presented in those tables include epidemiological data and parameters which are significantly different (Tables 5–8).

## 4. Discussion

Blood lead level increased five times after examined exposure period. Observed elevations of blood lead levels were caused by inadequate adherence of workers to work safety procedures. Workers were in conditions of exposure to lead for 12 hours a day. They did not properly use the personal protective equipment, such as protective clothes, masks, and goggles, probably because they neglected or were unaware of possible adverse health effects of lead poisoning. The main source of lead in the working environment is the manufacturing process of melting raw materials which releases lead to the atmosphere around the steelwork's furnace as industrial dust. Wind-blown historical dust and slag storage piles are the secondary sources of lead exposure [15].

Calcium regulates many different cellular functions, such as contraction, secretion, metabolism, gene expression, cell survival, and death. Due to the interaction with stereospecific sites for divalent cations, lead may potentially impair all of the calcium-dependent processes [16]. In the present study, serum calcium level significantly increased after a short-term lead exposure. This increase may be due to the competitive displacement of calcium from its binding sites in cells by lead. In lead-exposed individuals, the concentration of lead is 90 times higher in red blood cells than in the plasma [17]. Lead ion is transported into the erythrocytes through calcium transport systems and may compete with calcium ions [18]. In consequence, calcium uptake by erythrocytes may decrease and result in elevated calcium level in serum which was observed in the present study. On the other hand, lead is also believed to trigger opposite mechanisms leading to the increase of calcium level in red blood cells. It has been proposed that lead-induced oxidative stress may induce calcium influx by ROS-mediated activation of calcium channels and suppression of ($Ca^{2+}$, $Mg^{2+}$)-ATPase activity which is responsible for calcium efflux. Besides, lead ions directly inhibit ($Ca^{2+}$, $Mg^{2+}$)-ATPase activity [16, 17]. In cardiomyocytes, lead has been shown to activate the cascade of Src and ERK 1/2 which activates the $\alpha$-1 subunit of L-type calcium channels. This activation results in increased calcium influx [19]. The same mechanism may operate in red blood cells. The abovementioned mechanisms explain increased calcium level reported in erythrocytes of workers chronically exposed to lead [16] and in human erythrocytes exposed to lead in vitro [17]. In accordance, a negative correlation ($R = -0.41$, $p < 0.01$) between blood lead level and plasma calcium level was shown in workers chronically exposed to lead [20]. This observation may be also due to the inhibitory effect of lead on 1$\alpha$-hydroxylase in renal tubules. As a result, lead inhibits synthesis of calcitriol resulting in a decrease in calcium absorption in the intestine and its reabsorption in renal tubules [21]. The complexity of mentioned interactions between lead and calcium may result in divergent results of studies which are methodologically different. Besides, the analysis of confounders showed that smoking habits affect the influence of lead exposure on serum calcium level. In a group of nonsmokers, the increase of serum calcium level due to the exposure was significantly higher than in a group of smokers.

The interactions between magnesium and lead are less studied. Magnesium is known to be a calcium antagonist and also serves as an essential element for cell functioning being a cofactor in more than 300 enzymatic reactions. Protein and DNA biosynthesis, anaerobic energy production, and the hydrolysis and transfer of phosphate groups are believed to be the most important biochemical processes that require magnesium ions [22]. Analogically to calcium levels, serum magnesium levels significantly increased after a short-term exposure to lead compared to baseline. This elevation could be also caused by the increased release of magnesium from tissues due to its displacement from binding sites by lead ions. Consistently, Chiba et al. [23] found decreased magnesium level in erythrocytes of workers chronically exposed to lead (PbB = 32.52 ± 9.49 $\mu$g/dl) compared to unexposed control group, while plasma magnesium level in this group of workers was the same as in the control group. However, a positive association between blood lead and serum magnesium levels was shown in a group of children environmentally exposed to high doses of lead (PbB = 19.9 ± 17.93 $\mu$g/dl) [2].

Selenium is the next metal that competes with lead. Selenium is involved in the antioxidant defense as a cofactor for glutathione peroxidase (GPx) and plays a role in tissue respiration. Selenoproteins also have the antioxidant properties and help to eliminate reactive oxygen species overproduced

Table 3: The activities of antioxidant enzymes, the levels of oxidative stress markers and ceruloplasmin. S: serum; E: erythrocyte; L: leukocyte.

| | Before exposure | | After exposure | | Relative change (%) | $p$ value |
|---|---|---|---|---|---|---|
| | Mean | SD | Mean | SD | | |
| S-SOD (NU/ml) | 16.84 | 2.47 | 17.42 | 2.33 | 3 | 0.238 |
| E-SOD (NU/mg Hb) | 178.69 | 20.18 | 175.77 | 24.23 | −2 | 0.535 |
| L-SOD (NU/mg P) | 16.80 | 1.94 | 16.89 | 3.97 | 1 | 0.894 |
| L-CuZn-SOD (NU/mg P) | 11.14 | 2.08 | 11.76 | 3.35 | 6 | 0.373 |
| L-Mn-SOD (NU/mg P) | 5.66 | 1.86 | 5.21 | 3.50 | −8 | 0.487 |
| E-CAT (kU/g Hb) | 371.27 | 72.38 | 393.73 | 81.89 | 6 | 0.200 |
| L-CAT (U/mg P) | 38.18 | 10.61 | 43.66 | 14.51 | 14 | 0.078 |
| S-MDA ($\mu$mol/l) | 2.12 | 0.57 | 2.37 | 0.72 | 12 | 0.097 |
| S-LPH ($\mu$mol/l) | 4.72 | 3.19 | 6.90 | 4.66 | 46 | 0.005 |
| S-LPS (RF/ml) | 1076.05 | 152.85 | 1140.59 | 172.47 | 6 | 0.107 |
| E-LPS (RF/g Hb) | 2354.00 | 538.19 | 2037.71 | 482.85 | −13 | 0.010 |
| S-CER (mg/dl) | 39.43 | 5.95 | 40.62 | 6.83 | 3 | 0.324 |

Table 4: Correlations between lead-induced changes of the levels of lead, MDA, and LPH and the changes of the levels of essential metals, activities of antioxidant enzymes, and the levels of oxidative stress markers and ceruloplasmin. S: serum; E: erythrocyte; L: leukocyte; D: a difference between the levels at baseline and at the end of the study period.

| | B-Pb-D ($\mu$g/dl) | S-MDA-D ($\mu$mol/l) | S-LPH-D ($\mu$mol/l) |
|---|---|---|---|
| Ca-D (mg/dl) | 0.18 | 0.18 | 0.25 |
| Mg-D (mg/dl) | 0.27 | 0.14 | 0.08 |
| Se-D ($\mu$g/dl) | 0.11 | −0.09 | 0.11 |
| Fe-D ($\mu$g/dl) | 0.04 | 0.27 | −0.07 |
| Zn-D ($\mu$g/dl) | 0.07 | −0.33 | −0.29 |
| Cu-D ($\mu$g/dl) | 0.17 | −0.24 | −0.24 |
| S-SOD-D (NU/ml) | −0.08 | −0.11 | −0.05 |
| E-SOD-D (NU/mg Hb) | 0.13 | 0.15 | 0.01 |
| L-SOD-D (NU/mg P) | −0.58 | −0.29 | −0.46 |
| L-CuZn-SOD-D (NU/mg P) | −0.15 | −0.34 | −0.37 |
| L-Mn-SOD-D (NU/mg P) | −0.55 | 0.07 | −0.07 |
| E-CAT-D (kU/g Hb) | −0.18 | −0.08 | −0.04 |
| L-CAT-D (U/mg P) | 0.01 | −0.04 | −0.15 |
| S-MDA-D ($\mu$mol/l) | 0.03 | 1.00 | 0.78 |
| S-LPH-D ($\mu$mol/l) | 0.14 | 0.78 | 1.00 |
| E-LPS-D (RF/g Hb) | 0.18 | 0.05 | 0.14 |
| S-LPS-D (RF/ml) | 0.03 | 0.47 | 0.42 |
| S-CER-D (mg/dl) | 0.07 | 0.24 | 0.17 |

by the metals' action. Some animal studies have shown that lead-induced oxidative stress could be reduced by the administration of selenium alone or the combination of selenium and other antioxidants [24]. In our previous study, we showed decreased level of selenium in workers chronically exposed to medium and high doses of lead compared to the unexposed control group [6]. Results of the present study indicate that a short-term exposure to lead does not significantly affect serum selenium level. However, selenium level was significantly higher after the studied period of lead exposure in a group of workers who had not a history of occupational exposure to lead than in workers with such a history. Analogical difference in selenium level due to exposure was observed between subgroups of workers with low and high BMI. These observations suggest an existence of a defense mechanism against lead toxicity which is efficient in individuals with lower BMI and without a history of occupational lead exposure.

Similarly to selenium, serum level of iron was also not significantly affected by the studied short period of lead exposure. Iron is an essential trace element which plays an important role in the synthesis of metalloproteins, such as hemoglobin or myoglobin. In an experimental study on rats, a significant reduction in the concentration of serum iron following short- and long-term lead administrations to rats was reported. Authors of this study postulate that lead in the plasma binds to transferrin molecules displacing iron. As a result, unbound iron might be excreted through the kidneys [25]. Besides, an inverse relation between blood lead levels and iron status was reported in children environmentally exposed to lead diagnosed with anemia [26, 27]. This association between the levels of lead and iron is likely due to their sharing of the same transporters, such as the divalent metal transporter 1 (DMT1) and ferroportin 1 (FP1). Consequently, iron status may over- or underregulate the intestinal absorption of lead [28]. However, workers are exposed to lead primarily through the respiratory tract and upregulation of intestinal lead absorption by decreased body iron content should have marginal significance in occupational exposure. Consistently, in our previous study, we did not show any association between blood lead level and serum iron level in a group of chronically lead-exposed workers [6].

The inverse association between lead body burden and zinc status has been also found. These metals also compete in binding to metal transporters, including metallothionein-like transport protein responsible for the metals' intestinal absorption [29]. In the present study, serum zinc level significantly increased after lead exposure compared to baseline. This observation confirms that intestinal absorption of lead

Table 5: The comparison between subgroups of workers without a history of occupational exposure to lead (N-HOE) and workers witch such a history (HOE). B: whole blood; S: serum; L: leukocyte; D: a difference between the levels at baseline (1) and at the end of the study period (2).

| | N-HOE $n = 18$ | | HOE $n = 18$ | | *p value* |
|---|---|---|---|---|---|
| | Mean | SD | Mean | SD | |
| Age (years) | 37.72 | 14.17 | 44.58 | 12.37 | 0.125 |
| Percentage of smokers (%) | 0.72 | 0.46 | 0.63 | 0.50 | 0.569 |
| BMI (kg/m$^2$) | 25.35 | 3.81 | 26.13 | 3.68 | 0.530 |
| B-Pb-1 ($\mu$g/dl) | 4.16 | 1.62 | 16.95 | 5.32 | <0.001 |
| B-Pb-2 ($\mu$g/dl) | 46.52 | 10.98 | 51.26 | 16.37 | 0.311 |
| B-Pb-D ($\mu$g/dl) | 42.36 | 11.04 | 34.33 | 16.89 | 0.028 |
| Se-1 ($\mu$g/dl) | 68.64 | 9.25 | 71.23 | 9.93 | 0.424 |
| Se-2 ($\mu$g/dl) | 78.45 | 9.70 | 70.73 | 8.56 | 0.016 |
| Se-D ($\mu$g/dl) | 9.81 | 14.25 | −0.51 | 12.85 | 0.029 |
| L-SOD-1 (NU/mg P) | 17.34 | 1.88 | 16.25 | 1.89 | 0.091 |
| L-SOD-2 (NU/mg P) | 16.00 | 4.56 | 17.79 | 3.15 | 0.180 |
| L-SOD-D (NU/mg P) | −1.35 | 4.03 | 1.53 | 3.98 | 0.038 |
| L-CAT-1 (U/mg P) | 39.13 | 11.08 | 37.24 | 10.35 | 0.600 |
| L-CAT-2 (U/mg P) | 38.46 | 8.84 | 48.87 | 17.26 | 0.029 |
| L-CAT-D (U/mg P) | −0.67 | 9.89 | 11.63 | 22.27 | 0.039 |
| S-LPH-1 ($\mu$mol/l) | 3.52 | 2.12 | 5.91 | 3.66 | 0.022 |
| S-LPH-2 ($\mu$mol/l) | 6.53 | 4.76 | 7.27 | 4.67 | 0.644 |
| S-LPH-D ($\mu$mol/l) | 3.01 | 3.96 | 1.36 | 5.52 | 0.309 |

Table 6: The comparison between subgroups of smokers and nonsmokers. B: whole blood; E: erythrocyte; L: leukocyte; D: a difference between the levels at baseline (1) and at the end of the study period (2).

| | Nonsmokers $n = 11$ | | Smokers $n = 25$ | | *p value* |
|---|---|---|---|---|---|
| | Mean | SD | Mean | SD | |
| Age (years) | 40.09 | 13.62 | 41.40 | 13.93 | 0.795 |
| BMI | 27.42 | 3.51 | 25.17 | 3.65 | 0.094 |
| B-Pb-1 ($\mu$g/dl) | 10.42 | 7.18 | 10.82 | 8.03 | 0.886 |
| B-Pb-2 ($\mu$g/dl) | 49.33 | 10.94 | 49.04 | 15.60 | 0.956 |
| B-Pb-D ($\mu$g/dl) | 38.91 | 12.25 | 38.23 | 16.13 | 0.902 |
| Ca-1 (mg/dl) | 110.48 | 5.85 | 113.46 | 6.14 | 0.184 |
| Ca-2 (mg/dl) | 120.04 | 4.89 | 114.65 | 9.07 | 0.018 |
| Ca-D (mg/dl) | 9.55 | 8.62 | 1.19 | 10.56 | 0.027 |
| E-SOD-1 (NU/mg Hb) | 168.74 | 18.76 | 183.07 | 19.55 | 0.048 |
| E-SOD-2 (NU/mg Hb) | 174.51 | 29.20 | 176.31 | 22.37 | 0.841 |
| E-SOD-D (NU/mg Hb) | 5.77 | 25.72 | −6.76 | 28.63 | 0.221 |
| L-CuZn-SOD-1 (NU/mg P) | 10.44 | 2.15 | 11.45 | 2.01 | 0.186 |
| L-CuZn-SOD-2 (NU/mg P) | 13.24 | 2.23 | 11.11 | 3.59 | 0.078 |
| L-CuZn-SOD-D (NU/mg P) | 2.80 | 3.80 | −0.34 | 3.98 | 0.034 |
| L-CAT-1 (U/mg P) | 35.78 | 8.49 | 39.24 | 11.41 | 0.374 |
| L-CAT-2 (U/mg P) | 37.14 | 7.78 | 46.53 | 15.93 | 0.023 |
| L-CAT-D (U/mg P) | 1.36 | 12.38 | 7.29 | 20.06 | 0.373 |

in occupational exposure has limited significance. Zinc is essential for cellular metabolism as a central part of over 300 enzymes and proteins [6]. Therefore, as in the case of calcium and magnesium, observed elevation of zinc level may be due to its displacement from protein binding sites in cells. By contrast, the level of plasma copper significantly decreased after a short-term exposure to lead compared to baseline. At the same time, the level of ceruloplasmin, an acute-phase protein that binds copper, did not change significantly. Lead competes with copper analogically to zinc [30]. Therefore, there must exist an additional mechanism that decreases copper level due to the lead action independent of ceruloplasmin metabolism and function. Interestingly, we found a significantly elevated level of copper and ceruloplasmin in chronically lead-exposed workers [6]. This increase in the copper level might have been secondary to the increase of ceruloplasmin level related to the inflammatory processes to be triggered by lead. In light of this, a short-time exposure seems to be not enough to induce such proinflammatory conditions.

Both zinc and copper are necessary for the activity of cytoplasmic and extracellular isoenzymes of SOD, while iron is a cofactor for CAT. SOD utilizes superoxide anions to hydrogen peroxide which is degraded by CAT. Both enzymes serve as a part of the antioxidant defense mechanism against lead-induced oxidative stress [31]. Lead is able to modify expression and activities of CAT and SOD via many mechanisms. On the one hand, lead may induce expressions and activities of CAT and SOD through increased generation of their substrates. On the other hand, activities of CAT and SOD may decrease as a result of lead's binding to thiol groups of their active sites or lead's interactions with their cofactors. Consequently, activities of SOD and CAT in lead-exposed individuals are determined by the sum of opposite mechanisms. This explains divergent results of animal and human studies in this field [5]. In the present study, activities of both enzymes did not change after exposure to lead compared to baseline. However, there were negative correlations between the change of blood level and changes of the activities of leukocyte SOD and Mn-SOD due to lead exposure. The analysis of confounders provided some additional information. In a group of workers, who had a history of occupational exposure to lead, the activities of CAT and SOD in leukocytes were elevated due to the short-term exposure to lead, while in workers without such a history, activities of these enzymes were decreased. These observations suggest an existence of a defense mechanism against lead toxicity that had developed during previous episodes of exposure. The confounding role of smoking habits, age, and BMI also should not be neglected. In a group of nonsmokers, the leukocyte CuZn-SOD activity increased due to the studied lead exposure, while in smokers, the activity of this isoenzyme slightly decreased. Conversely, smokers had significantly higher baseline CAT activity than nonsmokers. The baseline leukocyte activities of CAT were also significantly higher in younger workers and those with lower BMI compared to the group of older workers and those with higher BMI. However, the changes of CAT activities in those groups due to the studied lead exposure were not

Table 7: The comparison between the subgroups of younger and older workers based on the median of age (37 years). B: whole blood; S: serum; L: leukocyte; D: a difference between the levels at baseline (1) and at the end of the study period (2).

| | Younger workers $n = 19$ | | Older workers $n = 17$ | | *p value* |
|---|---|---|---|---|---|
| | Mean | SD | Mean | SD | |
| Age (years) | 29.47 | 5.25 | 53.67 | 6.39 | <0.001 |
| Percentage of smokers (%) | 0.74 | 0.45 | 0.61 | 0.50 | 0.428 |
| BMI (kg/m$^2$) | 24.92 | 3.70 | 26.63 | 3.62 | 0.164 |
| B-Pb-1 ($\mu$g/dl) | 8.61 | 7.18 | 12.97 | 7.53 | 0.080 |
| B-Pb-2 ($\mu$g/dl) | 48.24 | 15.08 | 49.71 | 13.21 | 0.756 |
| B-Pb-D ($\mu$g/dl) | 39.63 | 15.52 | 36.76 | 14.12 | 0.561 |
| L-CAT-1 (U/mg P) | 41.16 | 10.22 | 34.85 | 10.31 | 0.046 |
| L-CAT-2 (U/mg P) | 46.43 | 16.44 | 40.57 | 11.72 | 0.232 |
| L-CAT-D (U/mg P) | 5.27 | 20.38 | 5.72 | 15.77 | 0.942 |
| S-MDA-1 ($\mu$mol/l) | 1.98 | 0.43 | 2.29 | 0.68 | 0.104 |
| S-MDA-2 ($\mu$mol/l) | 2.04 | 0.49 | 2.73 | 0.78 | 0.003 |
| S-MDA-D ($\mu$mol/l) | 0.07 | 0.55 | 0.45 | 1.10 | 0.193 |
| S-LPH-1 ($\mu$mol/l) | 3.35 | 2.72 | 6.24 | 3.04 | 0.005 |
| S-LPH-2 ($\mu$mol/l) | 5.17 | 3.54 | 8.84 | 5.09 | 0.016 |
| S-LPH-D ($\mu$mol/l) | 1.81 | 3.68 | 2.60 | 5.91 | 0.633 |
| S-LPS-1 (RF/ml) | 1113.71 | 186.24 | 1033.95 | 92.30 | 0.119 |
| S-LPS-2 (RF/ml) | 1075.00 | 157.34 | 1213.90 | 162.47 | 0.014 |
| S-LPS-D (RF/ml) | −38.71 | 226.46 | 179.95 | 187.42 | 0.004 |

Table 8: The comparison between subgroups of workers with lower and higher BMI based on the median of BMI (25.6 kg/m$^2$). B: whole blood; L: leukocyte; D: a difference between the levels at baseline (1) and at the end of the study period (2).

| | Low BMI $n = 17$ | | High BMI $n = 19$ | | *p value* |
|---|---|---|---|---|---|
| | Mean | SD | Mean | SD | |
| Age (years) | 37.44 | 14.16 | 44.84 | 12.22 | 0.097 |
| Percentage of smokers (%) | 0.72 | 0.46 | 0.63 | 0.50 | 0.569 |
| BMI (kg/m$^2$) | 22.65 | 1.96 | 28.69 | 2.28 | <0.001 |
| B-Pb-1 ($\mu$g/dl) | 9.84 | 7.56 | 11.57 | 7.69 | 0.494 |
| B-Pb-2 ($\mu$g/dl) | 50.68 | 15.57 | 47.32 | 12.59 | 0.475 |
| B-Pb-D ($\mu$g/dl) | 40.84 | 13.76 | 35.77 | 15.53 | 0.302 |
| Se-1 ($\mu$g/dl) | 66.88 | 10.40 | 72.67 | 8.03 | 0.069 |
| Se-2 ($\mu$g/dl) | 77.45 | 9.72 | 72.03 | 9.44 | 0.099 |
| Se-D ($\mu$g/dl) | 10.56 | 13.77 | −0.64 | 13.03 | 0.017 |
| L-SOD-1 (NU/mg P) | 17.21 | 1.52 | 16.43 | 2.22 | 0.237 |
| L-SOD-2 (NU/mg P) | 15.08 | 4.39 | 18.52 | 2.76 | 0.007 |
| L-SOD-D (NU/mg P) | −2.13 | 3.42 | 2.09 | 3.90 | 0.002 |
| L-Mn-SOD-1 (NU/mg P) | 5.61 | 1.84 | 5.70 | 1.92 | 0.889 |
| L-Mn-SOD-2 (NU/mg P) | 3.83 | 1.59 | 6.44 | 4.27 | 0.024 |
| L-Mn-SOD-D (NU/mg P) | −1.78 | 2.12 | 0.74 | 4.68 | 0.049 |
| L-CAT-1 (U/mg P) | 42.16 | 10.35 | 34.62 | 9.76 | 0.031 |
| L-CAT-2 (U/mg P) | 45.12 | 10.16 | 42.36 | 17.72 | 0.576 |
| L-CAT-D (U/mg P) | 2.96 | 13.84 | 7.73 | 21.33 | 0.437 |

significantly different. Surprisingly, the activities of SOD and Mn-SOD in leukocytes decreased after the studied lead exposure period in a group of workers with lower BMI, while an opposite trend was observed in those with higher BMI. However, these differences in SOD and Mn-SOD activities were not associated with differences in oxidative stress parameters. Therefore, their significance is limited.

The activities of antioxidant enzymes are associated with oxidative stress intensity. We showed inverse correlations between the changes of leukocyte SOD and CuZn-SOD activities and the changes of MDA and LPH levels due to the studied lead exposure. The ability of lead to induce oxidative stress via impairment of the antioxidant defenses has been widely studied in humans chronically exposed to lead [5, 32]. In the present study, a short-term exposure to lead resulted in increased LPH level by 46%. The levels of serum MDA and LPS did not change significantly. Consistently, in our previous study [8], we showed increased total oxidant status (TOS) level in leukocytes, unchanged leukocyte and erythrocyte MDA level, and decreased erythrocyte glutathione pool due to a short-term lead exposure. Therefore, it seems that the primary products of lipid peroxidation, such as LPH or TOS value, are better in estimating oxidative stress intensity in acute or subacute lead exposure. Additively, the analysis of confounders showed that older workers had greater levels of LPH at baseline and were more susceptible to develop oxidative stress due to lead exposure than the younger population. The possible influence of smoking habits and BMI on measured parameters of oxidative stress was not shown. Surprisingly, subacute exposure to lead resulted in significantly decreased level of LPS in

erythrocytes. This parameter serves as a marker of ageing. Lead has been shown to induce eryptosis. In this process, old and damaged erythrocytes are removed from circulation [33]. Therefore, the level of erythrocyte LPS may decrease after exposure to lead due to the elevated removal of the pool of erythrocytes with the highest levels of LPS.

## 5. Conclusions

The plasma and serum levels of essential metals are modified by a short-term exposure to lead in occupationally exposed workers. These modifications are partially different from those observed in a long-term exposure.

A short-term exposure to lead induces oxidative stress associated with elevated levels of LPH. A greater susceptibility to develop oxidative stress due to such exposure is related positively to a higher age of workers. This susceptibility may be a result of an age-related decrease in the CAT activity.

Activities of antioxidant enzymes, such as CAT and SOD, were not significantly affected by a short-term exposure to lead in all examined individuals. However, workers with a history of occupational exposure to lead may develop defensive mechanisms against lead-induced oxidative stress resulting in increased activities of CAT and SOD due to the subsequent episode of exposure.

## Conflicts of Interest

The authors declare that there are no conflicts of interest regarding the publication of this article.

## References

[1] Y. S. Reddy, Y. Aparna, B. A. Ramalaksmi, and B. D. Kumar, "Lead and trace element levels in placenta, maternal and cord blood: a cross-sectional pilot study," *The Journal of Obstetrics and Gynaecology Research*, vol. 40, no. 12, pp. 2184–2190, 2014.

[2] Y. S. Reddy, R. Pullakhandam, K. V. Radha Krishna, P. Uday Kumar, and B. Dinesh Kumar, "Lead and essential trace element levels in school children: a cross-sectional study," *Annals of Human Biology*, vol. 38, no. 3, pp. 372–377, 2011.

[3] G. Flora, D. Gupta, and A. Tiwari, "Toxicity of lead: a review with recent updates," *Interdisciplinary Toxicology*, vol. 5, no. 2, pp. 47–58, 2012.

[4] L. Patrick, "Lead toxicity, a review of the literature. Part 1: exposure, evaluation, and treatment," *Alternative Medicine Review*, vol. 11, no. 1, pp. 2–22, 2006.

[5] A. Kasperczyk, G. Machnik, M. Dobrakowski, D. Sypniewski, E. Birkner, and S. Kasperczyk, "Gene expression and activity of antioxidant enzymes in the blood cells of workers who were occupationally exposed to lead," *Toxicology*, vol. 301, no. 1-3, pp. 79–84, 2012.

[6] A. Kasperczyk, A. Prokopowicz, M. Dobrakowski, N. Pawlas, and S. Kasperczyk, "The effect of occupational lead exposure on blood levels of zinc, iron, copper, selenium and related proteins," *Biological Trace Element Research*, vol. 150, no. 1-3, pp. 49–55, 2012.

[7] Y. Li, M. Li, Q. Lv et al., "Relationship of lead and essential elements in whole blood from school-age children in Nanning, China," *Journal of Trace Elements in Medicine and Biology*, vol. 32, pp. 107–111, 2015.

[8] M. Dobrakowski, N. Pawlas, E. Hudziec et al., "Glutathione, glutathione-related enzymes, and oxidative stress in individuals with subacute occupational exposure to lead," *Environmental Toxicology and Pharmacology*, vol. 45, pp. 235–240, 2016.

[9] Y. Oyanagui, "Reevaluation of assay methods and establishment of kit for superoxide dismutase activity," *Analytical Biochemistry*, vol. 142, no. 2, pp. 290–296, 1984.

[10] L. H. Johansson and L. A. Borg, "A spectrophotometric method for determination of catalase activity in small tissue samples," *Analytical Biochemistry*, vol. 174, no. 1, pp. 331–336, 1988.

[11] R. Richterich, *Chemia kliniczna*, PZWL, Warszawa, 1971.

[12] E. Södergren, J. Nourooz-Zadeh, L. Berglund, and B. Vessby, "Re-evaluation of the ferrous oxidation in xylenol orange assay for the measurement of plasma lipid hydroperoxides," *Journal of Biochemical and Biophysical Methods*, vol. 37, no. 3, pp. 137–146, 1988.

[13] H. Ohkawa, N. Ohishi, and K. Yagi, "Assay for lipid peroxides in animal tissues by thiobarbituric acid reaction," *Analytical Biochemistry*, vol. 95, no. 2, pp. 351–358, 1979.

[14] S. K. Jain, "In vivo externalization of phosphatidylserine and phosphatidylethanolamine in the membrane bilayer and hypercoagulability by the lipid peroxidation of erythrocytes in rats," *The Journal of Clinical Investigation*, vol. 76, no. 1, pp. 281–286, 1985.

[15] F. Goodarzi, H. Sanei, M. Labonté, and W. F. Duncan, "Sources of lead and zinc associated with metal smelting activities in the Trail area, British Columbia, Canada," *Journal of Environmental Monitoring*, vol. 4, no. 3, pp. 400–407, 2002.

[16] M. A. Quintanar-Escorza, M. T. González-Martínez, I. O. del Pilar, and J. V. Calderón-Salinas, "Oxidative damage increases intracellular free calcium $[Ca^{2+}]_i$ concentration in human erythrocytes incubated with lead," *Toxicology in Vitro*, vol. 24, no. 5, pp. 1338–1346, 2010.

[17] M. A. Quintanar-Escorza, M. T. González-Martínez, L. Navarro, M. Maldonado, B. Arévalo, and J. V. Calderón-Salinas, "Intracellular free calcium concentration and calcium transport in human erythrocytes of lead-exposed workers," *Toxicology and Applied Pharmacology*, vol. 220, no. 1, pp. 1–8, 2007.

[18] J. V. Calderón-Salinas, M. A. Quintanar-Escorza, C. E. Hernández-Luna, and M. T. González-Martínez, "Effect of lead on the calcium transport in human erythrocyte," *Human & Experimental Toxicology*, vol. 18, no. 3, pp. 146–153, 1999.

[19] M. Fioresi, M. R. Simões, L. B. Furieri et al., "Chronic lead exposure increases blood pressure and myocardial contractility in rats," *PLoS One*, vol. 9, no. 5, article e96900, 2014.

[20] J. I. Anetor, O. A. Ajose, J. A. Adebiyi et al., "Decreased thiamine and magnesium levels in the potentiation of the neurotoxicity of lead in occupational lead exposure," *Biological Trace Element Research*, vol. 116, no. 1, pp. 43–51, 2007.

[21] N. N. Dongre, A. N. Suryakar, A. J. Patil, I. A. Hundekari, and B. B. Devarnavadagi, "Biochemical effects of lead exposure on battery manufacture workers with reference to blood pressure, calcium metabolism and bone mineral density," *Indian Journal of Clinical Biochemistry*, vol. 28, no. 1, pp. 65–70, 2013.

[22] A. Kasperczyk, M. Dobrakowski, J. Zalejska-Fiolka, S. Horak, and E. Birkner, "Magnesium and selected parameters of the non-enzymatic antioxidant and immune systems and oxidative stress intensity in the seminal plasma of fertile males," *Magnesium Research*, vol. 28, no. 1, pp. 14–22, 2015.

[23] M. Chiba, A. Shinohara, K. Matsushia, H. Watanabe, and Y. Inaba, "Indices of lead-exposure in blood and urine of lead-exposed workers and concentrations of major and trace elements and activities of SOD, GSH-Px and catalase in their blood," *The Tohoku Journal of Experimental Medicine*, vol. 178, no. 1, pp. 49–62, 1996.

[24] N. Pawlas, M. Dobrakowski, A. Kasperczyk, A. Kozłowska, A. Mikołajczyk, and S. Kasperczyk, "The level of selenium and oxidative stress in workers chronically exposed to lead," *Biological Trace Element Research*, vol. 170, no. 1, pp. 1–8, 2016.

[25] M. Moshtaghie, P. Malekpouri, M. R. Dinko, and A. A. Moshtaghie, "Changes in serum parameters associated with iron metabolism in male rat exposed to lead," *Journal of Physiology and Biochemistry*, vol. 69, no. 2, pp. 297–304, 2013.

[26] A. A. Hegazy, M. M. Zaher, M. A. Abd El-Hafez, A. A. Morsy, and R. A. Saleh, "Relation between anemia and blood levels of lead, copper, zinc and iron among children," *BMC Research Notes*, vol. 3, no. 1, p. 133, 2010.

[27] N. B. Jain, F. Laden, U. Culler, A. Shankar, S. Kazani, and E. Garshick, "Relation between blood lead levels and childhood anemia in India," *American Journal of Epidemiology*, vol. 161, no. 10, pp. 968–973, 2005.

[28] G. Fan, G. Du, H. Li et al., "The effect of the hemochromatosis (HFE) genotype on lead load and iron metabolism among lead smelter workers," *PLoS One*, vol. 9, no. 7, article e101537, 2014.

[29] M. Ahamed, S. Singh, J. R. Behari, A. Kumar, and M. K. Siddiqui, "Interaction of lead with some essential trace metals in the blood of anemic children from Lucknow, India," *Clinica Chimica Acta*, vol. 377, no. 1-2, pp. 92–97, 2007.

[30] F. L. Cerklewski and R. M. Forbes, "Influence of dietary copper on lead toxicity in the young male rat," *The Journal of Nutrition*, vol. 107, no. 1, pp. 143–146, 1977.

[31] S. Kasperczyk, E. Birkner, A. Kasperczyk, and J. Zalejska-Fiolka, "Activity of superoxide dismutase and catalase in people protractedly exposed to lead compounds," *Annals of Agricultural and Environmental Medicine*, vol. 11, no. 2, pp. 291–296, 2004.

[32] A. Kasperczyk, L. Słowińska-Łożyńska, M. Dobrakowski, J. Zalejska-Fiolka, and S. Kasperczyk, "The effect of lead-induced oxidative stress on blood viscosity and rheological properties of erythrocytes in lead exposed humans," *Clinical Hemorheology and Microcirculation*, vol. 56, no. 3, pp. 187–195, 2014.

[33] I. C. Aguilar-Dorado, G. Hernández, M. A. Quintanar-Escorza, M. Maldonado-Vega, M. Rosas-Flores, and J. V. Calderón-Salinas, "Eryptosis in lead-exposed workers," *Toxicology and Applied Pharmacology*, vol. 281, no. 2, pp. 195–202, 2014.